

NORTHEAST UTILITIES



THE CONNECTICUT LIGHT AND POWER COMPANY
WESTERN MASSACHUSETTS ELECTRIC COMPANY
HOLYOKE WATER POWER COMPANY
NORTHEAST UTILITIES SERVICE COMPANY
NORTHEAST NUCLEAR ENERGY COMPANY

General Offices • Selden Street, Berlin, Connecticut

P.O. BOX 270
HARTFORD, CONNECTICUT 06141-0270
(203) 665-5000

October 18, 1984

Docket No. 50-423
B11346

Director of Nuclear Reactor Regulation
Mr. B. J. Youngblood, Chief
Licensing Branch No. 1
Division of Licensing
U. S. Nuclear Regulatory Commission
Washington, D. C. 20555

- References:
- (1) W. G. Council to B. J. Youngblood, Millstone Nuclear Power Station, Unit No. 3, Technical Review Meeting Summary, Structural Confirmatory Items, dated June 26, 1984.
 - (2) B. J. Youngblood to W. G. Council, Millstone Nuclear Power Station, Unit No. 3, Docket No. 50-423 (NUREG-1031), dated August 2, 1984.

Dear Mr. Youngblood:

Millstone Nuclear Power Station, Unit No. 3
Transmittal of Responses to Safety
Evaluation Report (SER) Confirmatory Items

Enclosed are Northeast Nuclear Energy Company's responses to SER Confirmatory Items 6, 9 and 22 (Reference 2). Confirmatory Items 6, 9 and 22 correspond respectively to Items I, IV, and III discussed with your Mr. Nilesh Chokshi and Mr. David Jeng, Structural and Geotechnical Engineering Branch and Mr. Bob Palla, Containment Systems Branch, on June 14, 1984 (Reference 1).

8411010303 841018
PDR ADDOCK 05000423
E PDR

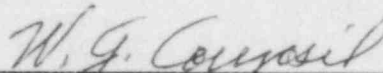
Bool
1/40

If there are any questions or concerns related to the information contained herein, please contact our licensing representative, Ms. C. J. Shaffer, at (203) 665-3285.

Very truly yours,

NORTHEAST NUCLEAR ENERGY COMPANY
et. al.

BY NORTHEAST NUCLEAR ENERGY COMPANY
Their Agent



W. G. Council
Senior Vice President

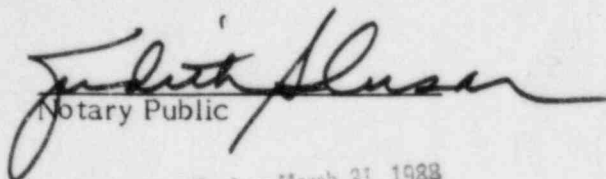


By: W. F. Fee
Executive Vice President

cc: Mr. Nilesh Chockshi - NRC-SGEB
Mr. David Jeng - NRC-SGEB
Mr. Bob Palla - NRC-CS

STATE OF CONNECTICUT)
) ss. Berlin
COUNTY OF HARTFORD)

Then personally appeared before me W. F. Fee who being duly sworn, did state that he is Executive Vice President of Northeast Nuclear Energy Company, a Applicant herein, that he is authorized to execute and file the foregoing information in the name and on behalf of the Applicants Licensees herein and that the statements contained in said information are true and correct to the best of his knowledge and belief.



Notary Public

My Commission Expires March 31, 1988

Structural Audit Item 41 - (Item I from June 14 meeting with NRC)

Discussion of Stone & Webster Engineering Corporation's Missile Barrier Interaction Topical Report (SWEC-7703)

RESPONSE:

- A. Additional data is required to justify ductility ratio and impulse values for the auto impact study. The applicant will provide this information.
- B. Ductility Ratio - The applicant will (1) survey all Category I structures exterior walls above ground level and prepare a table of panel sizes, (2) identify any panels less than 24 in. thick and (3) identify the limiting panel size. If the limiting panel size should be less than 10' x 10', we will then look at the ductility ratio.

ITEM A

As requested, the applicant has submitted the data required to justify the automobile impact and impulse parameters. They are derived in Appendix C of SWECO 7703 Time History Analysis for Overall Structural Response (enclosed). The following, which is extracted from Appendix C pages C-3 and C-5, specifically explains the derivation of the magnitude and duration of the automobile impact force used in the analysis.

The square wave force F 3 representation of body-chassis crushing strength is based on the results of a test performed by Sandia Laboratories. The test consisted of projecting an automobile head-on against a reinforced concrete barrier. The following data describe the test:

Weight of auto:	Originally 2,715 lb, modified for test to 3,330 lb
Impact velocity:	76.3 fps
Damage to barrier:	None
Damage to automobile	26 in. crushing

The average crushing resistance of the body and chassis can be determined by calculating their kinetic energy and dividing that energy by the crushing distance. Assuming 16 percent of the original weight to be engine and transmission this calculation gives:

$$26 R/12 = (3.3 \cdot 2.715 \times .16) 76.3^2/64.4$$
$$R = 119.6 \text{ kips}$$

Since the automobile used in the example is heavier than the one tested, the crushing resistance R is greater. Assuming resistance proportional to weight, there results

$$R = 119.6 \times 4000/2714 = 176 \text{ kips}$$

For conservatism, this is increased to 300 kips.

In order to know the duration of the square wave force F_3 , it is necessary to monitor the velocity of the missile mass M_3 . This is done as follows:

$$V_3 = (I_3 - \sum F_e^3 dt) / M_3$$

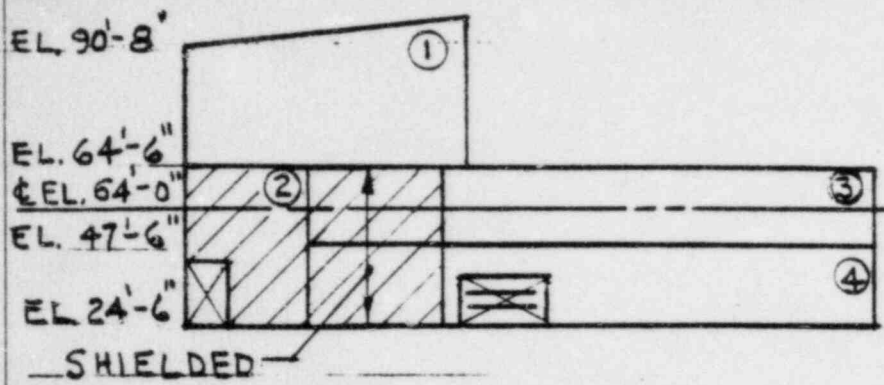
When the missile velocity V_3 decreases to the velocity of the barrier, the mass M_3 no longer pushes on the barrier with force F_3 . From this time on, the barrier and missile M_3 are assumed to travel together until the barrier stops. I_3 is the original momentum of missile mass M_3 .

Utilizing the above method along with the missile spectra submitted in FSAR Table 3.5-13, the ductility ratios submitted in FSAR Table 3.5-14 were calculated.

ITEM B

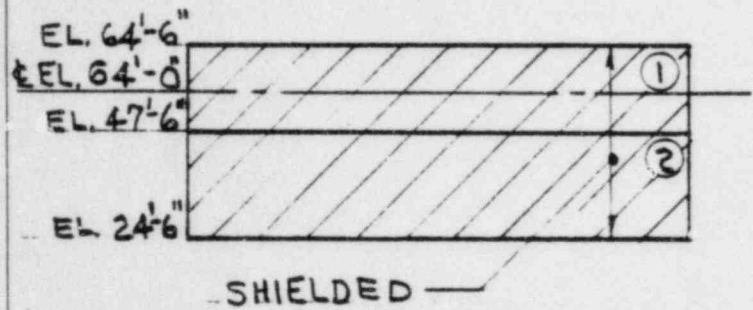
As requested, the applicant has performed a survey of all exterior wall panels to a height of 30 ft above grade which provide tornado missile protection. All walls providing protection from tornado missiles are a minimum 2 ft thick. The results of the survey are as indicated on the attached sheets. Those panels which provide missile protection, but are naturally shielded by other structures are so indicated. The results of the survey indicate that there is only one panel with a dimension less than 10 ft which would be subjected to impact by the automobile missile. However, this panel is shielded such that the automobile impacts close to the 2 ft roof support and the impact load is transferred directly into the roof. (G.6 Line Wall in Fuel Building. Page 7 of Attachment).

The results of the survey show the exterior walls are adequately protected against tornado missiles.



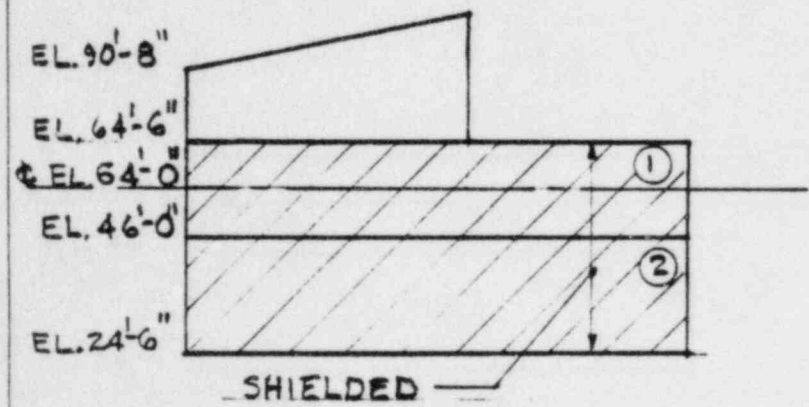
PENET NO.	LENGTH	HEIGHT
①	57'-0"	26'-0"
②	23'-0"	40'-0"
③	94'-0"	17'-0"
④	94'-0"	23'-0"

CONTROL BLDG-NORTH WALL
 DWG 12179-EC-10G (17-17)



PANEL NO.	LENGTH	HEIGHT
①	102'-0"	17'-0"
②	102'-0"	23'-0"

CONTROL BLDG-EAST WALL
 DWG 12179-EC-10G (14-14)



PANEL NO.	LENGTH	HEIGHT
①	117'-0"	18'-6"
②	117'-0"	21'-6"

NOTE: ALL WALLS AND ROOFS
 ARE 2'-0" THICK MIN
 AND HAVE #11@10" EW
 ALL DIMS ARE APPROX

CONTROL BLDG-SOUTH WALL
 DWG 12179-EC-10G (18-18)

JO 12179

POWER INDUSTRY GROUP		TITLE NUSCO-MILLSTONE #3 TORNADO MISSILE BARRIER PANEL SIZES OF CAT I STRUCTS	SCALE: NO SCALE	
CHECKED			DATE: JUNE 26, 84	
CORRECT			SKETCH NUMBER	
APPROVED			PG 1	
REVISIONS	②	③	④	⑤

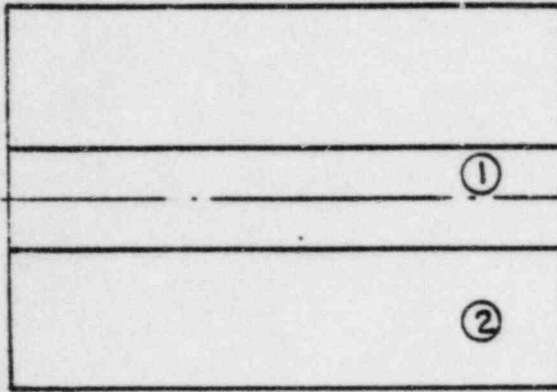
EL 90'-8"

EL 64'-6"

EL 64'-0"

EL 47'-6"

EL 24'-6"



PANEL N°	LENGTH	HEIGHT
1	102'-0"	17'-0"
2	102'-0"	23'-0"

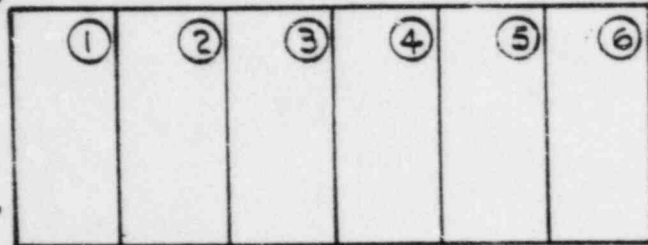
CONTROL BLDG - WEST WALL
 DWG 12179 - EC - 104 (20-20)

JO 12179

		TITLE NUSCO - MILLSTONE #3 TORNADO MISSILE BARRIER PANEL SIZES OF CAT I STRUCTS.	SCALE: NO SCALE
CHECKED			DATE: JUNE 26, 84
CORRECT			SKETCH NUMBER
APPROVED			
REVISIONS	(2) (3) (4) (5)		262

EL 64'-0" -----

EL 39'-0"



EL 14'-6"

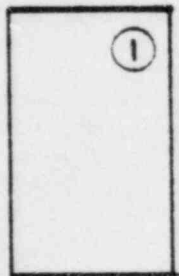
PANEL NO	LENGTH	HEIGHT
① To ⑥	20'-0"	24'-6"

CW PUMP HOUSE ~ LONG WALLS

DWG 12179-EC-14 H

EL 64'-0" -----

EL 39'-0"



EL 14'-6"

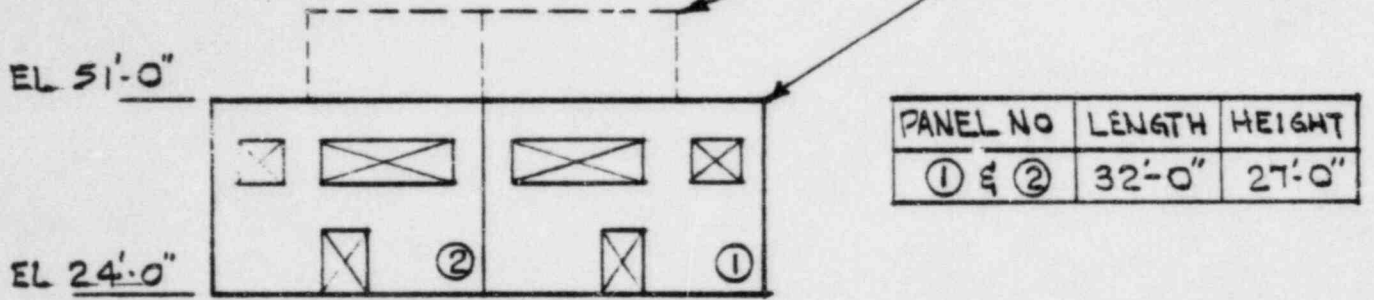
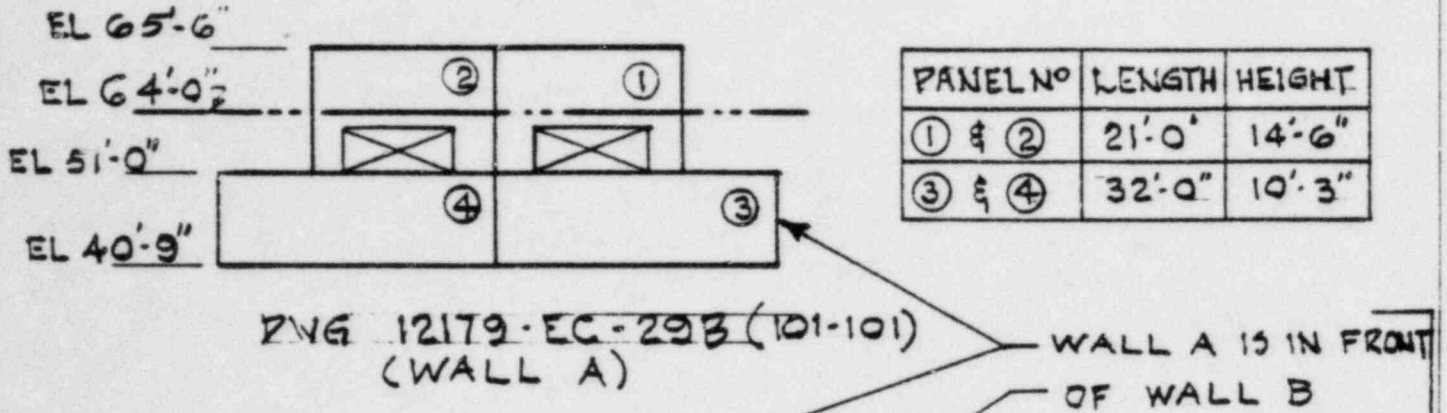
PANEL NO	LENGTH	HEIGHT
①	15'-0"	24'-6"

C.W. PUMP HOUSE ~ END WALL

DWG 12179-EC-14 H

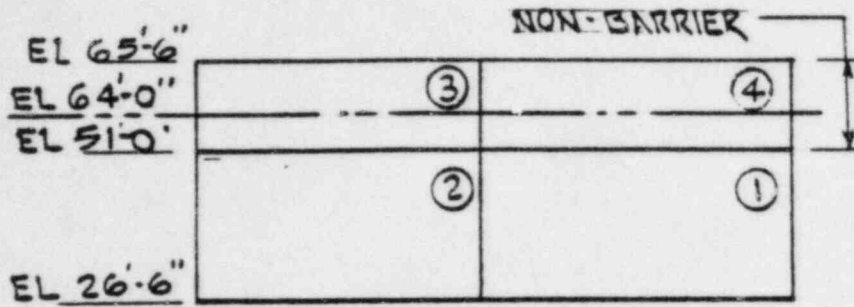
JO 12179

CHECKED		TITLE NUSCO MILLSTONE #3 TORNADO MISSILE BARRIER PANEL SIZES OF CAT I STRUCT	SCALE: NONE
CORRECT			DATE: JUNE 26, 84
APPROVED			SKETCH NUMBER
REVISIONS			PG 3
②	③	④	⑤



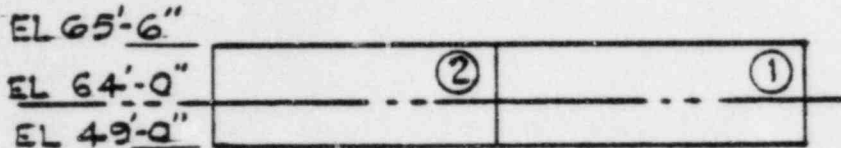
JO 12179

CHECKED		TITLE NUSCO MILLSTONE #3 TORNADO MISSILE BARRIER PANEL SIZES OF CAT I STRUCT.	SCALE: NONE		
CORRECT			DATE: JUNE 26, 84		
APPROVED			SKETCH NUMBER		
REVISIONS	②		③	④	⑤



PANEL NO	LENGTH	HEIGHT
① & ②	32'-2"	24'-6"
③ & ④	32'-2"	14'-6"

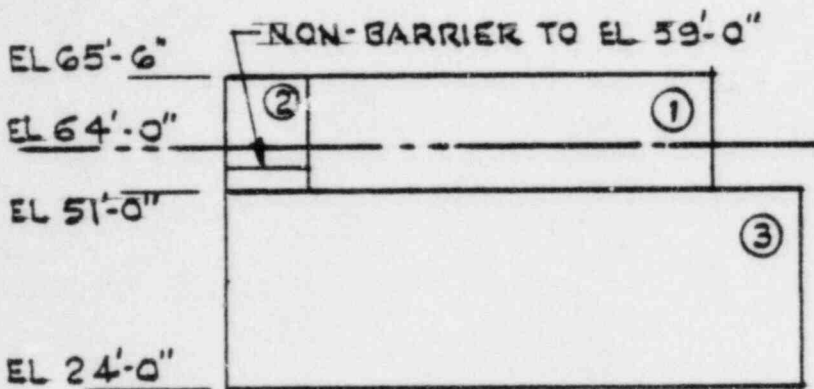
DWG 12179-EC-29F (13-13)



PANEL NO	LENGTH	HEIGHT
① & ②	32'-2"	16'-6"

EMER. GEN. ENCL ~ WEST WALL

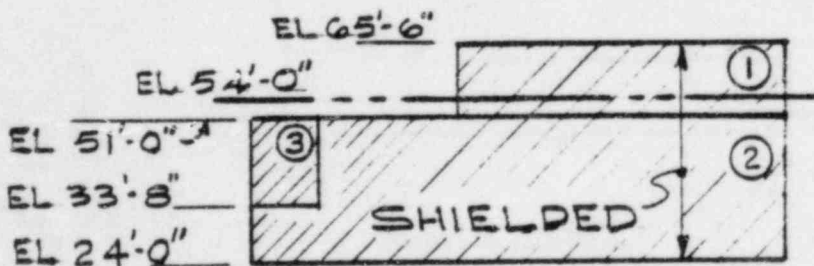
DWG 12179-EC-29K (107-107)



PANEL NO	LENGTH	HEIGHT
①	53'-0"	14'-6"
②	NON-BARRIER	
③	71'-6"	27'-0"

EMER. GEN. ENCL ~ NORTH WALL

DWG 12179-EC-29E (9-9)



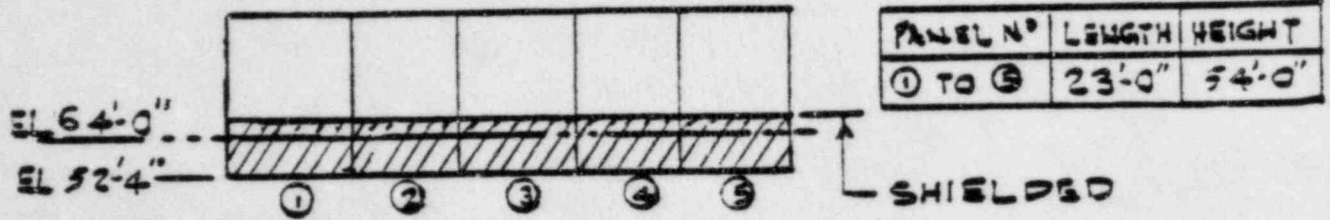
PANEL NO	LENGTH	HEIGHT
①	59'-6"	14'-6"
②	97'-0"	27'-0"
③	6'-0"	17'-4"

EMER. GEN. ENCL ~ SOUTH WALL

DWG 12179-EC-29G (14-14)

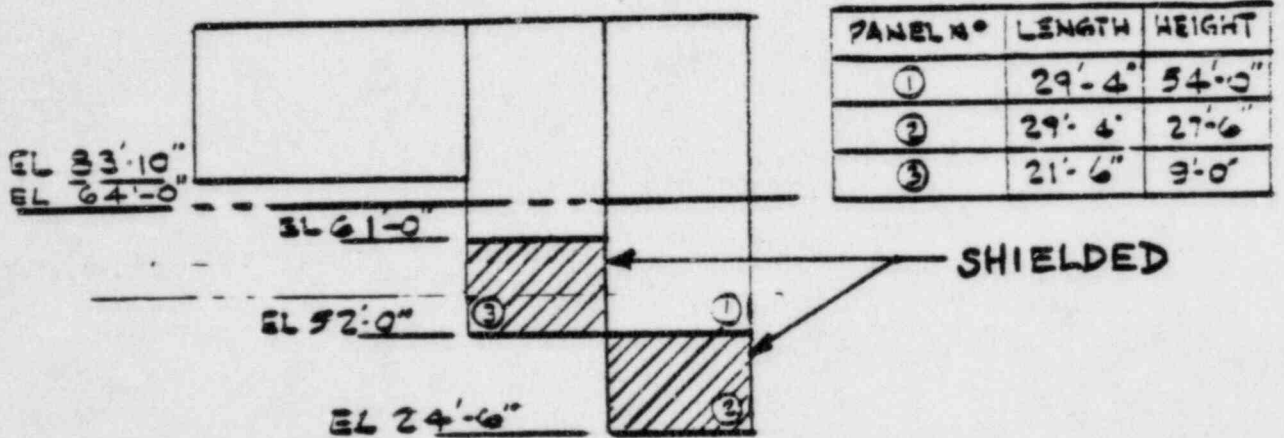
J012179

CHECKED		TITLE NUSCO MILLSTONE #3 TORNADO MISSILE BARRIER PANEL SIZES OF CAT I STRUCT	SCALE: NONE
CORRECT			DATE: JUNE 26, 84
APPROVED			SKETCH NUMBER
REVISIONS			PG 5
②	③		④



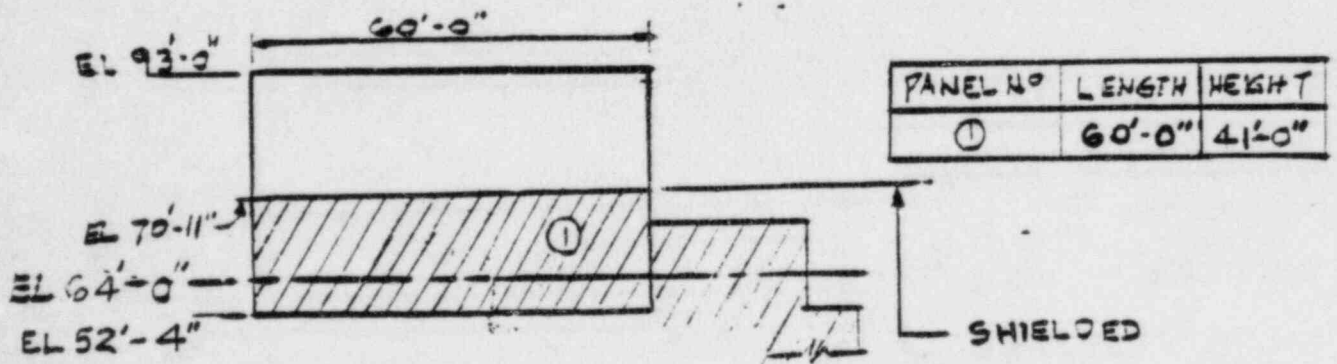
PANEL N°	LENGTH	HEIGHT
① TO ⑤	23'-0"	54'-0"

FUEL BLOG - 50.6 LINE WALL
DWG 12179-EC-38K F P



PANEL N°	LENGTH	HEIGHT
①	29'-4"	54'-0"
②	29'-4"	27'-6"
③	21'-6"	3'-0"

FUEL BLOG - 51.2 LINE WALL
DWG 12179-EC-38T

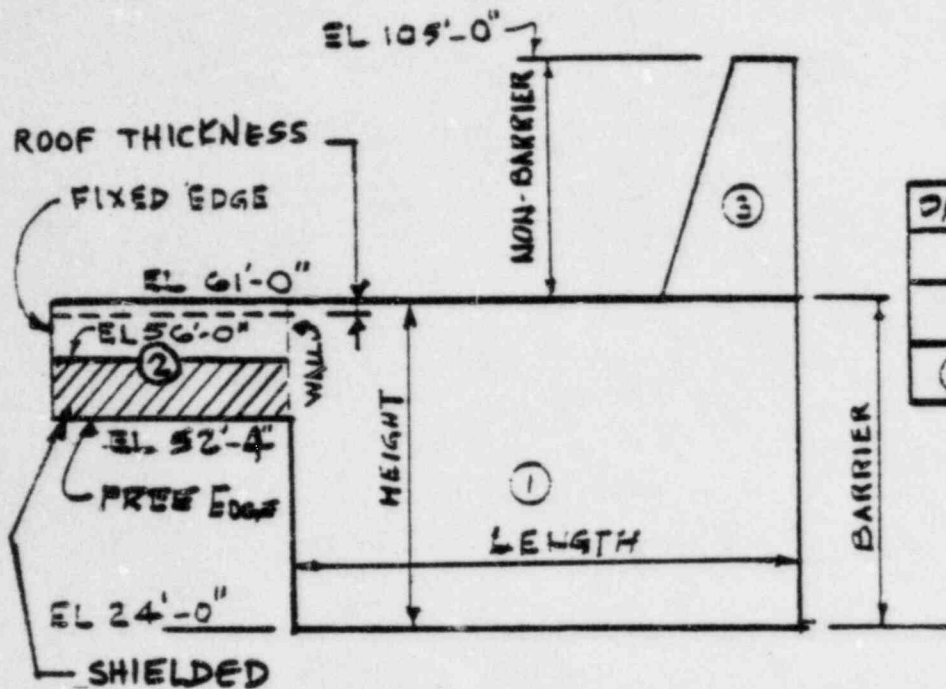


PANEL N°	LENGTH	HEIGHT
①	60'-0"	41'-0"

FUEL BLOG - 53.8 LINE WALL
DWG 12179-EC-38G

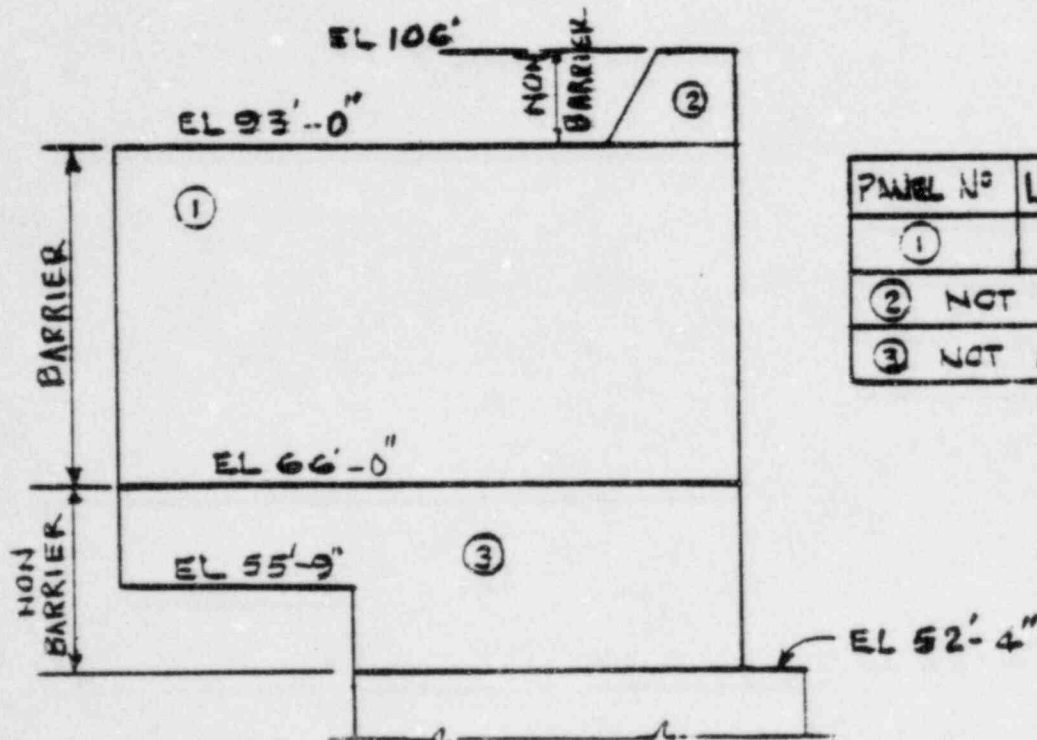
J.O.12179

POWER INDUSTRY GROUP	TITLE NUSCO - MILLSTONE #3	SCALE: NONE
CHECKED	TORNADO MISSILE BARRIER	DATE: JUNE 26, 84
CORRECT	PANEL SIZES OF CAT I STRUCT	SKETCH NUMBER
APPROVED		
REVISIONS ②	③	④



PANEL NO	LENGTH	HEIGHT
①	38'-0"	37'-0"
②	27'-0"	8'-8"
③	NOT A BARRIER	

FUEL BLDG - WALL 6'-6" WEST OF G.6 LINE
DWG 12179-EC-38Q (63-63)

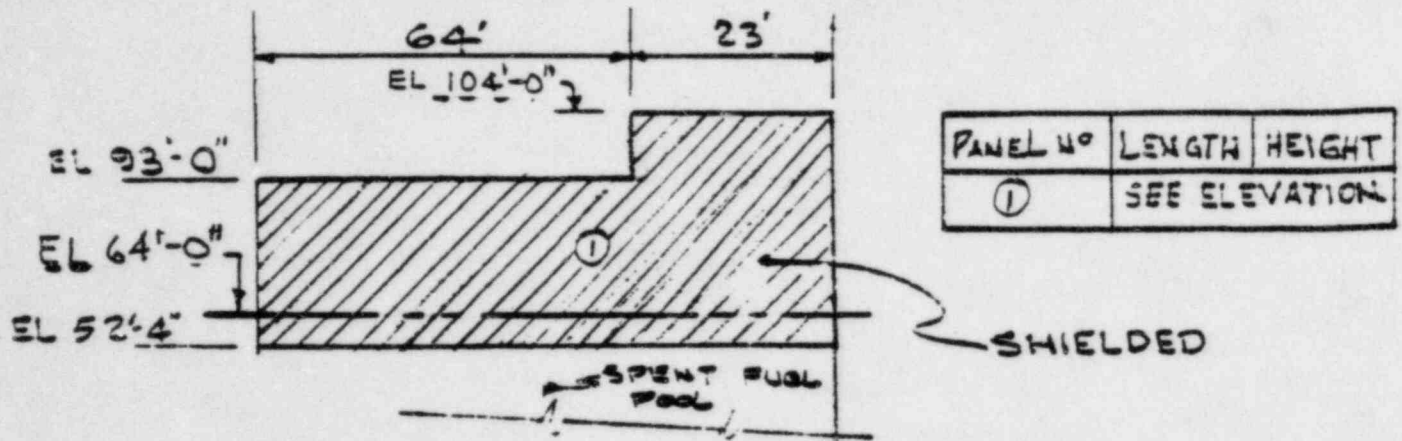


PANEL NO	LENGTH	HEIGHT
①	64'-0"	27'-0"
②	NOT A BARRIER	
③	NOT A BARRIER	

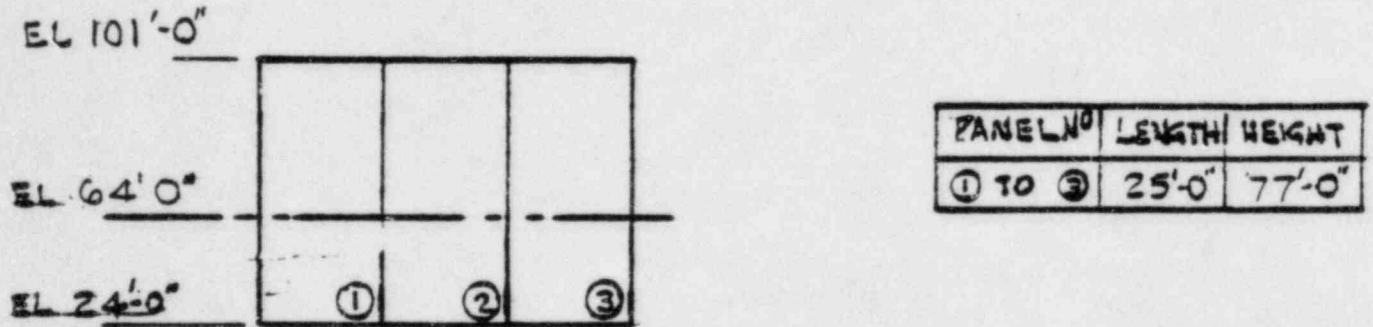
FUEL BLDG - G.5 LINE WALL
DWG 12179-38L (75-75)

JD 12179

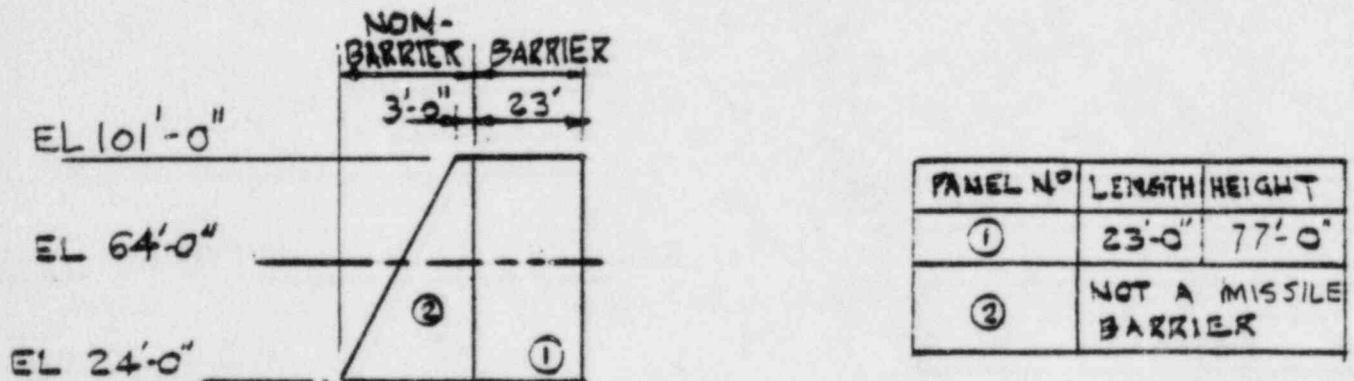
POWER INDUSTRY GROUP	TITLE	SCALE
CHECKED	NUSCO - MILLSTONE #3	SCALE: NONE
CORRECT	TORNADO MISSILE BARRIER	DATE: JUNE 26 84
APPROVED	PANEL SIZES OF CAT I STRUCT.	SKETCH NUMBER
REVISIONS (2)	(3)	(4)
		P: T



FUEL BLDG - G-LINE WALL
DWG 12179-EC-38X (80-80)



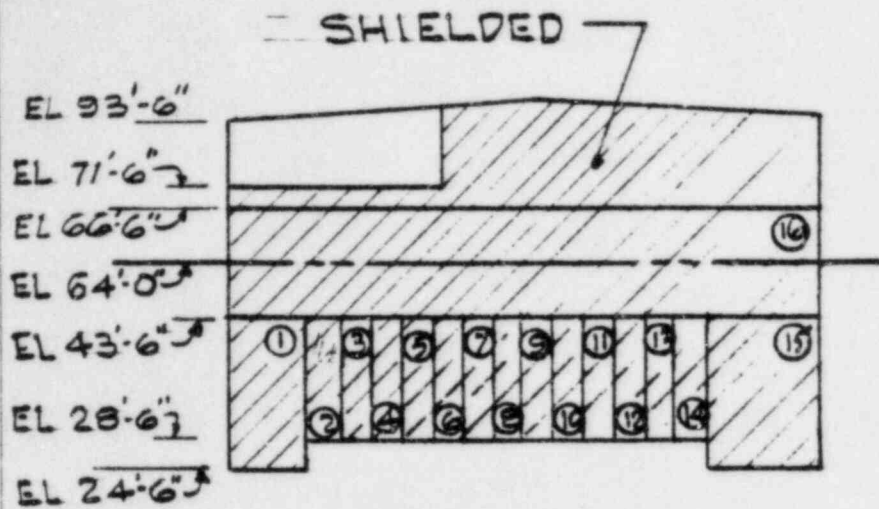
FUEL BLDG CANOPY - SOUTH & NORTH WALLS
DWG 12179-EC-38Z & 38Y



FUEL BLDG CANOPY-EAST WALL
DWG 12179-EC-385 (6-6)

J.O 12179

POWER INDUSTRY GROUP	TITLE	NUSCO - MILLSTONE #3	SCALE	NONE
CHECKED		TORNADO MISSILE BARRIER	DATE	JUNE 26 84
CORRECT		PANEL SIZES OF CAT I STRUCT	SKETCH NUMBER	
APPROVED				
REVISIONS	②	③	④	⑤



PANEL NO	LENGTH	HEIGHT
1	11'-0"	17'-0"
2	6'-6"	15'-0"
3, 8 & 14	6'-0"	15'-0"
4, 5, 6 & 7	7'-0"	15'-0"
9, 10, 11, 12, 13	5'-0"	15'-0"
15	4'-0"	19'-0"
16	129'-6"	23'-0"

AUX BLDG ~ F.9 LINE WALL
 DWG 12179-EC-37B (2-2)

JO 12179

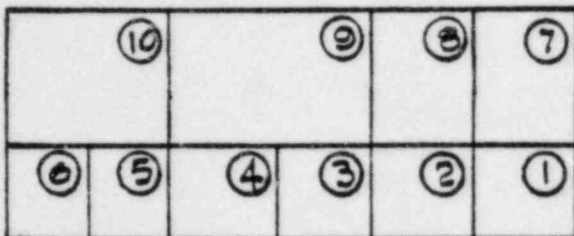
CHECKED		TITLE NUSCO MILLSTONE #3 TORNADO MISSILE BARRIER PANEL SIZES OF CAT I STRUCT	SCALE: NONE
CORRECT			DATE: JUNE 26, 84
APPROVED			SKETCH NUMBER
REVISIONS			7610
②	③	④	⑤

EL 64'-0"

EL 56'-9"

EL 36'-6"

EL 24'-6"



ESF BLDG ~ EAST WALL

DWG 12179-EC-32G (4-4)

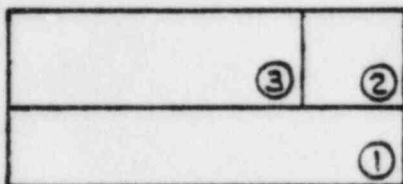
PANEL NO	WIDTH	HEIGHT
① & ②	23'-0"	12'-0"
③	27'-6"	12'-0"
④ & ⑥	21'-0"	12'-0"
⑤	22'-9"	12'-0"
⑦ & ⑧	23'-0"	20'-3"
⑨	48'-6"	20'-3"
⑩	43'-9"	20'-3"

EL 64'-0"

EL 56'-9"

EL 36'-6"

EL 24'-6"



ESF BLDG ~ SOUTH WALL

DWG 12179-EC-32J

PANEL NO	WIDTH	HEIGHT
①	57'-0"	12'-0"
②	11'-0"	20'-3"
③	47'-0"	20'-3"

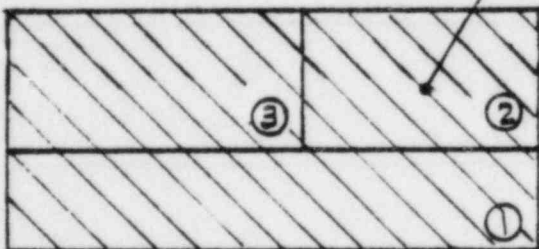
EL 64'-0"

EL 56'-9"

SHIELDED

EL 36'-6"

EL 24'-6"



ESF BLDG ~ NORTH WALL

DWG 12179-EC-32G

PANEL NO	WIDTH	HEIGHT
①	78'-0"	12'-0"
②	38'-0"	20'-3"
③	40'-0"	20'-3"

JD 12179

CHECKED		TITLE NUSCO MILLSTONE #3 TORNADO MISSILE BARRIER PANEL SIZES OF CAT I STRUCT	SCALE: NONE
CORRECT			DATE: JUNE 26, 84
APPROVED			SKETCH NUMBER
REVISIONS			PG 11
②	③	④	⑤

SWECO 7703
EMTR-801
September 1977

APPENDIX C
TIME HISTORY ANALYSIS FOR OVERALL
STRUCTURAL RESPONSE

Stone & Webster Engineering Corporation

TABLE OF CONTENTS

<u>Section</u>	<u>Title</u>	<u>Page</u>	<u>Section</u>	<u>Title</u>	<u>Page</u>
C.1	PURPOSE.	C-1	C.3.5	Numerical Solution for Equation of motion . . .	C-4
C.2	SUMMARY.	C-1	C.3.6	Analytical Solution for Equation of Motion . . .	C-5
C.3	SINGLE MASS TIME HISTORY ANALYSIS OF BARRIER STRUCTURAL RESPONSE	C-1	C.3.7	Williamson and Alvy Solution	C-7
C.3.1	General Description. . .	C-1	C.3.8	Comparison of Numerical and Analytical Methods with Williamson and Alvy results . .	C-8
C.3.2	Allowable Barrier Deflection	C-2	C.3.9	Application to Other Missiles	C-9
C.3.3	Barrier Equilibrium Equation and Transformation Factors. . .	C-3	C.4	CONCLUSIONS.	C-9
C.3.4	Missile Force for Load Type 1.	C-4	C.5	REFERENCES	C-10

LIST OF TABLES

<u>Table Number</u>	<u>Title</u>	<u>Table Number</u>	<u>Title</u>
C.3-1	4000 lb Auto V = 59 Meters/Sec - Instantaneous Momentum Transfer Span = 10.0 ft	C.3-5	4000 lb Auto V = 59 Meters/Sec 650 lb Engine 3350 lb Body and Frame Span = 15.0 ft
C.3-2	4000 lb Auto V = 59 Meters/Sec - Instantaneous Momentum Transfer Span = 15.0 ft	C.3-6	4000 lb Auto V = 59 Meters/Sec 650 lb Engine 3350 lb Body and Frame Span = 30.0 ft
C.3-3	4000 lb Auto V = 59 Meters/Sec - Instantaneous Momentum Transfer Span = 30.0 ft	C.3-7	Barrier Deflection and Ductility for Tornado-borne Missiles Plus 360 mph Tornado Wind
C.3-4	4000 lb Auto V = 59 Meters/Sec 650 lb Engine 3350 lb Body and Frame Span = 10.0 ft	C.3-8	Comparison of Barrier Ductility Predicted by Analytical and Numerical Methods with Williamson and Alvy Method

LIST OF FIGURES

<u>Figure Number</u>	<u>Title</u>
C.3-1	Effect of Tensile Membrane Action on Supported Circular Slab

APPENDIX C
TIME HISTORY ANALYSIS
FOR OVERALL STRUCTURAL RESPONSE

C.1 PURPOSE

The purpose of this Appendix is to develop methods for determining overall barrier deflection due to missile impact, static loads, and other dynamic loads acting together in a load combination equation.

C.2 SUMMARY

The deflection of a barrier due to missile impact, static loads and other dynamic loads acting together in a load combination equation is determined by solving the equation of motion for the barrier by two independent methods which give the same results and employ the same assumptions.

The equation of motion for a barrier is solved; a) by numerical integration and, b) in closed analytical form. In both solutions the barrier is represented by an equivalent mass and a nonlinear spring which can describe the barrier force deformation relationship.

The missile is characterized by its mass and striking velocity. In addition, the average impact force between missile and barrier is required.

The missile-barrier contact force acts to decelerate the missile and to accelerate the barrier, and continues to act until a common velocity at the impact point is attained. Thereafter, missile and barrier move together until they come to rest at the maximum barrier deflection.

If the duration of the impact interval (to achieve a common velocity) is very short compared to the time in which the barrier comes to maximum displacement, the impact can be treated on the basis of an instantaneous impulse between missile and barrier, considerably simplifying the analysis. The representation of the missile as an instantaneous impulse is realistic only when the duration of impact is short compared to the time it takes the barrier to come to maximum displacement. Otherwise, the instantaneous impulse method is too conservative and a square wave of force versus time is used to transfer the missile momentum to the barrier.

The permissible ductility ratio, μ , limiting barrier deflection for bending,

compression, and shear, is defined as the ratio of the maximum acceptable displacement x_m to the displacement at the effective yield point x_y in bending.

Where barriers are required to carry other loads or where there is only one barrier provided to stop a missile and protect against secondary missiles, the maximum allowable ductility is 10 or less depending on how shear and compression influence the flexural response of the barrier.

Where reinforced concrete barriers are not required to carry other loads and where a second barrier such as a wall or floor is located between the primary barrier and the missile protected area, the primary barrier may be designed to act in tension, similar to a mechanical pipe whip restraint. In this case, the maximum barrier deflection is based on half of the ultimate uniform strain in the rebar. This limit for reinforced concrete barriers acting in tension is the same as the limit for pipe whip restraints.

C.3 SINGLE MASS TIME HISTORY ANALYSIS OF BARRIER STRUCTURAL RESPONSE**C.3.1 General Description**

Structural response to missile impact is calculated here using a single equivalent mass and a nonlinear (elasto-plastic) spring to model the dynamic response characteristics of the barrier. The single equivalent mass in the equation of motion for the barrier is the sum of the barrier equivalent mass plus any missile mass in contact with the barrier, traveling at the same velocity as the barrier. When the impulse is short compared with the duration of the barrier response, the barrier mass, not the barrier structural resistance to deformation, stops the missile. In this case, structural response is based upon an initial impulse of zero duration described below. This produces the same structural response as obtained by Williamson and Alvy⁽²⁾, Eq. (14).

On the other hand, when the impulse of the missile acting on the barrier is not short enough to be treated as instantaneous, the interaction between missile and barrier is

represented by means of a constant force acting for a finite time. The magnitude of that force is determined by the crushing resistance of the missile or the penetration resistance of the barrier, whichever governs. The force remains constant until either the missile and barrier have reached the same velocity or the barrier has come to rest. In the former case, the combined system - missile with barrier - continues to deflect until brought to rest by the barrier's resistance to deformation. Depending on the parameters of the system, the final deflection obtained for an interaction of finite duration may be considerably smaller than when the entire momentum transfer is assumed to take place instantaneously, as is illustrated later.

The analytical and numerical methods presented here do take into account four types of static and dynamic loadings, as required by the load combination equation in the SAR.

- Load Type 1: static loads (static pressure differential or weight of a horizontal barrier)
- Load Type 2: dynamic suddenly applied constant load (fluid jet, or dynamic pressure differential)
- Load Type 3: square wave impulse of finite duration (force of penetration or crushing missile)
- Load Type 4: initial impulse of essentially zero duration (i.e., very much shorter than the duration of the barrier structural response)

The mass of the missile which applies its load to the barrier via a square wave, Load Type 3, is M_s . The mass of the missile associated with an instantaneous transfer of momentum, Load Type 4, is M_m .

The physical mechanism of the missile-barrier interaction is as follows: The impact force decelerates the missile and accelerates the barrier. The deflection of the barrier is aided by any static and dynamic forces normal to its surface and by any initial impulse; the barrier deflection is opposed by the barrier's structural resistance, initially elastic and finally plastic, represented by a bilinear resistance-deflection relation. The constant plastic resistance is determined by yield-line theory, taking no credit for any catenary or curvature influence. The missile and barrier continue to move under the action of the various forces, usually until both have achieved a common velocity. After that, the missile and barrier are assumed to form a single degree of freedom system

having kinetic energy which is dissipated in producing further deflection. A somewhat different physical process can sometimes occur when the plastic structural resistance is larger than the constant missile contact force. In that case, the barrier may come to rest before the missile and the barrier reach a common velocity.

C.3.2 Allowable Barrier Deflection

Where only one barrier is placed between a missile source and a missile protected zone or where a barrier is required to carry other loads, the maximum barrier deflection is expressed in terms of a ductility ratio, $\mu = X_m/X_y$. The maximum allowable ductility ratios for different loading conditions are specified by the NRC⁽¹⁾.

The maximum allowable ductility ratio of 10 or less, specified by the NRC, can be a small fraction of the deflection capacity of a barrier. The limit of 10 is based on tests of simply supported beams such as those reported by Gaston, Siess, and Newmark⁽²⁾.

Simply supported two-way slabs, end restrained two-way slabs, and end restrained beams all have considerably more deflection capacity to failure than do simply supported beams. This is because the reinforcing bars act in catenary tension after the flexural hinge capacity is exhausted. For two-way slabs, there is an additional resisting force due to the formation of compression rings in the barrier about the point of applied load. Anderson, Hansen, Murphy, Newmark and White⁽³⁾ described the additional capacity of these barriers in design of blast resistant structures. Section 4-7 of Anderson et al.⁽³⁾ states:

The Catenary Effect. The yield line theory gives only a partial explanation of the behavior of a plate or slab supported on more than two opposite sides and loaded laterally. In addition to the bending action that has been discussed, there is a complex membrane action as well.

In the case of a square plate with four-side support, the bulging at the center tends to pull opposite sides of the plate toward each other. This effect is strongest for a central strip and does not exist for a strip adjacent to a supported edge. As a consequence, the middle area of the plate is in tension and the outer parts in compression. This has two effects: a) the membrane action supplies some load carrying capacity, and b) the tension and compression fields alter the plastic hinge moments to be used in the yield line theory. It should be noted that the membrane action, just mentioned, is not confined to two-way slabs. A similar effect will be encountered in one-way slabs and beams the ends of which are so anchored as to prevent movement toward

each other during flexure. In this case, the lengthening of the member as it deflects gives rise to tension which carries a part of the applied load, thus increasing the load capacity of the member, especially at large deflections."

Wood⁽¹⁾ describes membrane tension in two-way slabs. Figure C.3-1 taken from Wood⁽¹⁾ shows that two-way slabs have considerably increased force capacity and deflection capacity above that determined using bending yield line analysis and a ductility of 10 based on simply supported beams.

The tension mechanism described above for two-way slabs and beams anchored at their ends is used in barrier design when:

1. There is a second barrier between the primary barrier acting in tension and the missile protected area. The second barrier is designed to stop scabbing particles from the primary barrier,
2. the primary barrier is not required to carry other loads,
3. the missile geometry is such that it cannot slip between the rebar pattern, and
4. the rebar is continuous in the barrier and fully developed in the barrier support.

The maximum deflection of reinforced concrete barriers acting in tension is determined by the maximum allowable strain in the rebar. For barriers acting in tension, meeting the conditions (1.) through (4.) above, the maximum allowable rebar strain is half of the ultimate uniform strain of the rebar. This is analogous to the maximum strain permitted by the NRC⁽¹¹⁾ for mechanical pipe whip restr. lnts.

C.3.J Barrier Equilibrium Equation and Transformation Factors

The basic equation of motion of the barrier is

$$M_e a = F_e - R_e \quad (C.3-1)$$

where

$M_e = M_{be} + M_1$: Prior to the missile and barrier reaching a common velocity, M_e equals barrier equivalent mass M_{be} , plus the mass, M_1 , associated with the initial impact of zero duration, Load Type 4. Thereafter,

$M_e = M_{be} + M_1 + M_2$: After missile and barrier reach a common velocity, M_e equals the sum of the barrier equivalent mass M_{be} plus the missile mass from Load Types 3 and 4.

- a = barrier acceleration
- F_e = sum of static and dynamic forces or equivalent forces causing changes of motion
- R_e = equivalent barrier resistance to deformation

Prior to missile mass M_1 and barrier reaching a common velocity, F_e equals

$$F_e = F_{e1} + F_{e2} + F_{e3}$$

where F_{e1} , F_{e2} and F_{e3} are equivalent forces for load types one, two, and three in Section C.3.1. After missile mass M_1 and barrier reach a common velocity, F_e equals

$$F_e = F_{e1} + F_{e4}$$

Load Type 4 from Section C.3.1 is a very high force from a hard missile or component which is on the barrier for a very short interval of time. This force causes the barrier equivalent mass, M_{be} plus the missile mass M_1 , to have an initial velocity before loads F_{e1} or F_{e4} cause any motion. This velocity is

$$V_0 = I_4 / (M_{be} + M_1)$$

Load Type 4 is not applied to the barrier explicitly. Rather, the barrier is given an initial velocity which results from the impulse I_4 of load F_{e4} . The impulse is applied to the combined mass of the barrier and the missile M_1 , since they are assumed to travel together after impact.

Load Type 1 is a static load which causes the barrier to have an initial displacement before loads F_{e1} and F_{e4} cause any motion. This displacement is

$$X_0 = F_{e1} X_y / R_{ey}$$

where X_y and R_{ey} are the displacement and resisting force of the barrier at its effective yield point.

In order to know when the missile force F_{e1} terminates, it is necessary to monitor the velocity of the missile mass M_1 . This is done as follows

$$V_1 = (I_1 - \sum F_{e1} dt) / M_1$$

When the missile velocity V_1 decreases to the velocity of the barrier, the mass M_1 no longer pushes on the barrier with force F_{e1} . From this time on, the barrier and missile M_1 are assumed to travel together until the barrier stops. I_1 is the original momentum of missile mass M_1 .

Although the barrier deflection pattern takes on different configurations in the elastic and plastic stages, the values used for the mass and load transformation factors, K_e and K_p , are determined for the plastic configuration since the barrier deflection is predominantly in the plastic range. The barrier equivalent mass M_{be} is determined from

$$F_e = K_e F \quad (C.3-2)$$

where

M_0 = total mass in barrier yield mechanism

K_m = mass transformation factor so that the model and prototype barriers have the same kinetic energy and same displacement

$$K_m = \sum a_0 \cdot dA / M_0 \quad (C.3-3)$$

where

a_0 = mass per unit area of barrier
 d = normalized displacement of barrier

dA = increment of barrier area

The equivalent forces acting on the barrier from the missile, other dynamic loads and static loads are determined as follows

$$F_e = K_e F \quad (C.3-4)$$

where

K_e = load transformation factor determined so that the model and prototype forces do the same work on the barrier assuming same displacements for model and prototype barriers.

$$K_e = \sum f \cdot dA / F \quad (C.3-5)$$

where

f = force per unit area of barrier mechanism

F = total force on barrier

A different equivalent force is determined for each load acting on the barrier.

The barrier equivalent resisting force R_e is determined from

$$R_e = R \quad (C.3-6)$$

where

R = barrier resisting force for a concentrated load producing a specified displacement

C.3.4 Missile Force for Load Type 2

The missile force for Load Type 2 in Section C.3.1 is determined by one of the following methods:

1. The force for Load Type 2 is equal to the kinetic energy of the missile divided by the distance the missile permanently deforms. This method is used when there is no significant penetration or shear plug

movement compared with missile deformation in actual tests.

2. If actual test data for (1.) above are not available, then the Load Type 2 for constant cross-section missiles is the lesser of missile material yield stress or 50 ksi confined concrete bearing stress times the net cross-sectional area of the missile.
3. If the missile does not maintain a constant cross-section at the point of impact, Load Type 2 is set equal to the peak of a force-crush curve for the missile, where the area under the curve equals the kinetic energy of the missile. If the area under the force-crush curve is less than the kinetic energy of the missile, the momentum corresponding to the balance of the energy is applied as instantaneous impulse, Load Type 2.

C.3.5 Numerical Solution for Equation of Motion

The numerical solution for the barrier equation of motion is performed starting from an instant of time when the displacement and velocity of the barrier and the missile and the forces acting on them are known. The numerical solution of the barrier equation of motion given here is accomplished in a manner similar to Biggs^(*), Chapter 1. The differences are: a) the barrier has an initial velocity from an instantaneous impulse of high force capacity missile components, b) the applied force of the missile remains on the barrier until missile and barrier come to a common velocity; then it is taken off, and c) the mass of the high force capacity missile components M_1 and the mass M_2 of the lower force capacity missile components which penetrate or crush significantly are added to the equivalent mass of the barrier after they attain a common velocity with the barrier.

Equation C.3-1 establishes the acceleration. The velocity and position of the barrier at the end of a time interval dt are

$$V_n = V_{n-1} + a dt \quad (C.3-7)$$

$$X_n = X_{n-1} + V_{n-1} dt + .5 a dt^2 \quad (C.3-8)$$

where

V_n = velocity at end of time interval dt

V_{n-1} = velocity at beginning of time interval dt

X_n = barrier displacement at end of time interval dt

- x = barrier displacement at beginning of time interval dt
- a = barrier acceleration assumed constant during time interval
- dt = time increment for numerical integration of the equations of motion. It is set between 2 and 20 microseconds depending on the time duration of missile force.

The example used for illustration is an automobile weighing 4,000 lb (1,810 kg) which strikes a 2 ft reinforced concrete barrier at 194 fps (59 meters per second), NRC(7). The engine and transmission are assumed to weigh 650 lb and assumed to be a rigid component which applies a concentrated impulse to the barrier of 3.85 kip-sec. The remaining 3,350 lb of body and chassis carry a momentum of 20.15 kip-sec. The crushing resistance of this component is assumed to be 300 kips and to be essentially constant as long as crushing continues.

The assumption of body-chassis crushing strength is based on the results of a test performed by Sandia Laboratories(4). The test consisted in projecting an automobile head-on against a reinforced concrete barrier. The following data describe the test:

- Weight of auto: originally 2,715 lb, modified for test to 3,330 lb
- Impact velocity: 76.3 fps
- Damage to barrier: none
- Damage to automobile: 26 in. crushing

The average crushing resistance of the body and chassis can be determined by calculating their kinetic energy and dividing that energy by the crushing distance. Assuming 16 percent of the original weight to be engine and transmission this calculation gives:

$$26 R/12 = (3.3 - 2.715 \times .16) 76.3^2/64.4$$

$$R = 119.6 \text{ kips}$$

Since the automobile used in the example is heavier than the one tested, the crushing resistance R is greater. Assuming resistance proportional to weight, there results

$$R = 119.6 \times 4000/2715 = 176 \text{ kips}$$

For conservatism, this is increased to 300 kips for the example.

Table C.3-1 through C.3-6 give the results of the numerical solution for 24 in. barriers with spans of 10 ft, 15 ft, and

30 ft. Two different load conditions are considered for each span. They are:

1. 4,000 lb auto body and auto engine considered as applying a zero duration impulse (Load Type 4). This gives identical results to Williamson and Alvy Equation 14.
Impulse: 24 kip-sec.
2. auto body with 20.15 kip-sec momentum considered as applying a square wave impulse with crush force of 300 kips (Load Type 3), and auto engine with 3.85 kip-sec momentum considered as a pure impulse (Load Type 4).

The top half of each table gives the data on missile, barrier, and other loads acting on the barrier. The bottom half presents a summary of the numerical integration of the barrier equation of motion.

Table C.3.7 gives the deflection and ductility of tornado-borne missiles listed in NUREG-75/087, Section 3.5.1.4(7). This table shows that the ductility is less than 10 for all missiles when the barrier is loaded simultaneously with tornado wind.

C.3.6 Analytical Solution for Equation of Motion

This analytical solution is presented to verify the numerical solution in Section C.3.5 and to offer an alternative to a computer program for the single mass time history analysis of barrier deflection.

The analysis predicts the structural response of an elasto-plastic missile barrier to any combination of the four kinds of loads given in Section C.3.1.

Load Types 2 - 4 are specifically treated in the analytical development that follows, and in which the static loading is assumed to be zero. The result is a system of formulas which permit the determination of both the maximum structural deflection x_m and the ductility ratio $\mu = x_m/e$, where e = the elastic limit deflection of the barrier. The duration of the impact phase of the process can also be found if required.

The effect of a simultaneous static loading is determined by means of a correction of the results of the purely dynamic loading analysis, as is discussed later.

Two different situations occur, according to whether the elastic limit is reached before or after the end of the impact phase.

The impact phase ends when the missile and the barrier (at the point of impact) have the same velocity. Following that time the missile and barrier are assumed to remain in contact and to decelerate together until motion ceases. Under some conditions, the barrier comes to rest before the missile does. This happens for high momentum missiles where the force stopping the missile (Load Type 3) is less than the barrier resistance, R.

The final result of the analysis is expressed in terms of ϵ , the ratio of the final deflection to the elastic limit deflection of the barrier.

The following symbols are used:

- ϵ ($= x_y$) = elastic limit deflection of barrier (ft)
- F = constant missile impact force (lbs), Load Type 3
- $F^0 = F + P$
- G = $3RmV/F^0 \sqrt{MR\epsilon} = \tan \gamma$
- I = Initial impulse (lb-sec) = $m_1 V = 3mV$, Load Type 3
- M_{be} = equivalent mass of barrier (slugs) (Eq. C.3-1)
- M = $M_{be} + m$
- m = missile mass associated with force F (=M)
- m_1 = missile mass associated with initial impulse I (=M)
- $m = m_1$ = total impacting mass
- P = suddenly applied constant force of indefinite duration Load Type 2 (Eq. C.3-3)
- Q = equivalent static force, Load Type 1 (Eq. C.3-3)
- R = constant plastic equivalent resistance of barrier (Eq. C.3-5)
- t = time (sec)
- t_1, t_2, \dots = durations of successive stages of response
- V = impact velocity of missile (fps)
- x = deflection of barrier (ft)
- x_1, x_2, \dots = deflection at ends of successive stages
- x_y ($=\epsilon$) = elastic limit deflection
- y = displacement of missile mass m after impact
- \dot{x}, \dot{y}, \dots = $dx/dt, dy/dt, \dots$
- $\mu = m_1/m$
- $\lambda = R/M\epsilon$
- $\gamma = \tan^{-1} G$
- $\epsilon = \text{final deflection}/\epsilon = \text{ductility ratio}$

Case A. ELASTIC LIMIT IS REACHED DURING PENETRATION/CRUSHING STAGE

Stage 1: $0 \leq x \leq \epsilon, \dot{y} > \dot{x}$

Equations of motion are

$$\begin{aligned} \ddot{y} &= -F/m & \ddot{x} &= R/M\epsilon - F^0/M \\ \dot{y} &= V - Ft/m & \dot{x} &= \frac{F^0}{M} t - \frac{R}{M\epsilon} \sin \lambda t \end{aligned}$$

$$\dot{x} = \frac{F^0}{M} \sin \lambda t + \frac{I}{M} \cos \lambda t$$

Find time t_1 when $\dot{x} = \dot{y}$ by setting $\dot{x} = \dot{y}$. Then $\cos (\lambda t_1 + \gamma) = (1-R/F^0) \cos \gamma$

where (C.3-9)

$$\gamma = \tan^{-1} 3RmV/F^0 \sqrt{MR\epsilon} = \tan^{-1} G$$

If $(1-R/F^0) \cos \gamma \leq -1$, the barrier remains elastic.

The condition for Case A to occur is:

$$\sin \lambda t_1 + G \cos \lambda t_1 + \frac{F^0}{F^0} \frac{M}{m} (\lambda t_1) \leq \frac{MG}{MB} \quad (C.3-10)$$

Stage 2: This stage ends when $\dot{y} = \dot{x}$.

Equations of motion (new time origin) are

$$\ddot{y} = -\frac{F}{m} (t_1 + t) \quad \ddot{x} = \frac{F^0 - R}{M}$$

$$\begin{aligned} \dot{x} &= \frac{F^0 \epsilon \lambda}{R} \sin \lambda t_1 + \frac{I}{M} \cos \lambda t_1 \\ &\quad + \frac{F^0 - R}{M} t \end{aligned}$$

$$\begin{aligned} x &= \epsilon + \frac{F^0 \epsilon \lambda}{R} \sin \lambda t_1 + \frac{I \epsilon}{M} \cos \lambda t_1 \\ &\quad + \frac{F^0 - R}{2M} t^2 \end{aligned}$$

Then, equating $\dot{x} = \dot{y}$ find t_2 from

$$\lambda t_2 = \frac{MG/M\epsilon - M\lambda t_1/m - \sin \lambda t_1 - G \cos \lambda t_1}{1 - \sqrt{m/M} - R/F^0} \quad (C.3-11)$$

However, if $R > F^0$ the barrier mass, M may come to rest at time t_1 before $\dot{y} = \dot{x}$. To determine if this happens (only possible if $R > F^0$) calculate t_1' from

$$\lambda t_1' = \frac{\sin \lambda t_1 + G \cos \lambda t_1}{R/F^0 - 1} \quad (C.3-11A)$$

If $t_1' \leq t_1$ or if λt_1 from Eq. C.3-11 is negative, then motion ceases at t_1' .

$$\begin{aligned} \epsilon &= \epsilon + \frac{F^0}{R} (\lambda t_1') \left[\sin \lambda t_1 + G \cos \lambda t_1 \right. \\ &\quad \left. + (1-R/F^0) \frac{t_1'}{\epsilon} \right] \quad (C.3-12A) \end{aligned}$$

However, if $F^0 > R$ or if $\lambda t_1' > t_1$, then Stage 3 follows, in which masses M and m move together until they come to rest at a final barrier deflection x_1 .

During Stage 3 the deceleration is

$$-\ddot{x} = \frac{R-P}{M+m}$$

At the beginning of Stage 3, velocity and deflection are Stage 2 final values

$$\dot{x}_1 = \frac{F^0 \epsilon \lambda}{R} \sin \lambda t_1 + \frac{I}{M} \cos \lambda t_1 + \frac{F^0 - R}{M} t_1$$

$$x = e - \frac{F'e}{R} \cos \lambda t_1 + \frac{Ie}{M} \cos \lambda t_1 + \frac{F-R}{2M} t_1^2$$

The final deflection $x_1 = x_2 + (\dot{x}_1)^2 / 2\ddot{x}_1$, and

$$\begin{aligned} x_1 &= \frac{x}{e} = 1 - \frac{F'}{R} (\lambda t_1) \left[\sin \lambda t_1 + G \cos \lambda t_1 \right. \\ &\quad \left. + \frac{1}{2} \left(1 - \frac{R}{F'} \right) \lambda t_1 \right] + \\ &\quad + \frac{1}{2} \frac{Ie}{M} \left(\frac{F'}{R} \right)^2 \left[\sin \lambda t_1 + G \cos \lambda t_1 \right. \\ &\quad \left. - \left(1 - \frac{R}{F'} \right) \lambda t_1 \right]^2 \end{aligned} \quad (C.3-12)$$

$$\begin{aligned} \text{and } \lambda t_1 &= \frac{1}{\sqrt{2}} \frac{Ie}{M} \left(\frac{F'}{R} \right) \left[\sin \lambda t_1 \right. \\ &\quad \left. + G \cos \lambda t_1 + \left(1 - \frac{R}{F'} \right) \lambda t_1 \right] \end{aligned}$$

Case 3: PENETRATION/CRUSHING STAGE ENDS BEFORE ELASTIC LIMIT IS REACHED

Stage 1: Ends when $\dot{y} = \dot{x}$, $x < e$

Equations of motion are the same as for Stage 1 of Case A.

Stage 1 end at time t_1 when $\dot{y} = \dot{x}$. This time is given by the equation

$$\sin \lambda t_1 + G \cos \lambda t_1 = \frac{F'}{F'} \frac{M}{M} (\lambda t_1) = \frac{MG}{2M} \quad (C.3-13)$$

The condition for Case B to occur is

$$\cos \lambda t_1 - G \sin \lambda t_1 \geq 1 - \frac{R}{F'} \quad (C.3-14)$$

Velocity and deflection at the end of Stage 1 are

$$\begin{aligned} \dot{x}_1 &= \frac{F'e\lambda}{R} \sin \lambda t_1 + \frac{F'}{M} \cos \lambda t_1 \\ x_1 &= \frac{F'e}{R} (1 - \cos \lambda t_1) + \frac{F'}{2M} \lambda \sin \lambda t_1 \end{aligned}$$

Stage 2: Ends when barrier comes to rest. Use work and energy principle. At the end of Stage 1, the strain and kinetic energies are

$Rx_1^2/2e$ and $\frac{M+m}{2} (\dot{x}_1)^2$, respectively. At the end of Stage 2 the strain energy = $R(x_2 - e/2)$, and the kinetic energy = 0. Then

$$Rx_1^2/2e + \frac{M+m}{2} (\dot{x}_1)^2 = R(x_2 - e/2)$$

and then

$$\begin{aligned} x_2 &= \frac{x_1}{e} = \frac{1}{2} \left[1 - \frac{F'}{R} \left[(1 - \cos \lambda t_1) + G \sin \lambda t_1 \right] \right. \\ &\quad \left. + \frac{1}{2} \frac{M+m}{M} \left[\sin \lambda t_1 + G \cos \lambda t_1 \right]^2 \right] \end{aligned} \quad (C.3-15)$$

or, alternatively

$$\begin{aligned} u &= \frac{1}{2} + \left(\frac{F'}{R} \right)^2 \left[1 - \cos \lambda t_1 + \sin \lambda t_1 + G - \frac{1}{2} G^2 \right. \\ &\quad \left. + \frac{M}{2M} (F' - \lambda t_1 + G \cos \lambda t_1)^2 \right] \end{aligned} \quad (C.3-16)$$

The limiting condition for Case B occurs with only an initial impulse $I = m_1 V$ and no force F . Then, since $M = M_{be} + \bar{m}_1$,

$$u = \frac{1}{2} \left(1 + \frac{I^2}{R \bar{m}_1} \right) / \left(1 - \frac{P}{R} \right) \quad (C.3-17)$$

The results that have been presented for dynamic response with no accompanying static loading can be corrected as follows when a static load Q also acts.

A uniformly distributed constant static loading can be represented for the dynamic analysis by means of an equivalent concentrated constant force Q , according to Eq. C.3-3. Since this force is capable of doing work during a structural displacement it contributes to the final deflection of the system. Its importance depends on its magnitude compared to the structural resistance (R) of the barrier.

Allowance for the effect of Q on maximum deflection is made as follows: The force Q alone produces in the barrier an elastic deflection Qe/R which uses up a fraction Q/R of its elastic limit deflection e , leaving what can be called a pseudo-elastic limit deflection e' ($e' = e - Qe/R$). Likewise, the presence of Q reduces the remaining available plastic resistance from the value R to $R - Q = R'$, where R' can be termed the pseudo-plastic resistance.

The dynamic loads can next be applied to the new substitute system characterized by e' and R' instead of the actual e and R . The calculations lead to a value of x_m' (Eq. C.3-12, C.3-12A, C.3-15, or C.3-16 as the case may be) which is the final deflection of the system beyond or in addition to the starting deflection e' caused by Q . Finally, the actual maximum deflection of the barrier relative to its unstrained configuration is

$$x_m = x_m' + e'$$

and the ductility ratio is

$$\mu = x_m/e = \frac{x_m'}{e} + \frac{Q}{R}$$

C.3.7 Williamson and Alvy Solution

The Williamson and Alvy⁽³⁾ method of calculating structural response is broken down into, (a) the case with missile penetration and (b) the case with no penetration. This method is used as a basis of comparison by the NRC⁽⁴⁾. The tornado missile which produces the most structural response is the 4,000 lb auto which does not penetrate the barrier.

Therefore, the case of no penetration in Williamson and Alvy is discussed here in detail. Because the penetration of missiles of concern to nuclear power plant design varies so widely for the spectrum of missiles and because the penetration of any given design basis missile is not documented, structural response is not based on penetration. Rather, it is based on the force of the missile on the barrier.

Equation 14 in Williamson and Alvy establishes how much reinforcing steel is needed in a barrier of given thickness for a missile with momentum equal to M_m times V_m . This method of calculating structural response does not necessarily predict structural response for moving objects striking barriers at a nuclear facility.

Equation 14 is derived here in a more direct way than given in Williamson and Alvy (3).

The kinetic energy and momentum of the missile are

$$KE_m = .5 M_m V_m^2$$

$$\text{Momentum} = M_m V_m$$

The velocity of the barrier after impact is determined by assuming that the missile and barrier remain together after impact. By conservation of momentum, the velocity of the barrier and missile moving together after impact is

$$V_{b+m} = V_m M_m / (M_m + M_{be}) \quad (C.3-18)$$

The kinetic energy after impact is

$$KE_{b+m} = .5 M_m^2 V_m^2 / (M_m + M_{be}) \quad (C.3-19)$$

where

- M_m = mass of missile
- V_m = velocity of missile
- M_{be} = equivalent mass of barrier
- V_{b+m} = velocity of missile and barrier traveling together after impact

The kinetic energy of the system after impact is absorbed by structural response. The structural properties are

R = equivalent barrier plastic resisting force

X_y = barrier yield displacement
 X_m = maximum barrier displacement
 μ = ductility defined by X_m/X_y

Equating the energy of structural response to the kinetic energy of the system after impact gives

$$RX_m = .5 RX_y = .5 M_m^2 V_m^2 / (M_m + M_{be}) \quad (C.3-20)$$

$$R^2 = (.5/X) X = .5 M_m^2 V_m^2 / (M_m + M_{be}) \quad (C.3-21)$$

where the barrier stiffness k is defined by

$$X_y = R/k \text{ and } X_m = \mu X_y \quad (C.3-22)$$

The period T of the system is

$$T = 2\pi \left((M_{be} + M_m) / k \right)^{1/2} \quad (C.3-23)$$

The resisting force of the barrier R then becomes

$$R = \frac{2\pi M_m V_m}{T} \left(\frac{1}{2\mu - 1} \right)^{1/2} \quad (C.3-24)$$

Equation C.3-24 is the same as Equation 14 in Williamson and Alvy (3).

Equation C.3-24 produces the same deflection as Load Type 4 for the missile where the momentum of the missile is transferred to the barrier as an initial velocity before the barrier offers any structural response.

C.3.8 Comparison of Numerical and Analytical Methods with Williamson and Alvy Results

The method proposed by Williamson and Alvy for predicting the structural response of a missile barrier to impact by a nonpenetrating missile is based on the assumption that the duration of the impact is very short compared to the time required for the barrier to reach its maximum deflection. The loading is treated as a concentrated impulse. This assumption is too conservative, as is evident from consideration of the data presented in the Table C.3-8.

A missile having a certain finite crushing strength will exert a total force of approximately that amount during the impact interval. The duration of the crushing process is then determined from consideration of the initial momentum. When that crushing or loading interval is not extremely short compared to the total reaction interval, consideration of that fact is necessary. The methods of analysis presented here take account of the fact that the crushing and/or penetrating interval is of finite duration. (Note that all the results presented in Table C.3-8 use the same data given in Tables C.3-1 through C.3-6.)

The reason for conservatism in the Williamson and Alvy method is that it only allows the equivalent of Load Type 4 in Section C.3.1. In this load case, the momentum of the missile is transferred to the barrier before the barrier offers structural resistance.

In Table C.3-8, Load Type A is a zero duration impulse, Load Type 4, which gives results identical to those of Williamson and Alvy. Load B is the combination of an initial rigid mass impulse of 1.35 kip-sec with a square wave impulse of 10.15 kip-sec and force 100 kips, Load Types 1 and

.. It is apparent in Table C.3-8 that for the short span the difference is considerable but that it remains very significant for the longer spans as well.

C.3.9 Application to Other Missiles

The method of determining barrier structural deflection to missile impact loads, static loads, and other dynamic loads required by a load combination equation, given in Sections C.3.1 through C.3.4, has many possible applications for predicting the effects of missiles striking reinforced concrete barriers at nuclear power plants.

An example is a whipping ruptured pipe striking a reinforced concrete barrier.

The whipping pipe motion during impact is considerably more complicated than the head-on impact of an auto or tornado driven pipe striking end-on. A whipping pipe may strike a barrier near the pipe elbow. It may also strike sequentially along a line when a long section of pipe impacts the barrier. In the first case, structural deflection is calculated using a circular yield mechanism around the point where the elbow strikes. In the second case, structural deflection is calculated using a rectangular yield mechanism surrounding the line of impact.

As a whipping pipe strikes a barrier, the metal on the impact side of the pipe exerts a large force to bring it to a sudden stop. Then a lower force is exerted on the barrier as the pipe crushes. If the pipe has sufficient energy, it will not be stopped by the time the back surface of the pipe arrives at the barrier. In this case a second force of large magnitude is exerted on the barrier to stop the rear surface of the pipe.

The momentum of the front surface of the pipe in the impact area is assumed to act like Load Type 4 in Section C.3.1, an instantaneous impulse. The crushing of a pipe is represented by Load Type 3 where the magnitude of the square wave is the maximum force from force deflection crush curves for pipes, from Peech et al.⁽³⁾, needed to absorb the energy of the whipping pipe. The energy of a whipping pipe used to determine the maximum force from crush curves is the total kinetic energy of a whipping pipe less the kinetic energy of the initial impact surface of the pipe, given above as an instantaneous impulse.

If the total crush energy of the elbow, defined by Peech et al.⁽³⁾ is not sufficient to absorb the kinetic energy of the whipping pipe, remaining after the front surface of the pipe has impacted the barrier as an instantaneous impulse, the excess kinetic energy is absorbed as an instantaneous impact, Load Type 4, of the rear side of the pipe impacting the

barrier. The two Type 4 loads representing the front and rear surfaces of the pipe impacting the barrier are applied for simplification and conservatism at the beginning of the impact process.

C.4 CONCLUSIONS

The conclusions to be drawn from this Appendix are:

1. A 2 ft thick reinforced concrete barrier with No. 11 rebar at 10 in., on centers each way and each face, having concrete strength of 3 ksi and rebar yield strength 40 ksi can withstand the impact of the tornado-generated missiles given in NUREG-75/087, Section 3.5.1.4(7) combined with tornado wind. The ductility is less than 10.
2. The methods of analysis formulated in this Appendix can be used to conservatively design barriers for structural response. These methods apply to tornado-generated missiles, whipping pipes, aircraft, dropped equipment, and ruptured components from pressurized and rotating systems and equipment.
3. Structural response is limited to a ductility of 10 or less if the barrier is carrying other loads or if it is the only barrier separating the missile from a missile protected zone.
4. Reinforced concrete barriers are designed to go into the tension resisting mechanism for anchored beam barriers and membrane tension of two-way slab barriers when there is a second barrier downstream of the primary barrier which can stop secondary concrete missiles and when the primary barrier is not required to carry other loads. The maximum barrier tension strain in this case is the same as is permitted for pipe whip restraints, NUREG-75/087, Section 3.6.2.(11)
5. Estimating structural response for barriers at nuclear power facilities using the method for non-penetrating missiles in Williamson and Alvy⁽³⁾ is too conservative. The method presented in this Appendix is used by Stone & Webster.
6. The method of calculating structural response given in this Appendix is the same whether the missile penetrates or not, and does not depend on a

determination of the depth of penetration. Since penetration of missiles of concern to nuclear power plants is not well documented, the method of determining structural response given in this Appendix is used by Stone & Webster instead of the method given in Williamson and Alvy for penetrating missiles.

C.5 REFERENCES

- (1) Wood, R.E., "Plastic and Elastic Design of Slabs and Plates", The Ronald Press Co., New York, N.Y., 1961.
- (2) ASTM-A615-75, "Standard Specification for Deformed and Plain Billet Steel Bars for Concrete Reinforcement."
- (3) Williamson, R.A., and Alvy, R.R., "Impact Effects of Fragments Striking Structural Elements," Holmes & Narver, Inc., Anaheim, California, Revised November 1973.
- (4) Stephenson, A.E., "Tornado Vulnerability Nuclear Production Facilities," Sandia Laboratories, Environmental test Department, April 1975.
- (5) Peech, J.M., Rosner, R.E., Pirotn, S.D., East, G.E. and Goldstein, N.A., "Local Crush Rigidity of Pipes and Elbows", Transactions of the 8th International Conference on Structural Mechanics in Reactor Technology, San Francisco, California, 15-19 August 1977.
- (6) Biggs, J.M., "Introduction to Structural Dynamics", McGraw-Hill Book Company, 1964.
- (7) NUREG-75/087, Section 3.5.1.2, "Missiles Generated by Natural Phenomena", U.S. Nuclear Regulatory Commission.
- (8) NUREG-75/087, Section 3.5.3, "Barrier Design Procedures", U.S. Nuclear Regulatory Commission.
- (9) Gaston, J.R., Siess, C.P., and Newmark, N.M., "An Investigation of the Load-Deformation Characteristics of Reinforced Concrete Beams Up to the Point of Failure", Civil Engineering Studies, Structural Research Series No. 40, University of Illinois, December 1952.
- (10) Anderson, P.E., Hansen, R.J., Murphy, H.L., Newmark, N.M., and White, M.P., "Design of Structures to Resist Nuclear Weapons Effects", ASCE-Manuals of Engineering Practice-No. 42, American Society of Civil Engineers, 1961.
- (11) NUREG-75/087, Section 3.6.2, "Determination of Break Location and Dynamic Effects Associated with the Postulated Rupture of Piping," U.S. Nuclear Regulatory Commission.

TABLE C.3-1
 4,000 LB AUTO V-59 METERS/SEC ** INSTANTANEOUS MOMENTUM TRANSFER SPAN = 10.0 FT

DATA ON MISSILE, BARRIER, AND LOAD COMBINATION EQUATION

BARRIER YIELD MECHANISM SPAN = 10.0 FT ** BARRIER THICKNESS = 24.0 "
 P = 0.007632 = AS/10*01 = STEEL RATIO ** DEPTH TO CENTROID OF TENSION STEEL = 20.44 "
 FC = 3.0 KSI ** FY = 40. KSI ** YIELD LINE FORCE = 12.6-MP

0.0 KIPS EQUIVALENT STATIC FORCE ** LOAD 3
 0.0 KIPS EQUIVALENT CONSTANT DYNAMIC FORCE ** LOAD 2

0.0 KIP-SEC MISSILE IMPULSE RESISTED BY FORCE AT BARRIER SUPPORT PLUS BARRIER INERTIA DURING MOMENTUM TRANSFER ** LOAD 3
 24.000 KIP-SEC MISSILE IMPULSE RESISTED ONLY BY BARRIER INERTIA DURING MOMENTUM TRANSFER ** LOAD 4
 97.5 FPS BARRIER INITIAL VELOCITY DUE TO LOAD 4

BARRIER EQUIVALENT WEIGHT	MISSILE WEIGHT LOAD 3	MISSILE WEIGHT LOAD 4	BARRIER PLASTIC FORCE	BARRIER YIELD FORCE	BARRIER PERIOD
KIPS	KIPS	KIPS	KIPS	FT	SEC
3.927	0.000	4.000	1402.2	0.0116	0.0003

RESULTS OF TIME HISTORY ANALYSIS FOR MISSILE IMPACT WITH OTHER LOADS

TIME HISTORY ORDER	DURATION OF LOAD 3	SEC	MISSILE FORCE LOAD 3	KIPS	FORCE AT TIME OF MAX BARRIER SUPPORT DEFLECTION	KIPS	MAXIMUM BARRIER DEFLECTION	FT	MAXIMUM BARRIER VELOCITY	FT/SEC	FINAL BARRIER RESISTING MECHANISM
1	0.0	0.0	1402.2	0.016250	0.7900	60.42	97.49				

TABLE C.3-2

4,000 LB AUTO V-59 METERS/SEC**INSTANTANEOUS MOMENTUM TRANSFER SPAN = 15.0 FT

DATA ON MISSILE, BARRIER, AND LOAD COMBINATION EQUATION

BARRIER YIELD MECHANISM SPAN = 15.0 FT ** BARRIER THICKNESS = 24.0 "
 P = 0.007632 = AS/(B*D) = STEEL RATIO ** DEPTH TO CENTROID OF TENSION STEEL = 20.44 "
 FC = 3.0 KSI ** FY = 40. KSI ** YIELD LINE FORCE = 12.4*MP

0.0 KIPS EQUIVALENT STATIC FORCE ** LOAD 1
 0.0 KIPS EQUIVALENT CONSTANT DYNAMIC FORCE ** LOAD 2
 0.0 KIP-SEC MISSILE IMPULSE RESISTED BY FORCE AT BARRIER SUPPORT PLUS BARRIER INERTIA DURING MOMENTUM TRANSFER ** LOAD 3
 24.000 KIP-SEC MISSILE IMPULSE RESISTED ONLY BY BARRIER INERTIA DURING MOMENTUM TRANSFER ** LOAD 4
 60.2 FPS BARRIER INITIAL VELOCITY DUE TO LOAD 4

BARRIER EQUIVALENT HEIGHT	MISSILE HEIGHT LOAD 3	MISSILE HEIGHT LOAD 4	BARRIER PLASTIC FORCE	BARRIER EFFEC. YIELD DEFLECTION	BARRIER PERIOD
KIPS	KIPS	KIPS	KIPS	FT	SEC
0.035	0.000	4.000	1482.2	0.0262	0.0130

RESULTS OF TIME HISTORY ANALYSIS FOR MISSILE IMPACT WITH OTHER LOADS

1 TIME HISTORY NUMBER	2 DURATION OF LOAD 3 SEC	3 MISSILE FORCE LOAD 3 KIPS	4 FORCE AT BARRIER SUPPORT KIPS	5 TIME OF MAX BARRIER DEFLECTION SEC	6 MAXIMUM BARRIER DEFLECTION FT	7 MAXIMUM BARRIER DUCTILITY	8 MAXIMUM BARRIER VELOCITY FT/SEC	9 FINAL BARRIER RESISTING MECHANISM
1	0.0	0.0	1482.2	0.0000	0.5013	17.36	60.21	MEMBRANE TENSION

TABLE C.3-3

4,000 LB AUTO V-59 METERS/SEC**INSTANTANEOUS MOMENTUM TRANSFER SPAN 30.0 FT

DATA ON MISSILE, BARRIER, AND LOAD COMBINATION EQUATION

BARRIER YIELD MECHANISM SPAN = 30.0 FT ** BARRIER THICKNESS = 24.0 "
 P = 0.007632 = AS/IB²D_v = STEEL RATIO ** DEPTH TO CENTROID OF TENSION STEEL = 20.44 "
 FC = 3.0 KSI ** FV = 40. K% ** YIELD LINE FORCE = 12.6*MP

0.0 KIPS EQUIVALENT STATIC FORCE ** LOAD 1
 0.6 KIPS EQUIVALENT CONSTANT DYNAMIC FORCE ** LOAD 2
 0.0 KIP-SEC MISSILE IMPULSE RESISTED BY FORCE AT BARRIER SUPPORT PLUS BARRIER INERTIA DURING MOMENTUM TRANSFER ** LOAD 3
 24.000 KIP-SEC MISSILE IMPULSE RESISTED ONLY BY BARRIER INERTIA DURING MOMENTUM TRANSFER ** LOAD 4
 19.4 FPS BARRIER INITIAL VELOCITY DUE TO LOAD 4

BARRIER EQUIVALENT HEIGHT	MISSILE HEIGHT LOAD 3	MISSILE HEIGHT LOAD 4	BARRIER PLASTIC FORCE	BARRIER EFFEC. YIELD DEFLECTION	BARRIER PERIOD
KIPS	KIPS	KIPS	KIPS	FT	SEC
35.342	0.000	4.000	1402.2	0.1047	0.0553

RESULTS OF TIME HISTORY ANALYSIS FOR MISSILE IMPACT WITH OTHER LOADS

1 TIME HISTORY INTRDER	2 DURATION OF LOAD 3 SEC	3 MISSILE FORCE LOAD 3 KIPS	4 FORCE AT BARRIER SUPPORT KIPS	5 TIME OF MAX BARRIER DEFLECTION SEC	6 MAXIMUM BARRIER DEFLECTION FT	7 MAXIMUM BARRIER DUCTILITY	8 MAXIMUM BARRIER VELOCITY FT/SEC	9 FINAL BARRIER RESISTING MECHANISM
1	0.0	0.0	1402.2	0.010938	0.2115	2.02	19.44	BENDING YIELD LINE

TABLE C.3-4

4,000 LB AUTO V-59 METERS/SEC** 650 LB ENGINE - 3,350 LB BODY AND FRAME SPAN = 10.0 FT

DATA ON MISSILE, BARRIER, AND LOAD COMBINATION EQUATION

BARRIER YIELD MECHANISM SPAN = 10.0 FT ** BARRIER THICKNESS = 24.0 "
 P = 0.007632 = AS/(B*D) = STEEL RATIO ** DEPTH TO CENTROID OF TENSION STEEL = 20.44 "
 FC = 3.0 KSI ** FY = 40. KSI ** YIELD LINE FORCE = 12.6*MP

0.0 KIPS EQUIVALENT STATIC FORCE ** LOAD 1
 0.0 KIPS EQUIVALENT CONSTANT DYNAMIC FORCE ** LOAD 2
 20.150 KIP-SEC MISSILE IMPULSE RESISTED BY FORCE AT BARRIER SUPPORT PLUS BARRIER INERTIA DURING MOMENTUM TRANSFER ** LOAD 3
 3.850 KIP-SEC MISSILE IMPULSE RESISTED ONLY BY BARRIER INERTIA DURING MOMENTUM TRANSFER ** LOAD 4
 27.1 FPS BARRIER INITIAL VELOCITY DUE TO LOAD 4

BARRIER EQUIVALENT HEIGHT	MISSILE WEIGHT LOAD 3	MISSILE WEIGHT LOAD 4	BARRIER PLASTIC FORCE	BARRIER EFFEC. YIELD DEFLECTION	BARRIER PERIOD
KIPS	KIPS	KIPS	KIPS	FT	SEC
3.927	3.350	0.650	1402.2	0.0116	0.0061

RESULTS OF TIME HISTORY ANALYSIS FOR MISSILE IMPACT WITH OTHER LOADS

1 TIME HISTORY INRDER	2 DURATION OF LOAD 3 SEC	3 MISSILE FORCE LOAD 3 KIPS	4 FORCE AT BARRIER SUPPORT KIPS	5 TIME OF MAX BARRIER DEFLECTION SEC	6 MAXIMUM BARRIER DEFLECTION FT	7 MAXIMUM BARRIER DISTORTION	8 MAXIMUM BARRIER VELOCITY FT/SEC	9 FINAL BARRIER RESISTING MECHANISM
1	0.003520	300.0	1402.2	0.003520	0.0517	4.45	27.20	BENDING YIELD LINE

TABLE C.3-5
 4,000 LB AUTO V=59 METERS/SEC+ 650 LB ENGINE - 3,350 LB BODY AND FRAME SPAN = 15.0 FT

DATA ON MISSILE, BARRIER, AND LOAD COMBINATION EQUATION

BARRIER YIELD MECHANISM SPAN = 15.0 FT BARRIER THICKNESS = 24.6 "
 P = 0.007632 = AS/(B*H) = STEEL RATIO DEPTH TO CENTROID OF TENSION STEEL = 20.44 "
 FC = 3.0 KSI FY = 40. KSI YIELD LINE FORCE = 12.5*W*P

0.0 KIPS EQUIVALENT STATIC FORCE LOAD 3
 0.0 KIPS EQUIVALENT CONSTANT DYNAMIC FORCE LOAD 2
 20.150 KIP-SEC MISSILE IMPULSE RESISTED BY FORCE AT BARRIER SUPPORT PLUS BARRIER INERTIA DURING MOMENTUM TRANSFER LOAD 3
 3.850 KIP-SEC MISSILE IMPULSE RESISTED ONLY BY BARRIER INERTIA DURING MOMENTUM TRANSFER LOAD 4
 13.1 FPS BARRIER INITIAL VELOCITY DUE TO LOAD 4

BARRIER EQUIVALENT HEIGHT	MISSILE WEIGHT LOAD 3	MISSILE WEIGHT LOAD 4	BARRIER PLASTIC FORCE	BARRIER EFFEC. YIELD DEFLECTION	BARRIER PERIOD
KIPS	KIPS	KIPS	KIPS	FT	SEC
0.035	3.350	0.650	1402.2	0.0262	0.0130

RESULTS OF TIME HISTORY ANALYSIS FOR MISSILE IMPACT WITH OTHER LOADS

1	2	3	4	5	6	7	8	9
TIME HISTORY NUMBER	DURATION OF LOAD 3	MISSILE FORCE LOAD 3	FORCE AT BARRIER SUPPORT	TIME OF MAX BARRIER DEFLECTION	MAXIMUM BARRIER DEFLECTION	MAXIMUM BARRIER VELOCITY	MAXIMUM BARRIER VELOCITY	FINAL BARRIER RESTING MECHANISM
	SEC	KIPS	KIPS	SEC	FT	FT/SEC	FT/SEC	
1	0.004540	300.0	1402.2	0.004540	0.0370	1.45	13.20	BENDING YIELD LINE

TABLE C.3-6
 4,000 LB AUTO V=59 MP/TERS/SEC 650 LB ENGINE - 3,350 LB BODY AND FRAME SPAN = 30.0 FT

DATA ON MISSILE, BARRIER, AND LOAD COMBINATION EQUATION

BARRIER YIELD MECHANISM SPAN = 30.0 FT BARRIER THICKNESS = 24.6 "
 P = 0.007632 = AS/(B*D) = STEEL RATIO DEPIN TO CENTROID OF TENSION STEEL = 20.44 "
 FC = 3.0 KSI FY = 40. KSI YIELD LINE FORCE = 12.6MP

0.0 KIPS EQUIVALENT STATIC FORCE LOAD 1
 0.0 KIPS EQUIVALENT CONSTANT DYNAMIC FORCE LOAD 2

20.150 KIP-SEC MISSILE IMPULSE RESISTED BY FORCE AT BARRIER SUPPORT PLUS BARRIER INERTIA DURING MOMENTUM TRANSFER LOAD 3
 3.050 KIP-SEC MISSILE IMPULSE RESISTED ONLY BY BARRIER INERTIA DURING MOMENTUM TRANSFER LOAD 4
 3.4 FPS BARRIER INITIAL VELOCITY DUE TO LOAD 4

BARRIER EQUIVALENT HEIGHT	MISSILE WEIGHT LOAD 3	MISSILE WEIGHT LOAD 4	BARRIER PLASTIC FORCE	BARRIER YIELD DEFLECTION	BARRIER PERIOD
KIPS	KIPS	KIPS	KIPS	FT	SEC
35.342	3.350	0.650	1402.2	0.1047	0.0553

RESULTS OF TIME HISTORY ANALYSIS FOR MISSILE IMPACT WITH OTHER LOADS

TIME HISTORY NUMBER	DURATION OF LOAD 3	MISSILE FORCE LOAD 3	FORCE AT BARRIER SUPPORT	TIME OF MAX BARRIER DEFLECTION	MAXIMUM BARRIER DEFLECTION	MAXIMUM BARRIER DUCTILITY	MAXIMUM BARRIER VELOCITY	FINAL BARRIER RESISTING MECHANISM
1	0.019330	309.0	027.7	0.019330	0.0505	0.56	4.19	ELASTIC

TABLE C.3-7

BARRIER DEFLECTION AND DUCTILITY FOR
TORNADO-BORNE MISSILES PLUS 360 MPH TORNADO WIND*

<u>Missile</u>	<u>Velocity (meters per second)</u>	<u>Momentum kip-sec</u>	<u>Barrier Span (ft)</u>	<u>Barrier Deflection (ft)</u>	<u>Barrier Ductility</u>
114.6 lb wood plank	83	0.97	10	0.0038	0.33
114.6 lb wood plank	83	0.97	30	0.0121	0.12
286.6 lb 6 in. Sch 40 pipe	52	1.52	10	0.0034	0.30
286.6 lb 6 in. Sch 40 pipe	52	1.52	30	0.0162	0.16
8.8 lb 1 in. steel rod	51	0.05	10	0.0004	0.04
8.8 lb 1 in. steel rod	51	0.05	30	0.0048	0.05
1124.4 lb utility pole	55	6.30	10	0.0114	0.98
1124.4 lb utility pole	55	6.30	30	0.0523	0.50
749.6 lb 12 in. Sch 40 pipe	47	3.59	10	0.0125	1.08
749.6 lb 12 in. Sch 40 pipe	47	3.59	30	0.0327	0.31
4000.0 lb auto	59	24.00	10	0.0520	4.47
4000.0 lb auto	59	24.00	30	0.0629	0.60

* Barrier data: 2 ft concrete $f'_c = 3$ ksi No. 11 rebar Grade 40 10 in. on center each way and each face

TABLE C.3-8

COMPARISON OF BARRIER DUCTILITY RATIOS PREDICTED BY ANALYTICAL
AND NUMERICAL METHODS WITH WILLIAMSON AND ALVY METHOD

Missile: Auto: weight = 1810 kg, velocity = 59 mps

Barrier: 24 in. concrete No. 11 rebar at 10 in. on center each way and each face

<u>Line No.</u>	<u>Span (ft)</u>	<u>Missile Load Type</u>	<u>Analytical Method</u>	<u>Numerical Method</u>	<u>Williamson & Alvy Method</u>
1	10	A*	68.42	68.42	68.42
2	10	B**	4.56	4.45	N.A.
3	15	A	19.14	19.14	19.14
4	15	B	1.47	1.45	N.A.
5	30	A	2.02	2.02	2.02
6	30	B	0.56	0.56	N.A.

*A 24 kip-sec initial impulse for auto body and engine

**B 3.85 kip-sec initial impulse for engine and 20.15 kip-sec square wave for auto body with 300 kip crush strength

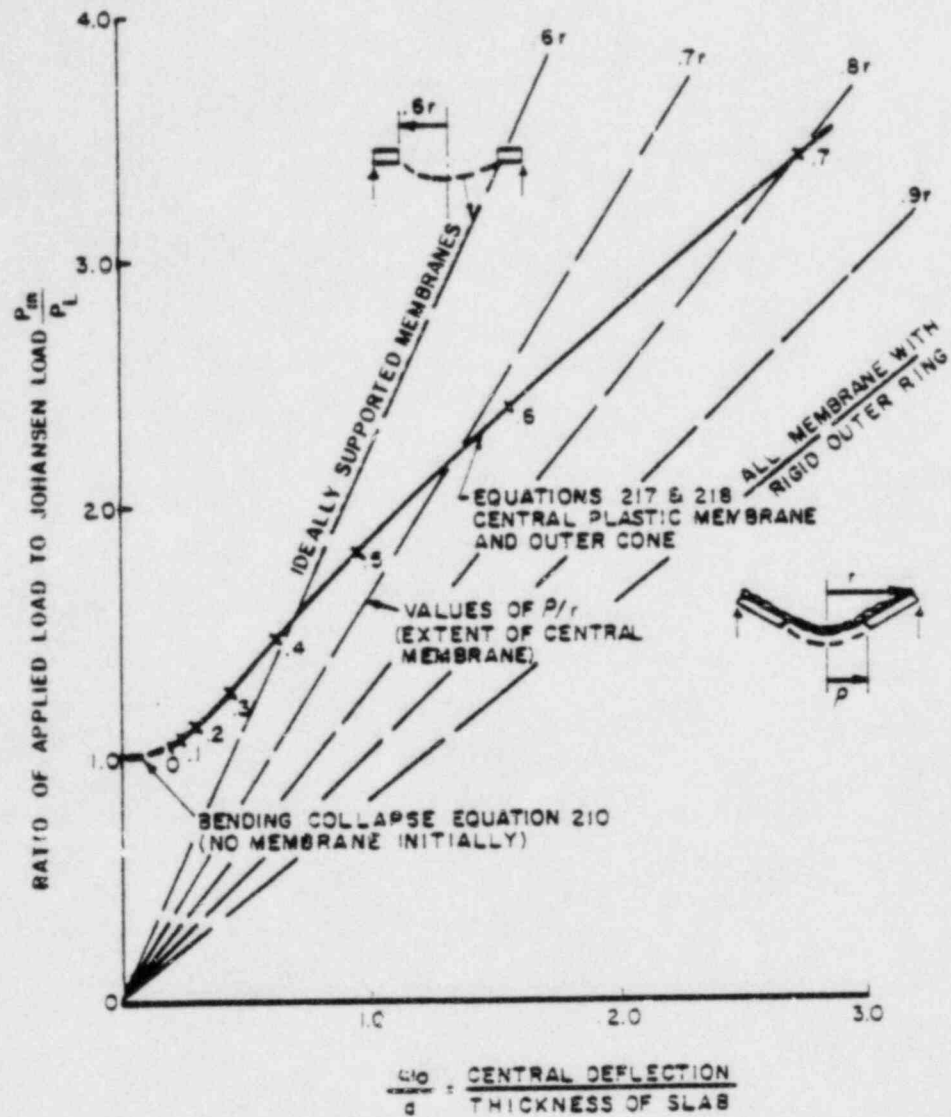


FIGURE C.3-1

EFFECT OF TENSILE MEMBRANE ACTION ON SUPPORTED CIRCULAR SLAB

(From Fig. 96a in Wood⁽¹⁾)

Structural Audit Item 15 - Containment Failure Mode (Item IV from June 14 meeting with NRC)

Item A: The applicant will provide reference for the use of 160 psi shear value for containment concrete.

Response: Copies of reference papers listed below are enclosed.

References

- 9) The Shear Strength of Reinforced Concrete Members. (By the joint ASCE-ACI Task Committee 426 on Shear and Diagonal Tension), Journal of Structural Division, ASCE, June 1973. pp. 1091-1185.
- 10) White, R.N. and Holley, M.J., Jr. Experimental Studies of Membrane Shear Transfer Journal of the Structural Division, ASCE, August 1972, pp. 1835-1852.
- 11) Hofbeck, J.A., Ibrahim, I.O., and Mattock, A.H. Shear Transfer in Reinforced Concrete. ACI Journal, February 1969, pp. 114-128.

Item B: The applicant will make the headings to Tables 2-4, 2-6, and 2-7 consistent (mean or median of normal distribution).

Response: The headings in Tables 2-4, 2-5, 2-6, and 2-7 have been changed to make them consistent with each other and assumed to be normally distributed. The revised tables are attached with this response.

Item C: The applicant has presently defined the median containment overpressure at which the leak criteria is exceeded. The applicant will also provide the lower bound pressure at which the leak criteria is exceeded.

Response: The lower bound pressure exceeding the leak criteria is 114 psig in Zone II where most of the piping penetrations and access hatches are located. (Refer to Table 15-2 attached with previous response to Item 15)

Item D: The critical pressure for the buckling analysis for the equipment hatch door appears high. The applicant will review the analysis and provide comment.

Response: The Failure Mode Analysis made by W. J. Woolley and Co. for Equipment hatch and personnel airlock has been reviewed and summarized below. The revised Table 5-2 is attached with this response.

Summary of the review of the analysis by W. J. Woolley & Co.:

Buckling pressures for the equipment hatch and personnel air lock in the analysis by Woolley & Co. is based on classical shell theory and experimental results by Hunag referred to in the September 1964 issue of Journal of Applied Mechanics. This analysis gives an upper bound for the buckling pressure.

This analysis has been reviewed using the NASA SP-8032 document "Buckling of Thin-Walled Doubly Curved Shells," which accounts for uncertainties between theory and experiments and for differences between assumed and actual boundary conditions. This gives a lower bound for buckling pressure. In the Containment Failure Mode Analysis Report, the lower bound of the buckling pressure is shown in Table 5-2.

Item E: A table similar to Table 8-2 will be provided varying only the corresponding material properties for indication of the first yield of the liner.

Response: A new Table 8-3 of Mean Failure pressures varying only material properties for indication of the first-yield of liner is attached with this response.

TABLE 2-4

REINFORCEMENT STEEL MATERIAL STRENGTH

Rebar Type	Yield Strength (psi)			Tensile Strength (psi)		
	Min. Spec. Strength*	Mean Test Strength**	Standard Deviation	Min. Spec. Strength	Mean Test Strength	Standard Deviation
#18, GR-50	50,000	56,504	2,159	70,000	89,396	3,576
#14, GR-50	50,000	58,948	2,943	70,000	93,897	4,882
#4-8, GR-40	40,000	50,900	5,635	70,000	81,692	10,048
#9-11, GR-40	40,000	49,619	5,390	70,000	83,250	7,130

*Used in original design

**Used in this study



TABLE 2-5

CADWELD SPLICE STRENGTH RESULTS

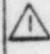
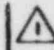
<u>Type of Break</u>	<u>Min. Spec Strength (psi)</u>	<u>Mean Test Strength (psi)</u>	 <u>Standard Deviation (psi)</u>
Bar	62,500	89,179	2,990
Sleeve	62,500	85,619	3,988
Pull out	62,500	85,573	5,436

TABLE 2-6

CONCRETE COMPRESSIVE STRENGTH EVALUATION


<u>Structure</u>	<u>Specified Strength (psi)*</u>	<u>Mean Test Strength (psi)</u>	 <u>Aging Factor</u>	<u>Actual Strength (psi)**</u>	<u>Standard Deviation</u>
Containment-Mat	3,000	4,437	1.15	5,102	249
Containment-Wall	3,000	4,381	1.14	4,994	354
Containment-Dome	3,000	4,674	1.16	5,442	415

*Used in original design

**Used in this study

TABLE 2-7

STEEL LINER MATERIAL STRENGTH

<u>Property</u>	<u>Specified Value (psi)*</u>	<u>Mean Value (psi)**</u>		<u>Standard Deviation (psi)</u>
Cylinder Plates (SA 537 Class 2)				
Yield Strength	60,000	78,582		5,559
Tensile Strength	80,000	90,812		4,893
Dome Plates (SA 537 Class 1)				
Yield Strength	50,000	57,093		5,363
Tensile Strength	70,000	78,453		3,845

NOTE:

1/4 in. liner material (containment mat) is made of same material as cylinder plates.

*Used in original design

**Used in this study


TABLE 5-2

FAILURE MODES AND PRESSURES OF EQUIPMENT HATCH ASSEMBLY
AND PERSONNEL AIR LOCK

<u>Failure Mode</u>	<u>Failure Pressure (psig)</u>
Equipment Hatch Assembly	
Bending stress intensity in spherical cap reaches ultimate stress	170
Buckling of hatch	163
Weld failure at junction of hatch barrel and cylinder liner	>194
Manway failure	230
Personnel Air Lock	
Bending stress in spherical cap reaches ultimate stress	>194
Buckling of hatch	302
Unseating of O-ring	153

NOTE:

> Means actual value exceeds value given.

TABLE 8-3 

MEAN FAILURE PRESSURES AND TOTAL VARIATIONS

Zone	Mean Failure Pressure (psig)	Material Coefficient of Variation (β)	Standard Deviation (psig)	Mean Failure Pressure (psig)	
				+One Standard Deviation	-One Standard Deviation
I @ C ₁	140	0.0525	±7.35	147.0	133.0
II @ C ₂	128	0.0465	±5.95	134.0	122.0
III @ C ₄	132	0.0622	±8.21	140.0	124.0
IV @ C ₅	≥145	0.0622	±9.01	154.0	136.0
Containment Mat					
Section B ₁	155	0.0491	±7.61	163.0	147.0
Section B ₃	140	0.0493	±6.90	147.0	133.0
Piping Penetrations					
Main Steam	128	0.0707	±9.04	137.0	119.0
Feedwater	131	0.0707	±9.26	140.0	122.0

NF = axial force due to prestressing;
 p, r, s, t = constant parameters;
 U = subscript denoting upper bound;
 X, XA, XB, XC, XD = variables;
 Y = configuration variable;
 z = objective function;
 α, γ = constant parameters;
 δ = coefficient equalling +1 or -1; and
 σ = stress

JOURNAL OF THE STRUCTURAL DIVISION

THE SHEAR STRENGTH OF REINFORCED CONCRETE MEMBERS

By the Joint ASCE-ACI Task Committee 426 on Shear and Diagonal
Tension of the Committee on Masonry and Reinforced Concrete
of the Structural Division

CHAPTER 1

1.1 Introduction

In the design of concrete structures an adequate margin of safety must be provided against any mode of failure that might occur under the forces that act upon the structure during its lifetime. One general type of failure that must be prevented is the so-called "shear failure," which in reality is a failure under combined shearing force and bending moment, plus, occasionally, axial load, or torsion, or both. Such failures reduce the strength of structural elements below the flexural capacity and considerably reduce the ductility of the elements. Especially for the latter reason, shear failures are generally considered undesirable.

The understanding and knowledge of the shear transfer mechanisms in various types of concrete structural elements has progressed significantly since the previous report issued by this Committee (7). This advance has occurred in three ways: though greater understanding of the fundamental mechanisms of shear transfer, better quantitative evaluation of the shear strength of structures, and the study of new types of structures or loading conditions.

This report reviews recent research results and design proposals in an attempt to establish the current state-of-the-art in our knowledge of shear transfer in reinforced concrete structures. Although specific design recommendations are not presented, it is hoped that this report will help

Note.—Discussion open until November 1, 1973. To extend the closing date one month, a written request must be filed with the Editor of Technical Publications, ASCE. This paper is part of the copyrighted Journal of the Structural Division, Proceedings of the American Society of Civil Engineers, Vol. 99, No. ST6, June, 1973. Manuscript was submitted for review for possible publication on February 12, 1973.

designers, researchers, and specification writers to arrive at simple, universally applicable design concepts. Despite the tremendous number of references on this subject, the question of shear strength is far from being settled. In some instances the explanations of behavior and the design concepts that are presented are somewhat speculative and may change as more information becomes available.

Throughout the report an attempt is made to compare the shear transfer mechanisms in various types of members. The different modes of shear failure are listed in this chapter but will be discussed more fully in subsequent chapters. The strength of concrete under combined loadings is discussed briefly in Chapter 2, followed by a review of the fundamental methods of shear transfer commonly found in various structural members. Use will be made of this information in subsequent chapters.

Considering the importance of the shear problem in beams, Chapter 3 analyzes the nature of the shear strength of beams, the factors affecting strength, and the design of beams to prevent shear failures.

Chapter 4 deals with special types of members such as deep beams, brackets, walls, etc. A future continuation of this report will consider the shear strength of slabs.

Although this report covers the subject extensively, some peripheral material such as the historical background presented in the previous report

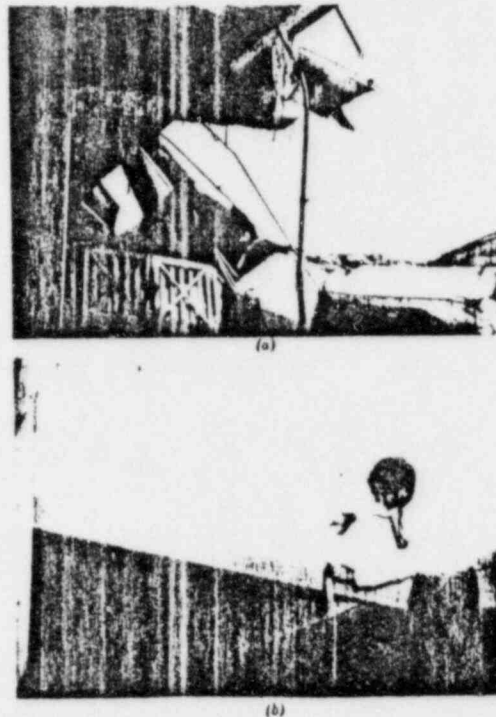
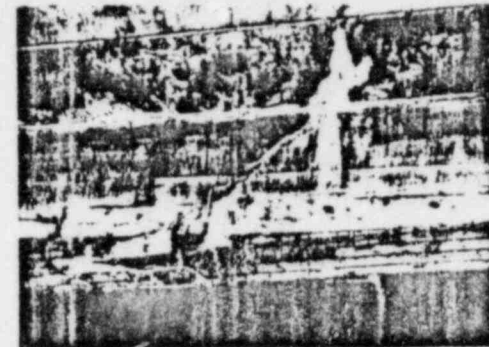


FIG. 1.1.—Shear Failure and Inclined Cracks in Continuous Roof Beams

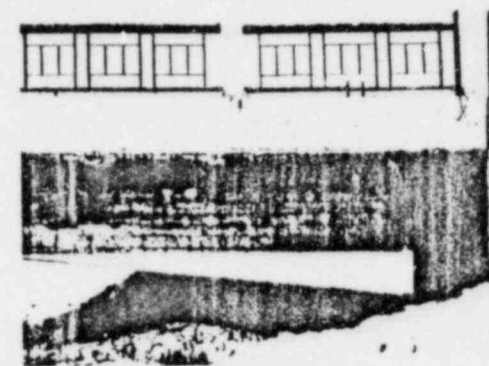
of the Shear Committee (7) and in other papers (24,88) is not repeated herein. In addition, the interaction of shear and torsional effects is not considered. Design recommendations for this type of loading are given in Ref. 6, 41, and 114, and also in the reports of ACI Committee 438, "Torsion."

1.2 Shear Failures and Shear Distress in Structural Members

Shear distress and failures have been reported in beams, columns, walls, slabs, brackets, and other members. In general, each type of



(a)



(b)

FIG. 1.2.—Inclined Cracks in T-Beam Highway Bridge

member exhibits different modes of cracking and failure, although the mechanisms by which shear is transferred within the member may be similar. For a beam subjected to a concentrated load, the major variable affecting the mode of failure is probably the ratio of the distance, a , from the load to the support to the depth of the member, d . As shown in Section 3.1, this ratio can also be expressed in terms of M/Vd . The latter form can be used to describe a wider variety of loading conditions, and therefore is frequently used in design recommendations. The relative magnitude of the flexural stresses, shear stresses, and vertical compress-

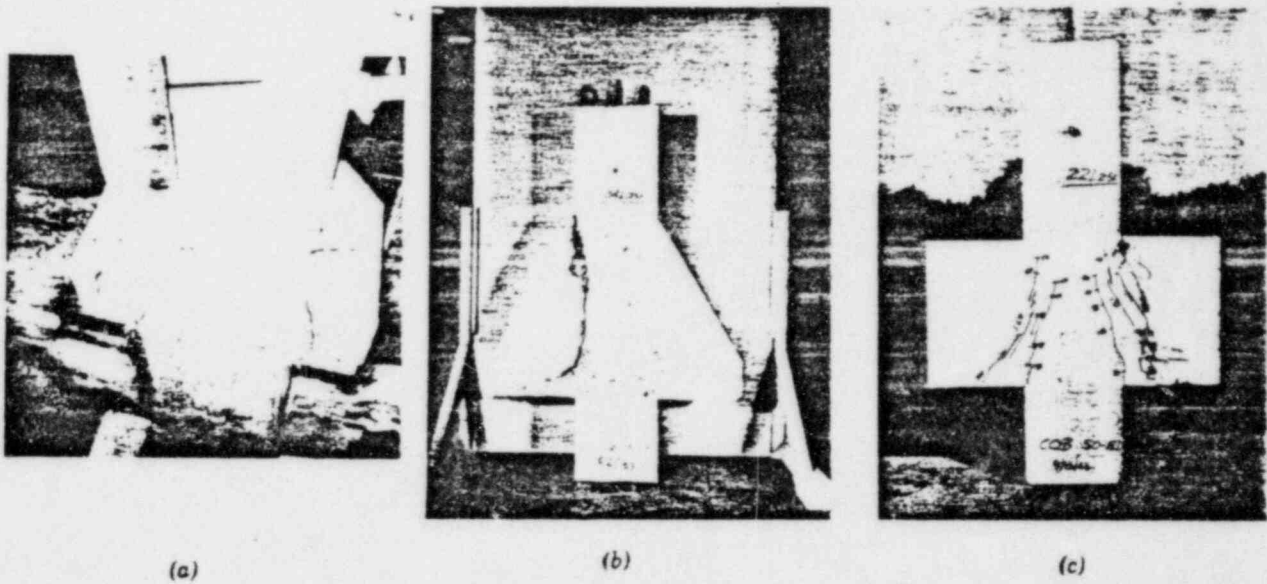


FIG. 1.3.—Shear Failures in Corbels: (a) Precast Building; (b) Laboratory Test; (c) Laboratory Test (Photos Courtesy of Portland Cement Association)

tion stresses varies, causing changes in behavior, as the M/Vd ratio is varied.

(a) Beams

Reinforced concrete and prestressed concrete beams of moderate slenderness (a/d or $M/Vd = 2-6$) develop inclined cracks due to

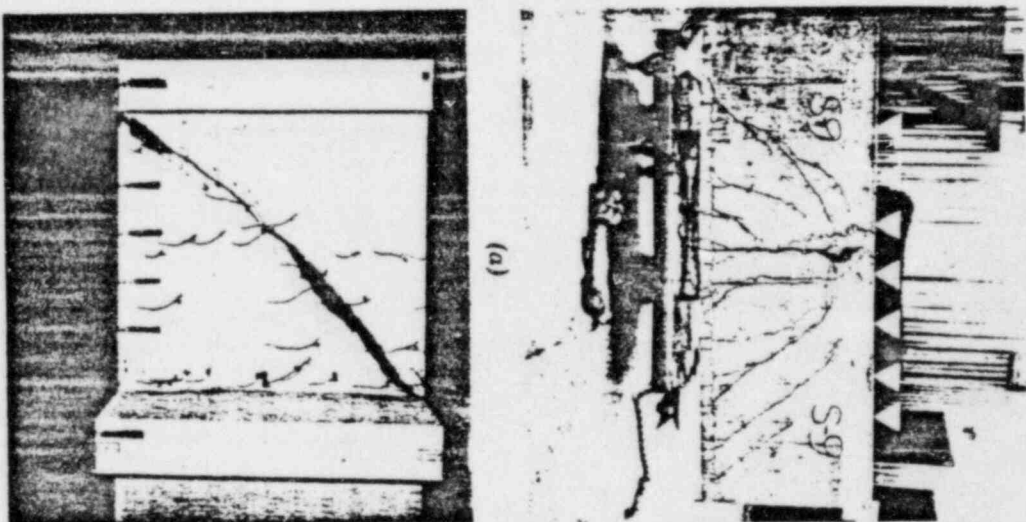


FIG. 1.4.—Shear Failures in Deep Beams

the combination of shear and flexural stresses. As explained in Chapter 3, beams may exhibit a number of different modes of shear failure, the most common of which is the crushing or shearing of

the compression flange over the inclined crack which is often accompanied or initiated by splitting along the tension reinforcement.

Fig. 1.1(a) shows a shear failure in a continuous roof beam supporting precast roof panels. This failure, in an Air Materiel Warehouse, led to a revision in the shear provisions in the 1956 ACI Building Code and subsequently to considerable research into shear strength. An inclined crack in a beam and slab roof is shown in Fig. 1.1(b).

Fig. 1.2 shows inclined cracks in a three-span continuous highway bridge. This bridge has not collapsed although the cracks are wide and deflections and corrosion of the reinforcement have become a problem.

(b) Deep Beams

Shearing failures of deep beams, brackets, and similar members differ considerably from those in normal beams, as shown in Figs. 1.3 and 1.4. This is largely due to the much steeper inclined cracks in deep members. This, in turn, changes the relative importance of the various shear transfer mechanisms as compared to normal beams. The shear strength of deep members is discussed in Chapter 4.

Figure 1.3(a) shows inclined cracks in corbels supporting precast beams in an industrial building. Similar failures in laboratory specimens are shown in Fig. 1.3(b) and (c). Fig. 1.4 shows inclined cracks in laboratory tests of deep beams.

(c) Shear Walls

Depending on their height to width ratio, shear walls represent a special case of beams or deep members. Such members may have significant axial compressions and occasionally axial tensions due to gravity loads and overturning moments. The transverse loads are generally applied to such walls by floor slabs attached to the full width of the wall, and frequently are cyclic in nature.

(d) Columns

Columns may fail in shear in earthquakes. These failures appear to be of two types: either similar to that in an axially loaded beam involving inclined cracking, as shown in Fig. 1.5(a); or complete destruction of the column core apparently prior to inclined cracking, as shown in Fig. 1.5(b). Shear failures in columns are discussed in Section 4.9.

(e) Beam-Column Joints

Inclined cracks may develop within the joints in reinforced concrete structures subjected to unbalanced gravity loads or seismic loads. Fig. 1.6 shows such a crack in a parking garage subjected only to gravity loads. This problem is discussed in Section 4.8.

(f) Construction Joints and Joints in Precast Construction

Frequently shearing forces must be transferred across an interface such as a construction joint in a shear wall, the interface between a beam and a composite slab, or at the supports of precast elements. This action will be referred to as interface shear transfer and will be discussed more fully in Sections 2.2.2 and Chapter 4.

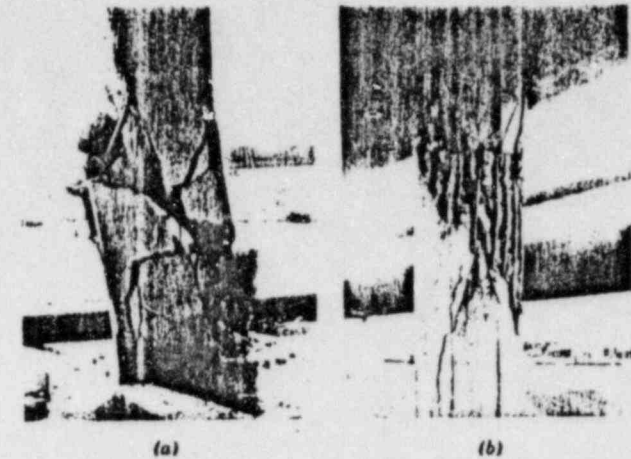


FIG. 1.5.—Shear Failures in Columns in San Fernando Earthquake (Photos Courtesy of National Bureau of Standards)



FIG. 1.6.—Inclined Crack in Beam-Column Joint



FIG. 1.7.—Shear Failures in Slabs: (a) Exterior Column in Building; (b) Exterior Column in Laboratory Test; (c) Interior Column in Laboratory Test (Photos Courtesy of Portland Cement Association)

(g) Slabs and Footings

So-called punching shear failures occur in slabs and footings in the manner shown in Fig. 1.7. The shear capacity decreases as the moment transferred from the column to the slab, or vice versa, increases. Therefore, failures are more likely for exterior column connections, or connections where moment transfer occurs because of either the loading conditions or the location of perforations adjacent to the column. This type of member will be discussed in a future committee report.

1.3 Design for Shear

The last report of the Shear Committee, published in 1962, presented a basic design procedure for reinforced concrete members subjected to shear forces. The recommendations from this report still are the basis for such design in North America and are contained in the 1971 ACI Building Code (6). Two significant changes have occurred during the past decade:

1. The 1962 report dealt primarily with beams and punching shear failures in slabs. Since then, considerable work has been done on shear in deep beams, brackets, walls, etc., and this has led to design equations for such members. The development of these equations will be discussed in later chapters, particularly in Chapter 4.

2. The basic philosophy of the ACI Building Code with respect to shear failures has changed. Stirrup reinforcement restrains growth of inclined cracking, providing increased ductility and a warning in situations in which the sudden formation of inclined cracking in an unreinforced web may lead directly to distress. Such reinforcement may be of great value where members are subjected to unexpected tensile forces, settlements, or catastrophic loadings. For these reasons the 1971 ACI Building Code requires a minimum amount of shear reinforcing in most members.

During the next decade it is hoped that the design regulations for shear strength can be integrated, simplified, and given a physical significance so that designers can approach unusual design problems in a rational manner.

CHAPTER 2

2. Basic Mechanisms of Shear Transfer

2.1 Failure Criteria for Concrete

The various modes of shear failure all involve cracking or crushing of concrete under complex states of stress as, e.g., when diagonal cracking, shear-compression failure, splitting, or web crushing occurs. Several studies in recent years have attempted to use refined concrete failure theories to investigate shear failure mechanisms.

The strength of concrete under combined shear and direct stresses seems to be predicted well by the octahedral stress theory (25). In this regard several investigators have emphasized that the intermediate principal stress is important in failure theories of concrete subjected to complex three-dimensional states of stress (142). In many applications,

however, such as the study of relatively slender beams, it is sufficiently accurate to use simpler theories of failure, and these are generally used in discussions of the shear strength of structures.

The simplest cracking criterion is based on the principal tensile stress or principal tensile strain theories of failure. These approaches have been shown to be useful in predicting tensile failure when applied to certain simple states of stress (46) and have been shown to give reasonable

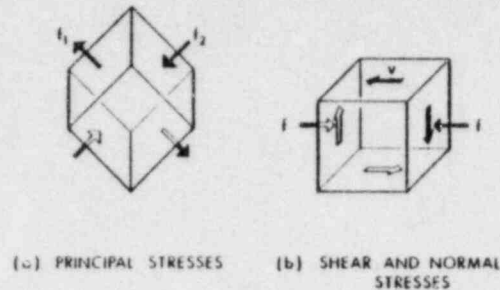


FIG. 2.1.—Biaxial States of Stress

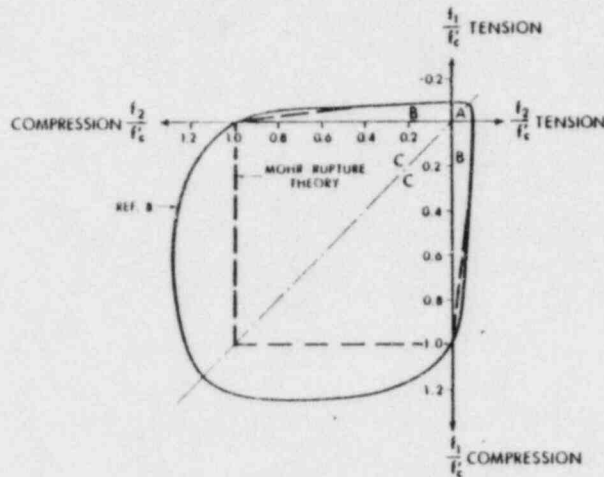


FIG. 2.2.—Biaxial Strength of Concrete

results when applied to the tensile cracking of a beam under combined shear and bending moment (105).

In pure flexure or combined flexure and axial load the limiting compressive strain concept gives reasonable predictions of failure loads. For the computation of plastic hinge relations the value of the limiting strain is sometimes taken to be a function of the M/Vd ratio (44).

Frequently the stresses in a structure can be idealized to a biaxial state of stress with the stress in the third direction equal to zero as

shown in Fig. 2.1(a) and 2.1(b). Kupfer, Hilsdorf, and Rüsçh (110) and more recently Liu, et al. (121) have shown that as f_1 and f_2 are varied,

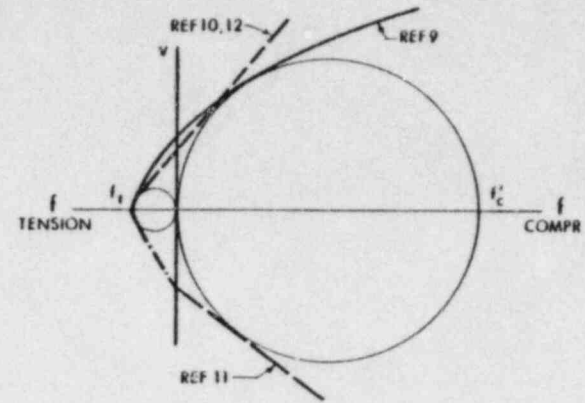


FIG. 2.3.—Possible Mohr Rupture Envelopes for Concrete

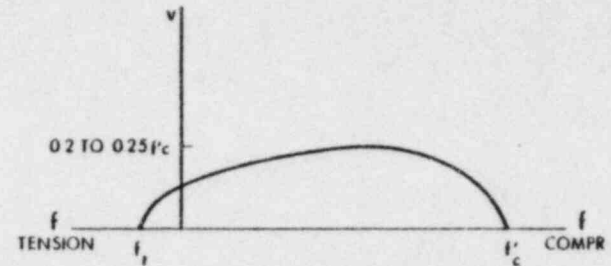


FIG. 2.4.—Combinations of f and v Corresponding to Failure of Element Shown in Fig. 2.1(b)—See Refs. 70, 168, 192

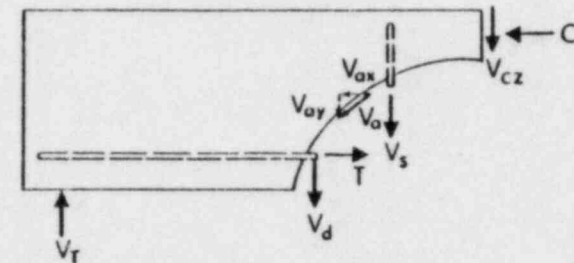


FIG. 2.5.—Forces Acting at Inclined Crack

the element shown in Fig. 2.1(a) will have the strengths shown by the solid lines in Fig. 2.2. This diagram is symmetrical about a 45° axis and can be divided into quadrants A, B, and C as shown. Biaxial tension

(Quadrant A) has relatively little effect on the tensile strengths and biaxial compression (Quadrants C) tends to increase the compressive strength over that for uniaxial compression. Combined tension and compression loadings significantly reduce both the tensile and compressive stresses at failure, however, as shown by the quadrants labelled B. The latter case is particularly important when shears are present since they give rise to principal tensile and principal compressive stresses on elements in the web of a beam.

Alternatively, Mohr's Theory of Failure yields acceptable strength predictions for either of the cases shown in Fig. 2.1 except that conservative results are obtained in quadrants C of Fig. 2.2. Parabolic (192) and straight line (70,198) envelopes similar to those shown in Fig. 2.3 have been proposed for the family of Mohr's circles representing failure conditions. Any stress condition that corresponds to a Mohr's circle that is tangent to or intersects this envelope is assumed to represent a failure condition. For the loading shown in Fig. 2.1(a) this failure theory leads to a strength diagram similar to that shown in dashed lines in Fig. 2.2. The dashed and solid lines differ because the effects of the intermediate principal stress are ignored in the Mohr Theory.

Based on either the Mohr Theory of Failure or the Kupfer, Hilsdorf, and Rüschi diagrams, relationships have been derived for the strength of elements stressed as shown in Fig. 2.1(b) (70,168,192). One such relationship is plotted in Fig. 2.4. This envelope presents all the combinations of shearing and axial stresses on the vertical plane of the element shown in Fig. 2.1(b) which result in failure of the element.

The implication of such a diagram is that the presence of shearing stresses will reduce the compression strength of concrete. Combined shear and compression may occur in columns or in the compression zones of beams.

In recent years a number of more complex failure theories have been proposed (39,150,169). These are particularly important when large triaxial stresses exist as in reactor vessels. A state of triaxial stress also exists in the compression zone under the column in a slab and as a result this region has a high capacity for shear and axial forces.

2.2 Mechanisms of Shear Transfer in Reinforced Concrete

Shear is transmitted from one plane to another in various ways in reinforced concrete members. The behavior, including the failure modes, depends on the method of shear transmission. Our appreciation of some of the principal shear mechanisms is relatively recent and therefore the definite evaluation of the contribution of these shear carrying components is yet only tentative.

The main types of shear transfer are the following: (a) Shear stress in the uncracked concrete; (b) interface shear transfer; (c) dowel action; (d) arch action; and (e) shear reinforcement.

These mechanisms occur to widely varying extents in various types of structural elements. For example, the forces in a reinforced concrete beam with a diagonal crack are shown in Fig. 2.5. The longitudinal forces, T and C , are related to the flexural resistance of the member. The forces at the diagonal tension crack, V_{ax} and V_{ay} , are due to interface shear

transfer (also called aggregate interlock). The V_s and V_d forces are the forces in the stirrups and the "dowel shear" carried by the longitudinal steel, respectively and V_{cz} = the shear carried by the compression zone. Thus,

$$V_T = V_s + V_{cz} + V_d + V_{ay} \dots \dots \dots (2.1)$$

Most modern design procedures assign portions of the total shear to the compression zone and to the stirrups. However, it has become evident in recent years that the shear carried by the longitudinal steel (dowel effect) and the interface shear transfer along the crack significantly affect the capacity and mode of failure (60,179). These basic concepts will be described briefly in this chapter with specific cases looked at in more detail in subsequent chapters.

2.2.1 Shear Transfer by Concrete Shear Stress

The simplest method of shear transfer is by shearing stresses. This occurs in uncracked members or in the uncracked portions of structural members. The interaction of shear stresses with tensile and compressive stresses produces principal stresses which may cause inclined cracking or a crushing failure of the concrete. The strength of concrete subjected to principal stresses or combined shear and normal stresses is shown in Figs. 2.3 and 2.4, respectively.

2.2.2 Interface Shear Transfer

There are several instances in which shear must be transferred across a definite plane or surface where slip may occur. Researchers have called this mechanism aggregate interlock, surface roughness shear transfer, shear friction, tangential shear transfer. Since none of these names are sufficiently general, "interface shear transfer" is used in this report to denote the tangential shear force transmitted across a crack or plane (such as a construction joint). Several types of interface shear transfer are described in this section.

If the plane under consideration is an existing crack or interface, failure usually involves slippage or relative movement along the crack or plane. If the plane is located in monolithic concrete, a number of diagonal cracks occur across the interface and failure involves a truss action along the plane.

(a) Shear Transfer Behavior of Uncracked Concrete with Reinforcement Normal to Shear Plane

Several researchers have studied shear transfer across monolithic shear planes. A typical specimen is shown in Fig. 2.6. Before cracking shear is transmitted by stress across the shear plane. At higher loads short diagonal cracks form across the shear plane (Fig. 2.7). Failure is prevented by transverse reinforcement. Steel bars and the compression between the diagonal cracks form a truss which resists further loads. Failure occurs when the compression diagonals crush under the combined action of axial and shear forces. For ductile behavior it is necessary to proportion the bars so that they yield before the diagonals crush. Although shear is transferred across a definite plane, this mechanism is not strictly interface shear

transfer since appreciable shear is not transferred across a crack. In addition to the truss mechanism, shear is also carried by dowel action. However, the shear transferred by that action is small if the bars yield before failure.

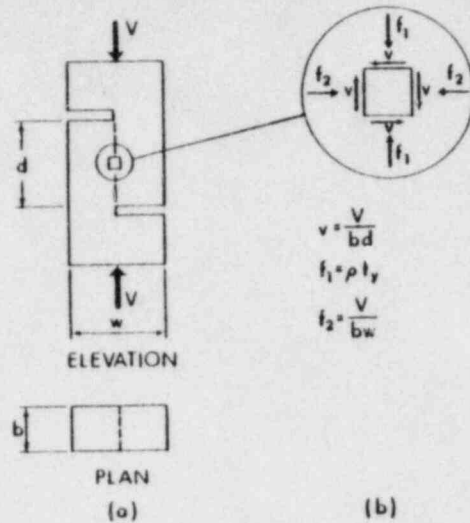


FIG. 2.6.—Shear Transfer Test Specimen (87)

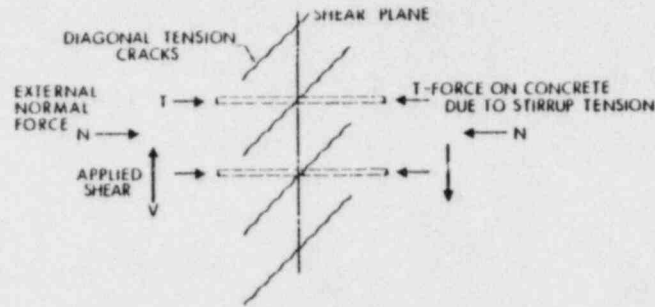


FIG. 2.7.—“Truss” Formed After Diagonal Tension Cracking (134)

(b) Shear Transfer Behavior of Initially Cracked Concrete with Reinforcement Normal to Shear Plane

If an initially cracked specimen is tested, shear can be transmitted only if lateral confinement or transverse steel exists. The irregularities of the surfaces of the two sides of the crack ride up on each other and this tends to open the crack and create forces in the transverse steel (Fig. 2.8).

At failure the shear capacity was found to be proportional

to the amount of average restraining stress ρf_y , equal to the transverse steel percentage multiplied by the yield stress (87). This proportionality is similar to the situation in the case of simple friction, and therefore this approach has been called

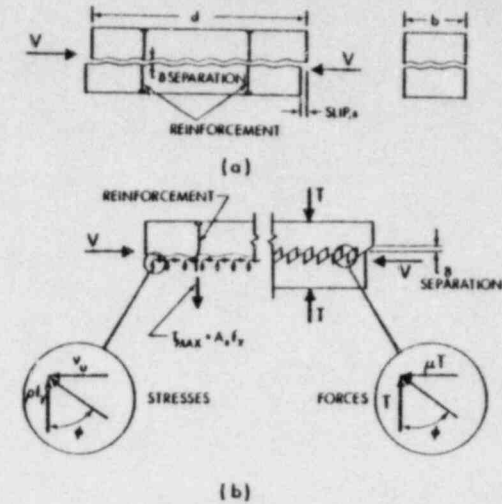


FIG. 2.8.—Shear-Friction Analogy

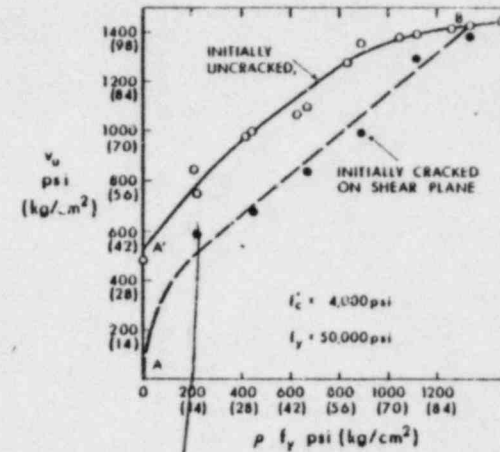


FIG. 2.9.—Variation of Shear Strength with Reinforcement Parameter ρf_y (87)

“shear-friction hypothesis,” although strictly speaking, friction does not play an appreciable role. The shear at failure can be written as (87,134)

$$V_u = A_s f_y \tan \phi \dots \dots \dots (2.2)$$

in which A_s = the total area of transverse steel and $\tan \phi$ = the equivalent coefficient of friction.

In addition, some shear is transferred by dowel action of the reinforcement crossing the crack.

Because the "coefficient of friction" along the crack is independent of the concrete strength, so also is the shearing strength, V_u , provided the shearing stresses do not exceed some limiting value. Similarly direct stresses parallel to the shear plane will not affect either the friction or dowel action and, as a result, the shearing strength is the same whether the shearing forces, V , in Fig. 2.6(a) are due to compression forces as shown or tension forces.

In a heavily reinforced shear plane or one subjected to a normal compressive stress, the shear resistance due to friction and dowel action may reach the shear corresponding to failure of an initially uncracked specimen having the same characteristics. In such a case the crack locks and the behavior and strength are similar to those for an initially uncracked section.

(c) Test Results

Test results obtained by Mattock and his co-workers (87,134) for specimens similar to Fig. 2.6(a) are shown in Fig. 2.9. The ultimate shear stress increases almost linearly with the index, ρf_y , from a finite value for ρf_y equal to zero to a limit dependent on the concrete strength for high ρf_y values. With a monolithic shear plane, strengths are consistently greater than with a precracked shear plane. For a precracked shear plane the strength decreases rapidly with decreasing ρf_y , for ρf_y values less than 200 psi (14 kg/cm²). For ρf_y lying between A and A' and B in Fig. 2.9, failure is relatively gentle and is due to a breakdown of the concrete after the reinforcement crossing the shear plane yields. For ρf_y values lying between B and C , failure occurs abruptly before the reinforcement yields. In this region the failure loads are similar for uncracked and precracked specimens, as explained previously.

Hanson (79) used push-off specimens similar to those in Fig. 2.6(a) to examine the effects of the roughness of a bonded surface and the length of the surface. For low ρf_y values and a rough bonded surface, the ultimate shear stresses were similar to those measured by Mattock (134) for a monolithic shear plane. For a smooth bonded surface and a low ρf_y value, the stresses were similar to those for precracked specimens. For both types of specimen the ultimate shear strength decreased about 100 psi (7 kg/cm²) for an increase in the bonded length from 6 in. to 24 in. (15 cm to 60 cm). This represented a 20% to 50% reduction for the rough bonded and smooth bonded surfaces, respectively. The addition of shear keys stiffened the connection at low slips but had no significant effect on its strength.

Fenwick and Paulay (60) and Loeber (122) studied shear

transfer in precracked unreinforced push-off specimens. In one group of tests the crack width was held constant and variations in the size of the aggregate from 3/8 in. to 3/4 in. (1 cm to 2 cm) had no effect on the shear stress-slip curve or the ultimate strength. For shear stresses between 200 psi and 1,000 psi (14 kg/cm² and 70 kg/cm²) the shear stress-slip curve was practically linear, and the stiffness increased as the width of the crack decreased. In a second group of tests the crack width was increased at 0.002 in. (0.05 mm) per 100 psi (7 kg/cm²) of shear stress. There was a continuous degradation of the aggregate interlock mechanism on the shear plane with increasing load and for a 4,000 psi (280 kg/cm²) concrete, failure occurred at a shear stress of about 900 psi (63 kg/cm²).

To simulate the deformations at an inclined crack in a beam, Taylor (179) tested blocks of concrete in a device that maintained a constant ratio between the opening normal to the crack, ΔN , and the shearing movement along the crack, ΔS . The ultimate shearing stresses and the deformations developed both decreased linearly as $\Delta N/\Delta S$ increased. The shear transfer strength was a function of the roughness of the fracture surface. In some very high strength concretes, fractures crossed the aggregates, leaving a relatively smooth fracture surface, and consequently a relatively low shear transfer at failure.

Tests at the Portland Cement Association have shown that interface shear transfer is a viable mechanism even under fatigue loading for the transfer of shear between concrete paving slabs (40,144). The shear transferred for a given slip decreases with cycling and with increasing load and increasing crack width. However, 90% of the decrease occurs during the first 5×10^5 loading cycles and the decrease diminished with increasing aggregate size and hardness.

For a shear stress ranging from 0 psi to 820 psi (57 kg/cm²) repeated 33 times for a 4,000 psi (280 kg/cm²) concrete, Loeber (122) found there was no sudden breakdown of the shear transfer mechanism. Although the permanent slip increased with cycling, the stiffness increased also.

White and Holley (193) applied cyclic shear forces to 1.5-ft by 2.0-ft by 3.0-ft (45-cm by 60-cm by 90-cm) specimens precracked by wedging them in two. These tests were designed to simulate seismic conditions in a nuclear containment vessel. Even after 50 cycles, more than 120 psi (8.5 kg/cm²) shear stress could be carried for the crack width and the size of restraining rod used. The shear stiffness decreased during cycling even though the external clamping rods did not reach yield.

In tests in which the parameter, ρ , was varied by varying both the bar spacing and the bar size, Mattock, et al. (87,134) found no marked variation in the effect of ρf_y . Similarly, the effect of the yield strength of the stirrups was found to be

properly reflected by the parameter, ρf_y .

As shown in Fig. 2.9, a limiting shear strength of about $0.3 f'_c$ was observed for both precracked and monolithic specimens with concrete strengths of 4,000 psi (280 kg/cm²). A similar limit was observed for strengths varying from 2,500 psi to 4,000 psi (175 kg/cm² to 280 kg/cm²). In tests with an applied compressive stress normal to the shear plane, the shear strength was found to increase in proportion to the sum of the normal stress and ρf_y , and to reach a limiting shear strength of about $0.45 f'_c$.

No tests have been carried out on specimens having a tensile stress normal to the shearing surface.

2.2.3 ~~Shear Reinforcement~~

If reinforcing bars cross a crack, shearing displacements along the crack will be resisted, in part, by a dowelling force in the bar. The dowel force gives rise to tensions in the surrounding concrete and these in combination with the wedging action of the bar deformations produce splitting cracks along the reinforcement (14, 69). This in turn decreases the stiffness of the concrete around the bar and therefore the dowel force. Following splitting, the doweling force is a function of the stiffness of the concrete directly under the bars and the distance from the point where the doweling shear is applied to the first stirrups supporting the dowel (14). Compression failure under the bar sometimes affects this behavior, especially in slabs or in mass concrete.

Although dowel action has been studied by a number of investigators (14, 69, 107, 149, 178), dowel tests are characterized by the large number of variables that have to be considered to cover all likely bar layouts. So far, reliable results are available only for a few practical cases.

Relative to other shear transfer mechanisms, the dowel shear force is generally not dominant in beams. On the other hand, its role in the failure mechanisms of some types of structural elements is important. In beams, splitting cracks develop along the tension reinforcement at inclined cracks as a result of the dowel effects. This allows the inclined cracks to open, which in turn reduces the interface shear transfer along the diagonal crack and thus leads to failure.

In slabs, some investigators (10, 102) credit dowel action with about 30% of the total shear.

2.2.4 ~~Shear Reinforcement~~

In deep beams and slabs part of the load is transmitted to the supports by arch action. This is not a shear mechanism in the sense that it does not transmit a tangential force to a nearby parallel plane. However, arch action does permit the transfer of a vertical concentrated force to a reaction in a deep member and thereby reduces the contribution of the other types of shear transfer.

For arch action to develop, a horizontal reaction component is required at the base of the arch. In beams this is usually provided

by the tie action of the longitudinal bars. Frequently deep beams will fail due to a failure of the anchorage of these bars. In beams arch action occurs not only outside the outermost cracks but also between diagonal tension cracks. Part of the arch compression is resisted by dowel forces and therefore splitting cracks may develop along the bars. It was found that stirrups close to the base of diagonal cracks can provide support to the arches (69, 99).

In slabs, arching action may occur around interior columns. Here the horizontal reaction is provided by the in-plane stiffness of the slab adjacent to the punching region (131).

2.2.5 ~~Shear Reinforcement~~

It has been customary to view the action of web reinforcement in beams as part of a truss. Although this analogy helps to simplify design concepts and methods, it does not consider the various types of shear transfer methods properly.

It is also helpful to examine the action of shear reinforcement from the viewpoint of how it aids the several kinds of shear transfer action. In addition to any shear carried by the stirrup itself, when an inclined crack crosses shear reinforcement, the steel may contribute significantly to the capacity of the member by increasing or maintaining the shear transferred by interface shear transfer, dowel action, and arch action. Thus, shear reinforcement restricts the widening of inclined cracks in beams and thus slows the decrease of interface shear transfer quite effectively. Its action is similar in other situations, such as in corbels or other types of members. The effects of web reinforcement in beams and deep members are discussed in Chapters 3 and 4.

CHAPTER 3

3. Behavior and Strength of Beams Failing in Shear

3.1 Modes of Inclined Cracking and Shear Failure

Shear failures of beams are characterized by the occurrence of inclined cracks. In some cases inclined cracking is immediately followed by member failure and in other cases, the inclined cracks stabilize and substantially more shear force may be applied before the member fails.

Inclined cracks in the web of a beam may develop either before a flexural crack occurs in their vicinity or as an extension of a previously developed flexural crack. The first type of inclined crack is often referred to as a "web-shear crack" [Fig. 3.1(a)]; the second type is often identified as a "flexure-shear crack;" and the flexural crack causing the inclined crack is referred to as the "initiating flexural crack" [128, 174, and Fig. 3.1(b)].

In addition to the primary cracks (flexural and the two types of inclined cracks), secondary cracks often result from splitting forces developed by the deformed bars when slip between concrete and steel reinforcement occurs, or from dowel action forces in the longitudinal bars transferring shear across the crack.

The manner in which inclined cracks develop and grow and the type

of failure that subsequently develops is strongly affected by the relative magnitudes of the shearing stress, v , and flexural stress, f_x . As a first approximation, these stresses may be defined as:

$$v = \alpha_1 \frac{V}{b_w d} \text{ and } f_x = \alpha_2 \frac{M}{bd^2} \quad (3.1)$$

in which α_1 and α_2 are coefficients depending on several variables, including geometry of the beam, the type of loading, the amount and arrangement of reinforcement, the type of steel, and the interaction between steel and concrete. The values, V and M , are the shear and moment at a given section, respectively; b = the width of the flange; b_w = the

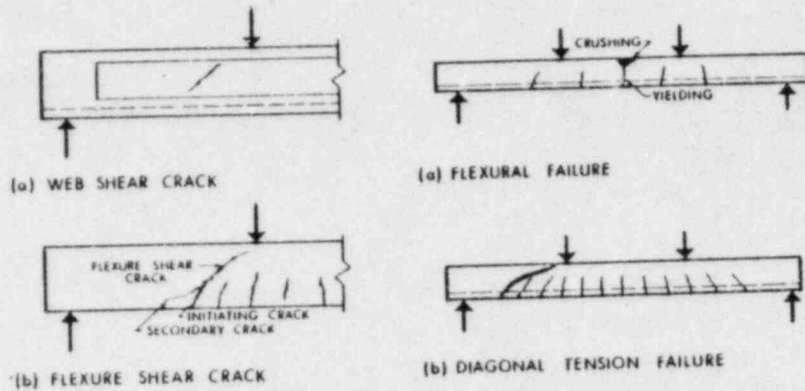


FIG. 3.1—Types of Inclined Cracks

FIG. 3.2—Failures of Slender Beams

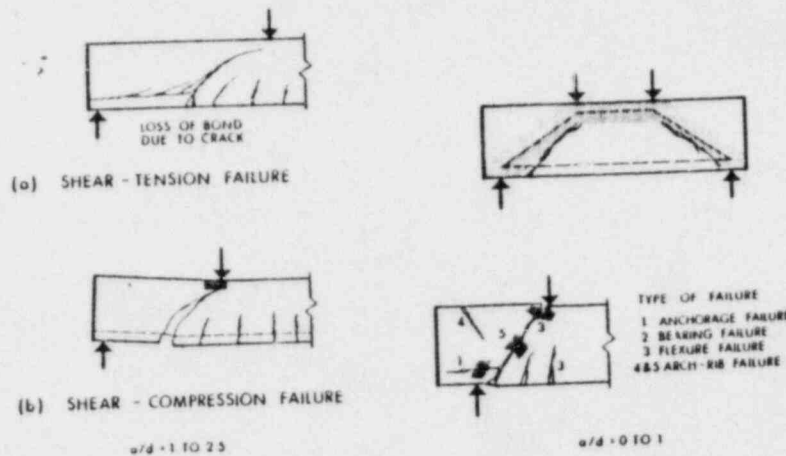


FIG. 3.3—Typical Shear Failures in Short Beams

FIG. 3.4—Modes of Failure of Deep Beams

width of the web; and d = the effective depth of the beam. The ratio f_x/v is therefore

$$\frac{f_x}{v} = \frac{\alpha_2 M b_w}{\alpha_1 V d b} = \alpha_3 \frac{M b_w}{V d b} \quad (3.2)$$

in which $\alpha_3 = \alpha_2/\alpha_1$. The shear, V , is a measure of moment gradient; $V = dM/dx$; and for beams subjected to concentrated loads may be expressed by $V = M/a$, in which a is called the "shear span." Then

$$\frac{f_x}{v} = \alpha_3 \left(\frac{a}{d}\right) \left(\frac{b_w}{b}\right) \quad (3.3)$$

and the variation in the inclined cracking load and shear capacity of rectangular beams may be conveniently considered as a function of varying a/d , i.e., the ratio of shear-span to depth (24).

In short deep members the vertical normal stresses, f_v , become significant as the value of a/d decreases below 2 to 2.5 and this leads to an additional increase in the shear strength.

When all other things are kept constant, the influence of the a/d ratio on the cracking of a rectangular simply supported reinforced concrete beam can be illustrated by considering beams of varying slenderness with two symmetrically placed concentrated loads placed a distance, a , from the supports.

(a) Normal and Long Beams of Rectangular Cross Section ($a/d > 2.5$)

Very shallow beams will usually fail in flexure [Fig. 3.2(a)]. The first crack will form due to flexural tension at the cross section of maximum moment. As the beam load increases prior to failure, the tensile cracking may spread to regions of lesser moment, but failure occurs in flexure near the section of maximum moment.

For a beam with somewhat smaller value of a/d , the fatal crack may well be a flexure-shear crack, as shown in Fig. 3.1(b). Such a crack may cause the beam to fail before its full flexural capacity is developed.

In moderately slender beams one of the cracks may continue to propagate through the beams with further load until at some stage it becomes unstable and extends through the beam as shown in Fig. 3.2(b). This type of failure is called a "diagonal tension failure."

(b) Short Beams: $1 < a/d < 2.5$

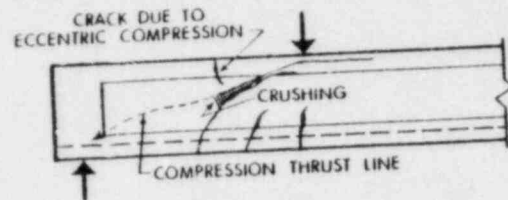
A curved tensile crack in a region of combined moment and shear may also trigger one of two additional modes of failure. A secondary crack may propagate backward along the longitudinal reinforcement from the inclined crack, perhaps because of dowel action in the longitudinal reinforcement [Fig. 3.3(a)]. This crack will cause a loss of bond. As the main reinforcement begins to slip, the wedging action of the bar deformations contributes to a splitting of the concrete and a further propagation of the crack, resulting in an anchorage failure of the longitudinal reinforcement, called a "shear-tension" failure (11). Prior to such a failure, the beam acts as a tied arch.

Alternatively, the concrete above the upper end of the inclined

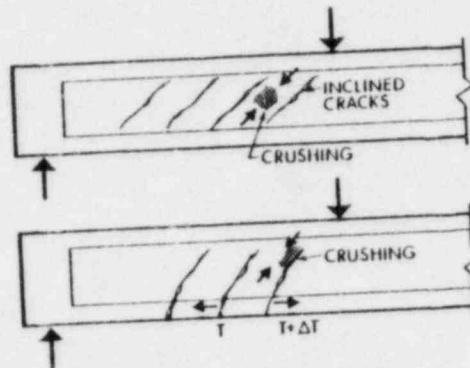
crack may fail by crushing [Fig. 3.3(b)] resulting in a "shear-compression" failure.

(c) Deep Beams: $0 < a/d < 1$

In the design of deep beams, shearing stresses and vertical normal stresses require more consideration than flexural stresses. Significant principal compression and tensions, respectively, exist along and across the line joining the load and the reaction, and inclined cracks occur immediately inside the reaction plates (Fig. 3.4). In some cases the cracks appear to be initiated by flexural cracks originating in



(a) ARCH-RIB FAILURE



(b) WEB-CRUSHING FAILURE

FIG. 3.5.—Typical Shear Failures in I-Beams

this region, and in other cases by the principal tensions across the line joining the load and reaction, as in an indirect tension test.

After inclined cracking occurs, a deep beam without web reinforcement transforms almost immediately into a tied-arch which can fail in a number of ways (50,54). The numbers in Fig. 3.4 correspond to the following modes of failure: (1) Anchorage failure of the tension reinforcement, usually combined with a dowel splitting effect; (2) crushing failure at the reactions; (3) flexural failure—either of the steel reinforcement due to yielding or fracture, or of the "crown of the arch" when the concrete crushes; or (4) tension failure of

the "arch-rib" by cracking over the support; followed by (5) crushing along the crack. The tension at Point 4 is produced by the eccentricity of the thrust which acts essentially along the inclined crack.

The strength of deep beams will be discussed more fully in Chapter 4.

(d) I-Beams

In a beam with a narrow web, such as an I-beam, the shearing stresses in the web are much larger in relation to the flexural stresses than they are in a rectangular beam, as is shown by Eq. 3.3. Consequently a tensile crack may begin in the web due to principal tensile stresses associated with the shearing stresses. Such a crack has been called a "web-shear" crack [Fig. 3.1(a)] and is inclined nearer to 45° than flexure-shear cracks because of the dominance of the shearing stresses over the flexural stresses in the web. Additional cracks may also begin in flexural tension.

The I-beams may fail in flexure, diagonal tension, shear-tension, shear-compression, or in the various modes of failure already described for deep beams. Fig. 3.5(a) shows an "arch-rib" failure similar to that of a deep rectangular beam. Fig. 3.5(b) shows a "web-crushing" failure which can occur in a thin-webbed beam with web reinforcement when a thin web element, isolated by diagonal cracks, crushes under the diagonal compression forces (116,153). It should be noted that the mechanics of failure will differ somewhat in the two beams shown in Fig. 3.5(b) depending on whether the lower flange is cracked or not (11). The European Concrete Committee (41) distinguishes between these two cases for design purposes.

3.2 Development of Inclined Cracks in Reinforced and Prestressed Concrete Beams

Because all types of "shear-failure" are affected by or result from inclined cracks due to diagonal tensile stresses, it is essential to understand, at least empirically, the factors affecting the formation of such cracks.

(a) Web-Shear Cracks

Web-shear cracks of the type shown in Fig. 3.1(a) form in a part of the beam that is as yet uncracked in flexure. Generally this type of cracking only occurs in highly prestressed beams with thin webs.

A web-shear crack occurs when the stresses at some point in the uncracked beam reach a limiting value. Based on a limiting principal tensile stress theory of failure, it has been shown that for those portions of beams actually susceptible to this type of cracking, the web-shear cracking load may be predicted with reasonable accuracy by calculating the shearing force required to cause principal tensile stresses equal to the tensile strength of the concrete at or near the neutral axis of the beam (128). More recently it has been shown that a slightly better prediction of the cracking load results from the use of Mohr's Failure Theory for concrete subjected to combined shear and normal stress (100).

From a Mohr's Circle it can be shown that the shear stress, v_{cw} ,

corresponding to reaching the tensile strength of the concrete, f_t , at the neutral axis of a beam with an average axial stress of f_p is:

$$V_{cw} = f_t \sqrt{1 + \frac{f_{pc}}{f_t} + \frac{V_p}{b_w t}} \quad (3.4)$$

In Eq. (11.12) of the ACI Code this is approximated by the straight line function (5):

$$v_{cw} = 3.5 \sqrt{f'_c} + 0.3 f_{pc} + \frac{V_p}{b_w d} \quad (3.5)$$

in which V_p = the vertical component of the prestressing force.

The latest revisions to the Soviet design regulations and prestressed concrete follow a similar approach except that the tensile strength of the concrete, f_t , is defined considering the effect of the principal compression force using a diagram similar to the upper left quadrant of Fig. 2.2 (197).

(b) Flexure-Shear Cracks

Flexure-shear cracks of the type shown in Fig. 3.1(b) form in a part of a beam already cracked due to flexure. Although these cracks are the most common type of crack observed in reinforced and prestressed concrete beams, the mechanism by which they form is not entirely understood.

In a beam containing flexural cracks, the variation in steel stress from crack to crack sets up forces on the cantilever elements or "teeth" between the flexural cracks [see Fig. 3.2(b)] which tend to cause bending and shearing deflections of the teeth (60,96,129). As the teeth deflect prior to inclined cracking the dowelling forces and aggregate interlock stresses developed between the teeth tend to prevent relative deflections of the teeth, thus delaying the formation of further cracks. The rate of propagation of the flexural cracks and the stage at which the inclined cracks develop in a given beam is a function of the magnitudes of the flexural and shearing stresses at the head of the crack (7,105,129). These, in turn, are a function of the M/Vd and b_w/b ratios, as shown in Eq. 3.3, the height of the flexural crack and the amount of shear transferred by interface shear transfer and dowelling.

In tests of rectangular beams Taylor (180) has shown that approximately one third of the total applied shear was transferred by the compression zone above flexural cracks in the shear spans prior to the formation of inclined cracks. The balance was presumably transferred by interface shear transfer and dowel action. These measurements suggest that a significant shear stress can exist at the upper ends of flexural cracks in the shear spans. Broms (28) has shown that the nonuniform stresses between cracks lead to "secondary shear stresses" which are particularly severe near the top of flexural cracks in the shear spans. These secondary shear stresses, combined with the stresses necessary to balance the applied loads,

cause major diagonal principal tensile stresses at the head of the flexural cracks.

A number of semirational expressions have been developed to predict the flexure-shear cracking load of reinforced concrete beams. The best known is the ACI Code equation for reinforced concrete, developed by ACI-ASCE Committee 326 (7):

$$\frac{V_c}{b_w d} = 1.9 \sqrt{f'_c} + \frac{2,500 \rho_w V d}{M} \leq 3.5 \sqrt{f'_c} \quad (3.6)$$

in which V_c = the shear carried by the concrete, taken equal to the inclined cracking shear; $\sqrt{f'_c}$ is a measure of the tensile strength of the concrete; M and V = the moment and shear at the point under consideration; and ρ_w = the amount of longitudinal reinforcement at that point related to the web thickness. This equation was derived considering the principal tensile stresses at the top of a flexural crack in the shear span.

For flexure-shear cracking in prestressed concrete beams, the inclined cracking load can be expressed in terms of the shear necessary to cause a flexural crack at a point located $d/2$ to d toward the reaction from the section under consideration, plus an increment of shear assumed to be necessary for this flexural crack to develop into an inclined crack (128,174). The 1963 ACI Code (5,6) equation for flexure-shear cracking in prestressed beams was expressed in this form:

$$V_u = \frac{M_{cr}}{\frac{M}{V} - \frac{d}{2}} + 0.6 \sqrt{f'_c} b_w d \quad (3.7)$$

in which the first term predicts the shear necessary to cause the initiating flexural crack and the second term expresses the additional increment of shear. The external moment required to cause a flexural crack at the point under consideration is M_{cr} . This equation was slightly simplified in the 1971 ACI Code (126). Since the effect of inclined prestressing tendons is included in the flexural cracking moment, M_{cr} , it is not necessary to add the additional term, V_p , to this equation.

Recently Mattock (133) extended Eq. 3.7 to reinforced concrete beams with or without axial loads. To do this, the steel percentage, ρ , and the modular ratio, n , were included in the expression as shown in Eq. 3.8

$$V_u = \frac{M_{cr}}{\frac{M}{V} - \frac{d}{2}} + \left(1.75 - \frac{0.036}{n\rho} + 4.0 n\rho \right) b_w d \sqrt{f'_c} \quad (3.8)$$

Statistical studies of tests of reinforced concrete beams suggest that the most significant variables affecting the shear at flexure-shear cracking are the tensile strength of the concrete, f_t , or $\propto \sqrt{f'_c}$; the

longitudinal reinforcement ratio, ρ ; the ratio of flexural tension to shearing stresses measured by the (M/Vd) or $(M/Vd\rho)$ ratio; the effective depth of the beam, d ; and perhaps the ratio of compression to tension reinforcement (101,199). Perhaps the best known statistically derived equation was presented by Zsutty (199).

$$v_c = 59 \sqrt{f'_c \rho \frac{d}{a}} \text{ (psi)} \dots \dots \dots (3.9)$$

Placas and Regan derived a similar equation starting from a failure theory for concrete (153).

3.3 Forces in Beams with Diagonal Tension Cracks

Traditionally, the transfer of shear across a section in a cracked beam has been explained using a "truss analogy" in which the beam is represented by a truss with parallel chords and a web composed of diagonal concrete compression struts and vertical or inclined stirrups acting in tension (7,88). In the 70 yr since this analogy was first proposed, it has formed the principal basis for the interpretation of forces in beams and for the design of reinforced concrete beams for shear. On the other hand, recent studies have shown that several significant components of shear force shown in Fig. 2.5 are not included in the basic truss analogy. These will be examined in the following paragraphs.

(a) Beams without Web Reinforcement

A number of experimental investigations have been carried out on beams without stirrups to assess the relative magnitude of the forces shown in Fig. 2.5. Acharya and Kemp (1) showed that only 40% of the total shear on a section can be carried by the compression zone if the stress conditions at the head of the crack are to be compatible with an accepted failure criterion for concrete subjected to combined shear and normal force (Section 2.2.1). Experimental work has subsequently been carried out by Fenwick and Paulay (60), Taylor (179), and Gergely (69) in which a variation of compression zone shear between 20% and 40% of the total shear on beams was found. This range depended mainly on the shape and nature of the cracks in the beams.

A number of investigations by Krefeld and Thurston (107), Parmelee (149), Fenwick and Paulay (60), Gergely (69), Taylor (178), Baumann (14), and many others have been carried out on dowel action indicating that the dowel shear force is between 15%-25% of the total shear force (see Section 2.2.3).

As discussed in Section 2.2.2, interface shear transfer tests have been carried out by Fenwick and Paulay (60), and Taylor (179), and Mattock, et al. (134), among others. Gergely (69) conducted tests in which interface shear transfer was eliminated by preforming smooth sided cracks in beams. These tests and those by Taylor indicate that between 33%-50% of the total force on a beam may be carried by interface shear transfer.

The figures given in the preceding were measured on rectangular beams without web reinforcement at loads near their failure load. Different distributions of shear force apply for lesser loads on the

beams. Thus, before cracking, a parabolic distribution of shear stress across a beam can be expected and after cracking, as the shear displacements across the cracks increase, dowel and interface shear transfer action become increasingly significant.

(b) Beams with Web Reinforcement

Web reinforcement has three primary effects on the strength of a beam: (1) It carries part of the shear, V_s ; (2) it restricts the growth of the diagonal tension crack width and thereby helps maintain the interface shear transfer, V_{at} ; and (3) it holds the longitudinal bars and increases their dowel capacity, V_d . In addition to these three actions, stirrups may transfer a small force across the crack by dowel action and they tend to enhance the strength of the compression zone by confining the concrete.

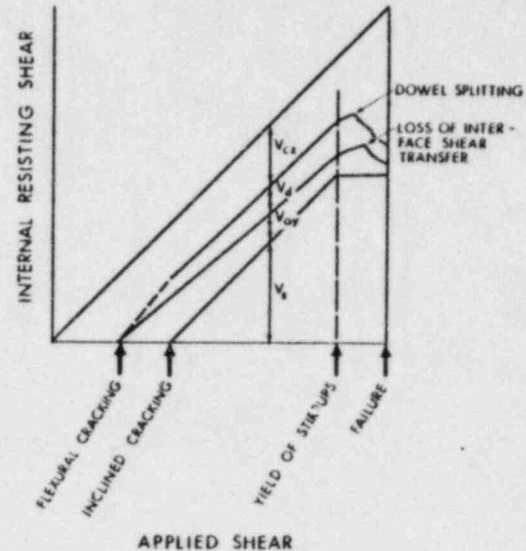


FIG. 3.6.—Distribution of Internal Shears in Beam with Web Reinforcement

If a stirrup happens to be near the bottom of a major diagonal crack, it is very effective in maintaining the dowel force and restraining the splitting failure, provided that the stirrups are of sufficient size, are well anchored, and are spaced close enough together that each potential diagonal crack reaches the tension steel near a stirrup (99).

The mechanism of a shear failure is not yet completely understood, although some careful tests have demonstrated it quantitatively in specific cases (1,60,69,179). The internal shearing force components at a crack such as the one shown in Fig. 2.5 are related to the applied shear in Fig. 3.6. Prior to flexural cracking all the shear is carried by the uncracked concrete. Between flexural and inclined

cracking, the external shear is resisted by the concrete, V_{ct} ; the interface shear transfer, V_{ay} ; and by dowel action, V_d . Following the formation of inclined cracks, a portion of the shear is carried by the web reinforcement, V_s . When the shear carried by the web reinforcement can no longer increase due to its yielding, any additional shear must be carried by V_{ct} , V_d , and V_{ay} . As the inclined crack widens, the interface shear transfer, V_{ay} , decreases, forcing V_d and V_{ct} to increase at an accelerated rate until either splitting (dowel) failure occurs or the compression zone fails due to combined shear and compression.

In the case of beams without stirrups, beam failure may be caused by the breakdown of any of the components of force transfer across the section with different mechanisms dominating in beams of different types. For example, in some tests it is possible to see dowel splitting at the tension steel level before the beam collapses and in other tests, dowel failure and beam collapse occur simultaneously. In some cases it is also possible to see spalling from the sides of inclined cracks before beam failure, indicating that failure of the interlock mechanism is imminent.

Each of the ways in which force is carried across beams, apart from the force carried by stirrups, has a load deformation curve which initially rises rapidly, followed by a falling portion. In the case of the force carried in the compression zone, the falling portion of the curve follows that of concrete under a combined shear and compressive stress system. Dowel failure has a very steep falling portion, except where the dowel is restrained from splitting by stirrups enclosing the longitudinal bars. The failure of the interface shear transfer can be very abrupt, particularly if a crack is inclined over most of its length and the predominant movement across the crack tends to open the crack rather than to shear it (179). Because of this it is very difficult to say which mechanism of force transfer breaks down to cause beam failure from the more ductile behavior of beams with stirrups.

(c) T-Beams and Prestressed Concrete Beams

In T-beams the interface shear transfer is probably less important than in rectangular beams due to the proportionately smaller width of cracked concrete. In addition, V_{ct} is concentrated over the web while the flexural compressive stresses are distributed over a greater width. This leads to a higher ratio of shear to compression than in a rectangular beam. Fig. 2.3 and 2.4 suggest that the magnitude of V_{ct} and the way in which the compression zone fails may change as a result (153).

The role of interface shear transfer and dowel effects has not yet been studied in the case of prestressed concrete beams having flexure-shear cracks. Prestressing strands carry less dowel force and produce smaller wedging action, therefore splitting should occur later than in a reinforced concrete beam. Furthermore, inclined cracks also occur later because of the prestressing effect. On the other hand, once started, the inclined crack tends to develop more rapidly

than in a reinforced concrete beam because of the smaller steel percentage, and tends to widen fairly quickly, leading to a rapid decrease in V_{ay} . Once splitting initiates, the strand can bend at the crack and does not inhibit the rotation that accompanies the opening of the crack. As a result, V_d is small. The shear capacity of a prestressed beam is approximately equal to the sum of V_s and V_{ct} . The term, V_{ct} , appears to depend on the depth of the compression zone, which in turn is a function of the load at which inclined cracking occurs.

3.4 Factors Affecting the Shear Strength and Serviceability of Beams

Most current building codes express the shear strength of beams in terms of an equation of the form:

$$V_u = V_c + V_s \dots \dots \dots (3.10)$$

in which V_c = the shear "carried by the concrete" at ultimate including V_{ct} , V_d , and V_{ay} in Eq. 2.1; and V_s = the shear carried by transverse reinforcement. For simplicity, the factors affecting the shear strength will be discussed in terms of their effect on V_c or on V_s , assuming these can be separated.

3.4.1 Effect of Cross Section

(a) Effect of Size

Leonhardt and Walther (116) studied the effect of beam size by testing two series of similar specimens without web reinforcement. The first series consisted of four completely similar specimens in which the cross section varied from 2 in. x 3.1 in. (5 cm x 8 cm) to 8 in. x 12.6 in. (20 cm x 32 cm). In this series, the bar diameter was proportional to the external dimensions and the number of bars was constant. In the second series, the cross section varied from 4 in. x 7 in. (10 cm x 18 cm) to 9 in. x 21.3 in. (22.5 cm x 67 cm), the ratios of depth were different from the ratios of widths, the bar diameter was constant, and the number of bars was varied to maintain the same steel percentage. The shear stress at failure decreased 37% between the smallest and largest specimen in the first series and decreased 21% in the second series. The greater strength decrease in the first series was explained on the basis of poorer bond quality with increasing bar diameter. The high shear strength of small scale beams has also been reported by Swamy (176) who attributed it to the influence of the high value of the modulus of rupture of the material and the increase in strength produced by extreme strain gradients in small specimens.

Kani (98) tested beams of various depths and the same concrete strength, steel percentage, and a/d ratio. The shear stress at failure decreased with increasing beam depth. In these tests the beam width was held constant at 6 in. (15 cm) as the depth was varied. As the depth increased the splitting forces due to the wedging bond action of the reinforcement increased and as a result, the failures of the two deeper series of beams

involved splitting along the reinforcement while those in the shallower beams did not.

In all three test series mentioned in the foregoing, one mix design was used for all beam sizes. It is possible that part of the loss of strength can be accounted for by the fact that although the cracks were wider in the deep beams than in the shallow beams, the surface of the cracks had the same roughness in both cases so that the contribution of aggregate in 'lock to their shear capacity was different. Similar size effects have been observed in punching shear tests of model slabs when the same mix was used for various size models (141).

Tests by Taylor (181) have shown much less size effect if the size of the coarse aggregate is changed in the same proportion as the beam size. Taylor also showed that if large beams with normal b/d ratios ($d/b < 4$) are tests, the loss of strength is not as serious as that reported by Kani. For beams with $d/b > 4$ Taylor has proposed that the design value of v_c , the shear stress carried by the concrete, should be reduced by 40%.

The beams tested by Leonhardt and Walther, Kani and Taylor to study the effect of size on shear strength did not have web reinforcement. It appears reasonable to expect that while V_c has a scale effect, V_s has not, so that the effect of size on beams with web reinforcement is small. Statistical analysis (101) of test results confirms that the beam depth has no significant effect on the ultimate strength of beams with web reinforcement. This is confirmed in part by tests of two 4 ft (122-cm) deep "wall beams" with web reinforcement (37). In these tests the shear at inclined cracking was about 50% of that predicted by the ACI Building Code, but the early inclined cracking did not lead to a reduction in the shear capacity of the beams.

(b) Effect of Shape

(i) b/d Ratio of Rectangular Beams

The effect of the b/d ratio in rectangular beams has been studied by Diaz de Cossio (55), Leonhardt and Walther (116), Kani (98), and Iyengar, et al. (91). Diaz de Cossio found that shear strength of beams without web reinforcement increases with b/d ratio. Leonhardt and Walther tested slab strips and also found slightly higher nominal ultimate shear stresses than in normal beams, perhaps due to anti-elastic bending effects. However, Kani did not find any significant change in strength when the beam width was increased from 6 in. to 24 in. (15 cm to 60 cm) and statistical studies by Iyengar, et al. of a large amount of data showed no significant effect of b/d in the range from $1/4 \leq b/d \leq 1$. In slabs, the critical range of b/d is about 4 to 10 and in

this range, some strength enhancement may occur.

(ii) Circular Sections

Farodji and Diaz de Cossio (58) tested circular beams with and without transverse reinforcement. In general, the cross sections resembled those of spiral columns. The maximum value of the ratio between concrete cover and external diameter was about 1/10 in the specimens.

It was found that the usual equations for rectangular sections are applicable to circular sections if the external diameter is used for the effective depth, and the gross area of the circular section for the product, bd . These findings are reflected in Ref. 6.

(iii) T-Beams and I-Beams

Tests of 24 simply-supported T-beams were reported by Placas and Regan (153). In one series the web thickness was kept constant at 6 in. (15 cm) and the flange widths varied from 6 in. to 42 in. (15 cm to 109 cm). All the beams had the same longitudinal and web reinforcement except that the rectangular beam had compression reinforcement to replace the flange. As shown in Fig. 3.7 the beams with 12-in. (30-cm) or wider flanges had about 20% greater ultimate shear strength than the rectangular beam. Placas (153) and Leonhardt (114) have suggested that only the portion of the flange immediately adjacent to the web can transmit a component of the shear in the compression zone. As a result, the compression is distributed over the width of the flange while the shear is concentrated above the web, leading to a critical state of stress in this area. Placas and others (72) have observed that the compression zone of a T-beam will frequently fail due to shearing in the region over the web rather than crushing.

Zsutty (201) has proposed that Eq. (3.11) be used to calculate the shear, V_c , carried by the concrete:

$$V_c = v_c (b_w d + 2h_f^2) \dots \dots \dots (3.11)$$

in which h_f = the thickness of the flange.

For design purposes, however, it seems reasonable to ignore the strengthening effect of the flange and to continue to compute $V_c = v_c b_w d$.

In pan-joint floors the webs generally taper from top to bottom. Although this is not serious in the positive moment region, the section of least width occurs in the compression zone in the negative moment region. In tests of beams simulating the negative moment region of a continuous pan-joint, Hanson (75) found that V_c should be based on the width at the bottom of the web.

Leonhardt and Walther (116) tested a series of beams with constant flange width but varying web thicknesses,

with the sections shown near the top of Fig. 3.8. All the beams for each loading had the same stirrup capacity, V_s . As shown in this figure the failure loads decreased as the web width was reduced. The rectangular and thick web T-beams failed by shear compression and shearing of the compression flange while the thinnest web T-beams failed by crushing of the web due to oblique compression

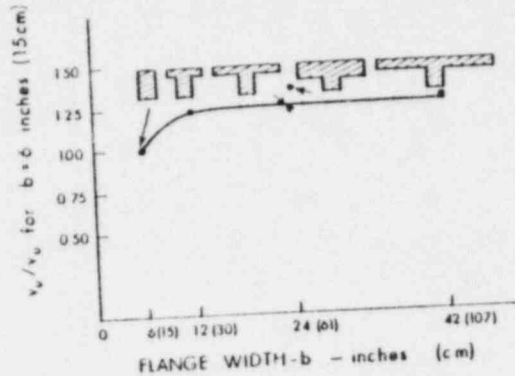


FIG. 3.7.—Effect of Flange Width (153)

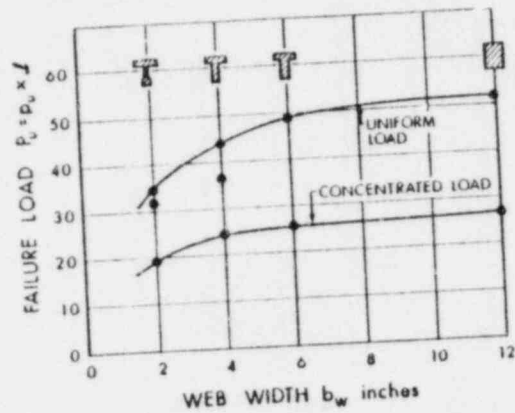


FIG. 3.8.—Effect of Web Thickness on Shear Strength (116)

stresses in the manner discussed in Section 3.1(d) of this report. The inclined cracking load, V_{cr} , and the stresses in the stirrups also depended on the web width. At any shear V , the stresses in the stirrups were approximately a function of $V - V_{cr}$.

The crushing of thin webs of I- or T-beams due to diagonal compression has been studied by a number of

authors (114,116,153) who have used the truss analogy to suggest that the inclined compression stress in the web varies from $f_c = V/b_w d$ for 45° stirrups to twice this value for vertical stirrups.

Recent tests by Demorieux (51) on panels loaded in compression in one direction and loaded in the transverse direction by tensile forces in transverse reinforcement to simulate the conditions in the web of a beam, suggest that the crushing strength of the concrete in the web will be about 2/3 of that in a cylinder test. This agrees with strengths obtained from biaxially loaded concrete (Fig. 2.2). Placas (153) has suggested the web crushing is also affected by the stiffness of the web reinforcement.

For design purposes the CEB-FIP (41) limits the shear in thin webs as a function of the principal tension and compression stresses in the web. For the normal case of reinforced or prestressed concrete beams without transverse prestressing their limit can be reduced to 0.2 times the design compressive strength with vertical stirrups or 0.25 times the design compressive strength with 45° stirrups to prevent crushing of the webs. Accounting for differences in load factors and design strengths, these correspond to $v_u = V_u/\phi b_w d = 0.18 f'_c$ and $0.22 f'_c$, respectively, in ACI practice. For the practical range of web reinforcement ratios, the equation suggested by Placas and Regan corresponds to $v_u = (15 \text{ to } 20) \sqrt{f'_c}$ for vertical stirrups and $v_u = (25 \text{ to } 50) \sqrt{f'_c}$ for 45° stirrups.

3.4.2 Effect of Reinforcement Details

(a) Percentage of Longitudinal Reinforcement

Tests (97,153,158) and analyses (133,153) have shown that the shear strength of reinforced concrete beams drops significantly if the longitudinal reinforcement ratio is decreased below 1.2% to 1.5% based on the web thickness as shown in Fig. 3.9. For the analysis of the strength of beams a number of equations are proposed for v_c .

Mattock (133) and Zsutty (199) have proposed Eqs. 3.8 and 3.9, respectively, while Rajagopalan and Ferguson (158) have fitted the following equation to test data:

$$v_c = (0.8 + 100\rho) \sqrt{f'_c} \leq 2.0 \sqrt{f'_c} \dots \dots \dots (3.12)$$

The 1971 British Standard Code of Practice (27) presents a table of values of v_c that are a function of $\rho_w = A_s/b_w d$ and the 1971 CEB Recommendations (41) reduce the allowable shear stress if ρ_w is less than 1.5% at $2d$ from the support. The various design equations are compared to tests in Fig. 3.9.

The effect of steel percentage may be explained in two ways: (1) The dowel shear, V_d , will be smaller if ρ is reduced; and

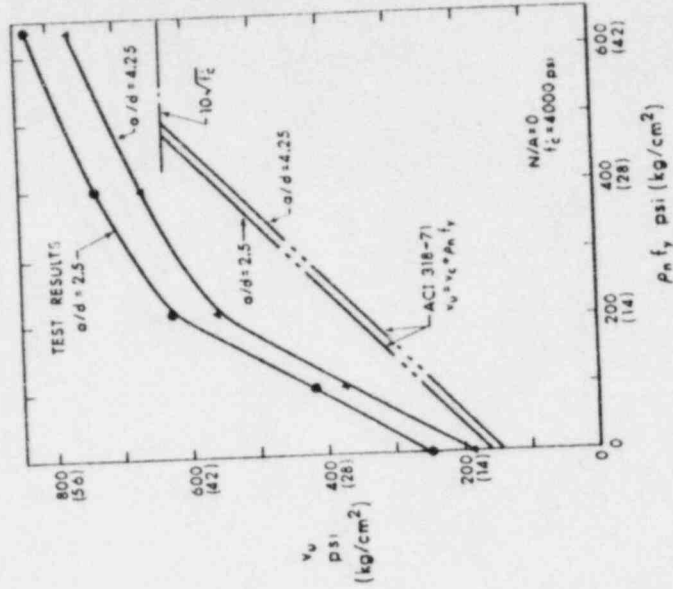


FIG. 3.10.—Effect of Variation in a/d on Relationship Between v and $\rho n f_y$ (72)

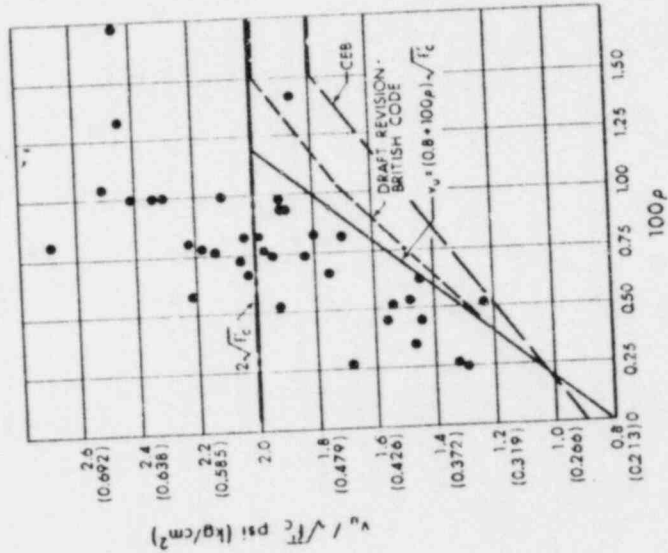


FIG. 3.9.—Effect of Longitudinal Reinforcement Ratio, ρ , on v_c (158)

(2) as ρ is reduced, the flexural cracks extend higher into the beam and are wider, reducing both the shear capacity of the compression zone and the interface shear transfer.

(b) Yield Strength of Longitudinal Reinforcement

Mathey and Watstein (132) have reported tests on beams with high yield strength longitudinal reinforcement. For a/d ratios from 1.5 to 3.8 they found that the shear strength was independent of the yield point. If, however, the increase in yield strength was offset by a reduction in ρ to give a constant moment capacity, they found a reduction in shear strength. This finding was corroborated by Taylor (183) who suggested that the shear strength decreased as the steel stress at inclined cracking increased. The reasons presented in section 3.4.2(a) to explain the effect of ρ also can be used to explain the effect of the yield strength on V_c when ρ is constant or varied.

(c) Cut-Off and Bent-Up Reinforcement

Major inclined cracks frequently develop near the ends of reinforcing bars cut off in a zone of tension. Adjacent to a cutoff point the stresses and deformations are decreasing in the cutoff bars and increasing in the remaining bars. This, combined with the eccentric pull in the cutoff bars, leads to a state of high shearing and diagonal tensile stresses in the vicinity of the cutoff. Baron (13) has shown that the changes in moment arm in this region lead to increased shears in the cutoff zone.

Tests by Ferguson and Matloob (65), Baron (13), and Bresler and Scordelis (26) show that:

1. Cutting off bars in a tension zone will lower the shear strength of a beam.
2. Closely spaced stirrups in the cutoff zone will prevent premature failure. The ACE-381-71 rules seem adequate in this regard.
3. Bending bars up instead of cutting them off will largely nullify these ill effects, probably because the bend discontinuity is less severe. On the other hand, a major inclined crack frequently occurs at the bend point.

(d) Web Reinforcement

The ACI procedure for designing stirrups assumes that the shear not carried by the concrete after inclined cracking is resisted by stirrups or bent bars acting essentially according to the truss analogy. Recent studies (26,72,85) have shown, however, that small amounts of web reinforcement have a significantly larger effect on the shear strength than predicted by the modified truss analogy. This is shown in Fig. 3.10 (72). While no adequate explanation of this effect has been presented, it has been noted that the horizontal projection of the inclined cracks tends to decrease as the web reinforcement

ratio, v_n , increases, so that the increase in the number of stirrups crossed by a crack is less than the increase in ρ_n . Web reinforcement near the bottom of diagonal cracks is very effective in preventing dowel splitting cracks and in increasing the bond strength by providing confinement. Kani (99) and Gergely (69) claim that isolated stirrups at the bottom of diagonal cracks would prevent shear failure in most cases, but of course, the position of cracks is not known in design. However, their tests indicate that the primary role of web reinforcement is the restriction of the width of diagonal tension cracks. These authors believed that the interface shear transfer does not decrease appreciably until some splitting occurs at the bar and therefore additional stirrups crossing diagonal cracks are not necessary.

The maximum yield strength of web reinforcement was empirically set at 60,000 psi (4200 kg/cm²) in the 1971 ACI Building Code because difficulties are encountered in bending higher strength stirrups and also to prevent excessively wide inclined cracks.

The 1971 ACI Building Code requires a minimum area of web reinforcement in most members when V_u exceeds 1/2 of the allowable V_c . This is intended to prevent or restrain shear failures in members where the sudden formation of inclined cracking may lead to distress. Such reinforcement may add valuable ductility where members are subjected to unexpected tensile forces, settlements or catastrophic loadings. The amount required corresponds to a nominal shearing stress resisted by stirrups of 50 psi ($\rho_n f_y = 50$ psi or 3.5 kg/cm²) and a minimum ratio of web reinforcement, ρ_n , between 0.00083 and 0.00125.

The European Concrete Committee (41) relates the minimum to the compressive strength of the concrete and the yield strength of the stirrups with a minimum of 0.0014 for deformed stirrups and 0.0025 for smooth mild steel stirrups. The Swiss Code (11) requires a minimum web reinforcement, $\rho_n f_y$, equal to half the nominal shear stress carried by the concrete. This corresponds to about 0.0010 for 2,200 psi (154 kg/cm²) concrete up to 0.00175 for 5,800 psi (410 kg/cm²) concrete. The increase in the minimum web reinforcement in this code is intended to reflect the fact that better concrete cracks at a higher stress and therefore at a higher load.

Placas (153) found that the horizontal projection of inclined cracks averaged 1.5d for beams with vertical stirrups and tended to be even greater in the case of inclined stirrups. The beneficial effect of the latter observation was offset by the inclination of the force in the stirrups. As a result he found vertical and inclined stirrups had equal efficiency. Leonhardt (116) and Bruce (29) also noted similar effects.

In view of its relative simplicity and applicability it appears

that the modified truss analogy used in the ACI Building Code is the best design method available at the present time for members subjected to statically applied loads, and this report advocates its continued usage for beams with $M/V_u > 2.5$. More study should be given, however, to the Soviet design procedure that involves both shear and moment equilibrium on inclined planes as outlined later in this chapter (20,21,138). This procedure gives the designer a better understanding of the behavior of the finished member than does the ACI procedure.

In Leonhardt and Walther's tests (116) beams with bent-up bars as shear reinforcement tended to have a lower shear strength and much wider cracks than similar beams with stirrups for several reasons: (1) Bent-up bars have more tributary area loading each bar; (2) they tend to cause longitudinal cracking or crushing at the bend points; (3) they do not confine the concrete in the shear region; and (4) they are less efficient in tying the compression flange and web together. As a result, the 1970 CEB Recommendations (41) require the use of vertical stirrups in addition to bent-up bars. This problem is also discussed by Robinson (163). The ACI Building Code (6) also limits the shear that can be resisted by bent bars.

The principal conclusions of tests carried out in Stuttgart on welded wire mesh stirrups were (117)

1. Mats with 2-in. to 4-in. (5-cm to 10-cm) spacing of the stirrup bar were best with respect to crack widths and compressive stresses in the web.
2. An equivalent yield strength of 60,000 psi (4200 kg/cm²) can be used in load factor design.

The Commentary to the 1971 ACI Building Code provides similar anchorage details for welded wire mesh stirrups.

In some cases it is convenient to use pairs of U-shaped stirrups, lapped in the web of the beam to form a rectangular stirrup. In such a stirrup the lap occurs in a region of diagonal cracking. The relatively few tests of this type of stirrup carried out to date suggest that the capacities of the stirrups are a function of the lap length, stirrup diameter, and cover (77). Allen and Huggins (4) suggest that a lapped stirrup will have the same capacity as a rectangular stirrup if the lap is long enough to develop the yield strength of the stirrup bars. Section 12.13.4 of ACI 318-71 has similar requirements.

(e) Reinforcement of Flanges

Studies made by J. R. Robinson (163) suggest that the behavior of the tension chord is affected by the mechanics of the transmission of forces between the longitudinal reinforcement and the concrete web. In that respect the importance of the reinforcement details cannot be overemphasized. The studies

of these details cannot be separated from the study of the bond and anchorage of the longitudinal and web bar including effects of transverse "binding" reinforcement used to prevent longitudinal splitting of the concrete along the main reinforcement. Robinson uses a truss analogy to design transverse reinforcement in both flanges. Leonhardt also presents these rules (114).

In tests of simply supported T-beams, Placas (153) observed that cracks may develop in the flange along the edge of the web. These cracks were parallel to the web rather than at a 45° angle, as frequently assumed. The model shown in Fig. 3.11 was used to explain this cracking. This figure shows the top of a portion of flange bounded by the web and midspan.

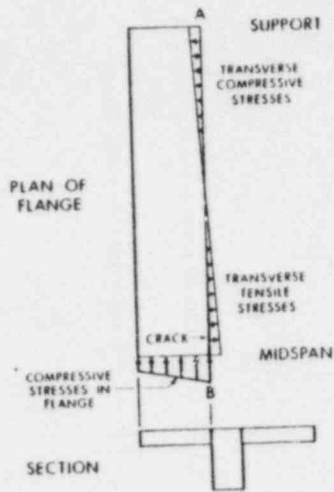


FIG. 3.11.—Flange Cracking in T-Beam

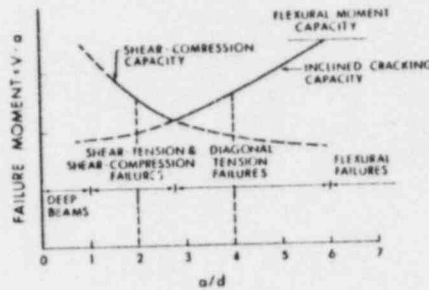


FIG. 3.12.—Variation in Shear Capacity with a/d for Rectangular Beams

Placas found that shear friction reinforcement across the surface, AB, would prevent failure. Johnson (93) has reported similar cracks and based on a shear-friction analysis recommends that the total amount of transverse reinforcement in the slab over the beam web should be:

$$\rho_t f_y \geq 1.26 v_u - 3.8 \sqrt{f'_c} \geq 80 \text{ (psi)} \quad (3.13)$$

Half of this reinforcement should be at the bottom face.

3.4.3 Effect of M/Vd Ratios and Types of Supports

(a) Span to Depth Ratios M/Vd

A number of authors (24) have presented figures similar to Fig. 3.12 showing that a/d or M/Vd is an important variable in defining the shear strength of a beam. This effect is explained in a conceptual fashion by Eqs. 3.2 and 3.3 and is discussed

in Ref. 7. This chapter will deal primarily with beams having a/d or M/Vd ratios greater than about two. Deeper beams will be considered in Chapter 4.

It is generally assumed that the M/Vd concept can be used equally well in simply supported and continuous beams. This is not entirely true, however, especially for the common range of M/Vd ratios for negative moment regions ($M/Vd = 2$ to 3). The initial development of flexure-shear cracking is similar in the various portions of a continuous beam and the equivalent simple beams (22). Once the inclined cracks have developed, the load carrying mechanism of a beam loaded on its top face and supported on the bottom changes from pure beam action to a type of tied arch action with a diagonal compression strut from the load to the reaction as shown in Fig. 3.13(b). As a result, the regions of tensile force in the longitudinal bars frequently extend past the point of inflection, as shown in Fig. 3.14(c), leading to possible anchorage failures in these regions (30,112,119,151,164). The meaning of the terms, a/d and M/Vd , becomes difficult to define in such a case. Ferguson (64) has proposed that the ratio, a_s/d , shown in Fig. 3.13(a) be used in place of M/Vd in Eq. 3.6 when computing v_c or that v_c be taken equal to $2\sqrt{f'_c}$ in all cases for continuous reinforced concrete beams.

For continuous prestressed concrete beams the inclined thrust shown in Fig. 3.13(b) appears to delay the development of inclined cracking in the region of contraflexure (84). Once inclined cracks occur in that region, however, the ultimate shear strength of prestressed concrete beams with web reinforcement is best calculated using the ACI Code formulas (84, 168).

(b) Directly and Indirectly Loaded Beams

In most beams tests the loads and reactions are applied on the top and bottom of the beam, respectively. Such beams are said to be "directly loaded." For directly loaded beams with a/d ratios less than 2.5 this leads to a significant vertical compressive stress component between the load and reaction and as a result the shear strength is increased. Thus, a portion of the increase shown in Fig. 3.12 between the inclined cracking and shear compression capacities of beams with a/d less than 2.5 is due to vertical stresses or arch action. For directly loaded beams having a/d ratios less than 2.5 the 1971 ACI Building Code Equation (11-12) allows an increase in v_c . Zsutty (200) has proposed Eq. 3.14 to account for the direct loading effects in short beams:

$$v_c = (\text{Eq. 3.9}) \left(\frac{2.5}{a/d} \right) \quad (3.14)$$

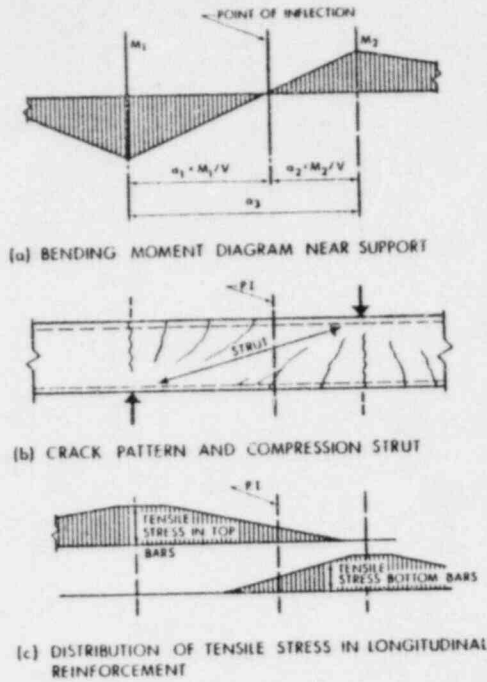


FIG. 3.13.—Behavior of Continuous Beams

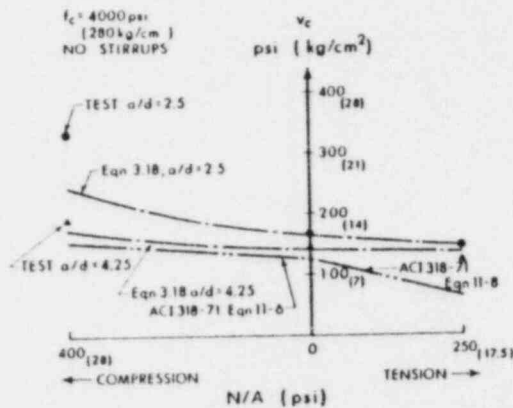


FIG. 3.14.—Variation of v_c with Axial Stress for Different Values of a/d (133)

Leonhardt (112) has proposed a similar equation.

Frequently in practice, beams are loaded or supported by intersecting beams so that the load transfer is by shear rather than by bearing on the top and bottom surface. These are referred to as "indirectly" loaded beams. A number of investigators have reported tests of such beams (15,61,119,177,182). For beams having a/d ratios greater than 2.5 to 3, there was no reduction in shear strength in such beams due to indirect loading provided that there was sufficient reinforcement in the intersection region to transfer the load from the supported member to the supporting member. Leonhardt, et al. (119) recommended the use of "hanger" reinforcement of stirrups or bent bars sufficient to transfer 80% of the shear force at the joint when beams of equal depth are connected and 100% of the shear force in the case in which the supported beam is connected only to the tension side of the supporting beam. Baumann and Rüsç (15) recommend hanger reinforcement for 100% of the load transferred. These stirrups should be provided within $d/2$ of the center of the joint in the members joined (115). In addition, it is good practice for the longitudinal reinforcement in the supported beam to pass over that in the supporting beam where possible.

For a/d less than 2.5, however, indirectly loaded beams are weaker than directly loaded beams because arch action cannot develop. Such beams tend to fail in diagonal tension at the inclined cracking load. Zsutty (200) shows that Eq. 3.9, developed to predict the shear strength of slender beams without web reinforcement, also applies for indirectly loaded short beams.

3.4.4 Effect of Type of Loading

(a) Repeated Loadings

From tests of 39 small beams without web reinforcement, Chang and Kesler (38) found that the inclined cracking shears and ultimate shears having a 50% probability at 2,000,000 cycles were 50% and 63% of the corresponding static strength. These beams failed either by crushing of the compression zone over the inclined crack or by a diagonal tension failure.

Price and Edwards (156) found the tensile fatigue strength of concrete at 3,000,000 cycles was about 60%-75% of the static tensile strength. This strength reduction may explain the reduced inclined cracking load in Chang and Kesler's beams.

Kokubu and Higai (103) report that beams with a/d ratios of 2 to 4 and no stirrups may fail due to fatigue fracture of the longitudinal reinforcement at the point where the inclined crack intersects the bar. In their tests, localized flexural stresses due to the dowel action in the reinforcement in this region led to fatigue failures at 51% to 70% of the static failure load. Similar beams developed shear compression failures in static tests. For beams with a/d of 5 the inclined cracking

and diagonal tension failure loads were each reduced by about 35%. On the basis of their tests, Kokubu and Higai have suggested that the shear strength corresponding to 10^6 cycles of load in each shear failure made is about 60% of the static failure load.

In tests of the cracking behavior of T-, I-, and rectangular reinforced concrete beams Kaar and Mattock (95) found that the stirrup stresses increased approximately 50% during the first 300,000 cycles of service load ($D + L$) and did not increase appreciably during another 700,000 cycles at the same load.

Prestressed concrete beams tested by Hanson, et al. (77,78) had an excellent shear fatigue resistance. Fatigue fractures of the web reinforcement were due primarily to flexural stresses in the stirrups due to dowelling. The range in the crack widths during repeated loading was an important factor in determining whether a shear fatigue failure would occur.

Burton and Hognestad (32) have shown that tack welding of stirrups to longitudinal reinforcement can significantly reduce the fatigue strength of the longitudinal bars. In their tests the stress range corresponding to failure at 5,000,000 cycles was 35% lower in beams with tack welded stirrups than in beams with tied stirrups.

(b) Dynamic Loadings

Extensive tests of simply supported reinforced concrete beams under dynamic loads indicate that the shear, moment, shear strength, and flexural strength all increase under a dynamic load with respect to the same load applied statically (166). However, the usable ultimate shear strength and the flexural yield strength increase in different proportions as do the contributions of the concrete and web reinforcement to the shear strength. In some cases the compression zones of beams failed prior to yield of the stirrups suggesting a need for an upper limit on shear strength under dynamic loads. For design, Seabold (166) has recommended the use of the modified truss analogy using Eq. 3.12 to compute V_c and using an amplified stirrup yield strength to account for the increase in yield strength under rapidly applied loads.

(c) Reversed Loadings

When a beam is subjected to reversals of loading, inclined cracks develop across the cracking caused by the preceding loading. Tests in which reversals of loading have been applied have shown that cross-inclined-cracking occurring before yielding of shear reinforcement does not destroy the integrity of the member (2,23), but uncertainty exists regarding the effect of reversals of loading on ultimate shear strength.

Alatorre and Casillas (2) tested 52 beams with a/d equal to 4.4 under reversed cycles of shear and moment. They report that the behavior was not significantly altered by the application of a few cycles of relatively high loads, except that there was

a trend to a lower stiffness with increasing loads. The ACI design equations were found to be conservative for these beams.

On the other hand, Japanese investigators (146) have proposed the use of a reduced capacity of stirrups in beams and girders subjected to seismic loadings as given by:

$$v_{\text{red}} = v_c + 0.5f_y(\rho_n - 0.002) \quad (3.15)$$

in which v_c is about equal to the ACI value. Thus the shear assumed to be carried by the web reinforcement is less than half that computed using the ACI recommendations.

Paulay (151) applied reversed cycles of high shearing force to deep members restrained at each end. In the first few cycles the beams behaved as predicted by the ACI Code Sections 11.4.2 and 11.6.1 but as load cycling continued the shear carried by the concrete decreased. Following yielding of the web reinforcement, a high load was carried by arch action. Failure generally occurred by crushing and shearing of the ends of the arch. Significant decreases in stiffness were observed as the test progressed.

The apparent discrepancies may be due to the severity of the loading cycles considered by the various investigators. In a beam loaded statically to failure without load cycle reversals, Eq. 2.1 suggests that portions of the shear are carried by the uncracked concrete above the inclined cracks, the dowel action of the reinforcement, and interface shear transfer across the crack. For statically loaded beams and beams subjected to nonreversing cyclic loads ACI 318-71 Chapter 11 gives conservative strength values. In a member containing x-shaped cracks due to load reversals, however, the compression zone is cracked and due to residual tension strains in the precompression reinforcement following a load reversal, the cracks may not close completely. Thus the shear transferred by the compression zone may be smaller than in a normal beam. Interface shear transfer is unreliable since it may be reduced by a "working back and forth" action along the cracks as the load is cycled. Finally, dowel action will only be dependable under cyclic loads if splitting along the longitudinal bars is restrained by closely spaced stirrups. Based on this reasoning, Bresler (23) has proposed that stirrups be provided for the full shear in beams where full reversal takes place.

3.4.5 Effect of Axial Loading

(a) Behavior of Axially Loaded Beams in Tests

In a group of three otherwise identical beams subjected to axial tension, no axial force, and axial compression, the initial flexural cracks would occur earliest in the beam with axial tension forces and would extend farther and be more nearly vertical in this beam. In all three beams, however, approximately the same additional increment of shear is required be-

tween flexural cracking in the shear span and inclined cracking. The inclined cracks would have essentially the same slope in all three beams, cutting across or growing out of pre-existing flexural cracks (72,133). As shown in Fig. 3.14, the effect of axial forces on the shear at inclined cracking may not be too significant (72) especially for slender beams or for tensile loadings. Axial tensile cracks which had formed prior to the application of the shear loading had very little effect on the behavior and strength of beams tested by MacGregor (125) but reduced the strength of beams tested by Haddadin, et al. (72) who recommend that the shear carried by the concrete be taken equal to zero if the average axial tensile stress exceeds $4\sqrt{f'_c}$.

(b) Calculation of Inclined Cracking Load

The inclined cracking load of axially loaded beams has been estimated through two distinct concepts. The first considers the principal tensile stresses at the head of a flexure crack. For beams without axial loads, such an analysis yielded Eq.

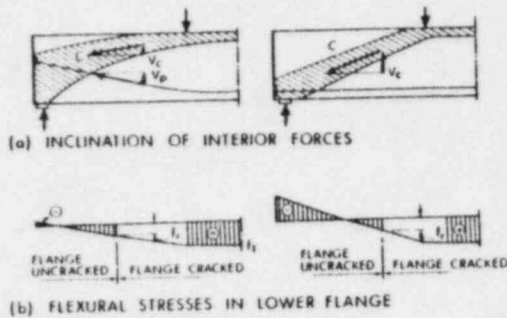


FIG. 3.15.—Effect of Draped Reinforcement on Interior Forces in Prestressed Beams (114)

3.6 presented in Section 3.2 of this report. Committee 326 (7) also showed that this equation could be applied to axially loaded beams if the term, M , is replaced by M_m in which:

$$M_m = M - N \left(\frac{4H - d}{8} \right) \dots \dots \dots (3.16)$$

N = axial load, positive in compression

If this is done, Eq. 3.6 can be rewritten as:

$$\frac{V_c}{b_w d} = 1.9 \sqrt{f'_c} + \frac{2,500 \rho_w V d}{M_m} \dots \dots \dots (3.17)$$

Tests by Haddadin, Hong, and Mattock (72) suggest that this equation accounts for the effects of axial loads in a reasonable manner as shown in Fig. 3.14.

Alternately, investigators (133) have attempted to predict inclined cracking in axially loaded members using the shear-increment concept, which postulates that the load causing a diagonal tension crack as a development of a flexure crack is equal to the sum of the load causing flexure cracks and the load increment required to transform the flexure crack to a diagonal tension crack. Eqs. 3.7 and 3.8 are examples of this approach. The inclusion of the modular ratio, n , and the steel percentage, ρ , in Eq. 3.8 possibly accounts for the greater dowel action due to increased steel area and the fact that flexural cracks tend to be narrower and do not extend as high if $n\rho$ is large.

Because Eq. 3.17 is frequently difficult to apply in design, ACI-318-71 allows the designer to use the simplified equations (Eqs. 11.6 and 11.8 of ACI-318-71) plotted in Fig. 3.15 to compute the shear carried by the concrete in beams subjected to axial forces. The CEB Recommendations (41) present similar equations.

The interaction diagrams for axial compression and shear presented in Section 2.1 of this report (Fig. 2.4) rise to a maximum for $f_c = 0.6 f'_c$ and then drop off. This suggests that for very high axial loads, care should be exercised in choosing the maximum shears at ultimate load because in this region an increase in axial load may lead to a decrease in shear strength.

(c) Effectiveness of Web Reinforcement in Beams with Axial Forces

Recent investigations at the University of Washington have shown that the presence of axial, tensile, or compressive forces does not alter the effectiveness of web reinforcement (72). These tests suggested that the use of the ACI stirrup design equation, Eq. 3.29, along with Eq. 3.17 to compute the shear in the concrete, led to an overconservative design for low percentages of web reinforcement and was adequately conservative for high web reinforcement ratios. Similar results were found for beams subjected to axial forces.

In beams subjected to high axial tensions, cracks may traverse the entire beam. Although large shears can be transferred across such cracks by interface shear transfer, inclined stirrups may be desirable to prevent shearing displacements along such cracks under repeated load conditions (125).

3.4.6 Effect of Prestressing

The ACI Code method of designing prestressed concrete beams to withstand shearing forces is based on the assumptions listed in Section 3.6.1. In this procedure stirrups are provided for:

$$V_s = V_u - V_c \dots \dots \dots (3.18)$$

The shear "carried by the concrete," V_c , is assumed to be equal to the inclined cracking shear as defined by Eq. 3.5 and 3.7 and as such, includes any vertical component of the prestressing force.

This assumption grew out of the extensive series of the prestressed concrete beams tested at the University of Illinois between 1954 and 1962 (85,128,148). The major difference in the behavior and shear strength of the portions of beams with flexural cracks in the tension flange and those portions without such cracks was recognized for the first time in this procedure. Adaptations of this procedure have been incorporated in the Canadian (34), Australian (82), and British (162) building standards. The following simplified equation for computing V_c , recently proposed by Hanson (126) for prestressed building members is also included in the 1971 ACI Code:

$$v_c = \frac{V_c}{b_w d} = 0.6 \sqrt{f'_c} + 700 \frac{V_u d}{M_u} \quad (3.19)$$

in which $2 \sqrt{f'_c} \leq v_c \leq 5 \sqrt{f'_c}$.

This equation is limited to members having an effective prestressing force at least equal to 40% of the tensile strength of the tensile reinforcement.

Although these equations were developed for small beams, Gustafson (71) has shown that the ACI design procedure based on Eqs. 3.5 and 3.7 gave satisfactory results for 45-ft span AASHTO III standard prestressed highway bridge beams with an overall depth of 45 in. The ratio of measured to ACI failure load was 1.133.

In recent years the ACI design procedure has been criticized by several noted European engineers (11,114) on three principal grounds:

1. No valid reason has yet been presented why V_c should equal the inclined cracking shear, V_{cr} . Bachmann and Thurlimann (11) suggest that V_c should be related to the size of the compression zone at failure. This, in turn, may be affected by the stage of loading at which inclined cracking develops, but this has not been proven to date.

2. The ACI equations for V_c are excessively conservative for a member containing both prestressed and normal tension reinforcement, an increasingly popular form of partial prestressing (33, 184). This latter observation has also been made by Burns and Pierce (31). Eq. 3.8, proposed by Mattock (133) to extend the range of the basic flexure-shear equation (Eq. 3.7), goes a long way to satisfying this complaint at the expense of increased complexity.

3. The ACI procedure is unnecessarily complex.

In a major series of tests of large prestressed concrete beams carried out in Stuttgart (114), the shear carried by the concrete, V_c , was only 10% to 60% of V_{cr} when the stirrups yielded. Although the shear, V_c , increased somewhat between stirrup yield and beam failure, it generally did not reach V_{cr} . Leonhardt (114) has recommended that the load corresponding to yielding of the stirrups should be taken as the failure load for design purposes. He also pointed

out the danger of web crushing failures.

Bachmann and Thurlimann (111), proposed the following design equations for reinforced, partially prestressed, and prestressed concrete beams. The equations have been checked against tests and form a part of the Swiss building regulations (11):

For regions with flexural cracks in the tension flange at design capacity

$$V_u = V_c + V'_u + V_p \quad (3.20)$$

in which V_p = vertical component of prestress

$$\frac{V_c}{b' d} = v_o \left(1 + \frac{f_{se} A_{sp}}{\Sigma f_{su} A_s} \right) \text{ but not more than } 1.5 v_o \quad (3.21)$$

$$v_o = 57 + 0.025 f'_c \quad (3.22)$$

in which $f_{se} A_{sp}$ = prestressing force after all losses; and $\Sigma f_{su} A_s$ = total force in tensile reinforcement at ultimate = $f_{ps} A_{sp} + f_y A_s$.

For regions of beams without flexural cracks in the tension flange at design capacity

$$V_u = V_c + V_N + V'_u + V_p \quad (3.23)$$

in which V_N = shear transferred by the uncracked tension flange = $0.2 f_{cp} b_w d$.

The sum of $V_c + V_N$ can be shown to closely approximate the web-shear cracking equation in the ACI Code (Eq. 3.5).

In a recent series of tests of prestressed and partially prestressed beams reported by Cafilisch and Thurlimann (33) the shear corresponding to yield of the stirrups was closely predicted by Eq. 3.20. The shear capacities ranged from 110% to 168% of this value. It was also concluded for these tests that $V_c + V_p$ were approximately equal to the inclined cracking load. Note, however, that for nonprestressed beams with small steel ratios, Eqs. 3.21 and 3.22 are unconservative compared to Eqs. 3.9 and 3.12.

The inequality of the inclined cracking load and the shear carried by the concrete is also suggested by tests of normal weight and lightweight concrete prestressed concrete T-beams with stirrups tested by Krauss and Bachmann (106). Although the average principal tensile stress at inclined cracking was 20% lower in the lightweight concrete beams than in the normal concrete beams, the average ratios of shear at yielding of the stirrups to that calculated with Eqs. 3.20 and 3.22 were 1.04 and 1.03, respectively, for lightweight and normal concrete.

Leonhardt (114) has recently used Fig. 3.15 to suggest that an increase in V_p should lead to a decrease in the shear in the concrete, V_c , in beams with cracked tension flanges. The bottom portion of the figure shows that flexural cracking extends over a greater length in the beam with draped cables than in the beam with straight cables. In addition, Leonhardt notes that if prestressing ducts with

a diameter greater than $b_w/10$ are placed in the web of a beam, one should use a reduced web thickness in calculating the diagonal crushing strength of the web. He proposes the use of a reduced b_w :

$$b_w \text{ reduced} = b_w - \frac{2}{3} \Sigma \phi \quad \dots \dots \dots (3.24)$$

in which ϕ = diameter of ducts.

MacGregor, Siess, and Sozen (127) in a series of tests of prestressed beams under simulated moving loads, concluded that the development of cracking in these beams was similar to that in beams tested under stationary loads and that the same basic equations could be used to analyze both groups.

DePaiva, Neville, and Guger (53), in a series of tests of continuous prestressed concrete beams with varying level supports, concluded that moderate relative movement of the supports did not significantly affect the behavior and strength of the beams in shear. The inclined cracking loads were closely predicted by equations similar to Eqs. 3.5 and 3.7.

Hanson, Hulsbos, and Van Horn (77,78) performed a series of fatigue tests of prestressed concrete I-beams containing web reinforcement. In their tests, prestressed concrete beams with enough web reinforcement to develop their flexural capacity were able to sustain large overloads without subsequent danger of a shear fatigue failure under design loads. Additional test data on the fatigue strength in shear of prestressed concrete I-beams have been reported by Price and Edwards (156).

3.4.7 Effect of Lightweight Aggregate Concrete

In 1962 the ACI-ASCE Shear Committee proposed an equation for the inclined cracking shear of the form:

$$\frac{V}{bd \sqrt{f'_c}} = \alpha_1 + \alpha_2 \frac{\rho Vd}{M \sqrt{f'_c}} \quad \dots \dots \dots (3.25)$$

A statistical analysis of test data for normal weight concrete beams resulted in the values of α_1 and α_2 given in Eq. 3.6.

An attempt was made to evaluate these constants for lightweight aggregate concrete as a single group on the basis of 74 tests conducted at the Portland Cement Association and University of Texas Laboratories (74). The test data involved nine different lightweight aggregates and it was concluded that a reasonably conservative choice of the two constants would result in extreme conservatism for some of the aggregates due to the fact that different aggregates produce concrete with different tensile strengths. As a result the tensile strength was included in the shear equation for lightweight aggregate concretes in the 1963 ACI Building Code, and Hanson. in his report on shear strength of structural lightweight concrete (74) stated:

"It has been found that diagonal tension strength of the lightweight concrete is affected by the same variables as affect the resistance of normal weight concrete. The difference between the types of materials is one of magnitude of diagonal tension resistance and not of fundamental difference in behavior."

Further testing and studies of lightweight beams were carried out at the Texas Transportation Institute (90) leading to the design rules in Section 11.3 of the 1971 ACI Code. Note that none of the beams studied in Refs. 74 and 90 had web reinforcement.

In companion tests of lightweight and normal weight prestressed concrete beams with stirrups discussed earlier in Section 3.4.6 (106) the inclined cracking load of the lightweight beams appeared to be a function of the lower tensile strength in these beams. The contribution of the concrete to the ultimate shear capacity appeared to be a function of its compression strength, however.

Recent studies of the shear failure phenomenon have suggested several other reasons why the shear strength of lightweight concrete members may differ from that of normal weight concrete:

1. It has been suggested (8) that the mode of bond failure may involve shearing or crushing of the concrete under the lugs rather than splitting as experienced with normal concretes.
2. The amount of shear transferred by interface shear transfer is probably less in lightweight concrete members due to the smoother crack surface.
3. Recent Soviet and Japanese tests have suggested that the strength of lightweight concrete may be less than that for normal weight concrete under biaxial tensile-compressive stress (197,143).

3.4.8 Factors Affecting Inclined Crack Widths

The control of crack widths at working loads is an important serviceability criteria for reinforced concrete structures. Although recent design recommendations include proposals for the control of the widths of tensile and flexural cracks, only the Soviet Code contains provisions for shear cracks. It has been reported (153) that inclined crack widths can not be satisfactorily predicted using this code. Relatively little test data are available at present with respect to spacing and widths of diagonal tension cracks. Measurements of the widths of shear cracks have been reported by Leonhardt and Walther (116), Placas and Regan (153), Haddadin (72), and others (95,125).

An unpublished statistical study of German data on inclined crack widths in beams of 12 in. to 18 in. in overall depth suggested that $(V - V_c)$, M/Vd , f'_c , d , stirrup diameter, and stirrup angle were significant variables in decreasing order of significance (125). A good correlation was found between crack width and stirrup strain. For a stirrup strain of 0.001, the maximum and average

crack widths calculated from the regression equation were about 0.012 in. and 0.005 in. (0.3 mm and 0.125 mm), respectively.

In a study conducted at PCA (95) the widths of flexural and diagonal cracks in girder webs were reported for I, Tee, and rectangular girders. It was concluded that longitudinal reinforcement spaced over the depth of the web of a Tee girder (face steel) was effective in controlling flexural cracking in the web but was less effective in controlling diagonal cracking. For flexural cracking it was found that for a given steel stress there was an apparent correlation between crack width and the area of concrete surrounding each bar regardless of the bar diameter. The only conclusion reported concerning diagonal cracks was that for a given amount of web reinforcement the width and spacing of diagonal cracks occurring in a girder web appeared to increase with increase in width of the web. In these tests, inclined crack widths were reported for three half size bridge girders with 75,000 psi (5300 kg/cm²) yield strength main reinforcement with a design ultimate capacity of 1.5D + 2.5L in which D and L refer to service dead and live load, respectively. Under a static load of 1(D + L) the maximum inclined crack widths ranged from 0.007 in. to 0.009 in. (0.18 mm to 0.23 mm) in the three beams. After 1,000,000 loading cycles between D and 1(D + L) the maximum inclined crack widths were 0.008 in. to 0.012 in. (0.2 mm to 0.3 mm).

Leonhardt and Walther (116) have made extensive crack width measurements on many types of beams. One series compared crack widths in otherwise similar beams with three different types of web reinforcement. As shown in Fig. 3.16, the crack widths were smallest in a beam with closely spaced inclined stirrups, followed by a beam with vertical stirrups. The widest cracks occurred in a beam with bent up bars.

Several authors have attempted to compute the width of inclined cracks. By integrating strains along a stirrup in the cracked web of a beam (20,125) the crack width, w, should be a function of:

$$w = fn \left[\int_0^{l_c} (\epsilon_s - \epsilon_c) dx \right] = fn \left(\frac{f_v}{E_s} l_c \right) \dots \dots \dots (3.26)$$

in which l_c = the distance between cracks along the stirrup; and $\epsilon_s = f_v/E_s$ and ϵ_c are the strains in the stirrup and surrounding concrete, respectively. By substituting expressions for f_v and l_c into Eq. 3.26, it is possible to derive an equation for the crack width.

Based on similar reasoning the test data, Placas and Regan (153) have proposed:

$$w_{max} = \frac{s \sin \alpha}{10^6 \rho_n (f'_c)^{1/3}} \left(\frac{V - V_c}{b_w d} \right) \dots \dots \dots (3.27)$$

Haddadin, Hong, and Mattock (72) found that the foregoing concept did not adequately explain the variation in crack widths, but

observed that for high values of the shear reinforcement ratio, $\rho_n f_y$, the maximum crack width at working load stabilized at about 0.006 in. (0.15 mm) if v_u is limited to $10 \sqrt{f'_c}$ as required by the

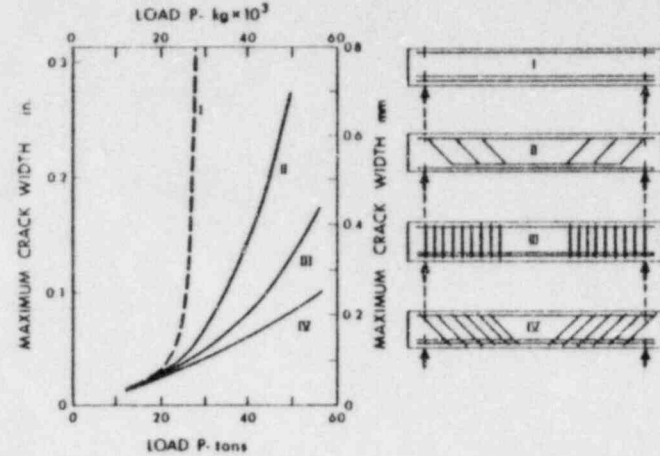
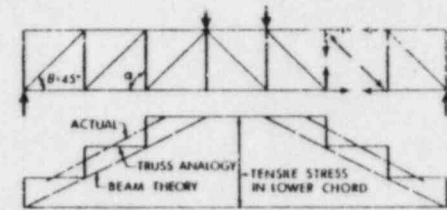
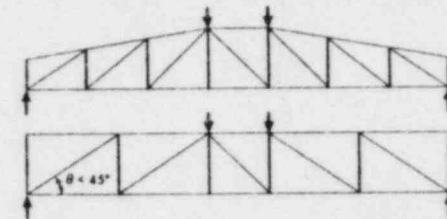


FIG. 3.16.—Effect of Type of Web Reinforcement on Width of Inclined Cracks (112)



(a) DISTRIBUTION OF FORCES IN CLASSICAL TRUSS ANALOGY



(b) MODIFIED TRUSS ANALOGIES

FIG. 3.17.—Truss Analogies

ACI Code. If it is assumed that the width of inclined cracks is a function of the stress in the stirrups, which in turn is a function of $(v - v_c)$, it may be possible to control crack widths at service

loads by limiting the value of $(v_u - v_c)$ at the ultimate load. Thus, for stirrups having a yield strength of 60,000 psi (4,200 kg/cm²) a load factor of 1.6 and an upper limit on $(v_u - v_c)$ of $8\sqrt{f'_c}$, the stirrup stress at service load $1(D + L)$ will be about 32,000 psi (2,200 kg/cm²) corresponding to a maximum crack width of about 0.013 in. (0.32 mm).

Carpenter and Hanson (37) have proposed a design method to limit the width of inclined cracks in beams with thin webs. This design method assumes all the shear in a cracked web is taken by vertical stirrups and uses the Kaar and Mattock (95) equation for flexural crack width to determine the allowable stress in the stirrups for a given crack width at service loads.

The widths of inclined cracks in large prestressed concrete beams were reported by Hanson, Hulsbos, and Van Horn (77,78). The widths of web-shear cracks were function of $V - V_{cr}$, ρ_n , and a/d . On the other hand, the width of flexure-shear cracks seemed insensitive to ρ_n . In general, the cracks were very wide and much more reinforcement than that required by the 1971 ACI Code would be necessary to hold the crack widths to acceptable values.

3.5 Methods of analysis of the Shear Strength of Beams

3.5.1 The Truss Analogy

At the beginning of this century Ritter and Morsch introduced the truss analogy for the design of web reinforcement in reinforced concrete beams (88). This analogy assumes that a reinforced concrete beam with inclined cracks can be replaced by the hinged jointed truss shown in Fig. 3.17(a). In its most common form the crack angle, θ , is assumed to be 45°. This model is extremely simplified, ignoring the shearing forces, V_{cr} , V_{ay} , and V_d in Fig. 2.5 and Eq. 2.1, and a number of authors have tried to improve it by sloping the compression chord as shown in Fig. 3.17(b) or by changing the slope of the compression diagonals (112). More important, perhaps, it does not attempt to satisfy compatibility.

Regardless of the shortcomings of the truss analogy, however, it is an excellent conceptual tool in the study of beams with web reinforcement. It indicates the presence of tensile stresses in stirrups and compression stresses in the concrete between the inclined cracks, and correctly shows the effect of variation in the stirrup angle on these stresses. It may be used to derive the basic equations for the design of web reinforcement. Finally, as shown in Fig. 3.17(a) it clearly and correctly shows that the stresses in the longitudinal tensile reinforcement in the shear span are larger than those predicted from beam theory. Thus it shows that the diagram indicating the tensile force in the longitudinal reinforcement is displaced toward the supports compared to that given by beam theory leading to possible bond or anchorage problems.

3.5.2 Equilibrium Analyses

Short beams or beams with web reinforcement may develop a shear compression failure, as shown in Fig. 3.3(b). Over the past three decades a number of authors (21,25,70,168,192,202) have at-

tempted to develop analyses for this type of failure. These usually involve summing moments about a point in the compression zone above the end of the inclined crack. Generally the effect of the shearing stresses in the strength of the compression zone (Section 2.1) is considered (25,70,168,192). Some analyses attempt to allow for dowel action (149) and others consider strain compatibility (192,153). Taylor has included the effect of loss of dowel action and interface shear transfer in an analysis (180).

In slender beams without stirrups, T-beams, and beams with compression reinforcement, the final failure may result from a shearing action in the compression flange. Placas (153) has presented an analysis of this mode of failure based on equilibrium of vertical forces on an inclined plane along an inclined crack. For many years the Soviet building codes have required a check of equilibrium of vertical forces and of moments in the design of concrete beams (20,21,138).

3.5.3 Statistical Estimates of Shearing Strength of Beams

Recently, several authors have presented statistical studies of the factors affecting the shear failure capacity of reinforced concrete beams (101,199). These studies suggest that the most significant variables affecting diagonal tension failures were the same as for inclined cracking (199). For shear compression failures the most significant variables appeared to be the concrete strength, the percentage of longitudinal reinforcement, the spacing, angle and ratio of the stirrups, and the a/d ratio. For beams with web reinforcement failing in shear-compression, the failure shear minus the shear carried by the web reinforcement differed, in general, from the shear corresponding to inclined cracking (101).

3.6 Approaches to Design of Beams for Shear Strength

Refs. 7 and 88 survey the historical development of methods of designing beams to resist shearing forces. This section will briefly review the basic assumptions in three current design procedures. The following section, 3.7, will list a number of requirements for a comprehensive design procedure to handle shear in beams.

3.6.1 American Concrete Institute

In 1962, ACI-ASCE Committee 326, "Shear and Diagonal Tension," presented a procedure for the shear design of reinforced concrete members (7) which was based on four assumptions (126):

1. For a beam without web reinforcement, the shearing force, V_{cr} , which causes the first diagonal cracking can be taken as the shear capacity of the beam. Eq. 3.6 for V_{cr} was derived in Ref. 7.
2. For a beam with web reinforcement, the concrete can be assumed able to carry a constant amount of shear, V_c , regardless of the stage of loading or the state of cracking. Thus, any web reinforcement needs to be designed to carry only that shear in excess of the concrete contribution as given by Eq. 3.18:

$$V_u = V_c + V_s \dots \dots \dots (3.18)$$

in which V_s = shear carried by web reinforcement.

3. The constant shearing force in the concrete, V_c , can be taken equal to that causing diagonal cracking, V_{cr} . Thus Eq. 3.18 becomes:

$$V_u = V_c + V_s \quad (3.28)$$

4. The shear force, V_s , resisted by the stirrups is calculated assuming the inclined crack has a horizontal projection of d :

$$V_s = \frac{A_s f_y d}{s} (\sin \alpha + \cos \alpha) \quad (3.29)$$

Because an equation similar to Eq. 3.29 can also be derived from the truss analogy the design procedure involving Eqs. 3.18 and 3.29 will be referred to as the "modified truss analogy" procedure.

About the same time, the same four assumptions were made in deriving design relationships for prestressed concrete although different procedures were used to define the inclined cracking shear (5). Although assumptions 1 and 4 are widely accepted as reasonable engineering approximations to the behavior of beams, the second and third assumptions have been strongly questioned (1.,114).

3.6.2 European Concrete Committee

The 1970 CEB-FIP Recommendations (41) present a design procedure somewhat similar to that of the ACI Code. Code. With the exception of certain slabs or wide beams, all members must have at least a minimum amount of web reinforcement. So other members the CEB recognizes three zones of behavior:

Zone A corresponds to a part of a structure having negligible probability of flexural or shear cracking. In this region it may be necessary to check whether failure can occur due to combined shear and compression.

Zone B corresponds to portions of members developing web-shear cracks and not having flexural cracks at ultimate. In this region of a beam, web reinforcement must be provided for the difference between the principal tensile stress at ultimate in an uncracked member and a reduced value of the tensile strength of the concrete. Failure due to crushing of the web must also be prevented.

Zone C corresponds to those portions of beams in which flexure-shear cracking can occur. The maximum shear is limited to prevent crushing of the web. Web reinforcement is designed using Eq. 3.18 and an equation similar to Eq. 3.29. The shear, V_c , carried by the concrete is a function of the amount of longitudinal reinforcement and the square root of the concrete strength. Depending on the amount and distribution of the web reinforcement, the tension force at a point in the flange of a beam is calculated using the moment existing at a distance from $0.2d$ to $1.5d$ from the section under consideration in the direction in which the absolute value of the moment increases.

For axially loaded and prestressed beams the design procedure involves checking zones B and C. In zone C the shear, V_c , carried by the concrete is increased as a function of the average prestress.

3.6.3 Soviet Building Regulations

The building codes of the Soviet Union use a completely different design procedure to check the shear strength of a member (20,21,138). First, a right cross section is designed for flexure and axial loads and then an inclined section is checked for shear. The design of the inclined section involves four steps. First, stirrups or bent bars are chosen considering equilibrium of vertical forces using Eq. 3.18. The shear carried by the concrete is assumed to be a function of the tensile strength of the concrete and the horizontal projection of the inclined crack, c . The value of c is taken as that length giving the minimum value of V_u from Eq. 3.18. The anticipated width of the inclined cracks is checked for working loads and the amount of stirrups is increased, if necessary, to limit the crack width. Once the transverse reinforcement has been chosen, it is necessary to check whether moment equilibrium can exist on the inclined section at ultimate. This is done by summing moments about the centroid of the compression block over the inclined crack. The depth of the compression zone is taken equal to that for flexure. In a few cases this check may lead to a revision in the longitudinal reinforcement. Finally, the maximum shear stress on the web is limited to prevent crushing of the inclined concrete struts in the web (20,21,138).

3.7 Summary of Shear Design Requirements for Beams

In this section of the basic requirements for the design of reinforced and prestressed concrete are reviewed in the light of the research data presented earlier in this chapter. This analysis is not intended as a building code or a recommended practice, but merely as a checklist for the future formulation of such documents. The design procedures described in the previous section are attempts to avoid most or all of the following modes of failure.

3.7.1 Significant Modes of Shear Failure

In the design of beams of normal proportions the modes of shear failure that must be considered directly or indirectly in any design procedure are:

1. Beams without web reinforcement having a/d ratios greater than 2 to 3 will fail upon or shortly after formation of an inclined crack. The failure is generally sudden with little warning.
2. The web reinforcement may yield followed by breakdown of aggregate interlock and dowel action. In this case, the final failure is generally due to crushing or shearing of the compression zone.
3. In beams having very thin webs, the webs may crush due to inclined compressive stresses prior to yielding of the stirrups.
4. The anchorages of the stirrups may fail prior to yield of the stirrups leading to a frequently sudden failure.
5. Due to inclined cracking, the stresses in the longitudinal rein-

forcement tend to be higher than those due to flexure. As a result, anchorage failures or other failures of the tension chord may occur.

6. The shear transfer from the web to the flanges of T- and I-beams may cause severe cracking which may lead to separation of the web from the flanges.

7. Excessive crack widths may constitute failure of the beam for serviceability reasons.

These various failure modes are discussed more fully in the following paragraphs:

(a) Shear Failure of Beams Without Web Reinforcement

Beams without web reinforcement having $a/d > 2$ to 3 will fail at or shortly after inclined cracking. For such members the inclined cracking load is the critical design parameter. The present ACI design equations for v_c overestimate the inclined cracking shear for beams having low steel percentages. For this reason, study should be given to adopting design equations similar to Eqs. 3.9 or 3.12 in place of $v_c = 2\sqrt{f'_c}$ and Eq. 3.6.

Because the failure of beams without stirrups is sudden with little warning, web reinforcement should be provided wherever possible. In the ACI Code this is accomplished by requiring a minimum amount of web reinforcement. In those cases in which this is not feasible, it may be desirable to reduce the member understrength factor, ϕ , in recognition of the undesirable mode of failure. This could also be accomplished by limiting the shear in an unreinforced web to one-half to two-thirds of v_c for a reinforced web.

(b) Shear Failure Initiated by Stirrup Yield

Probably the most common design case for beams involves failures initiated by stirrup yield. At failure, the shear force in the beam is resisted by stirrups and by the compression zone, dowel action, and interface shear transfer. The latter three components are frequently referred to as shear resisted "by the concrete."

At the present time the shear resisted by the stirrups at ultimate, V_u , is calculated by Eq. 3.29 derived from the truss analogy. Although this calculation tends to be conservative for low amounts of stirrups, the conservatism reduces as the stirrup ratio, $\rho_n = A_s/b_w s$, increases. For design purposes it appears that Eq. 3.29 is the best available and this report advocates its continued use.

Stirrups cannot be counted on to resist shear if they are not crossed by the inclined crack. For this reason, and because the ultimate dowelling shear is a function of the stirrup spacing, it is recommended that the stirrup spacing not exceed half the horizontal projection of the inclined crack, about $0.75d$. In addition, stirrups should be continued at least a distance, d , past the point where they theoretically are no longer required

to restrain inclined cracks starting at that point. Generally the requirement for minimum web reinforcement satisfies this.

Small diameter, closely spaced stirrups are desirable to control cracking. Welded wire fabric anchored according to the 1971 ACI Code (23) and the Commentary on this code is desirable in this respect.

Lapped U-shaped stirrups may sometimes be desirable and can be used, provided the laps are equal to a Class C splice (ACI 318-71) designed for the yield strength of the bars.

In the ACI Code the shear "carried by the concrete" is assumed equal to the inclined cracking shear, V_c . In view of the controversy surrounding this assumption, a complete reevaluation of V_c is required. In the meantime, it would seem reasonable to develop simpler expressions for V_c , particularly for prestressed concrete. Eqs. 3.9, 3.12, 3.19, and 3.21 seem to be particularly good starting points in such a study.

(c) Shear Failure Initiated by Web Crushing

In very thin webbed reinforced and prestressed concrete beams, failure may be initiated by crushing of the web prior to yielding of the stirrups. To prevent such a failure, the diagonal compression stresses and thus the shearing stresses must be limited. Thus, the maximum shearing stress, $v_u = V_u/\phi b_w d$, computed allowing for ducts, etc., in the web, should not exceed about $0.2 f'_c$ in beams with vertical stirrups and $0.25 f'_c$ in beams with 45° stirrups (41) as discussed in Section 3.4.1. Normally, such high shearing stresses will lead to unsightly diagonal cracks and should not be allowed except, possibly, close to prestressing ducts. The ACI 318-71 limits the shear to $v_u - v_c = 8\sqrt{f'_c}$. For reinforced concrete this limitation is more conservative than $0.2 f'_c$, if f'_c exceeds 2,500 psi. This may not be true for prestressed concrete or axially loaded members.

(d) Shear Failure Initiated by Failure of Stirrup Anchorages

In beams with a large amount of web reinforcement, cracks will cross many stirrups close to their upper anchorage. To behave as assumed in the design, it is imperative that these stirrups be well anchored. The stirrup anchorage requirements in the ACI Code are adequate in this respect.

(e) Shear Failure Initiated by Failure of Tension Chord

As shown by the truss analogy or other failure models (112), the stress in the longitudinal tensile reinforcement at a given point in the shear span is a function of the moment at a section located about d closer to the nearest section of maximum moment. The displacement of the actual tensile stress diagram compared to the diagram given by beam theory is a function of the web reinforcement ratio and the inclination of the web reinforcement, being most severe for small ratios of vertical stirrups. The ACI rule requiring that bars be extended d plus anchorage past the "theoretical cut-off point" is adequate for

beams having a moderate or high amount of web reinforcement, but may not be sufficient for very small values of the web reinforcement ratio, ρ_w .

In addition to the displacement of the tensile stress diagram, the choice of cutoff points for tensile bars must consider the possibility of increased shear cracking in the vicinity of the cutoff. The 1971 ACI Code adequately treats this problem in Section 12.1.6.

(f) Failure Initiated by Separation of Flanges and Web

A minimum amount of horizontal steel transverse to the beam axis is required in both tension and compression flanges to ensure the shear flow necessary for beam action. The relationships proposed by Robinson (163), Leonhardt (114), Placas (153), and Johnson (93), warrant further study in this regard.

(g) Serviceability Failure Due to Excess Inclined Crack Width

The width of inclined cracks in reinforced and prestressed concrete beams is a function of the stirrup strain, among other things. Studies presented in Section 3.4.8 suggest that limiting the maximum stirrup strain at working loads to 0.001 or limiting $(v_u - v_c)$ to $8\sqrt{f'_c}$ should prevent unsightly inclined cracks at working loads. For stirrups having a yield strength of 60,000 psi (4,200 kg/cm²) and for an extreme dead-to-live load ratio of 5, it can be shown that these two rules give similar results at service loads.

CHAPTER 4

4. Shear Strength of Special Members

4.1 Introduction

Chapter 11, Shear and Torsion, of the ACI Building Code (ACI 318-71) (6) contains separate special provisions for deep beams, brackets and corbels, beam-column connections, and shear walls. Quite often these special members have the characteristic of being relatively short and deep, having shear span to effective depth ratios, as measured by M/Vd , of less than about 2.5. Another common characteristic of many of these special members is that, in addition to main flexural reinforcement, they contain orthogonal reinforcement distributed throughout the member. Consequently, the usual methods of calculating flexural and shear strength may be conservative. More accurate methods are necessary if the aim of design is to provide shear capacity at least equal to flexural capacity.

Shear design provisions for special members are separated from those for ordinary beams in the ACI Code for two reasons. First, it is recognized that the method of load application, nature of loading, type of shear reinforcement, and reinforcement details have a substantial influence on the behavior of short, deep members. These factors are discussed in Section 4.2. It is worth noting specifically that the strength provisions of the ACI Code are largely based on static conditions. These provisions must be interpreted cautiously when they are extended to other load conditions, particularly earthquake and blast loadings.

Secondly, previous research on special members has been largely directed toward development of design recommendations, without regard to unification or compatibility. Committee 426 believes that considerable simplification in design can be achieved by research aimed at bridging the gaps between the design recommendations for these special members.

Consideration of shear-friction is one common method of looking at special members when the shear span to effective depth ratio is less than about one-half. This method is discussed in Section 4.3. The following Sections 4.4, through 4.9 present recent research findings and discuss design recommendations for specific special members.

4.2 Factors Affecting Behavior of Short, Deep Members

4.2.1 Method of Load Application

Concentrated loads or reactions may be applied to beams on the extreme compression or tension fibers, or through other structural members framing into the sides of the beam. While the former

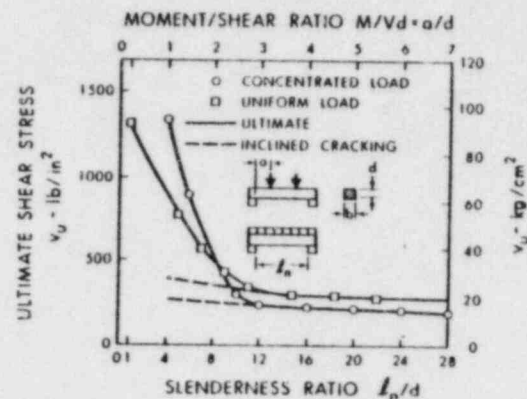


FIG. 4.1.—Reserve Shear Capacity of Deep Beams (113)

is the case most frequently simulated in the laboratory, the latter is more generally representative of actual structural systems. It was pointed out in Section 3.4.3(b) that the method of loading influences the behavior and shear strength of reinforced and prestressed concrete beams without shear reinforcement. These differences are significant in short, deep members (200).

The main effect of applying loads to a short, deep member without shear reinforcement, through bearing points on the top and bottom of the beam, fibers, is to increase the ultimate shear capacity above the shear causing inclined cracking (50,54) as shown in Fig. 4.1. The angle that the inclined cracking makes with the longitudinal axis of the member will also increase, particularly at very low M/Vd ratios of 1.0 or less. On the other hand, if the applied loads are distributed along the sides of a member, the shear strength and inclined cracking behavior will be about the same as in a similar

member with an a/d ratio of 2.5 or more (199).

4.2.2 Nature of Loading

Beam-column connections and shear walls are designed for wind and earthquake loadings which may cause reversals of shear. Under a wind loading, the main requirement is that a member develop its design ultimate strength. However, under an earthquake loading, it is essential that shear capacity be sustained while the member undergoes several cycles of reversed inelastic deformation.

When a member is subjected to reversals of loading, inclined cracks develop across the cracking caused by the preceding loading. Tests where reversals of loading have been applied have shown that cross-inclined-cracking occurring before yielding of shear reinforcement does not destroy the integrity of the member (2,35) but uncertainty exists regarding the effect of reversals of loading on ultimate shear strength. Most of the uncertainty has concerned the contribution of the concrete to the shear capacity of the member.

4.2.3 Type of Shear Reinforcement

As the M/Vd ratio of a short, deep member decreases from about 2.5 to 0, shear reinforcement perpendicular to the longitudinal axis becomes less effective than that in an ordinary beam (50,154). At the same time, distributed reinforcement parallel to the longitudinal axis will increase the shear capacity. As the a/d ratio approaches zero, this reinforcement may resist shear by the concept of shear-friction (87,134). Diagonal reinforcement is also effective in resisting shear (104,136) even though the ACI Building Code does not recognize its value in special members.

The ultimate shear capacity of a member may be governed by the crushing strength of the concrete in the web as discussed in Section 3.4.1. It is generally accepted that the nominal ultimate shear stress in members with adequate shear reinforcement may be at least equal to $10\sqrt{f'_c}$ and that there is an upper limit on the strength that can be developed by adding shear reinforcement to a member.

4.2.4 Reinforcement Details

The development of inclined cracking tends to cause an increase in the stress in flexural tension reinforcement at the base of the crack. The effect is greatest in members without shear reinforcement, as the stress in the main reinforcement at the base of the inclined crack will be controlled by the moment at a section through the top of the crack. It is least in members with effective shear reinforcement, since the position of the resultant compressive thrust will be least affected by the inclined cracking.

In short, deep members, inclined cracking may extend the full length of the shear span. If the shear reinforcement is not fully effective, high tensile stresses will develop in the longitudinal reinforcement at sections where the resultant moment is zero. Sufficient, adequately anchored reinforcement must be provided to resist this tension. This problem will be particularly severe in struts, piers, or spandrels containing an inflection point, especially if they are

subjected to reversals of loading. Adequate end anchorage of stirrups is also essential.

4.3 Shear Friction

The concepts of interface shear transfer were described in Section 2.2.2. For design the shear friction analogy given by Eq. 2.2 can be applied. It is important to note, however, that shear-friction gives unconservative answers if significant moments exist across the section. According to the ACI Code, shear friction should only be applied when the shear span to effective depth ratio, a/d or M/Vd , is less than one-half or when the deformations are parallel to the crack. For larger a/d ratios this procedure tends to overestimate the shear resisted by the concrete. Many practical design cases for deep beams, corbels, and shear walls fall within this range, and the applicability of shear friction to these cases is briefly considered in Sections 4.4, 4.5, and 4.6, respectively.

Design recommendations based on Eq. 2.2 are presented in Section 11.15 of the ACI Code and in Refs. 87 and 134. There are also cases in the connection of precast concrete members in which the concepts of shear friction are useful. Some of these are described in the PCI Design Handbook (155). Care must be exercised in the use of this and other design aids or procedures, however, that potential applications of shear friction satisfy the a/d restriction, and the shear friction reinforcement is adequately anchored.

There are many practical design problems that arise in the application of shear friction. Besides the limitation that the moment on the shear plane must be small, the influence of tension across the shear plane, biaxial orthogonal shearing, and reversed cyclic loading is not well known. The application of shear friction becomes questionable when the reinforcement is diagonal to the shear plane or when the reinforcement consists of very large bars. In some situations, reinforcement parallel to the shear plane may be desirable.

4.4 Deep Beams

4.4.1 Background

In early technical literature, it was common to include all types of short deep members in the general category of deep beams. However, recognition that the type of loading and other factors discussed in Section 4.2 have a substantial effect on the strength of short deep members led to distinctions between deep beams, brackets and corbels, and shearwalls.

In general, deep beams are regarded as members loaded on their extreme fibers in compression. Examples of this type of member are pile caps and transfer girders. Members loaded through floor slabs or diaphragms are closer to the conditions that are idealized for shearwalls.

4.4.2 Behavior of Deep Beams

Early analysis of reinforced concrete deep beams was based on the classical theory of elasticity, with the beam assumed to be homogeneous. Reinforcing was placed in regions where tensile stresses were above the estimated strength of the concrete. Some of the earliest work in this area was performed by Dischinger,

and distributed as a design aid by the Portland Cement Association (154).

Leonhardt and Walther (118) considered two states—the uncracked and the cracked. They found that the cracking followed the tensile stress trajectories; however, after cracking and stress redistribution, the elastic approach did not adequately describe the stress distributions of deep beams. Actual stresses exceeded theoretical stresses at sections near supports, and theoretical stresses exceeded actual stresses at sections near the center of the span.

Crack patterns and failures of deep beams have been observed under many different loading conditions—a single concentrated load (118,188), concentrated loads at the one-third points of the span (118,189), and uniform loads (47-49, 2,57,118,194). Some of these tests included beams subjected to dynamically applied loads (48,59,189).

In these investigations deep beams were observed to fail in either shear or flexure. Although the inclined cracking load was relatively independent of the a/d ratio, the ultimate strength increased as a/d decreased below about 3 as shown in Fig. 4.1. This was only true if the loads and reactions were opposite faces of the beam so that a compression thrust could develop between the load and the support. Load applied on the tension flange through a shelf resulted in lower strengths than did loads applied directly to the compression flange. Thus the ultimate shear stress, v_u , in a beam without web reinforcement is approximately equal to the inclined cracking shear stress, v_c , for members loaded at the tension flange and will be greater than v_c for directly loaded beams (50,118,199,200).

Many of the shear failures observed in tests were precipitated by anchorage and bearing problems, emphasizing the importance of careful detailing of members carrying large loads. When anchorage and bearing problems are avoided, the shear failures generally occur due to crushing of the concrete in the compressive region above an inclined crack, termed "shear compression," or due to propagation of an inclined crack, through the compressive region, and also to and along the longitudinal reinforcement, termed "diagonal tension." Beams with low span-to-depth ratios and small amounts of vertical web reinforcing exhibit brittle modes of failure. Dynamic loading also causes a more brittle mode of failure than does static loading.

Tests of small deep beams have shown that the number of cracks in a given region decreases significantly as the specimen size decreases, indicating that small specimens may be stiffer than larger specimens because of fewer cracks. Also, the small specimen is then a distorted model of the larger specimen.

In general, as the span-to-depth ratio, l_n/d , of a beam decreases, the angle of inclination of the shear cracks, θ_c , becomes greater than the value of 45° commonly assumed for ordinary reinforced concrete beams. The relationship of this parameter to the span-to-

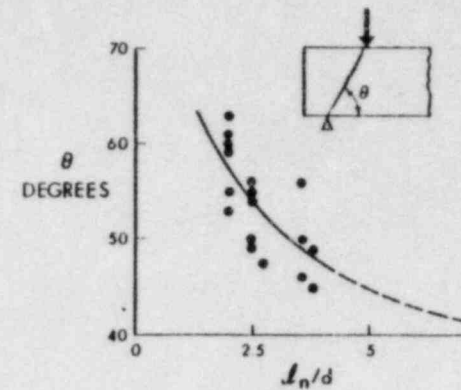
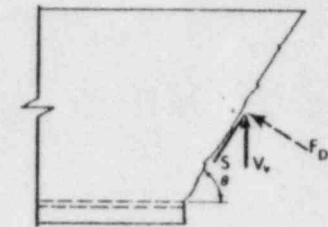
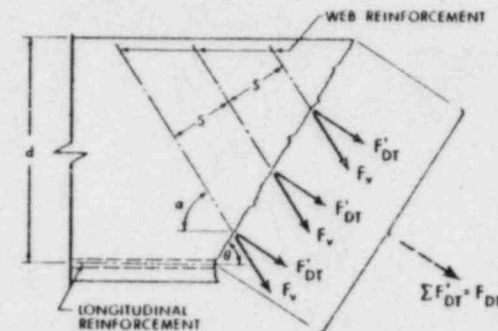


FIG. 4.2.—Inclination of Shear Cracks in Deep Beams (50)



(a) FORCES ON INCLINED CRACK PLANE



(b) FORCES IN STIRRUPS ALONG INCLINED CRACK PLANE

FIG. 4.3.—Derivation of Equations for Web Reinforcement in Deep Beams (50)

depth ratio of a beam is shown in Fig. 4.2 (50). In Fig. 4.2, the dashed portion of the line is carried out to the value associated with ordinary beams.

4.4.3 Development of Design Equations for Deep Beams

Members with an l_n/d ratio of less than 5 are classified in the ACI Code (6) as deep beams if they are loaded on the top face and supported on the bottom face. The CEB (42) defines deep beams as members with span to depth ratios of 2 or 2.5 for simple and continuous beams.

(a) Shear Carried by Concrete

Provisions in the ACI Code for shear capacity of deep beams follow the approach used for ordinary beams which assumes that the total shear capacity of a member is obtained by superposition of capacity of the concrete plus the capacity of the web reinforcement. The equations used in design are based on work by Crist (47,50) and de Paiva (54).

Recognition of the reserve shear capacity of a deep beam without web reinforcement led to development of the expression

$$v_c = \left[3.5 - 2.5 \frac{M_u}{(V_u d)} \right] \left[1.9 \sqrt{f'_c} + 2,500 \rho_w \frac{V_u d}{M_u} \right] \leq 6 \sqrt{f'_c} \quad (4.1)$$

for shear carried by the concrete. In this expression the second term in brackets gives the inclined cracking shear while the first term represents the increase in the shear over that causing cracking. The first term shall not exceed 2.5. Since dead load shears and moments may be significant in a deep beam, Eq. 4.1 is evaluated at a section located at 0.15 l_n from the face of the support for uniformly loaded beams and 0.5a but not more than d from the face of the support for beams subjected to concentrated loads.

Zsutty (200) has derived Eq. 4.2 for deep beams loaded on the top face and supported on the bottom face:

$$v_c = \left(\frac{2.5}{\frac{a}{d}} \right) \times (\text{Eq. 3.9}) \quad (4.2)$$

For indirectly loaded deep beams the arching action is less pronounced, and Zsutty has found good correlation with v_c as given by Eq. 3.9.

Ref. 43 reviews research on deep beams and corbels including 358 deep beam tests carried out in the Netherlands. The researchers concluded that a deep beam without web reinforcement tends to act as a truss composed of the longitudinal reinforcement and two diagonal concrete compression struts. This truss can fail due to yielding of the longitudinal reinforcement or due to a crushing failure of one of the concrete

struts. It was concluded that the concrete strength will not govern the strength of a beam without web reinforcement provided that:

$$V_u \leq \frac{4.8 b_w d f_{ct} k_b k_l}{1 + \left(\frac{a}{d} \right)^2} \leq 4 b_w d f_{ct} \left(\frac{k_b k_l}{b_w d} \right) \quad (4.3)$$

in which f_{ct} = the splitting tensile strength and k_b and k_l = the breadth and length of the loading plate.

When the strength was governed by yielding of the flexural reinforcement, the failure load of the beams and corbels was adequately predicted by the calculation of the yield moment according to conventional beam theory.

(b) Design of Shear Reinforcement

Deep beam test data indicate that horizontal web reinforcement contributes to shear capacity. To take this into account, an approach considering the force along a known inclined crack was developed (47,50) using the shear-friction analogy. Considering the forces acting along an inclined crack, as shown in Fig. 4.3(a):

$$S = F_{DT} \tan \phi \quad (4.4)$$

in which F_{DT} = the normal force on the inclined crack; $\tan \phi$ = the apparent coefficient of friction; and S = the shear force along the crack. The total transverse shear force acting at midlength of the crack, assuming S is uniformly distributed along the crack, is therefore:

$$V_v = S \sin \phi \quad (4.5)$$

The force V_v is assumed to represent the transverse resistance of the web reinforcing along the crack.

The normal forces on the inclined crack are assumed to be developed by the tension in the web reinforcing, as indicated in Fig. 4.3(b). The tension is developed in the reinforcing crossing the inclined crack when slip occurs along the crack. When slip occurs, the crack width is increased slightly because of the roughness of the crack, thus creating tensile stress in the reinforcing. Assuming that the stirrups are at the yield stress at the ultimate load condition:

$$F_v = A_v f_y \quad (4.6)$$

From the geometry of the forces in the stirrups:

$$F_{DT} = \Sigma (F'_{DT})_i = \Sigma F_{vi} \sin(\alpha_i + \theta) \quad (4.7)$$

$$\text{Therefore: } V_v = \Sigma F_{vi} \sin(\alpha_i + \theta) \tan \phi \sin \theta \quad (4.8)$$

which can be shown to lead to:

$$V_v = \frac{A_w f_y d}{s_i} \sin^2 (\alpha_i + \theta) \tan \phi \dots \dots \dots (4.9)$$

Eq. 4.9 represents the transverse capacity of a set of parallel web reinforcing crossing an inclined crack.

Considering an arbitrary number of parallel sets of web reinforcing crossing an inclined crack, the transverse capacity is given by:

$$V_v = d \tan \theta \sum_{i=1}^n \left[\frac{A_w f_y}{s_i} \sin^2 (\alpha_i + \theta) \right] \dots \dots \dots (4.10)$$

in which *i* corresponds to each set of parallel web reinforcing designated *i* = 1, 2, . . . , *n*. A specific case of interest is that of an orthogonal set of web reinforcing oriented coincident with the longitudinal axis of a beam. Then:

$$\alpha_1 = \alpha_v = 90^\circ \text{ (vertical web reinforcing)} \dots \dots \dots (4.11a)$$

$$\alpha_2 = \alpha_h = 0^\circ \text{ (horizontal web reinforcing)} \dots \dots \dots (4.11b)$$

Substituting into Eq. 4.10, and assuming that all sets of web reinforcing have identical *f_y*

$$V_v = f_y d \tan \phi \left[\frac{A_v}{s} \cos^2 \theta + \frac{A_{vh}}{s_h} \sin^2 \theta \right] \dots \dots \dots (4.12)$$

in which *A_v* and *s* refer to vertical web reinforcing and *A_{vh}* and *s_h* refer to horizontal web reinforcing.

A relationship of *θ* as a function of *l_n/d* has been determined experimentally (47) as shown in Fig. 4.4. A lower boundary of the test data is given by:

$$\cos^2 \theta = \frac{1}{12} \left(1 + \frac{l_n}{d} \right) \dots \dots \dots (4.13)$$

Using trigonometric identities:

$$V_v = f_y d \tan \phi \left[\frac{A_v}{s} \frac{1}{12} \left(1 + \frac{l_n}{d} \right) + \frac{A_{vh}}{s_h} \frac{1}{12} \left(11 - \frac{l_n}{d} \right) \right] \dots \dots \dots (4.14)$$

which is equal to F · s. 11-24 in the ACI Code when tan *φ* is set equal to one.

This derivation is based on the shear friction concept which is not normally applied to sections subjected to a significant moment. Shear friction was applied because there is a significant shearing action along the critical inclined crack. On the other hand, this analysis assumes the sole function of the web reinforcement is to create a compression force across the slip plane so that shear-friction can be mobilized. As *l_n/d* approaches or exceeds 5, however, a significant amount of shear

is transmitted directly by tension in the stirrups as implied by the truss analogy. A conventional truss analogy underestimates the effect of horizontal web reinforcement in deep beams.

Based on the 1962 Committee 326 report (7), the nominal shear stress, *v_n*, was limited to 8√*f_c'* for *l_n/d* less than 2 varying up to 10√*f_c'* for *l_n/d* greater than 5. For beams with *l_n/d* ≤ 2, the European Concrete Committee (CEB Ref. 42) limits the shear to a value, which when converted to ACI load factors and material understrength factors, is about:

$$V_{max} = 0.075 \phi b_w h f_c' \leq 0.075 \phi b_w l_n f_c' \dots \dots \dots (4.15)$$

This limitation was established to prevent diagonal crushing of the beam web near the support. The CEB value is about half that allowed by the 1971 ACI Code and is lower than the value given by Eq. 4.3.

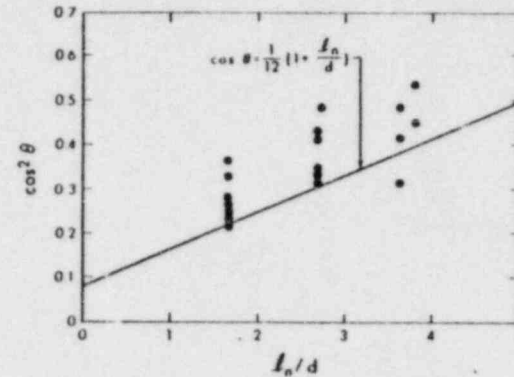


FIG. 4.4.—Crack Inclination Versus *l_n/d* (50)

Frequently the behavior and strength of a deep beam is strongly affected by the details of the supports and reinforcement. This problem is discussed extensively in Ref. 113. In addition, the European CEB has recently published detailed recommendations concerning the design, placement, and detailing of reinforcement, etc., for simply supported and continuous deep beams having span to depth ratios not greater than 2 and 2.5, respectively (42). Of particular interest are reinforcing details for the support regions and locations at which loads are applied below the top of a deep beam.

4.5 Brackets and Corbels

4.5.1 Review of Research

Brackets and corbels are structural members that project from the face of another structural member, usually a column as shown in Fig. 4.5. They are used extensively in precast concrete construc-

tion, to support other primary structural elements. Corbels are normally designed for a shear, V , caused by dead and live loads. In addition, a normal component, N , may be caused by restraint of horizontal deformations due to creep, shrinkage, and temperature changes in the supported members.

The provisions for design of corbels in Section 11.14 of the ACI Building Code are based upon an extensive research investigation carried out by Kriz and Raths (109). They tested a total of 195

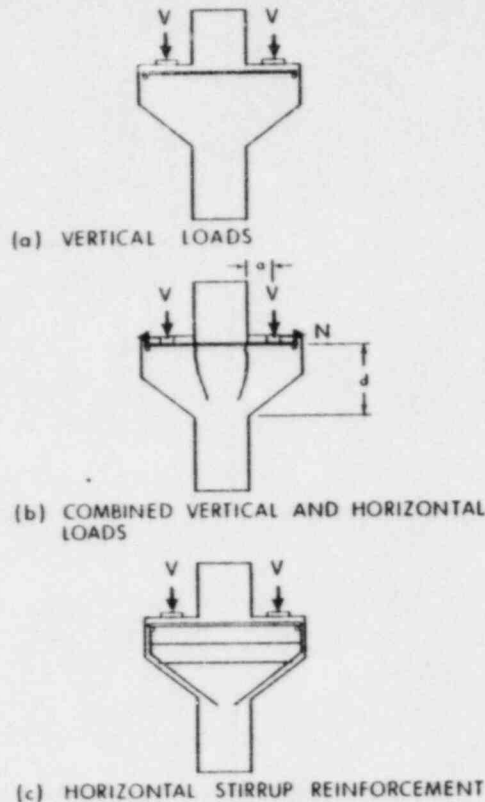


FIG. 4.5.—Specimens Tested by Kriz and Raths (109)

corbels, of which 124 were subjected to only vertical load, and 71 to combined vertical and horizontal loads. Variables included in their test program were as follows: size and shape of corbel, amount of main tension reinforcement and its detailing, concrete strength, amount of stirrups, ratio of shear span to effective depth, and the ratio of the horizontal force to the vertical force.

All of Kriz and Raths' specimens consisted of a length of 8 in. by 12 in. column with two corbels arranged symmetrically, as shown in Fig. 4.5. With the exception of 10 specimens in an explor-

atory series, the main tension reinforcement consisted of straight deformed bars anchored by bars of equal diameter welded across their ends. Figs. 4.5(a) and 4.5(b) present the different bearing details used when only vertical loads or combined vertical and horizontal loads were applied, respectively. Sixteen of the test specimens contained horizontal stirrup reinforcement, as shown in Fig. 4.5(c). It is important to note that none of the specimens included inclined reinforcement.

Kriz and Rath reported the following primary modes of failure:

1. Flexural tension failures occurred by crushing of the concrete at the bottom of the sloping face of the corbel after extensive yielding of the tension reinforcement.
2. Flexural compression failures involved crushing of the concrete at the base of the corbel before the reinforcement has yielded.
3. Diagonal splitting failures involved a sudden splitting along a line from the bearing plate to the base of the corbel followed by crushing of the portion below this. Fig. 1.3(b) shows such a failure.
4. Shearing failures involved a series of short inclined cracks along this weakened plane [Fig. 1.3(c)].
5. If the reinforcement was not correctly detailed, the corbel could fail by shearing off the portion outside the reinforcing bars. The right-hand corbel in Fig. 1.3(b) shows distress due to this type of action.
6. If the corbel was too shallow under the load the diagonal cracks sometimes intersected the sloping surface of the corbel.

From the analysis of their data and also data from tests on deep beams at the University of Illinois (54,194) and the University of Texas (62), Kriz and Raths suggested that the design shear capacity of corbels be computed from the following:

$$v_u = \frac{V_u}{\phi b d} 6.5 \sqrt{f'_c} (1 - 0.5^{d/a}) \frac{(1,000\rho)(1/3 + 0.4 N/V)}{10^{0.8N/V}} \dots \dots \dots (4.16)$$

For the special case in which $N = 0$, Eq. 4.16 reduces to:

$$v_u = \frac{V_u}{\phi b d} 6.5 \sqrt{f'_c} (1 - 0.5^{d/a})(1,000\rho)^{1/3} \dots \dots \dots (4.17)$$

A parametric plot of Eqs. 4.16 and 4.17 is presented in Fig. 4.6, which incorporates limits placed on these equations in the analysis. The figure may be entered on either the v_u or ρ scales, following parallel to the heavy black line to appropriate values of f'_c , a/d , and N/V .

It was concluded that closed horizontal stirrups having an area at least equal to 1/2 of A_s should be used in all corbels, and that this stirrup reinforcement should be placed not farther than 2 in. from the outer edge of the corbel, and that the total depth

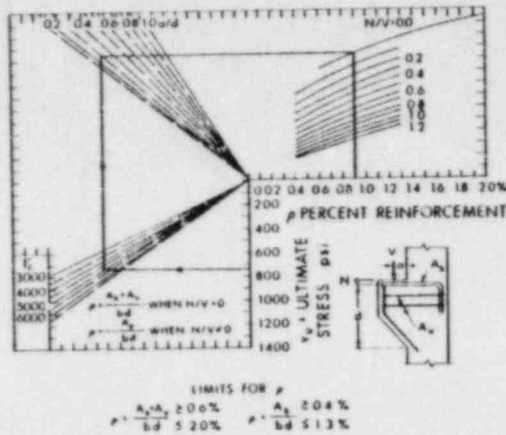


FIG. 4.6.—Design Chart for Corbels (109)

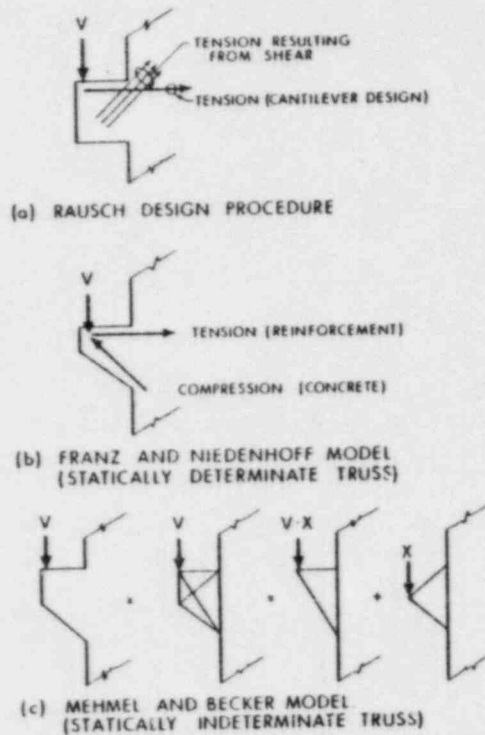


FIG. 4.7.—German Models for Design of Corbels and Brackets

of the corbel under the outer edge of the bearing plate should be not less than one-half the total depth of the corbel at the face of the column.

The Kriz and Rath tests are restudied in Ref. 43. When failure was initiated by yielding of the tension reinforcement, the failure load could be estimated by considering the specimen shown in Fig. 4.5(b) and summing moments about the center of the compression block at the bottom of the cracks. This led to Eq. 4.18 to predict the shear at yielding of the reinforcement

$$V_y = \frac{0.9 d A_s f_y}{a + \frac{dN}{V}} = \frac{0.9 A_s f_y}{\frac{a}{d} + \frac{N}{V}} \quad (4.18)$$

No special shear reinforcement was found necessary provided the shear force to be transmitted was less than the value given by Eq. 4.3 for values of:

$$\frac{a}{d} > 0.15 \sqrt{\frac{bd}{k_b k_t}} \quad (4.19)$$

For shorter shear spans there was a reduction in shear strength unless horizontal stirrups were provided.

The three different truss models shown in Fig. 4.7 have been proposed in Germany for the design of corbels. Rausch (159,160) has proposed that all the shear be transferred by 45° reinforcement and that reinforcement be provided at the top for the tension calculated from the cantilever design. Franz and Nienhoff (67) replaced the corbel with a statically determinate truss as shown in Fig. 4.7(b). For some circumstances they require transverse reinforcement to prevent slipping along the compression strut. This model was also used in Ref. 43. More recently, Mehmel and Becker (135) proposed the use of the indeterminate truss shown in Fig. 4.7(c) for design. The division of the applied shear between the two systems is a function of the a/d ratio and the depth of the edge of the corbel to its depth, d , at the column face.

In 1967, Mehmel and Freitag (136) reported an investigation comparing the strength of corbels designed by the methods of Rausch, Franz, and Nienhoff, and Mehmel and Becker. It is noteworthy that all of the corbels had a satisfactory ultimate strength. Highest load capacity was attained with corbels designed in accord with Rausch's method, containing heavy diagonal bars and stirrups. Mehmel's method gave designs with the most favorable ratio of weight of reinforcement to failure load, with corbels designed by the Franz-Nienhoff procedure second.

Somerville (171,172) has recently proposed a design analysis based on the Franz and Nienhoff model shown in Fig. 4.7(b). The depth of the corbel, d , is based on allowable shear obtained from an equation similar to Eq. 4.2. The compression force acts

on an inclined strut which is assumed to fail under a compression stress of $0.5 f'_c$. Once the depth of the compression strut is known, the force to be resisted by tension reinforcement is calculated by summing moments about the intersection of the strut and the face of the column. The stress in the tension reinforcement is computed from the distribution of strains on the vertical plane at the face of the column.

Ferguson (63) has reported tests of simulated bridge bent caps. Within the range, $0.5 < a/d < 1.2$ for $f'_c = 4,500$ psi, Ferguson recommended:

$$v_u = \left(320 + 140 \frac{d}{a} \right) \text{ psi} \quad (4.20)$$

In these tests the overhangs, containing tension bars which were

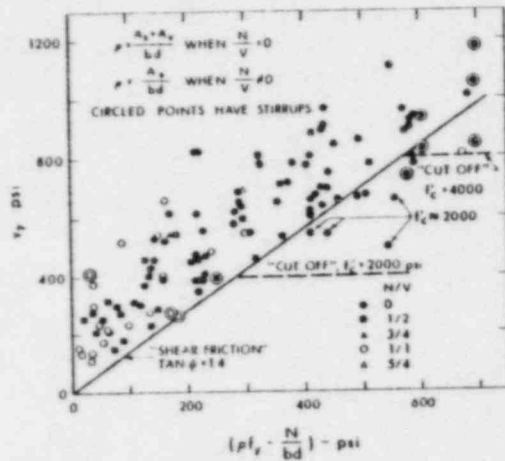


FIG. 4.8.—Comparison of Kriz and Rath's Tests with Shear Friction Equation

anchored by extending the bars beyond the loading point, behaved satisfactorily.

4.5.2 Development of ACI Code Design Equations

Although a corbel resembles one end of an inverted deep beam, the ACI Code (6) differentiates between the two types of members and includes special provisions for brackets and corbels in Section 11.14. The main reasons for this distinction are that corbels are generally trapezoidal in shape and vertical stirrups are ineffective in such members. In addition, the size of a corbel normally makes it difficult to anchor the reinforcement effectively.

The special provision for brackets and corbels in Section 11.14 applies only to members having a shear-span-to-depth ratio, a/d , of unity or less. Projecting members are no longer corbels when the a/d ratio is greater than one, and these members must be

designed using the shear provisions for ordinary concrete beams or deep beams. In practice, the reinforcement in a member of this type would be quite different, depending on whether the a/d ratio was slightly less than or greater than one.

The ACI Code equations (11-23 and 11-29) for the capacity of corbels are an attempt to simplify Eqs. 4.16 and 4.17 while retaining the same basic parameters.

When the a/d ratio is less than $1/2$, the corbel may be designed in accordance with the shear-friction provisions in Section 11.15 of the Code. For corbels subjected to vertical load only, both the horizontal stirrups and main reinforcement are considered effective as shear friction reinforcement. If the corbel is subjected to horizontal and vertical loads, just the main top reinforcement can be counted on as shear reinforcement. Although this phenomenon has not been adequately explained, it may be related to the effect of the horizontal force on the M/Vd or effective a/d ratio of the corbel (see Eq. 4.18). Fig. 4.8 shows that the shear-friction concept safely predicts the strength of the corbels tested by Kriz and Rath's (109). This plot includes all the Kriz and Rath's tests that satisfy the requirements of Section 11.14 of the ACI Code and have $a/d \leq 0.5$. Similar plots are given in Ref. 171.

4.6 Shear Walls

Shear walls are walls designed to resist the effects of lateral forces acting on buildings. These lateral forces are primarily due to wind or earthquake. The performance requirements for shear walls under wind loads are different than that for earthquakes. Walls designed for wind forces have to meet both strength and stiffness requirements. Walls designed for earthquakes must also satisfy requirements of ductility and energy absorption, damping characteristics and damage control, during several cycles of inelastic deformation.

The behavior of shear walls is complicated by the influence of boundary elements and multiple openings. Fig. 4.9(a) and 4.9(b) presents some typical examples. Lateral loads are usually introduced into shear walls through floor slabs framing into either one side or both sides of the wall. As a result, the lateral loads tend to be distributed across the width of the wall. Transverse walls or columns are often located at the extreme edges of the walls. They act with the wall, and usually contain most of the flexural reinforcement resisting the moment due to the lateral forces.

When a wall contains large openings, it can be considered to be made up of a system of piers and spandrels. Each individual pier or spandrel is, in effect, a shear wall element, with a shear span approximately equal to one-half of its height or length, respectively. In addition to shear, piers will also generally have tension or compression caused by gravity and overturning forces as well as shrinkage, creep, and differential settlement.

Some distinctions need to be made between tall and short walls. Reference should be made to the Committee 442 report (9) for a discussion of the behavior and analysis of tall walls. It is noteworthy that many

tall walls have rather low M/Vd ratios of perhaps 3 to 4. In general, the shear strength of a wall is of interest only for M/Vd ratios of less than 2, or for walls with a flanged cross section.

4.6.1 Experimental Investigations

Originally, the lateral load resisting system used was the masonry in-filled frame. It was believed that its lateral resistance was the sum of that of the frame plus that of the masonry in-fill acting independently. Tests on one-story shear walls (17), one-story frames (18), and full scale three-story frames (145) changed this "sum of the parts" concept. In other words, an interaction between the parts was recognized, making the behavior of an in-filled frame closer to that of a single structural unit. More recent investigations on single-story (196) and five-story frames (66) have further increased our knowledge of the mechanisms of failure of brick in-filled frames. Observations of the performance of this type of structure in earthquakes has verified the interaction of wall and frame.

Investigators in Japan (139,147,185,187) have been concerned primarily with the strength of low-rise concrete shear walls surrounded by a reinforced concrete or steel frame and subjected to load reversals. Japanese shear wall design provisions in the Architectural Institute of Japan Standards are described in Ref. 186 and will be outlined in Section 4.6.3.

In the United States, the Uniform Building Code (89) specifies requirements for structures under lateral forces. In the case of shear walls, the provisions are based on the recommendations of the Seismology Committee of the Structural Engineers Association of California. In the UBC, the shear strength of shear walls is based on experimental results of shear tests on directly loaded deep beams with and without web reinforcement (54,170).

While the UBC provisions represented an advancement in design, additional work, including that by Crist (50), Leonhardt and Walther (118), Cardenas and Magura (36), and Cardenas, et al. (35) has led to separate provisions for deep beams and shear walls in Chapter 11 of ACI 318-71 (6). These provisions recognize that there are important differences between deep beams and shear walls. First, deep beams are usually loaded through extreme fibers in compression. Under these conditions, shear carried by the concrete in a member without web reinforcement is greater than the shear causing diagonal tension cracking. Shear walls, however, are more like deep members indirectly loaded through lateral stubs or diaphragms [Fig. 4.9(a)]. This type of member, if it does not contain web reinforcement, may fail at a shear equal to or only slightly greater than the shear causing diagonal cracking (200). Secondly, deep beams are not usually subjected to axial loads, whereas the consideration of axial compression or tension is important in shear walls.

Research on spandrel beams, connecting elements of shear walls with openings, has been carried out by Paulay (151,154). Based on his work, Paulay suggests that the total shear force in the spandrel beam in a wall subjected to load reversals should be taken

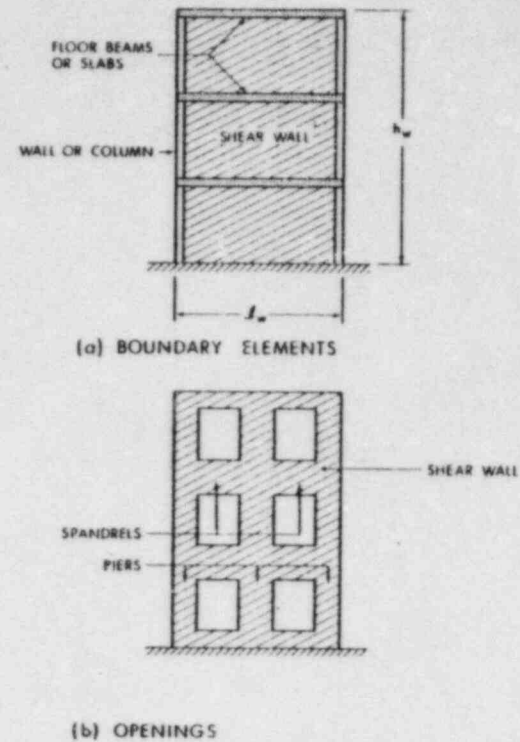


FIG. 4.9.—Elements Affecting Behavior of Shear Walls

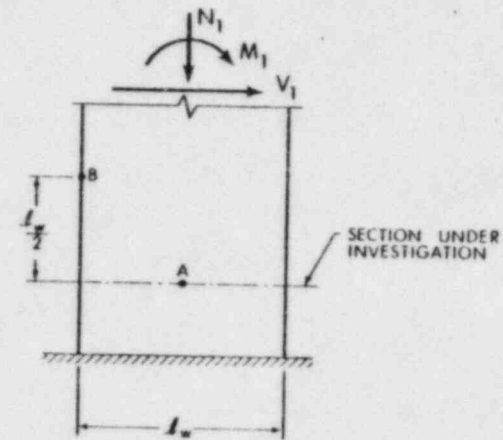


FIG. 4.10.—Critical Points for Inclined Cracking

by shear reinforcement. Paulay also tested a spandrel beam containing diagonal main reinforcement, and reports good strength and ductility for this case.

4.6.2 Flexural Strength

Research findings stress the importance of recognizing the flexural behavior and strength of walls. In the case of earthquake loadings, it is essential that the integrity of the wall be maintained during many excursions into inelastic behavior.

High-rise solid walls or in-filled frames behave basically like vertical cantilever beams subjected to combined axial loading and bending, and their flexural strength can be closely determined using assumptions applicable to reinforced concrete beam-columns. Low-rise walls also behave like vertical cantilever beams until they develop inclined cracking. Their behavior subsequently depends on the amount and arrangement of shear reinforcement. With adequate reinforcement, tests (35,151) indicate that walls or spandrels will develop at least 90% of the flexural strength determined using assumptions for ordinary beams given in the ACI Code.

Perforated shear walls may be controlled by the flexural strength of the spandrel beams or the secondary stresses in spandrels around the openings. As in the case of beams, the presence of openings may cause the wall section to be more critical for shear strength than flexural strength.

4.6.3 Shear Strength

In general, lateral forces are applied to walls through floor slabs which distribute the shear along the side of the wall. Consequently their shear capacity cannot be expected to benefit from bearing of concentrated loads on the extreme fibers, as is the case for deep beams. On the other hand, the floor slab may possibly act as an external stirrup, and thereby increase the strength of the wall.

The special provisions for design of walls in the ACI Code consider inclined cracking to occur at the section under investigation when a critical condition is reached at either point A or B shown in Fig. 4.10. At point A, web shear cracking is considered to occur when the principal tensile stress in the uncracked concrete section equals $4\sqrt{f'_c}$. At point B, a flexure shear crack is considered to initiate when the flexural tensile stress equals $6\sqrt{f'_c}$, and it is considered to be fully formed and therefore critical at the section under investigation when an additional shear force of $0.6hd\sqrt{f'_c}$ is applied. Here, h = the thickness of the shear wall, and d = the distance from the extreme compression fiber to the center of the tension reinforcement. These assumptions lead to the development of Eqs. 11-31 and 11-32 in the Code.

The design provisions require a minimum amount of shear reinforcement. Consequently the design shear capacity will always be at least equal to that causing cracking plus the contribution of the minimum shear reinforcement determined in accord with the "truss analogy." By providing additional shear reinforcement,

ultimate shear of $10hd\sqrt{f'_c}$ may be allowed on the wall.

A detailed development of the ACI Code design provisions for shear walls has been presented elsewhere (35). This reference includes a comparison of the design provision with available test results, showing that the provisions lead to a conservative prediction of shear strength for static loading conditions.

Fratessa and Zsutty (68) have studied the problems associated with design of shear walls for seismic loading conditions. Primarily because of cyclic loading under inelastic conditions, they have recommended a different approach to shear wall design than that contained in the ACI Code. In their report on shear walls to the Structural Engineers Association of the Northern California Seismology Subcommittee, they stress the need for consideration of energy absorption and damping, as well as strength, in the design of walls. They recommend that the shear stress carried by the concrete be limited to $2\sqrt{f'_c}$ and that the ultimate shear stress be limited to $8\sqrt{f'_c}$. When shear reinforcement perpendicular to the flexural reinforcement is required, an equal amount of reinforcement shall be provided normal to the shear reinforcement. In any case, a minimum of 0.25% reinforcement shall be provided in each direction. Similar requirements have been incorporated in the 1971 revision to the SEAOC requirements (167).

Shear walls designed by the Architectural Institute of Japan Standards (186) generally consist of a boundary frame with a panel wall which is frequently cast in place after the frame members are built. The wall is designed for a ductile failure in shear as an in-filled wall with deformation of the panel resisted by panel reinforcement and the boundary frame. The boundary frame is designed for a ductile flexural failure. The cracking shear for such a wall is given as:

$$V_1 = v_c hl_w \dots \dots \dots (4.21)$$

in which $v_c = 108 \text{ psi} + 0.015 f'_c$ for $3,000 \text{ psi} \leq f'_c \leq 5,000 \text{ psi}$. The ultimate horizontal shear capacity of such a wall is given by:

$$V_2 = V_w + \sum V_{col} \dots \dots \dots (4.22)$$

in which V_w = shear capacity of the reinforcement in the cracked wall = $\rho_n f_y b l_w$ and V_{col} = shear capacity of a column in the boundary frame

$$v_w = \frac{7}{8} bd [1.5 v_c + 0.5 f_y (\rho_n - 0.002)] \dots \dots \dots (4.23)$$

in which b , d , f_y , and ρ_n refer to the dimensions and shear reinforcement of the boundary column.

For ductility, V_1 must be less than V_2 and the first shear cracks must occur in the wall panel and not the boundary frame. To ensure that the latter occurs, the AIJ Standards specify limitations on the dimensions such that the maximum nominal shear stress in

the wall panel exceeds twice the maximum nominal shear stresses in the columns or beams. Since tests of such walls have shown that most such walls fail due to shear cracks that originate in the wall panel and extend diagonally across the boundary frame near the ends of its columns or beams, extra shear reinforcement is required in these parts of the boundary frame.

4.6.4 Recommended Research

Considerable research is needed to increase our knowledge of the behavior of shear walls and shear wall structures. Investigations

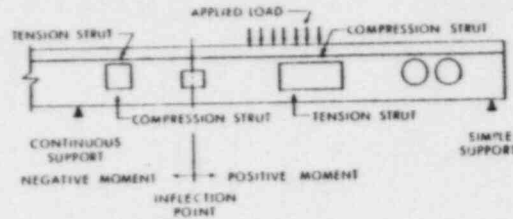


FIG. 4.11.—Openings in Concrete Beams

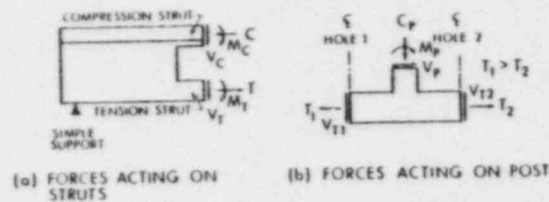


FIG. 4.12.—Forces Adjacent to Holes in Beam

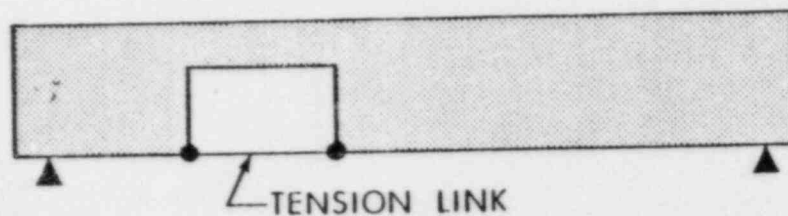


FIG. 4.13.—Lorentsen's Idealized Beam with Hole

of low-rise walls, wall panels, piers, and spandrels should provide improved design procedures that can include energy absorption and damping. Strength degradation and the decrease in stiffness due to reversals of loading and inelastic deformation need to be considered. In seismic design, a practical analysis procedure must be developed which can relate the appropriate horizontal force factors to the amount of inelastic deformation that takes place in a given structural system.

Experimental work evaluating minimum detailing requirements for stirrup anchorage and construction joint performance is needed. The effect of diagonal reinforcement should be studied. Effects of axial loads on piers need special study. Consideration of boundary members is needed.

4.7 Beams with Openings

Some of the various sizes and shapes of openings that might be placed in a typical T-shaped concrete beam are shown in Fig. 4.11. These openings may be located in regions of positive or negative moment, which will determine whether the struts above and below the openings are in tension or compression. When two openings are placed close to each other, the element between the openings is referred to as a post.

A free-body-diagram of a part of a beam that includes a section through an opening of depth H is shown in Fig. 4.12(a). It is evident that the opening does not greatly affect the resultant compressive force, C , and tensile force, T . However, the external shear, $V_c + V_T$, must be carried by a substantially reduced section, indicating that the shear capacity of the struts will be a controlling factor in design.

Similarly, when two openings are placed close together, as illustrated by the free-body-diagram in Fig. 4.12(b), it is evident that a shear, V_p , acts on the post between the openings. This shear is equal to the difference between either the resultant compressive or tensile forces acting on the struts of the adjacent holes.

In most cases, the struts are short deep members with low a/d ratios.

4.7.1 Theoretical Approaches

The forces acting on the struts of an opening are indeterminate to the third degree. A direct solution for these forces is difficult, and the reliability of the results is uncertain because of the need to account for flexural, shear, and axial deformations before and after cracking of the concrete.

Lorentsen (123) reduced the analysis to a single degree of indeterminacy by using the model shown in Fig. 4.13. He considered that the tension strut was divided into short sections by flexural cracks, and was therefore not able to transmit shear. To verify the model, tests were carried out on four T-shaped beams having a compression flange width of 39.4 in. (1 m) and an overall depth of 23.6 in. (60 cm). The thickness of the compression flange was 3.9 in. (10 cm) and the thickness of the stem was 11.8 in. (15 cm). Either one or two concentrated loads were applied, at the third points of the 19.7-ft (6.5-m) simply supported span. Each beam contained a rectangular hole having a length of 71 in. (180 cm) and a depth of 12.4 in. (31.5 cm) located at midspan.

The behavior of Lorentsen's test beams was in good agreement with his predictions, although he did observe that the tension strut carried substantial shear. He concluded that holes in beams should be kept away from inflection points if at all possible, and that additional stirrups should be placed near the sides of holes.

Nasser, et al. (140) presented assumptions that simplified the analysis of beams with holes, as follows:

1. The top and bottom struts behave similarly to the chords of a Vierendeel panel.
2. The struts, when they are not subject to transverse loads, have contraflexure points at their midlength.
3. The struts, when they have adequate stirrups, carry the external shear in proportion to their cross-sectional areas.
4. There is a diagonal force concentration at the corner induced by the chord shear, and its value is twice the simple shear force.

A series of 9 in. (22.9 cm) wide by 18 in. (45.5 cm) deep beams, designed in accordance with these assumptions, were made and tested by Nasser, et al. The beams were pierced by rectangular holes, usually 8 in. (20.3 cm) deep and 30 in. (76 cm) long. They were simply supported on a span of 12 ft. (3.65 m) and were subjected to a one- or two-point concentrated loading. Although the majority of their specimens failed in flexure, it was concluded that the proposed assumptions were valid for rectangular beams.

4.7.2 Tests on Joists

An extensive investigation of the effect of openings in the webs of continuous joists has been carried out at the laboratories of the Portland Cement Association (75,76). The investigation included both unreinforced openings and openings with reinforcement added to the struts and along the sides of the openings.

The test specimens had cross-sectional dimensions of a standard 16-in. (40.5-cm) deep joists with a 3-in. (7.6-cm) thick flange. They were built with a special stub simulating a continuous support. The loading approximated the shear and moment that would occur between inflection points of a continuous joist framing into a supporting beam.

The test results indicated that a specimen with an unreinforced opening close to the stub had a substantially greater strength than a specimen with an opening more than twice the depth of the web from the stub. Moving a square opening in an unreinforced web from middepth toward the tension fibers did not significantly affect the strength of the specimen; however, cracking at the hole did occur at a lower load. Size of opening did affect strength, but an unreinforced web containing a square opening of one-quarter the web depth, or a circular opening of three-eighths the web depth, did not reduce the strength of the specimen.

Tests were also carried out on specimens with stirrup reinforcement along the vertical sides of the opening. It was evident from the results that very large openings can be accommodated in the webs of joists without reducing their strength, provided that stirrup reinforcement with a yield capacity nearly equal to the shear at the hole is provided at its vertical edges. It was also evident that closely spaced multiple holes can be placed in a joist as long as each hole has side reinforcement. Specimens with multiple circular and oval holes failed in the struts when the width of the post was equal to or greater than three-eighths the depth of the web.

The addition of stirrups in the tensile strut was beneficial; however, the addition of longitudinal bars adjacent to the tension side of the hole decreased the strength.

Strain measurements confirmed that a point of axial compression occurred near the midlength of the compressive strut at the opening. The magnitude of the axial compression force could be calculated from the external bending moment. Until cracking, the distribution of shear between the regions above and below the opening was approximately in proportion to the cross-sectional area of the struts. After cracking, the compressive strut tended to carry all of the shear.

A conservative prediction of the strength of the specimens with square openings in unreinforced webs was obtained by calculating the load causing tensile cracking at the corner of the opening. A good prediction of the strength of the specimens with reinforced square openings that failed in the compressive strut was obtained by calculating the load causing either a diagonal tension failure or a crushing failure due to combined compression and shear (75).

4.7.3 Tests on Prestressed Beams

A series of 20-in. (50.5-cm) deep, simply supported prestressed concrete T-beams with web openings was tested at the University of Alberta (157). They were subjected to a symmetrical 2-point loading applied on a span of 20 ft (6.1 m). Failure of the beams with holes occurred after development of inclined cracking in the tensile struts and the formation of Vierendeel type mechanisms.

In addition to the laboratory tests at the University of Alberta, a special field test was carried out on a full-sized 120-ft (36.5 m) long prestressed beam (157). The beam failed under a loading which produced a moment at the center line of the beam equivalent to a 1.5 dead load plus 1.8 live load condition. The failure was believed to have occurred due to shear compression in the flange at the high moment side of the opening closest to the simply supported end of the beam.

More recent tests (165) at the University of Alberta were conducted to determine the effect of both vertical and longitudinal reinforcement in T-beams with multiple 8-in. by 16-in. (20.3-cm by 41.6-cm) rectangular openings separated by 8-in. (20.3-cm) wide posts. The 20-in. (50.5-cm) deep, 24-ft (7.3 m) long specimens were tested with a 20-ft (6.1-m) span length. It was found that increasing the vertical reinforcement in the posts increased the shear capacity of the specimens. However, increasing the amount of longitudinal reinforcement in the struts above and below the openings had little effect on the shear capacity. It was also found that placing inclined shear reinforcement in the lower struts had the effect of increasing capacity and localizing the failure in the posts.

4.7.4 Tests on Wall Beams with Doorway Sized Openings

Tests of two reinforced concrete beams with very large web openings have also been carried out at the laboratories of the Portland Cement Association (37). These test beams were half-scale

models of prototype wall beams having a total depth of 8 ft. (2.45 m) and web thickness of 6 in. Openings equivalent to a central corridor and a doorway were provided in these beams.

It was concluded that the design of these test specimens could be carried out in accordance with the provisions of the 1963 ACI Building Code. The assumptions that all of the shear at an opening is carried by the lintel and that zero bending moment exists at lintel midspan resulted in conservative predictions of load capacity. It was observed, however, that initial diagonal cracking in the solid web portions of the test beams occurred at about 50% of the load expected using provisions in the 1963 ACI Building Code. This early diagonal cracking did not result in a reduction of shear strength; however, additional stirrup reinforcement was required to control cracking.

4.8 Beam-Column JUNCTIONS

A connection must be as strong or stronger than the members framing into it. While the proper proportioning of joints is essential for adequate ductility under seismic loading, shear reinforcement in the joint may also be necessary for wind, dead, and live load conditions.

There are three major considerations for the design of beam-column junctions (92): (1) Provision of shear reinforcement sufficient to resist any internal shear in excess of that carried by the concrete; (2) provision of hoop reinforcement to ensure transmission of the column load through the joint under ultimate load conditions; and (3) adequate anchorage for the flexural reinforcement in the beams framing into the joint.

This discussion is concerned only with determination of the necessary amount of shear reinforcement. However, stirrups used as shear reinforcement are also effective for confinement of the column reinforcement.

N. Hanson and others (45,80,81,188) have reported tests on beam-column joints subjected to a series of reversed static loads to simulate seismic load conditions. Variables included the size and reinforcement of the column, amount of stirrup reinforcement through the joint, grade of reinforcement, and the number of beams framing into the joint. Each test included at least nine cycles of load applied at the ends of the beams, with five or more of the cycles requiring extensive inelastic behavior.

The forces acting on a beam-column junction are shown in Fig. 4.14. If an ultimate design condition is being investigated, the net shear on the joint is.

$$V_u = (A_{s1} + A_{s2})f_s - V_1 \dots \dots \dots (4.24)$$

Based on the requirements of the ACI Code (6) (ACI 318-71) the maximum shear contribution of the concrete is computed according to the provisions of Section 11.4.3.

When $V_u / \phi b_w d$ exceeds that which can be carried by the concrete, the required amount of stirrup reinforcement perpendicular to the axis of the column is computed from Eq. 11-13 of the ACI Code.

N. Hanson, et al. (87) found that when an area of reinforcement equal to 80% of that required by the ACI Code was used, the joint had adequate

strength and ductility for reversed loading conditions. For a joint without any stirrup reinforcement, the effective collapse load was 60% higher than that implied by code provisions. The difference between the strengths implied by the code and the measured strengths decreased as the column load increased. When the joint was restrained on two sides by beams with depths equal to the depth of the loaded beams, the strength and ductility characteristics for a joint without stirrup reinforcement were better than those of a joint without restraining beams but with adequate shear reinforcement. It was also found that there was little difference in the behavior of junctions made with Grade 40 or Grade 60 reinforcement.

The beam deflections in the tests reported in Ref. 81 corresponded to a ductility ratio of about 5. In similar tests involving larger ductility ratios (161) the shear contribution of the concrete appeared to diminish under cyclic loading and eventually all the stirrup ties across such a joint yielded even when the shear reinforcement was in excess of that

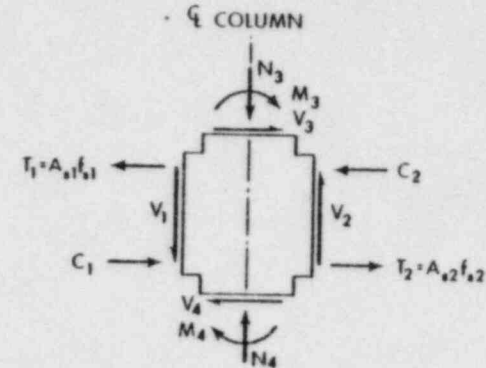


FIG. 4.14.—Forces Acting on Beam-Column Junction

suggested in the foregoing. In these tests a diagonal compression "strut" formed in the joint. The failure load was enhanced if the outer end of this strut was well anchored by ties and supplementary cross-ties in the joint.

The Soviet design procedure (191) for such joints considers the width of this strut to be 40% of the diagonal of the joint and assumes joint failure will occur when the average compression stress in this strut reached 80% of the concrete strength.

While it is clear from these results that stirrup reinforcement is necessary in some joints to provide adequate shear strength and ductility, extrapolation of these results to different joint details should be made with caution. Some correlation between these results and shear-transfer results should be possible. Shear transfer concepts imply that the distribution of the column reinforcement is important. Reinforcement distributed over the depth of the column for bending would be partially effective for transferring shearing forces across the shear plane. The steel in the

beam anchored on the far side of the inclined crack could effectively increase the shear strength by providing an additional normal compressive stress on the shear plane.

4.9 Columns

Columns may fail in shear during earthquakes due to the lateral forces resisted by the columns (56,120,173). This in turn may lead to major structural damage or collapse of the structure. This type of failure occurs mainly in tied columns and few, if any, spiral columns have failed in shear.

Two types of failure appear possible. In columns subjected to moments high enough to cause flexural cracking at the ends, shear failures will tend to resemble those in axially loaded beams [Fig. 1.5(a)]. For this type of failure the ACI Code Section 11.4.3 seems adequate. For short stocky columns subjected to high axial loads with small M/Vd ratios it has been hypothesized that shear failures may occur prior to flexural cracking [Fig. 1.5(b)]. Such failures would occur due to crushing of the concrete at an axial stress less than the concrete strength due to the effect of the shearing stress on the compression stress at failure (see Section 2.1). Yamada and Furui (195) have attempted to explain this type of failure using the Mohr rupture theory and diagrams similar to Fig. 2.4. Such diagrams show a reduction in the shear strength of members under extremely high axial loads. This behavior is reflected in the CEB design equations for shear-crushing failures in uncracked members (41). At present there is insufficient information available to make design recommendations concerning this type of failure. The ACI Code Eqs. 11-6 and 11-7 are believed to be safe for such failures for $N_u/f'_c A_g$ values less than 0.80, however.

Relatively few shear tests of reinforced concrete columns are reported in the literature. The tests of knee frames carried out in the late 50's at the University of Illinois (12,137) are compared to the ACI Code equations in Ref. 7. Section 3.4.5 of this report deals with the effect of axial loads on the shear strength of beams and can be applied to the design of columns in non-seismic areas.

Yamada and Furui (195) investigated the influence of shear span ratios, axial load level, and web reinforcement on the behavior of tied columns. The ductility decreased significantly as the axial load was increased where either the shear span ratio or web reinforcement was reduced. In columns with short shear spans a few inclined cracks formed, followed quickly by an explosive shear failure along a diagonal plane between the loads. As mentioned previously, the authors analyzed these failures using a Mohr rupture criterion with considerable success. The test columns with ties spaced at d or $d/2$ had very little ductility while one with ties spaced at $d/4$ had considerable ductility. The shearing strengths of the four columns with ties can be safely predicted using the 1971 ACI Code.

In a review of Japanese column tests Hirose and Goto (86) concluded that the effect of axial loads could be accounted for by using $[v_c + 0.1(N/A_g)]$ as the shear carried by the concrete. They also concluded that 50% to 75% as much web reinforcement as required by the second term in the brackets in Eq. 4.23 would ensure a ductility ratio of 2

or more while 100% to 150% as much would ensure a ductility ratio of 3 or more. The ACI Code requirements approximately correspond to the values given for a ductility ratio of 2.

The 1971 SEAOC Seismic Recommendations (204) require that the ultimate shear resistance be based on the core area of the column. The shear carried by the concrete is taken from the ACI Code except that v_c is taken as zero when N_u/A_g is less than $0.12f'_c$ because of the crossing inclined cracks that occur when such member is subjected to reversed loadings.

As mentioned in Section 3.4.1, a series of tests were performed on beams with a circular cross section and reinforcement similar to spiral columns (60). The results suggest that the usual ACI design equations for rectangular sections could be applied to circular sections if the external diameter is used in the place of the effective depth and the gross area for the product, bd .

4.10 Recommended Research

During the past 5 yr the understanding of the behavior of beams failing in shear has improved to the extent that a fairly realistic description of beam behavior can be presented. This is not yet true for the special types of members described in this chapter. During the next few years a concentrated effort is needed to develop realistic behavioral models of deep beams, corbels, shear walls, etc. These will be of value to the designer in considering unusual design problems and will form a basis for the future unification and simplification of design rules.

ACKNOWLEDGMENTS

This report was written by the Joint ASCE-ACI Task Committee on Shear and Diagonal Tension. Chapters 1 and 2 were initially drafted by a subcommittee chaired by P. Gergely. The subcommittees responsible for Chapters 3 and 4 were chaired by J. G. MacGregor and J. M. Hanson, respectively. These chapters were then edited and correlated by J. G. MacGregor and reviewed and balloted by the members of the Task Committee. A future Chapter 5 on the Shear Strength of Slabs is currently being written under the direction of N. M. Hawkins. The Task Committee wishes to acknowledge the guidance and help of T. Diaz de Cossio, formerly Chairman, who originally proposed the concept of this report, and D. J. Caldera and R. G. Mathey, both of whom contributed to the report while members of the Task Committee. This report was reviewed by some 50 people, many of whom proposed additions, corrections, and improvements. The Task Committee is grateful for the time and effort which went into these reviews. The typing of several drafts of this manuscript was done by the secretarial staff in the Department of Civil Engineering, University of Alberta. The costs of drafting and the reproduction of the final draft were borne by the National Research Council of Canada through Grant No. NRC A1673. Finally, the Task Committee wishes to thank the Headquarters staff of both the American Society of Civil Engineers and the American Concrete Institute for their advice and help during the preparation of this report.

This report is respectfully submitted by the Joint ASCE-ACI Task Committee

426 on Shear and Diagonal Tension of the Committee on Masonry and Reinforced Concrete of the Structural Division.

Eugene Buth
Alex Cardenas
Vincent R. Cartelli
Edward Cohen
Robert A. Crist
Marvin E. Criswell
H. A. R. de Paiva
Paul F. Fratessa
Peter Gergely
Anand B. Gogate

John M. Hanson
Neil M. Hawkins
Nat. W. Krahl
Adrian E. Long
Keith O. O'Donnell
Richard A. Parmelee
Raymond C. Reese
Frederic Roll
Harold P. J. Taylor
Theodore C. Zsutty
James G. MacGregor, Chairman

APPENDIX I.—REFERENCES

- Acharya, D. N., and Kemp, K. O., "Significance of Dowel Forces on the Shear Failure of Rectangular Beams with Web Reinforcement," *Proceedings, American Concrete Institute*, Vol. 62, Oct. 1965, pp. 1265-1278.
- Alatorre, G., and Cassillas, J., "Shear Strength Behavior of Concrete Beams Subjected to Alternate Loads," *Rilem International Symposium on the Effects of Repeated Loading of Materials and Structures*, Vol. IV, 1966.
- Albritton, G. E., "Static Tests of Reinforced Concrete Deep Beams," *Technical Report No. 1-676*, U.S. Army Engineers Waterways Experiment Station, Vicksburg, Miss., June, 1965.
- Allen, W. E., and Huggins, M. W., "Pilot Tests on the Effectiveness of Lapped Stirrups in Reinforced Concrete Beams," *O.J.H.R.P. Report No. 34*, Department of Civil Engineering, University of Toronto, Toronto, Canada, May, 1964.
- ACI Committee 318, "Commentary on Building Code Requirements for Reinforced Concrete (ACI-318-63)," *ACI SP-10*, Detroit, Mich., 1965, pp. 81-88.
- ACI Committee 318, "Building Code Requirements for Reinforced Concrete (ACI-318-71)," American Concrete Institute, Detroit, Mich., 1971.
- ACI-ASCE Committee 326, "Shear and Diagonal Tension," *Proceedings, American Concrete Institute*, Vol. 59, Jan., Feb., and Mar., 1962, pp. 1-30, 277-334, and 353-396.
- ACI Committee 408, "Bond Stress—The State-of-the-Art," *Proceedings, American Concrete Institute*, Vol. 63, Nov., 1966, pp. 1161-1190.
- ACI Committee 442, "Response of Buildings to Lateral Forces," *ACI Journal, Proceedings*, Vol. 68, No. 2, Feb., 1971, pp. 81-106.
- Anis, N. N., "Shear Strength of Reinforced Concrete Flat Slabs Without Shear Reinforcement," thesis presented to Imperial College, University of London, at London, England, in 1970, in partial fulfillment of the requirements for the degree of Doctor of Philosophy.
- Bachmann, H., and Thürlimann, B., "Shear Design of Beams and Slabs of Reinforced, Partially Prestressed or Prestressed Concrete" (in German) *Schweizerische Bauzeitung*, Vol. 84, No. 33/34, Aug., 1966, pp. 583-591 and 599-605. Translation by K. Zoluda, Portland Cement Association.
- Baldwin, J. M., Jr., and Viest, I. M., "Effect of Axial Compression on Shear Strength of Reinforced Concrete Frame Members," *ACI Journal*, Nov., 1958, pp. 635-654.
- Baron, M., "Shear Strength of Reinforced Concrete Beams at Points of Bar Cutoff," *American Concrete Institute Journal*, Vol. 63, Jan., 1966, pp. 127-134.
- Baumann, T., "Tests to Study the Dowel Action of the Bending Tension Reinforcement of Reinforced Concrete Beams," *Bericht Nr. 77*, Munich Technischen Hochschule, 1968 (English Translation by Portland Cement Association).
- Baumann, T., and Rüschi, H., "Shear Tests With Indirect Loading," (in German) *Deutscher Ausschuss Für Stahlbeton*, Vol. 210, Wilhelm Ernst und Sohn, Berlin, West Germany, 1970.
- Beaufait, F. W., "Behavior of Reinforced Concrete Deep Beams Under Static and Dynamic Loading, Literature Review and Pilot Study," *Miscellaneous Paper No. 1-874*, U.S. Army Engineers Waterways Experiment Station, Vicksburg, Miss., Mar., 1967.
- Benjamin, J. R., and Williams, H. A., "The Behavior of One-Story Brick Shear Walls," *Journal of the Structural Division, ASCE*, Vol. 84, No. ST4, Proc. Paper 1723, July, 1958, pp. 1723-1-1723-30.
- Benjamin, J. R., and Williams, H. A., "Behavior of Reinforced Concrete Shear Walls," *Transactions, ASCE*, Vol. 124, 1959.
- Birkeland, P. W., and Birkeland, H. W., "Connections in Precast Construction," *Journal of the American Concrete Institute*, Vol. 63, No. 3, Mar., 1966, pp. 345-368.
- Borishanski, M. S., "Calculation of the Shear Strength of Reinforced Concrete Flexural Members According to the Soviet Norms," (in French), *Bulletin d'Information No. 42*, Comité Européen du Béton, Paris, France, May, 1965.
- Borishansky, M. S., and Gvozdev, A. A., "Design of Bent-up Bars and Stirrups in Reinforced Concrete Elements Based in Ultimate Strength," *Stroitzdat*, Moscow, U.S.S.R., 1946 (in Russian).
- Bower, J. E., and Viest, I. M., "Shear Strength of Restrained Concrete Beams without Web Reinforcement," *Proceedings, American Concrete Institute*, Vol. 57, July, 1960, pp. 73-98.
- Bresler, B., "Behavior of Structural Elements, A Review," *Proceedings of the Disaster Mitigation Workshop*, University of California, Aug., 1972.
- Bresler, B., and MacGregor, J. G., "Review of Concrete Beams Failing in Shear," *Journal of the Structural Division, ASCE*, Vol. 93, No. ST1, Proc. Paper 5106, Feb., 1967, pp. 343-372.
- Bresler, B., and Pister, K. S., "Strength of Concrete Under Combined Stresses," *Proceedings, American Concrete Institute*, Vol. 55, Sept., 1958, pp. 321-345.
- Bresler, B., and Scordelis, A. C., "Shear Strength of Reinforced Concrete Beams—Series II," *Report No. 64-2*, Structures and Materials Research, Department of Civil Engineering, University of California, Berkeley, Calif., Dec., 1964.
- "Draft British Standard Code of Practice for Structural Use of Concrete," *British Standards Institution*, London, England, 1970.
- Broms, B. B., "Stress Distribution, Crack Patterns and Failure Mechanisms of Reinforced Concrete Members," *Proceedings, American Concrete Institute*, Vol. 61, Dec., 1964, pp. 1535-1558.
- Bruce, R. N., "The Action of Vertical, Inclined and Prestressed Stirrups in Prestressed Concrete Beams," *Journal of the Prestressed Concrete Institute*, Vol. 9, Feb., 1964.
- Burnett, E. F. P., and Jajoo, R. P., "Reinforced Concrete Beam-Column Connection," *Journal of the Structural Division, ASCE*, Vol. 97, No. ST9, Proc. Paper 8395, Sept., 1971, pp. 2315-2336.
- Burns, N. H., and Pierce, D. M., "Strength and Behavior of Prestressed Concrete Members with Unbonded Tendons," *Journal of the Prestressed Concrete Institute*, Vol. 12, No. 5, Oct., 1967, pp. 15-29.
- Burton, K. T., and Hognestad, E., "Fatigue Tests of Reinforcing Bars—Tack Welding of Stirrups," *American Concrete Institute Journal, Proceedings*, Vol. 64, May, 1967, pp. 244-252.
- Callisch, R., and Thürlimann, B., "Shear Tests on Partially Prestressed Concrete Beams," (in German) *Report 6504-2*, E. T. H. Zürich, Institut für Baustatik, 1970.
- Canadian Standards Association, "A135 Code for Prestressed Concrete Construction," Ottawa, Canada, 1962.
- Cardenas, A. E., et al., "Design Provisions for Shear Walls," *Proceedings, American Concrete Institute*, Vol. 70, Mar., 1973, pp. 221-230.
- Cardenas, A. E., and Magura, D. D., "Strength of High-Rise Shear Walls—Rectangular Cross Sections," *Response of Multistory Concrete Structures to Lateral Forces*, *American Concrete Institute Publication SP-36*, Detroit, Mich., 1973, pp. 119-150.
- Carpenter, J. E., and Hanson, N. W., "Tests for Reinforced Concrete Beams with

- Large Openings in Thin Webs," *Proceedings, American Concrete Institute*, Vol. 65, No. 9, Sept., 1969, pp. 756-766.
38. Chang, T. S., and Kesler, C. E., "Static and Fatigue Strength in Shear of Beams with Tensile Reinforcement," *American Concrete Institute Journal*, Proc. Vol. 54, June, 1958, pp. 1033-1057.
 39. Chen, W. F., and Drucker, D. C., "Bearing Capacity of Concrete Blocks or Rock," *Journal of the Engineering Mechanics Division, ASCE*, Vol. 95, No. FM4, Proc. Paper 6742, Aug., 1969, pp. 955-978.
 40. Colley, B. E., and Humphrey, H. A., "Aggregate Interlock at Joints in Concrete Pavements," *Highway Research Record No. 189*, 1967, pp. 1-8; *Bulletin D124*, Portland Cement Association Research and Development Lab.
 41. Comité Européen du Béton—Fédération Internationale de la Précontrainte, "International Recommendations for the Design and Construction of Concrete Structures," Cement and Concrete Association, London, England, 1970.
 42. Comité Européen du Béton, "International Recommendations for the Design and Construction of Deep Beams," *Information Bulletin No. 73*, Paris, France, June 1970, pp. 17-24.
 43. Commissie AB, "Deep Beams and Short Brackets," (in Dutch with English Summary) *Commissie Voer Vitvoering Van Research, Betonvereniging, Zoetermeer, Netherlands*, Feb., 1971, 152 pp.
 44. Corley, W. G., "Rotational Capacity of Reinforced Concrete Beams," *Journal of the Structural Division, ASCE*, Vol. 92, No. ST5, Proc. Paper 4939, Oct., 1966, pp. 121-146.
 45. Corley, W. G., and Hanson, N. W., "Design of Beam-Column Joints for Seismically Resistant Reinforced Concrete Frames," *Proceedings, Fourth World Conference on Earthquake Engineering, Santiago, Chile, Jan., 1969*.
 46. Cowan, H. J., "The Strength of Plain, Reinforced and Prestressed Concrete under the Action of Combined Stresses with Particular Reference to the Combined Bending and Torsion of Rectangular Sections," *Magazine of Concrete Research*, Vol. 5, No. 14, Dec., 1953.
 47. Crist, R. A., "Shear Behavior of Deep Reinforced Concrete Beams, Vol. II: Static Tests," *AFWL-TR-67-61*, Kirtland Air Force Base, N.M., Oct., 1967.
 48. Crist, R. A., "Shear Behavior of Deep Reinforced Concrete Beams, Vol. III: Dynamic Tests," *AFWL-TR-67-61*, Kirtland Air Force Base, N.M., Dec., 1968.
 49. Crist, R. A., "Shear Behavior of Deep Reinforced Concrete Beams, Vol. I: Summary of Testing," *AFWL-TR-67-61*, Kirtland Air Force Base, N.M., Dec., 1970.
 50. Crist, R. A., "Static and Dynamic Shear Behavior of Uniformly Reinforced Concrete Deep Beams," *AFWL-TR-71-74*, University of New Mexico (CERF) Kirtland Air Force Base, N.M., Nov., 1971, thesis presented to the University of New Mexico at Albuquerque, N.M., in partial fulfillment of the requirements for the degree of Doctor of Philosophy.
 51. Demorieux, J. M., "Tests of Tension-Compression on Models of the Webs of Reinforced Concrete Beams," (in French) *Annales de L'Institut Technique du Bâtiment et des Travaux Publics*, Vol. 22, No. 258, June, 1969, pp. 980-982.
 52. de Paiva, H. A. R., and Austin, W. J., "Behavior and Design of Deep Structural Members: Part 3, Tests of Reinforced Concrete Deep Beams," *AFSWC-TR-59*, Kirtland Air Force Base, N.M., March, 1960.
 53. de Paiva, H. A. R., Neville, A. M., and Guger, H. A., "Shear Moment Interaction in Continuous Prestressed Concrete I-Beams with Varying Level Supports," *Journal of the Prestressed Concrete Institute*, Vol. 12, No. 2, Apr., 1967, pp. 38-56.
 54. de Paiva, H. A. R., and Siess, C. P., "Strength and Behavior of Deep Beams in Shear," *Journal of the Structural Division, ASCE*, Vol. 91, No. ST5, Proc. Paper 4496, Oct., 1965, pp. 19-42.
 55. Diaz de Cossio, R., discussion of Reference 7, *ACI Journal*, Proc. Vol. 59, Sept. 1962, pp. 1323-1332.
 56. Diaz de Cossio, R., and Rosenbluth, E., "Reinforced Concrete Failures Due to Earthquakes," *American Concrete Institute Journal*, Vol. 58, Nov., 1961, pp. 571-584.
 57. Dill, A. F., "Strength and Behavior of Restrained Deep Reinforced Concrete Beams Under Static Loading," *AFWL, RTD-TDR-63-3092*, Kirtland Air Force Base, N.M., Sept., 1963.

58. Farodji, M. J., and Diaz de Cassio, R., "Diagonal Tension in Concrete Members of Circular Section," (in Spanish) *Ingeniería, Mexico*, Apr., 1965, pp. 257-280 (Translation by Portland Cement Assoc., *Foreign Literature Study No. 466*).
59. Feldman, A., "Behavior and Design of Deep Structural Members: Part 5, Resistance and Behavior of Reinforced Concrete Beams of Normal Proportions Under Rapid Loading," *AFSWC-TR-59-72*, Kirtland Air Force Base, N.M., Mar., 1960.
60. Fenwick, R. C., and Paulay, T., "Mechanisms of Shear Resistance of Concrete Beams," *Journal of the Structural Division, ASCE*, Vol. 94, No. ST10, Proc. Paper 2325, Oct., 1968, pp. 2325-2350.
61. Ferguson, P. M., "Some Implications of Recent Diagonal Tension Tests," *American Concrete Institute Journal*, Proc. Vol. 53, Aug., 1956, pp. 157-172.
62. Ferguson, P. M., Unpublished Data on Tests of Short Cantilever Beams Tested at the University of Texas, Austin, Tex.
63. Ferguson, P. M., "Design Criteria for Overhanging Ends of Bent Caps-Bond and Shear," *Final Report, Center for Highway Research, The University of Texas, Austin, Tex.*, Aug., 1964, 41 pp.
64. Ferguson, P. M., *Reinforced Concrete Fundamentals*, 3rd ed., John Wiley and Sons, New York, N.Y., 1973.
65. Ferguson, P. M., and Matloob, F. M., "Effect of Bar Cutoff on Bond and Shear Strength of Reinforced Concrete Beams," *American Concrete Institute Journal*, Vol. 56, July, 1959, pp. 5-24.
66. Fiorato, A. E., Sozen, M. A., and Gamble, W. L., "An Investigation of the Interaction of Reinforced Concrete Frames with Masonry Filler Walls," *SRS 330, Civil Engineering Studies, University of Illinois, Urbana, Ill.*, Nov., 1970.
67. Franz, G., and Niendenhoff, H., "The Reinforcement of Brackets and Short Deep Beams," *Beton und Stahlbetonbau*, Vol. 58, No. 5, (Translation No. 114, Cement and Concrete Association, London, England, Dec., 1964), May, 1963.
68. Fratessa, P. F., and Zsutty, T., "Strength and Performance of Concrete Shear Walls," *Report to the S.E.A.O.N.C. Seismology Subcommittee on Shear Walls, 1970*, 49 pp. also *Proceedings, S.E.A.O.C. 38th Annual Convention, 1969*, p. 72.
69. Gergely, P., "Splitting Cracks Along the Main Reinforcement in Concrete Members," *Report to Bureau of Public Roads, U.S. Department of Transportation, Cornell University, Ithaca, N.Y.*, Apr., 1969.
70. Gusalnick, S. A., "Strength of Reinforced Concrete Beams," *Transactions, ASCE*, Vol. 125, Paper No. 3036, 1960, pp. 603-645.
71. Gustafson, D. P., "Shear Behavior of Prestressed Concrete Bridge Girders," thesis presented to Tulane University, at New Orleans, La., in 1967, in partial fulfillment of the requirements for the degree of Doctor of Philosophy.
72. Haddadin, M. J., Hong, S., and Mattock, A. H., "Stirrup Effectiveness in Reinforced Concrete Beams with Axial Forces," *Journal of the Structural Division, ASCE*, Vol. 97, No. ST9, Proc. Paper 8394, Sept., 1971, pp. 2277-2298.
73. Hampe, P. A., and Bolsara, J. P., "An Experimental Study of Model Deep Beams, Report 1, Tests on One-Quarter Scale Simply Supported Beams," *Miscellaneous Paper W-68-3*, U.S. Army Engineers Waterways Experiment Station, Vicksburg, Miss., July, 1968.
74. Hanson, J. A., "Tensile Strength and Diagonal Tension Resistance of Structural Lightweight Concrete," *American Concrete Institute Journal*, Proc. Vol. 58, July, 1961, pp. 1-39.
75. Hanson, J. M., "Square Openings in Webs of Continuous Joists," *Research and Development Bulletin*, Portland Cement Association, 1969, 14 pp.
76. Hanson, J. M., Corley, W. G., and Hognestad, E., "Evaluation of Structural Concrete Members Penetrated by Service Systems," *RILEM-ASTM-CIB Symposium on the Performance Concept in Buildings*, Philadelphia, Pa., 1972.
77. Hanson, J. M., and Hulbos, C. L., "Ultimate Shear Tests of Large Prestressed Concrete Bridge Beams," *Paper SP-26-21, Proceedings of the Second International Symposium on Concrete Bridge Design, ACI Publication SP-26*, 1971, pp. 523-551.
78. Hanson, J. M., Hulbos, C. L., and Van Horne, D. A., "Fatigue Tests of Prestressed Concrete I Beams," *Journal of the Structural Division, ASCE*, Vol. 96, No. ST11, Proc. Paper 7705, Nov., 1970, pp. 2443-2464.
79. Hanson, N. W., "Precast-Prestressed Concrete Bridges—2. Horizontal Shear Connec-

- tions," *Journal of the Portland Cement Association, Research and Development Laboratories*, Vol. 2, No. 2, May, 1960, pp. 38-58.
80. Hanson, N. W., "Seismic Resistance of Concrete Frames with Grade 60 Reinforcement," *Journal of the Structural Division, ASCE*, Vol. 97, No. ST6, Proc. Paper 8180, June, 1971, pp. 1685-1700.
 81. Hanson, N. W., and Conner, H. W., "Seismic Resistance of Reinforced Concrete Beam-Column Joints," *Journal of the Structural Division, ASCE*, Vol. 93, No. ST5, Oct., 1967, pp. 533-560.
 82. Hawkins, N. M., "Shear Provisions of AS CA35 Code for Prestressed Concrete," *Civil Engineering Transactions, Institution of Engineers, Australia*, Sept., 1964, pp. 103-116.
 83. Hawkins, N. M., unpublished memorandum to Shear Committee, Nov., 1971.
 84. Hawkins, N. M., Sozen, M. A., and Siess, C. P., "Behavior of Continuous Prestressed Concrete Beams," *Proceedings of International Symposium on Flexural Mechanics of Reinforced Concrete, ACI Special Publication No. 12*, 1965.
 85. Hernandez, G., "Strength of Prestressed Concrete Beams with Web Reinforcement," thesis presented to the University of Illinois, at Urbana, Ill. in 1958, in partial fulfillment of the requirements for the degree of Doctor of Philosophy, University Microfilms, Ann Arbor, Mich.
 86. Hirosawa, M., and Goto, T., "Strength and Ductility of Reinforced Concrete Members Subjected to Shear, Moment, and Axial Load," *Transactions, Architectural Institute of Japan*, Nov., 1971.
 87. Hofbeck, J. A., Ibrahim, I. A., and Mattock, A. H., "Shear Transfer in Reinforced Concrete," *Journal of the American Concrete Institute*, Vol. 66, No. 2, Feb., 1969, pp. 119-128.
 88. Hognestad, E., "What do We Know About Diagonal Tension and Web Reinforcement in Concrete?," *Circular Series No. 64, University of Illinois Engineering Experiment Station*, Mar., 1952, 47 pp.
 89. International Conference of Building Officials, "Uniform Building Code," Pasadena, Calif., 1970.
 90. Ivey, Don L., and Butl, Eugene, "Shear Capacity of Lightweight Concrete Beams," *Proceedings, American Concrete Institute*, Vol. 64, Oct., 1967, pp. 634-643.
 91. Iyengar, K. T. S. R., Rangan, B. V., and Paloniswamy, R., "Some Factors Affecting Shear Strength of Reinforced Concrete Beams," *Indian Concrete Journal*, Vol. 42, Dec., 1968, pp. 499-505.
 92. Jirsa, J. O., "Cast-in-Place Joints for Tall Buildings," *State of Art Report No. 1 Technical Committee 21, Proceedings, International Conference on Tall Buildings* Lehigh University, Bethlehem, Pa., 1973.
 93. Johnson, R. P., "Longitudinal Shear Strength of Composite Beams," *American Concrete Institute Journal*, Vol. 67, June, 1970, pp. 464-466.
 94. Jungwirth, D., "Elektronische Berechnung des in einem Stahlbetonbalken in gewissen Zustand auftretenden Kraftzustandes unter besonderer Berücksichtigung des Querkraftbereiches," *Deutscher Ausschuss für Stahlbeton*, Vol. 211, Verlag Wilhelm Ernst und Sohn, Berlin, West Germany, 1970.
 95. Kaar, P. H., and Mattock, A. H., "High Strength Bars as Concrete Reinforcement: Part 4, Control of Cracking," *Journal of the PCA Research and Development Laboratories*, Vol. 5, No. 1, Jan., 1963, pp. 15-38.
 96. Kani, G. N. J., "The Riddle of Shear Failure and Its Solution," *Proceedings, American Concrete Institute*, Vol. 61, Apr., 1964, p. 441.
 97. Kani, G. N. J., "Basic Facts Concerning Shear Failure," *American Concrete Institute Journal*, Proc. Vol. 63, June, 1966, pp. 675-692.
 98. Kani, G. N. J., "How Safe are Our Large Reinforced Concrete Beams?," *American Concrete Institute Journal*, Proc. Vol. 64, Mar., 1967, pp. 128-141.
 99. Kani, G. N. J., "A Rational Theory for the Function of Web Reinforcement," *American Concrete Institute Journal*, Proc. Vol. 66, Mar., 1969, pp. 185-197.
 100. Kar, J. N., "Diagonal Cracking in Prestressed Concrete Beams," *Journal of the Structural Division, ASCE*, Vol. 94, No. ST1, Proc. Paper 5713, Jan., 1968, pp. 83-109.
 101. Kennedy, R. P., "A Statistical Analysis of the Shear Strength of Reinforced Concrete Beams," thesis presented to the Stanford University, at Stanford, Calif., in 1967

- in partial fulfillment of the requirements for the degree of Doctor of Philosophy.
102. Kinnunen, S., "Punching of Concrete Slabs with Two-Way Reinforcement with Special Reference to Dowel Effect and Deviation of Reinforcement from Polar Symmetry," *Trans. No. 198, Royal Institute of Technology, Stockholm, Sweden*, 1963.
 103. Kokubu, M., and Higai, T., "Shear Failure of Reinforced Concrete Beams Subjected to Repeated Loading," *Memories of Faculty of Engineering, University of Tokyo, Tokyo, Japan*, 1971, pp. 195-198.
 104. Kong, F. K., and Robins, P. J., "Web Reinforcement Effects on Lightweight Concrete Deep Beams," *American Concrete Institute Journal*, Vol. 68, No. 7, July, 1971, pp. 514-520.
 105. Krahl, N. W., Khachaturian, N., and Siess, C. P., "Stability of Tensile Cracks in Concrete Beams," *Journal of the Structural Division, ASCE*, Vol. 93, No. ST1, Proc. Paper 5098, Feb., 1967, pp. 235-254.
 106. Krauss, R., and Bachmann, H., "Bending and Shear Tests on Partially Prestressed Lightweight Concrete Beams," (in German) *Report No. 6504-4, Inst. für Baustatik, Swiss Federal Technical University, Zurich, Switzerland*, Oct., 1971.
 107. Krefeld, W. J., and Thurston, C. W., "Contribution of Longitudinal Steel to Shear Resistance of Reinforced Concrete Beams," *Journal of the American Concrete Institute*, Proc. Vol. 63, No. 3, Mar., 1966, pp. 325-344.
 108. Krefeld, W. J., and Thurston, C. W., "Studies of the Shear and Diagonal Tension Strength of Simply Supported Reinforced Concrete Beams," *American Concrete Institute Journal*, Apr., 1966.
 109. Kriz, L. B., and Raths, C. H., "Connections in Precast Concrete Structures—Strength of Corbels," *Journal, Prestressed Concrete Institute*, Vol. 10, No. 1, Feb., 1965, also *PCA Development Department Bulletin D85*.
 110. Kupfer, H., Hilsdorf, H., and Rüschi, H., "Behavior of Concrete under Biaxial Stress," *Proceedings, American Concrete Institute*, Vol. 66, Aug., 1969, pp. 656-666.
 111. Laupa, A., Siess, C. P., and Newmark, N. M., "Strength in Shear of Reinforced Concrete Beams," *Bulletin No. 428, Engineering Experiment Station, Urbana, Ill., University of Illinois, Urbana, Ill.*, Mar., 1955.
 112. Leonhardt, F., "Reducing the Shear Reinforcement in Reinforced Concrete Beams and Slabs," *Magazine of Concrete Research*, Vol. 17, No. 53, Dec., 1965, pp. 187-194.
 113. Leonhardt, F., "Deep Beams—Plane Structures Loaded Parallel to their Mid-Plane," (in French), *Bulletin D'Information No. 65, Comité Européen du Béton, Paris, France*, Feb., 1968, pp. 1-113.
 114. Leonhardt, F., "Shear and Torsion in Prestressed Concrete," *Lecture, Session IV, VI IIP Congress, Prague, Czechoslovakia*, 1970.
 115. Leonhardt, F., Koch, R., and Rostásy, F. S., "Hanger Reinforcement for Indirectly Loaded Prestressed Concrete Beams, Test Report and Recommendations," (in German) *Beton und Stahlbetonbau*, Vol. 66, Oct., 1971, pp. 233-241.
 116. Leonhardt, F., and Walther, R., "The Stuttgart Shear Tests, 1961," *Translation No. 111, Cement and Concrete Association, London, England*, 1964.
 117. Leonhardt, F., and Walther, R., "Welded Wire Mesh as Stirrup Reinforcement, Shear Tests of T-Beams, and Anchorage Tests," (in German) *Bautechnik*, Vol. 42, Oct., 1965, English translation by W. Dilger.
 118. Leonhardt, F., and Walther, R., "Wandartige Träger," *Deutscher Ausschuss für Stahlbeton*, Vol. 178, Wilhelm Ernst und Sohn, Berlin, West Germany, 1966.
 119. Leonhardt, F., Walther, R., and Dilger, W., "Shear Tests on Indirectly Loaded, Simple and Continuous Reinforced Concrete Beams," (in German) *Deutscher Ausschuss für Stahlbeton*, Vol. 201, Verlag Von Wilhelm Ernst Sohn, Berlin, West Germany, 1968.
 120. Lew, H. S., Leyendecker, E. V., and Dikkers, R. D., "Engineering Aspects of the 1971 San Fernando Earthquake," *Building Science Series 40, National Bureau of Standards, Washington, D.C.*, Dec., 1971, pp. 130-138.
 121. Liu, T. C. Y., Nilson, A. H., and Slate, F. O., "Biaxial Stress-Strain Relations for Concrete," *Journal of the Structural Division, ASCE*, Vol. 98, No. ST5, Proc. Paper 8905, May, 1972, pp. 1025-1034.
 122. Leober, P. J., "Shear Transfer by Aggregate Interlock," thesis presented to the University of Canterbury, at Christchurch, New Zealand, in 1970, in partial fulfillment of the requirements for the degree of Master of Engineering.

123. Lorensten, M., "Holes in Reinforced Concrete Girders," *Byggmastaren*, Vol. 41, No. 7, July, 1972, pp. 141-152, English translation from Swedish by the Portland Cement Association.
124. MacGregor, J. G., unpublished memorandum about Width of Shear Cracks, July, 1971.
125. MacGregor, J. G., "Shear Tests of T-Beams Subjected to Combined Shear Bending and Axial Tension," (in German) Otto-Graf Institute, Stuttgart, West Germany, 1972.
126. MacGregor, J. G., and Hanson, J. M., "Proposed Changes in Shear Provisions for Reinforced and Prestressed Concrete Beams," *ACI Journal*, Vol. 66, Apr., 1969, pp. 276-288.
127. MacGregor, J. G., Siess, C. P., and Sozen, M. A., "Behavior of Prestressed Concrete Beams Under Simulated Moving Loads," *Journal of the American Concrete Institute*, Vol. 63, No. 8, Aug., 1966, pp. 835-842.
128. MacGregor, J. G., Sozen, M. A., and Siess, C. P., "Effect of Draped Reinforcement on Research of Prestressed Concrete Beams," *Proceedings, American Concrete Institute*, Detroit, Mich., Dec., 1960, pp. 649-677.
129. MacGregor, J. G., and Walters, J. R. V., "Analysis of Inclined Cracking Shear in Slender Reinforced Concrete Beams," *Proceedings, American Concrete Institute*, Vol. 64, No. 10, Oct., 1967, pp. 644-653.
130. Mast, R. F., "Auxiliary Reinforcement in Concrete Connections," *Journal of the Structural Division, ASCE*, Vol. 94, No. ST6, Proc. Paper 6002, June, 1968, pp. 1485-1504.
131. Masterson, D. M., "A Study of the Punching Strength of Reinforced Concrete Flat Slabs," thesis presented to Queen's University, at Kingston, Canada, in 1971, in partial fulfillment of the requirements for the degree of Doctor of Philosophy.
132. Mathey, R., and Watstein, D., "Shear Strength of Beams without Web Reinforcement Containing Deformed Bars of Different Yield Strengths," *American Concrete Institute Journal*, Vol. 60, Feb., 1963, pp. 183-208.
133. Mattock, A. H., "Diagonal Tension Cracking in Concrete Beams with Axial Forces," *Journal of the Structural Division, ASCE*, Vol. 95, No. ST9, Proc. Paper 6776, Sept., 1969, pp. 1887-1960.
134. Mattock, A. H., and Hawkins, N. M., "Research on Shear Transfer in Reinforced Concrete," *Journal of the Prestressed Concrete Institute*, Vol. 17, No. 2, Mar., Apr., 1972.
135. Mehmel, A., and Becker, G., "Shear Tests of Short Cantilevers," *Der Bauingenieur*, 40, Heft 6, 1965, pp. 224-231.
136. Mehmel, A., and Freitag, W., "Investigation of the Strength of Reinforced Concrete Corbels," *Der Bauingenieur*, 42, Heft 10, 1967, pp. 362-369.
137. Morrow, J., and Viest, I. M., "Shear Strength of Reinforced Concrete Frame Members Without Web Reinforcement," *American Concrete Institute Journal*, Mar., 1957, pp. 833-869.
138. Murashev, V., Sigalov, E., and Baikov, V., "Design of Reinforced Concrete Structures," Mir Publishers, Moscow, U.S.S.R., 1968 (English).
139. Muto, K., and Kokusho, K., "Experimental Study on Two-Story Reinforced Concrete Shear Walls," Muto Laboratories, University of Tokyo, Tokyo, Japan, translated by T. Akagi, University of Illinois, Urbana, Ill., Aug., 1959.
140. Nasser, K. W., Acavalos, A., and Daniel, H. R., "Behavior and Design of Large Openings in Reinforced Concrete Beams," *American Concrete Institute Journal*, Vol. 64, No. 1, Jan., 1967, pp. 25-33.
141. Neth, V. W., "Model Studies on Punching of Reinforced Concrete Flat Slabs at Edge Columns," thesis presented to Queen's University, at Kingston, Canada, in 1971, in partial fulfillment of the requirements for the degree of Master of Science.
142. Newman, K., and Newman, J. B., "Failure Theories and Design Criteria for Plain Concrete," International Conference, Southampton, England, Apr., 1969.
143. Niwa, Y., Kobayashi, S., and Koyanagi, W., "Failure Criterion of Light-weight Aggregate Concrete Subjected to Triaxial Compression," *Memoires, Faculty of Engineering, Kyoto University, Kyoto, Japan*, 1967.
144. Nowlen, W. J., "Influence of Aggregate Properties on Effectiveness of Interlock Joints in Concrete Pavements," *Journal of the PCA Research and Development Laboratories, Bulletin D139*, Vol. 10, No. 2, May, 1968, pp. 2-8.

145. Ockleston, A. J., "Tests on the Old Dental Hospital, Johannesburg: Paper No. 3; The Effect of Floors and Walls on the Behavior of Reinforced Concrete Frameworks Subject to Horizontal Loading," The Concrete Association of South Africa, Johannesburg, South Africa, Nov., 1956.
146. Ogura, K., and Hirokawa, M., "Shear Design in New Recommendations of A. I. J. for Structural Design of Reinforced Concrete," *Proceedings, Third Regional Conference, ASCE-IABSE Joint Committee on Planning and Design of Tall Buildings*, Tokyo, Japan, Sept., 1971.
147. Ogura, K., Kokusho, K., and Matsoura, N., "Tests to Failure of Two-Story Rigid Frames with Walls," Part 24, *Experimental Study No. 6, Japan Society of Architects Report No. 18*, Feb., 1952, translated by T. Akagi, Univ. of Illinois, Urbana, Ill., Aug., 1959.
148. Oleson, S. E., Sozen, M. A., and Siess, C. P., "Investigation of Prestressed Reinforced Concrete for Highway Bridges"—Part IV: Strength in Shear of Beams with Web Reinforcements," *Bulletin No. 493, University of Illinois Engineering Experiment Station*, Urbana, Ill., 1967.
149. Parmalee, R. A., "A Study of the Ultimate Strength of Reinforced Concrete Beams," *Structural Engineering and Structural Mechanics Report #61-11*, University of California, Berkeley, Calif., Jan., 1961, 66 pp.
150. Paul, P., "Macroscopic Criteria for Flow and Fracture," Chapter 4, *Fracture*, Liebowitz, ed., Vol. 2, Academic Press, New York, N.Y., 1969.
151. Paulay, T., "Coupling Beams of Reinforced Concrete Shear Walls," *Journal of the Structural Division, ASCE*, Vol. 97, No. ST3, Proc. Paper 7984, Mar., 1971, pp. 843-862.
152. Paulay, T., "Simulated Seismic Loading of Spandrel Beams," *Journal of the Structural Division, ASCE*, Vol. 97, No. ST9, Proc. Paper 8365, Sept., 1971, pp. 2407-2419.
153. Placas, A., and Regan, P. E., "Shear Failures of Reinforced Concrete Beams," *Proceedings, American Concrete Institute*, Vol. 68, Oct., 1971, pp. 763-773.
154. Portland Cement Association, "Design of Deep Girders," *Concrete Information*, 10 pp.
155. Prestressed Concrete Institute, "PCI Design Handbook," Chicago, Ill., 1971.
156. Price, K. M., and Edwards, A. D., "Fatigue Strength in Shear of Prestressed Concrete I Beams," *American Concrete Institute Journal*, Vol. 68, Apr., 1971, pp. 282-292.
157. Regan, H. S., and Warwaruk, J., "Tee Members with Large Web Openings," *Journal, Prestressed Concrete Institute*, Vol. 12, No. 4, Aug., 1967, pp. 52-65.
158. Rajagopalan, K. S., and Ferguson, P. N., "Exploratory Shear Tests Emphasizing Percentage of Longitudinal Steel," *American Concrete Institute Journal*, Vol. 65, Aug., 1968, pp. 634-638.
159. Rausch, E., "Design of Bent Bars for Shear," *Der Bauingenieur*, Vol. 3, No. 7, Berlin, West Germany, Apr., 1972.
160. Rausch, E., "Shear in Reinforced Concrete Structures," *Der Bauingenieur*, Vol. 12, No. 32/33, Berlin, West Germany, Aug., 1931.
161. Renton, G. W., "The Behavior of Reinforced Concrete Beam Column Joints Under Cyclic Loading," thesis presented to the University of Canterbury, at Christchurch, New Zealand, in 1972, in partial fulfillment of the requirements for the degree of Master of Engineering.
162. Reynolds, G. C., "Shear Provisions for Prestressed Concrete in the Draft Unified Code," *Technical Report TRA432*, Cement and Concrete Association, London, England, Dec., 1969.
163. Robinson, J. R., "Influence of Transverse Reinforcement on Shear and Bond Strength," *American Concrete Institute Journal*, Vol. 62, Mar., 1965, pp. 343-362.
164. Rodriguez, J. J., et al., "Shear Strength of Two Span Continuous Reinforced Concrete Beams," *American Concrete Institute Journal*, Vol. 55, No. 10, Apr., 1959, pp. 1089-1130.
165. Sauve, J. G., "Prestressed Concrete Tee Beams with Large Web Openings," thesis presented to the University of Alberta, at Edmonton, Alberta, Canada, in 1970, in partial fulfillment of the requirements for the degree of Master of Science.
166. Seabold, R. H., "Dynamic Shear Strength of Reinforced Concrete Beams—Part III," *Technical Report R695*, Naval Civil Engineering Laboratory, Port Hueneme, Calif., Sept., 1970.

167. Seismology Committee, "Recommended Lateral Requirements, 1971 Revisions," Structural Engineers Association of California, 1971.
168. Sheikh, M. A., de Paiva, H. A. R., and Neville, A. M., "Calculation of Flexure-Shear Strength of Prestressed Concrete Beams," *Journal of the Prestressed Concrete Institute*, Vol. 13, No. 1, Feb., 1968, pp. 68-85.
169. Sih, G. C., and Liebowitz, H., "Mathematical Theories of Brittle Fracture," Chapter 2, *Fracture*, Liebowitz, ed., Vol. 2, Academic Press, New York, N.Y., 1969, pp. 68-190.
170. Slater, W. A., Lord, A. R., and Zipprodt, R. R., "Shear Tests of Reinforced Concrete Beams," National Bureau of Standards, Washington, D.C., 1926.
171. Sommerville, G., "The Behavior and Design of Reinforced Concrete Corbels," *Technical Report No. 42-472*, Cement and Concrete Association, London, England, Aug., 1972.
172. Sommerville, G., and Taylor, H. P. J., "The Influence of Reinforcement Detailing on the Strength of Concrete Structures," *The Structural Engineer*, Vol. 50, No. 1, Jan., 1972, pp. 7-19, Discussion, Aug., 1972, pp. 309-321.
173. Sozen, M. A., "The Caracas Earthquake of July 29, 1967," *American Concrete Institute Journal*, Vol. 65, May, 1968, pp. 394-401.
174. Sozen, M. A., and Hawkins, N. M., Discussion of Reference 7, *Proceedings*, American Concrete Institute, Vol. 59, Sept., 1962, pp. 1341-1347.
175. Sozen, M. A., Zwoyer, E. M., and Siess, C. P., "Strength in Shear of Beams Without Web Reinforcement," Investigation of Prestressed Concrete for Highway Bridges, Part I, *Bulletin No. 452*, University of Illinois Engineering Experiment Station, Apr., 1959, 69 pp.
176. Swami, R. M., and Qureshi, S. A., "Strength, Cracking and Deformation Similitude in Reinforced T-Beams under Bending and Shear," *Proceedings*, American Concrete Institute, Vol. 68, Mar., 1971, pp. 187-195.
177. Taub, J., and Neville, A. M., "Resistance to Shear of Reinforced Concrete Beams, Part I—Beams Without Web Reinforcement," *Proceedings*, American Concrete Institute, Vol. 57, Aug., 1970, pp. 193-220.
178. Taylor, H. P. J., "Investigation of the Dowel Shear Forces Carried by the Tensile Steel in Reinforced Concrete Beams," *Technical Report TRA 431*, Cement and Concrete Association, London, England, Nov., 1969.
179. Taylor, H. P. J., "Investigations of the Forces Carried Across Cracks in Reinforced Concrete Beams in Shear by Interlock of Aggregate," *Technical Report 42-477*, Cement and Concrete Association, London, England, 1970, 22 pp.
180. Taylor, H. P. J., "Fundamental Behavior of Reinforced Concrete in Bending and Shear," thesis presented to City University, at London, England, in 1971, in partial fulfillment of the requirements for the degree of Doctor of Philosophy.
181. Taylor, H. P. J., "Shear Strength of Large Beams," *Journal of the Structural Division*, ASCE, Vol. 98, No. ST11, Proc. Paper 9329, Nov., 1972, pp. 2473-2490.
182. Taylor, R., "Some Aspects of the Problem of Shear in Reinforced Concrete Beams," *Civil Engineering and Public Works Review*, London, England, May, 1963, pp. 629-632, 768-770.
183. Taylor, R., "Some Shear Tests on Reinforced Concrete Beams without Web Reinforcement," *Magazine of Concrete Research*, Vol. 12, No. 36, Nov., 1960, pp. 145-154.
184. Thürlimann, B., "A Case for Partial Prestressing," *Proceedings*, Structural Concrete Symposium, University of Toronto, Toronto, Ontario, Canada, May, 1971, pp. 253-301.
185. Tomii, M., "Introduction and Summary of Design Procedures of Concrete Shear Walls," Japan Joint Seminar, Feb., 1967.
186. Tomii, M., "Shear Walls," *State-of-the-Art Report 21-4*, *Proceedings*, ASCE-International Association for Bridge and Structural Engineering International Conference on Tall Buildings, 1973.
187. Tsuboi, Y., Suenaga, Y., and Shigenobu, T., "Fundamental Study on Reinforced Concrete Shear Wall Structures—Experimental and Theoretical Study of Strength and Rigidity of Two-Directional Structural Walls Subjected to Combined Stresses M.N.Q.," *Transactions of the Architectural Institute of Japan*, No. 131, Jan., 1967, *PCA Foreign Literature Study No. 536*, Nov., 1967.

188. Umemura, H., and Aoyama, H., "Evaluation of Inelastic Seismic Deflection of Reinforced Concrete Frames based on Test of Members," *Proceedings of the Fourth World Conference on Earthquake Engineering*, Chile, Nov. 1, 1969, pp. B2-81 to B2-108.
189. Untrauer, R. E., "Behavior and Design of Deep Structural Members: Part 4, Dynamic Tests of Reinforced Concrete Deep Beams," AFSWC-TR-59-72, Kirtland Air Force Base, N.M., May, 1960.
190. Varghese, P. C., and Krishnamoorthy, C. S., "Strength and Behavior of Deep Reinforced Concrete Beams," *Indian Concrete Journal*, Bombay, India, Mar., 1966.
191. Vasiliev, A. P., Bychenkov, Y. D., and Matkov, N. G., "Prefabricated Reinforced Concrete Multi-Story Frame Buildings in the USSR," *State of the Art Report 5*, Technical Committee 3, *Proceedings*, International Conference on Tall Buildings, Lehigh University, Bethlehem, Pa., 1973.
192. Walther, R., "Calculation of the Shear Strength of Reinforced Concrete and Prestressed Concrete by the Shear Failure Theory," *Translation No. 110*, Cement and Concrete Association, London, England.
193. White, R. M., and Holley, M. J., "Experimental Studies of Membrane Shear Transfer," *Journal of the Structural Division*, ASCE, Vol. 98, No. ST8, Proc. Paper 9145, Aug., 1972, pp. 1835-1852.
194. Winemiller, J. R., and Austin, W. J., "Behavior and Design of Deep Structural Members: Part 2, Tests of Reinforced Concrete Deep Beams with Web Reinforcement," AFSWC-TR-59-72, Kirtland Air Force Base, N.M., Aug., 1960.
195. Yamada, M., and Furui, S., "Shear Resistance and Explosive Cleavage Failure of Reinforced Concrete Members Subjected to Axial Load," *Final Report*, Eighth Congress of International Association for Bridge and Structural Engineering, New York, N.Y., 1968, pp. 1091-1102.
196. Yorulmas, M., and Sozen, M. A., "Behavior of Single-Story Reinforced Concrete Frames with Filler Walls," *Civil Engineering Studies Structural Research Series No. 337*, University of Illinois, Urbana, Ill., May, 1968.
197. Zalesov, A., personal Discussion with J. G. MacGregor, May, 1972.
198. Zia, P., "Torsional Strength of Prestressed Concrete Members," *Proceedings*, American Concrete Institute, Vol. 57, Apr., 1961, pp. 1337-1360.
199. Zsutty, T. C., "Beam Shear Strength Prediction by Analysis of Existing Data," *Proceedings*, American Concrete Institute, Vol. 65, Nov., 1968, p. 943, (Discussions May, 1969, p. 435.)
200. Zsutty, T., "Shear Strength Prediction for Separate Categories of Simple Beam Tests," *American Concrete Institute Journal*, Vol. 68, Feb., 1971, pp. 138-143.
201. Zsutty, T. C., unpublished memorandum to Reinforced Concrete Research Council, May, 1972.
202. Zwoyer, E. M., and Siess, C. P., "Ultimate Strength in Shear of Simply Supported Prestressed Concrete Beams Without Web Reinforcement," *Proceedings*, American Concrete Institute, Vol. 51, Oct., 1954, pp. 181-200.

APPENDIX II.—NOTATION

The following symbols are used in this paper:

- A_s = area of longitudinal tension reinforcement;
- A_{sp} = area of prestressing reinforcement;
- A_v = area of shear reinforcement within distance s , or area of shear reinforcement perpendicular to main tension reinforcement within distance s for deep beams;
- A_{vh} = area of shear reinforcement parallel to main tension reinforcement within distance s_h ;
- a = shear span, distance between concentrated load and face of support;

- z_m = right cable coordinate;
 α = reciprocal eigenvalue;
 γ = slope;
 $\Delta_x, \Delta_y, \Delta_z$ = corrective forces at right cable position;
 δ = positive correction value;
 $\theta_c^{(r)}$ = phase angle associated with C_r ;
 $\theta_g^{(r)}$ = phase angle associated with generalized forcing function;
 θ_j = phase angle associated with ϕ_j ;
 θ_{r0} = phase angle associated with initial displacement of ξ_r ;
 κ = convergence termination value;
 λ = eigenvalue;
 μ = rotated cable coordinate, damping coefficient = to real part of α ;
 ν = rotated cable coordinate;
 ξ = complex normal coordinate;
 τ = dummy variable of integration;
 T = linear transformation;
 Φ = eigenvector;
 ϕ = lower half of Φ ;
 ω = circular frequency;
 $\{ \}$ = column vector;
 $[\]$ = row matrix;
 $[\]$ = matrix;
 $[0]$ = null matrix;
 $\dot{}$ = time derivative d/dt ;
 $\ddot{}$ = second derivative with respect to time d^2/dt^2 ; and
 $*$ = complex conjugate.

NOTED
 JUL 20 1972
 BALTIMORE

Journal of the
STRUCTURAL DIVISION
 Proceedings of the American Society of Civil Engineers

EXPERIMENTAL STUDIES OF MEMBRANE SHEAR TRANSFER^a

By Richard N. White,¹ M. ASCE and Myle J. Holley, Jr.,² F. ASCE

INTRODUCTION

The problem in membrane shear transfer in seismically loaded reinforced concrete nuclear containment vessels prompted the experimental study reported herein on the effectiveness of shear transfer across cracks in concrete by a surface roughness interlock mechanism. Although the study was conducted within rather severe time and budget constraints, sufficient data was obtained to formulate preliminary design guidelines for containment structures. It is emphasized that the goal of the study was to shed light on one aspect of concrete strength that is relevant to one mode by which membrane shear may be transferred in a cracked reinforced concrete structure. The experimental results are most applicable to the containment design problem, but they also provide an improved understanding of a phenomenon that is of general interest to structural engineers. A long term research program is underway to further clarify this important problem.

The typical containment vessel for a nuclear power reactor is comprised, in part, of one or more concentric, axisymmetric shells, as shown in Ref. 4. The membrane stress state is conveniently described in terms of circumferential tension T_H , meridional tension T_V , and shear S , as shown in Fig. 1. If the vessel is of reinforced concrete (i.e., not prestressed) it must be assumed that cracks will occur, and the reinforcing bars (pattern and quantities) must be proportioned to provide internal equilibrium across any such cracks. Because the crack may have occurred under an earlier loading condition, it

Note.—Discussion open until January 1, 1973. To extend the closing date one month, a written request must be filed with the Executive Director, ASCE. This paper is part of the copyrighted Journal of the Structural Division, Proceedings of the American Society of Civil Engineers, Vol. 98, No. ST8, August, 1972. Manuscript was submitted for review for possible publication on December 6, 1971.

^aPresented at the April 19-23, 1971, ASCE Annual Meeting on Structural Engineering, held at Baltimore, Md. (Preprint 1395).

¹Assoc. Prof. of Structural Engrg., Cornell Univ., Ithaca, N.Y.

²Prof. of Civ. Engrg., MIT, Cambridge, Mass.

cannot be assumed that cracks necessarily define planes of principal tension. Thus, consider that cracks may be of any orientation and, accordingly, internal equilibrium both normal to and along the crack must be satisfied.

Shear resistance along a crack (i.e., resistance to slip) can be developed by components of the axial forces in bars which are inclined to the crack, by shear in bars crossing the crack (i.e., dowel action), and by surface roughness interlock. While dowel action probably provides a major contribution to the total resistance, the basis for accounting for such action in design has not yet been established. To provide such a basis will require many tests of large scale specimens with many bar arrangements, and subjected to a variety of biaxial load combinations. However, it has been possible to demonstrate that the surface roughness interlock mode can provide very large shear resistance along a crack, and that, at the very modest shear stress levels relevant to containment vessel design, the associated slip magnitudes are acceptably

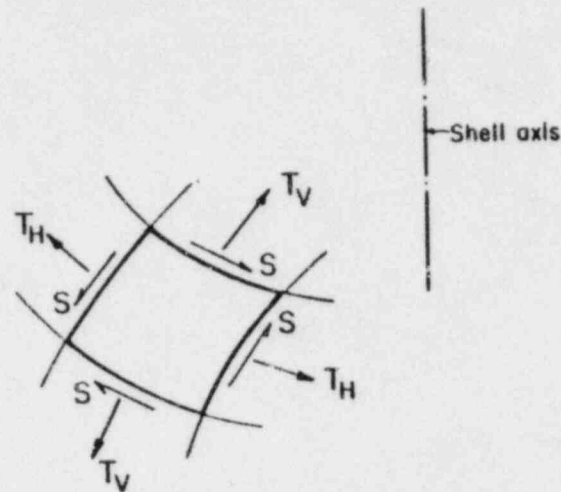


FIG. 1.—SHELL MEMBRANE STRESSES

small. Accordingly, dowel action can be disregarded, and shear resistance can be provided by surface roughness interlock and by components of bar axial forces when such bars are inclined to the crack plane.

Part I of this paper describes a program of tests which were conducted to establish conservative design stress levels for shear along a crack in a containment vessel. These tests differed from earlier investigations in that the possibility of an initial crack width was specifically accounted for, dowel action was excluded, and shear along the crack was cycled through many complete reversals. The latter provision reflects the fact that membrane shear stress in a containment vessel results from earthquake accelerations.

Part II contains recommendations for proportioning bars to resist membrane stresses in containment vessels. Both the two-directional arrangement and multidirectional arrangements are considered. In the former, reliance on surface roughness interlock is inescapable in the latter (three-directional

and four-directional arrangements), it is not essential to take advantage of surface roughness interlock, but it is sound practice and may be economically desirable to do so.

PART I—TEST PROGRAM

Summary of Test Program.—The present study was confined to a single mode of shear transfer—that of surface roughness interlock, neglecting dowel

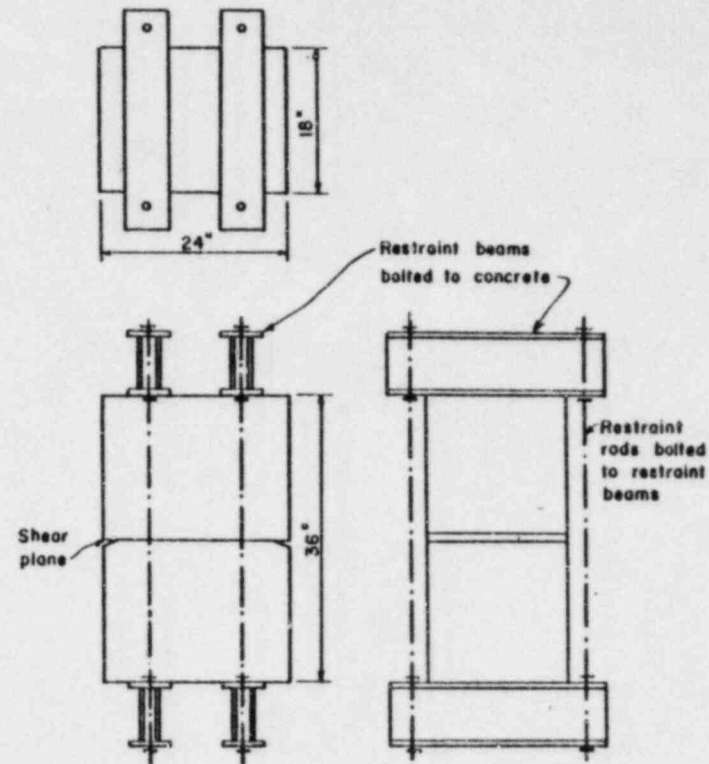


FIG. 2.—TEST SPECIMEN CONFIGURATION

forces and the other modes described previously. While some aspects of this phenomenon had been studied earlier (Refs. 2,3,6), the latter work was done on small specimens [3-1/2 in. by 3-1/2 in. (8.9 cm by 8.9 cm) in cross section by Fenwick, and on 7-in. (17.8 cm) and 9-in. (22.9 cm) thick concrete slabs by Nowlen, Colley and Humphrey]. It was believed that extrapolation of results on small specimens to concrete dimensions on the order of several feet was not warranted in light of meager understanding of the surface roughness interlock mode of shear transfer.

Sixteen large precracked concrete blocks were so loaded as to transmit

shear across the crack strictly by surface roughness interlock. Each block was subjected to reversing shear stresses in the range of 120 psi to 160 psi (84 N/cm² to 110 N/cm²) for a number of cycles (55 maximum) and subsequently to a much higher [300 psi (207 N/cm²) minimum] terminal shear stress. The primary response characteristics measured were: slip along the crack, change in crack width during loading, and magnitude of tensile clamping force in the external bars which held the precracked block together. The complete program is reported in Ref. 7.

The 1.5-ft by 2.0-ft by 3.0-ft (0.457-m by 0.61-m by 0.915-m) specimens (Fig. 2) were cracked to form two unconnected blocks, and then separated to a preset crack width. Further separation of the two halves of the specimen was restricted by four external rods fastened to the blocks. The amount of shear carried by the external rods was a fraction of 1%, thereby ensuring that the shear was transmitted across the crack solely by the mechanical interlock of the cracked surfaces.

A total of 16 specimens, identical in size and overall geometrical configuration, was tested. The cross-sectional area effective in resisting shear was 280 in.² (1,810 cm²) for specimens 1 through 6 and 240 in.² (1,550 cm²) for specimens 7 through 16. Nominal strength of the concrete was 3,000 psi (2,070 N/cm²). The primary variables employed in the study were: (1) size and gradation of aggregate; (2) size of clamping rods; (3) magnitude of applied cyclic shear stress; (4) numbers of cycles of shear load; and (5) width of preset crack. The quantities measured were: (1) slip of one block relative to the other; (2) change of crack width; and (3) magnitude of tensile force developed in the four clamping rods. A complete summary of specimen data and test results is available from the first writer.

Specimen Configuration, Precracking, and Loading.—The specimen geometry shown in Fig. 2 was selected on the basis of having a representative size as compared to elements of concrete in the actual structure. The height of 36 in. (0.915 m) is believed to represent, very conservatively, the clamping flexibility associated with the vertical reinforcing bars in typical secondary containment vessels.

Two different types of crack initiating grooves were used in the tests. The first was unsatisfactory because it produced a curved failure surface. The second groove design utilized a 2-in. (5.08-cm) deep combination V groove and sheet metal strip on the narrow faces of the specimen and three 2-in. (5.08-cm) wide sheet metal strips running through the specimen along the plane of the crack (see Fig. 3 for a typical failure surface).

The only steel items cast in the block were details needed for fastening the loading and restraining equipment in position. There were no steel elements cast in the vicinity of the shearing surface.

Heavy steel cross beams were bolted to the top and bottom surfaces of the specimen prior to cracking. The four-clamping rods were then attached to the beams with nuts. A test specimen complete with beams and clamping rods, and placed in the prestressed concrete test frame, is shown in Fig. 4.

The specimen was cracked by pushing a pair of cracking beams into the open V grooves on the narrow faces of the specimen. The cracking beam had a 1/2-in. (1.27-cm) round bar welded to its leading edge. The cracking beams were retracted immediately after cracking had occurred, and the width of the crack was set by adjusting the clamping rod nuts.

Shearing load was applied to the specimen by hydraulic rams acting against

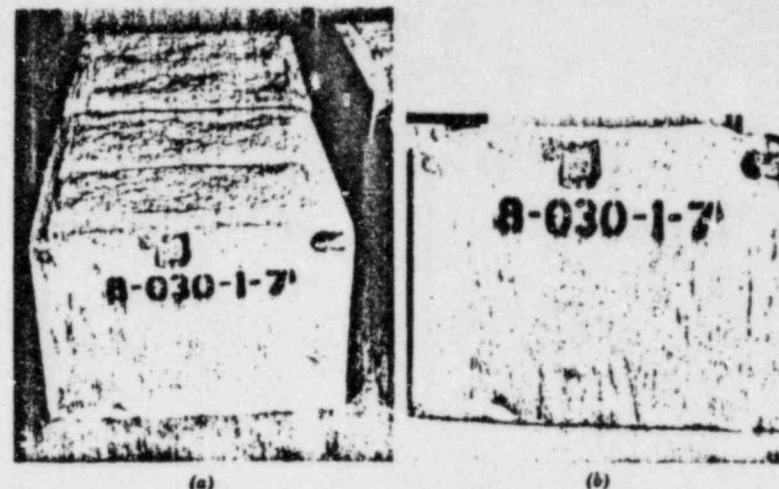


FIG. 3.—TYPICAL CRACK SURFACE, CRACK DETAIL 2; (a) SPECIMEN 8; (b) SIDE VIEW, SPECIMEN 8

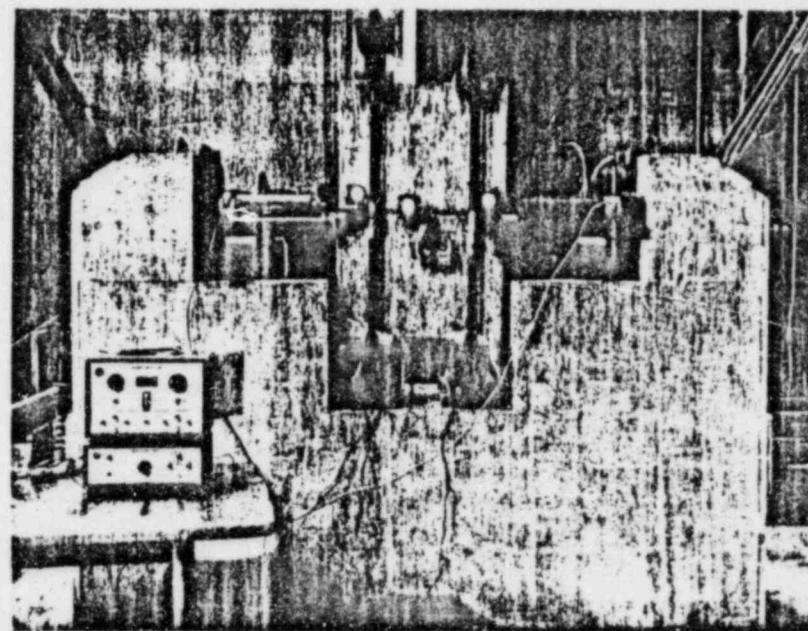


FIG. 4.—TEST SPECIMEN UNDER LOAD IN FRAME

heavy loading angles fastened to the upper half of the specimen; the reacting load was carried by the testing frame.

Following the cyclic loading, each specimen was loaded to a maximum (not ultimate) value of load. The maximum load level applied to any specimen was limited by bearing stresses under the loading angle and by the desire to keep the stresses in the clamping rods below the proportional limit.

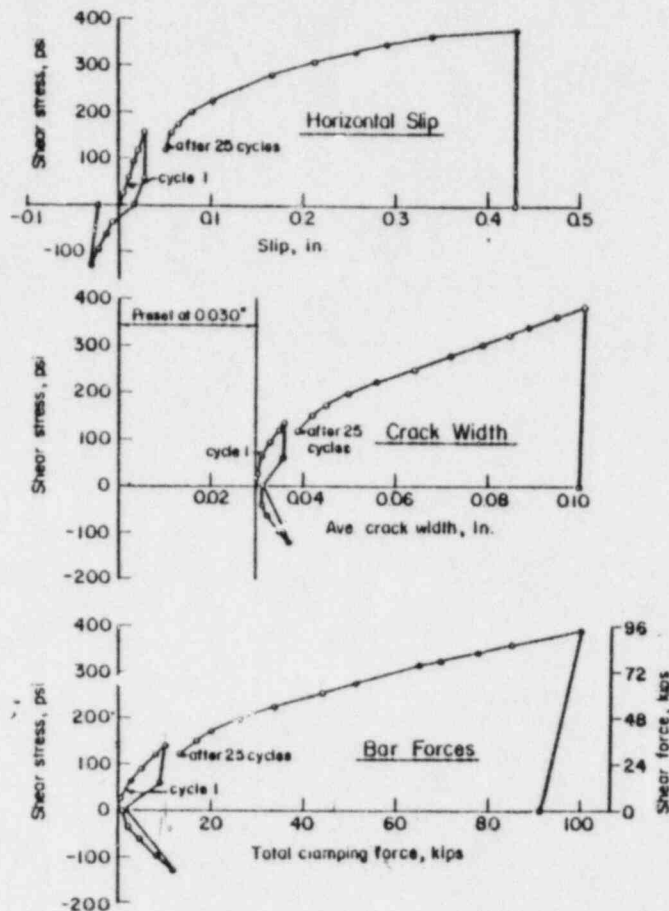


FIG. 5.—BEHAVIOR OF SPECIMEN 8 (1 psi = 0.6895 N/cm²; 1 in. = 25.4 mm; 1 k = 4448 N)

Concrete.—Two concrete mixes were designed for use in the test program; one with a coarse aggregate fraction in the size range of 1/2 in. (1.27 cm) to No. 4 (No. 7 aggregate according to ASTM C 33), and the second with a coarse aggregate fraction ranging from 1-1/2 in. (3.81 cm) to No. 4 (ASTM size No.

467). Both mixes used Type III high early strength Portland cement and were provided by a local ready mix supplier. The compressive strength of the mixes used for the last 10 specimens ranged from 2,750 psi to 3,280 psi (1,895 N/cm² to 2,260 N/cm²).

Sand was a locally available commercial product taken from glacial deposits. It consisted mainly of quartz; larger particles included some shale, sandstone, and limestone. The sand gradation conformed to the requirements of ASTM C 33 and had a fineness modulus of 3.15.

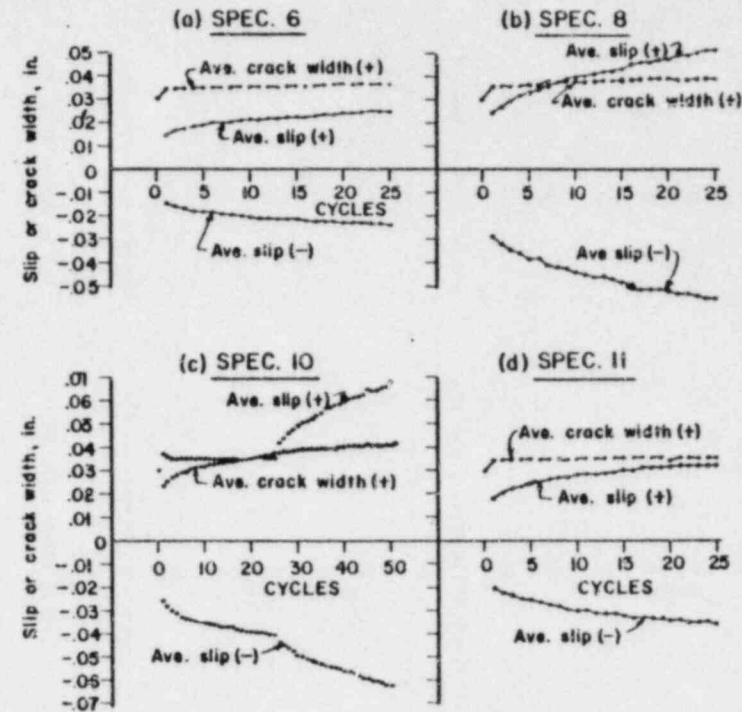


FIG. 6.—EFFECT OF LOAD CYCLING ON SLIP AND CRACK WIDTH, SPECIMENS 6, 8, 10, 11 (1 in. = 25.4 mm)

The coarse aggregate came from the same deposit as the sand. While the materials used in this program were not analyzed, previous analysis of a similar deposit indicated that the aggregate was made up of approximately 40% sandstone, 30% limestone, 20% shale, and 10% miscellaneous. A 5-cycle magnesium sulphate soundness test (ASTM C 88-69) yielded a loss of 3.6%. A Los Angeles abrasion test conducted on the A grading portion in accordance with ASTM C 131 gave a 21.8% wear (500 revolutions).

Test Results.—Only selected specimens will be reviewed herein; the interested reader should request a complete summary from the first writer.

There were five pairs of essentially identical specimens tested: Specimens

(5,6), (7,8), (9,10), (11,12), and (15,16). Single tests of interest include Specimens 3 and 14. Several of the early specimens tested are to be regarded as preliminary tests during which the procedures and techniques were perfected. In addition, Specimen 13 cracked at one exterior corner either prior to or during the first load cycle, and the test was discontinued immediately because proper crack width control became impossible.

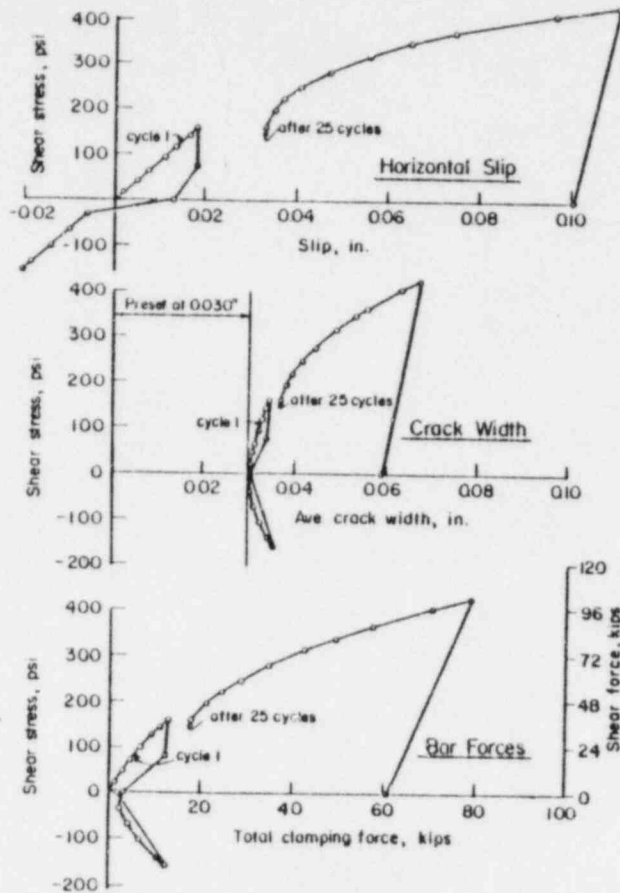


FIG. 7.—BEHAVIOR OF SPECIMEN 11 (1 psi = 0.6895 N/cm²; 1 in. = 25.4 mm; 1 k = 4448 N)

Test results for Specimens 8, 11, and 14 will be given below. Three basic types of data plots are included for each of these specimens: average slip versus shear load; average crack width versus shear load; and clamping forces versus shear load. These plots show the behavior for the first complete load cycle and for the final loading to a maximum value of shear load.

The effects of cycling are best illustrated by plotting slip and crack width as a function of cycle number; this type of plot is given for Specimens 6, 8, 10, 11, 14 and 16.

Specimen 8.—Parameter values for this specimen included No. 7 aggregate, 1-in. (2.54-cm) diameter clamping rods, crack detail type No. 2, a preset crack width of 0.030 in. (0.762 mm), and 25 cycles of ± 120 psi (83 N/cm²) cyclic shear stress. Test results are shown in Figs. 5 and 6(b).

The crack surface for Specimen 8, made with the joint detail No. 2 was quite flat (Fig. 3). First cycle slips of + 0.024 in., - 0.028 in. (+ 0.61 mm, - 0.71 mm) increased to + 0.051 in., - 0.055 in. (+ 1.30 mm, - 1.40 mm) after 25 cycles at 120 psi (83 N/cm²) shear. The slip increased at a decreasing rate as shown in Fig. 6(b).

The preset crack width of 0.030 in. (0.762 mm) increased by about 0.005 in. (0.127 mm) on the first cycle of loading. The maximum increase of about 0.009 in. (0.228 mm) was at the 25th cycle. The character of the change in crack width (Fig. 5) during the first load cycle was similar to that of the change in clamping force during the same loading (Fig. 5). The total clamping force existing at a shear stress of 160 psi (110 N/cm²) was about 45% of the applied shear load.

Specimen 11.—Parameter values for this specimen included No. 467 aggregate, 1.375-in. (3.50-cm) diam clamping rods, crack detail type No. 2, a preset crack width of 0.030 in. (0.762 mm), and 25 cycles at ± 164 psi (113 N/cm²) shear. Test results are given in Figs. 6(d) and 7.

This specimen was the first tested with the larger clamping rods. The increased stiffness resulting from the larger rods is revealed in the lower values of slip; cycled at 164 psi (113 N/cm²), the first cycle slips of + 0.018 in., - 0.020 in. (+ 0.46 mm, - 0.51 mm) increased to + 0.032 in., - 0.036 in. (+ 0.81 mm, - 0.91 mm).

The crack width increase at peak cyclic load varied only slightly from 0.005 in. (0.127 mm) during the cycling. The maximum value of slip reached during the loading to maximum was about 30% of the slip reached on Specimens 9 and 10, which were identical in all respects except for size of clamping rods. Total clamping force was about 25% of the total applied shear when the specimen was at 160 psi (110 N/cm²) shear.

Specimen 14.—Specimen 14 was similar to Specimen 11 with the exception of size of preset crack width and number of loading cycles. Results are given in Figs. 8 and 9(a). The first 25 cycles of load were applied with the crack set at 0.020 in. (0.508 mm), the smallest crack opening used on any specimen. Slips of [+ 0.014 in., - 0.014 in.] (+ 0.36 mm, - 0.36 mm) increased to [+ 0.022 in., - 0.024 in.] (+ 0.56 mm, - 0.61 mm). The crack was then set at 0.030-in. (0.762-mm) opening, and an additional 25 cycles of load applied. The first extra cycle increased the slips to [+ 0.029 in., - 0.032 in.] (+ 0.74 mm, - 0.81 mm), while the 25th increased them to + 0.040 in., - 0.044 in. (+ 1.01 mm, - 1.12 mm). Finally, the crack was set at 0.015 in. (0.381 mm) on one of the 24-in. (0.610-m) dimensions of the test specimen and 0.030 in. (0.762 mm) on the other, and 5 additional cycles of load were applied. The latter loading was done to establish the feasibility of loading a specimen with variable crack width through the 18-in. (0.458-m) thickness of the specimen.

The cycling effects are summarized in Fig. 9(a). The symmetry of the magnitude of positive and negative slips throughout this complex load history should be noted.

The degree of damage to the cracked surfaces after 50 load cycles was examined by loosening the clamping rods and allowing the blocks to reach an equilibrium position, with only the dead weight of the upper block attempting to close the crack. The crack closed to 0.026 in. (0.66 mm), which was less than the crack width at which it was being cycled. The crack was then closed

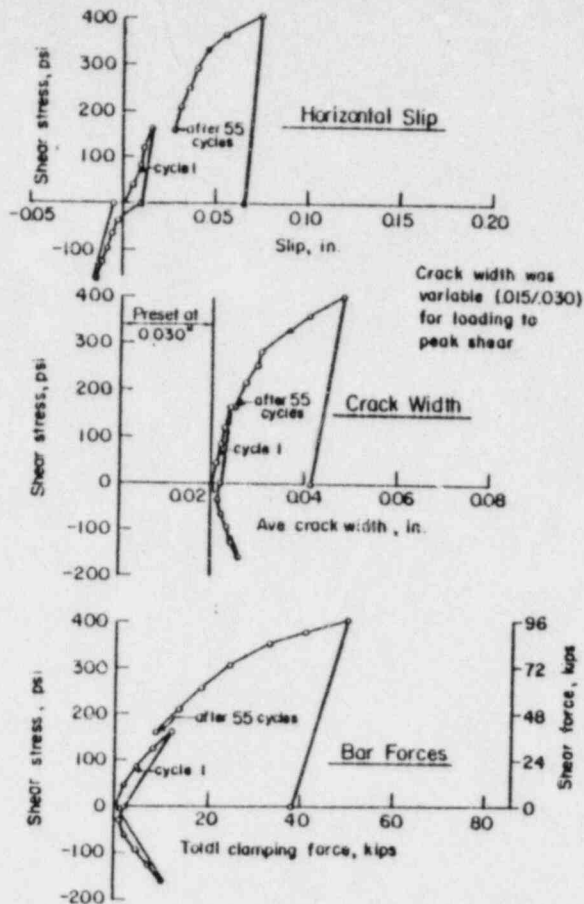


FIG. 8.—BEHAVIOR OF SPECIMEN 14 (1 psi = 0.6896 N/cm²; 1 in. = 25.4 mm; 1 k = 4448 N)

up to 0.015 in. (0.381 mm) on one side of the block by tightening the nuts on the clamping rods; this was accomplished with no difficulty with a hand wrench.

The increase in crack width during peak cyclic loads was about 0.005 in. (0.127 mm) for both cases of preset crack widths of 0.020 in. (0.508 mm) and 0.030 in. (0.762 mm). The specimen was subjected to its maximum load cycle

with the crack set at 0.015 in./0.030 in. (0.381 mm/0.762 mm). The specimen was very stiff and had a maximum average slip of only 0.074 in. (0.188 mm) [0.053 in. (0.134 mm) on the 0.015-in. (0.31-mm) side and 0.094 in. (0.238 mm) on the 0.030-in. (0.762-mm) side] at a shear stress of 427 psi. The total clamping force was also much lower than in preceding tests, being less than half the applied shear load at its maximum value of 427 psi (295 N/cm²).

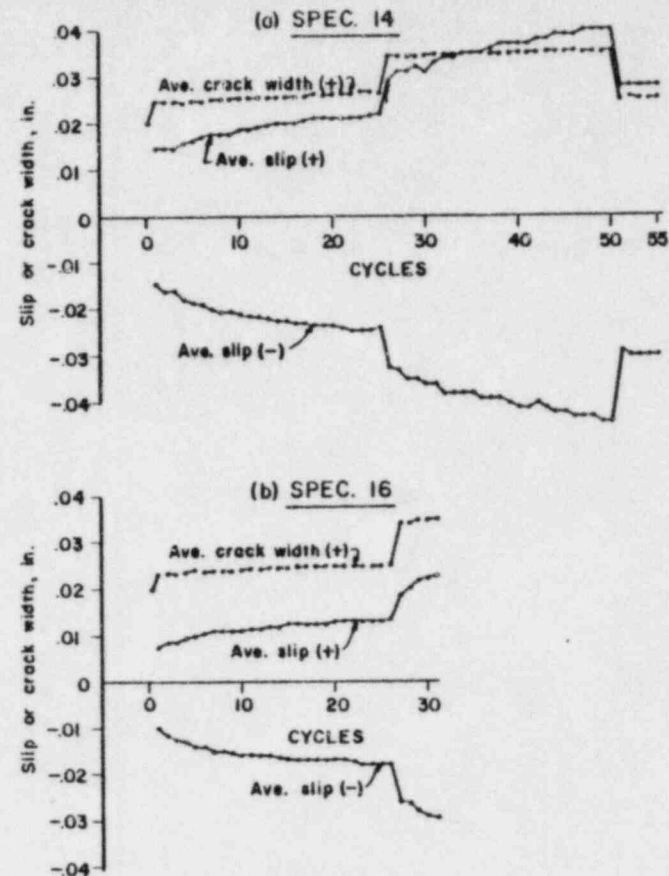


FIG. 9.—EFFECT OF LOAD CYCLING ON SLIP AND CRACK WIDTH, SPECIMENS 14 AND 16 (1 in. = 25.4 mm)

Analysis of Behavior; Parameter Evaluation.—Several behavioral aspects were common to all tests and will be given prior to evaluation of the various parameter effects. These aspects include:

1. Slip in the shear plane, and the width of the crack at the plane, both increased under cyclic shear loading (see Figs. 6 and 9).

2. Specimens were loaded to a terminal shear stress in the range of 300 psi to 450 psi (207 N/cm^2 to 310 N/cm^2) after the cycling; however, these high stress levels did not represent true ultimate strengths of the specimen in shear. All specimens undoubtedly possessed a higher shear capacity than that measured.

3. The forces in the clamping bars remained low during cycling; the total tensile force was in the range of 30% to 50% of the applied shear load at shearing stresses of 160 psi (110 N/cm^2) [for specimens with 1.375-in. (3.50-cm) diam bars]. For those specimens which had high slips [greater than about $3/8$ in. (0.95 cm)] during the final peak load cycle, the total clamping force was nearly equal to the applied shear load.

4. The significant damage to the integrity of the shearing surfaces occurred during the final load application and not during the cyclic loading. This conclusion was reached by comparison of surfaces which had experienced similar magnitudes of slip during cycling, but had markedly different slips

TABLE 1.—SUMMARY OF SELECTED DATA

Specimen number (1)	Cycle 1		Cycle 10		Cycle 25		Peak shear, in pounds per square inch (8)	Peak slip, in inches (9)	
	Positive loading, in inches (2)	Negative loading, in inches (3)	Positive loading, in inches (4)	Negative loading, in inches (5)	Positive loading, in inches (6)	Negative loading, in inches (7)			
8	0.024	0.028	0.040	0.044	0.061	0.055	405	0.394	
10	0.024	0.025	0.032	0.035	0.038	0.040	454	0.368	
11	0.018	0.020	0.028	0.030	0.032	0.036	446	0.111	
14	0.014	0.014	0.018	0.021	0.022	0.024	427	0.074 ^a	
15	0.010	0.012	0.014	0.016	0.018	0.018	442	0.010 ^b	
	Ratio								
8/10	1.08		1.26		1.36				
10/11	1.29		1.16		1.15				
11/14	1.35		1.49		1.48				
14/15	1.28		1.30		1.28				

^a With crack set at 0.015/0.030 in. prior to peak shear.
^b With crack set at 0.013 in.
 1 in. = 25.4 mm; 1 psi = 0.6895 N/cm².

during the final load application. Those specimens which had larger slips during the final load had a substantial amount of ground material in the joint, while the others had very little material in the joint and no noticeable surface damage.

5. With two exceptions (Specimens 3 and 4), the increase in crack width after 25 cycles was less than or equal to 0.010 in. (0.254 mm).

6. The magnitude of slip did not return to zero during the unloading of a specimen. Typical behavior is shown in Fig. 5; as the load was reduced to about half its peak cyclic value, the slip remained unchanged. As the load was further reduced, the slip decreased but did not vanish. Only upon loading from the opposite direction did not blocks pass through the neutral position (zero slip). Unloading from the negative cyclic loading produced the same type of behavior. The effect of varying the main parameters can be best summarized by comparing the magnitudes of shear surface slip measured in certain speci-

mens. Slip values for both positive and negative loading, for cycles 1, 10, and 25, are summarized in Table 1.

7. Slip decreases with increasing aggregate size. As shown in row 6 of Table 1, slip of the small aggregate specimen (No. 8) was 8% of 36% larger than slip of the large aggregate specimen (No. 10). The large aggregate becomes relatively more beneficial in resisting slip as the number of load cycles increases. Slip at peak shear (Col. 9 of Table 1) was also higher for the specimen with the small aggregate.

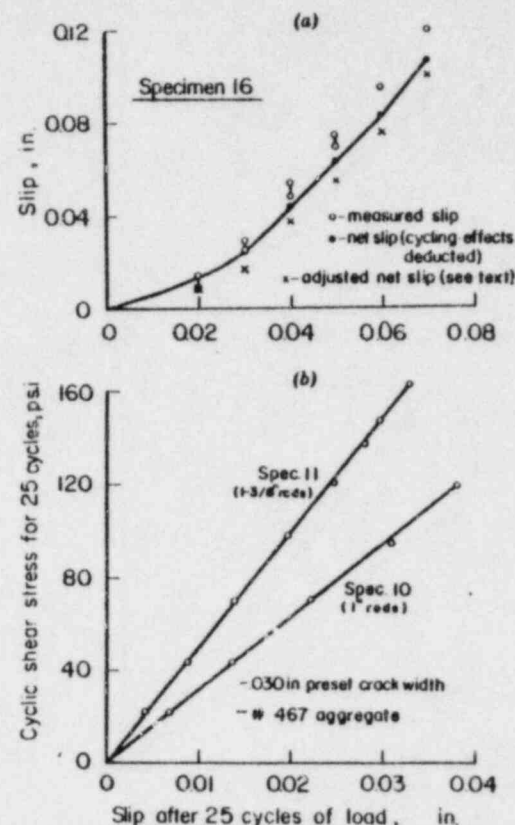


FIG. 10.—(a) SLIP VERSUS INITIAL CRACK WIDTH; (b) 25 CYCLE SLIP AS FUNCTION OF APPLIED SHEAR STRESS (1 psi = 0.6895 N/cm²; 1 in. = 25.4 mm)

8. Slip decreases with increasing size of clamping rods. A direct comparison of the effect of axial stiffness of the clamping rods on slip and shear stiffness is not possible because all specimens made with the larger rods (1.375-in. (3.50-cm) diam, $p = 2.5\%$) were cycled at a higher stress level than were the specimens made with smaller rods (1.0-in. (2.54-cm) diam, $p = 1.2\%$). However, the beneficial effects of higher clamping stiffness can be

shown by comparing Specimen 11, cycled at ± 164 psi (113 N/cm^2), with Specimen 10, cycled at ± 121 psi (84 N/cm^2) (Row 7 of Table 1). Both specimens were made with the large aggregate. Specimen 10 had slip values ranging from 15% to 29% higher than slips in Specimen 11. In addition, Specimen 11 was considerably stiffer when subjected to the maximum shear loading (see Col. 9 of Table 1). No direct comparison of Specimens 10 and 11 can be made at a stress of 120 psi (83 N/cm^2) on the first load cycle; the small rod specimen slipped 0.024 in. (0.61 mm) while the large rod specimen slipped only 0.014 in. (0.36 mm).

9. Slip decreases with decreasing initial crack width. Specimens 11 and 14 had initial crack widths of 0.030 in. and 0.020 in. (0.762 mm and 0.508 mm), respectively, while both had large clamping rods, large aggregate, and were cycled at ± 164 psi (113 N/cm^2). The ratios of slips of Specimen 11 to Specimen 14 are given in Row 8 of Table 1, and range from 1.35 to 1.49. The effect of larger initial crack widths, up to a maximum of 0.070 in. (1.78 mm), was examined on Specimen 16 which was cycled at ± 164 psi (113 N/cm^2). Results are summarized in Fig. 10(a) in terms of the average maximum slip which would result from successive single cycles of ± 164 psi (113 N/cm^2) shear stress with crack widths set at 0.020 in. (0.508 mm), 0.030 in. (0.762 mm), . . . , 0.070 in. (1.78 mm) on the same specimen. It should be emphasized that this curve is valid only for the specimen with large aggregate and large clamping rods cycled at ± 164 psi (113 N/cm^2). For this situation, the dependence of maximum average slip on increasing crack width is nearly linear for crack widths in the range of 0.030 in. to 0.070 in. (0.762 mm to 1.78 mm).

10. A specimen with variable crack width across its thickness exhibits less slip than a similar specimen with a uniform crack width equal to the average of the variable crack width; furthermore, it does not degrade any more rapidly than the uniform crack width specimen. The results from Specimens 14 and 15 form a basis for this conclusion. Both had large aggregate, large clamping rods, and were cycled at ± 165 psi (114 N/cm^2). Specimen 15 had an initial crack width of 0.010 in. (0.254 mm) on one side and 0.030 in. (0.762 mm) on the other, while Specimen 14 had a uniform crack width of 0.020 in. (0.508 mm). As shown in line 9 of Table 1, the uniform crack width specimen had slips about 30% higher than Specimen 15.

11. The amount of slip to be expected after 25 cycles of shear loading on specimens with large aggregate, and with a preset crack width of 0.030 in. (0.762 mm) is shown in Fig. 10(b). This plot was constructed from data on Specimens 10 and 11. It is seen that the accumulated maximum slip is a linear function of applied shear stress for both percentages of clamping rod.

12. The character of the load versus slip response for later cycles of loading was measured on a number of test specimens, normally at the 10th and 20th cycles. The characteristic shape of the first load-slip cycle response was maintained during subsequent cycles; specimens consistently exhibited an unloading stiffness higher than the loading stiffness.

PART II—RECOMMENDATIONS FOR DESIGN

Fig. 11 presents recommended design values of shear strength along a crack, in the surface roughness interlock mode, as a function of the reinforcing ratio of bars normal to the crack plane, or the equivalent (reduced) ratio for

bars inclined to the crack plane. Recommended values are given as a function of steel ratio, which is a measure of the clamping stiffness, because the tests demonstrated that the stress corresponding to a given slip displacement increased with increasing clamping stiffness. Embedded bars in a containment shell will have a substantially shorter effective length per crack than the external bars used in the test program. They will, therefore, provide greater clamping stiffness and will assure even better performance than was observed in the tests.

It will be noted that the shear stress values presented on Fig. 11 are very low compared, for example, with values proposed in the forthcoming revised ACI Building Code. For shear stress, along cracks (in short brackets and connection details, Refs. 1 and 5) the latter document permits values up to 53.7 psi at 800 psi (662 N/cm^2). The difference arises, of course, from the fact that the ACI Code values are intended to preclude failure while the values recommended herein were deliberately chosen to guarantee negligibly small

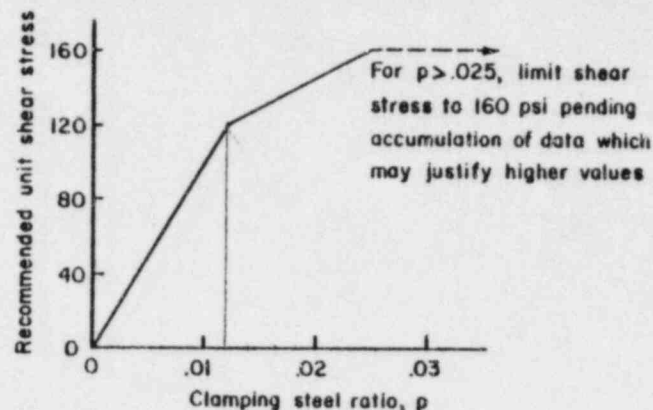


FIG. 11.—RECOMMENDED UNIT SHEAR STRESS LIMITS FOR SURFACE ROUGHNESS INTERLOCK MODE (1 psi = 0.6895 N/cm^2)

displacements. The concrete used in the test specimens was typical of containment structures and not of unusually high strength. Thus the values given on Figure 11 should be conservative for most containment vessel concretes. For mixes which depart significantly from the test specimen mixes, described in Part I, it would be prudent to conduct similar tests to establish appropriate shear strength values.

Two-Directional Bar Arrangements.—Because the circumferential and meridional stress components, T_H and T_V (Fig. 1), typically are dominant in the membrane stress state, and because bars are more economically placed in these directions, it is recommended that the two-directional arrangement shown in Fig. 12(a) be used whenever the membrane shear stress, S , corresponds to a unit shear stress not exceeding the values presented on Fig. 11. In these cases it is further recommended that the circumferential and meridional bars be proportioned for membrane forces $T_H + 1.5S$ and $T_V + 1.5S$, respectively. Because many different combinations of T_H , T_V and S must be con-

APPENDIX.—REFERENCES

1. Birkeland, P. W., and Birkeland, H. W., "Connections in Precast Concrete Construction," *Journal of the American Concrete Institute*, March, 1966.
2. Colley, B. E., and Humphrey, H. A., "Aggregate Interlock at Joints in Concrete Pavements," *Highway Research Record No. 189*, 1967, pp. 1-18.
3. Fenwick, R. C., "The Shear Strength of Reinforced Concrete Beams," thesis presented to the University of Canterbury, at Christchurch, New Zealand, in 1966, in partial fulfillment of the requirements for the degree of Doctor of Philosophy.
4. Gordon, C. T., and Klehm, W. L., "Conventionally Reinforced Nuclear Containments," *Journal of the Structural Division, ASCE*, Vol. 96, No. ST2, Proc. Paper 7065, Feb., 1970, pp. 199-219.
5. Hofbeck, J. F., Ibrahim, I. O., and Mattock, A. H., "Shear Transfer in Reinforced Concrete," *Journal of the American Concrete Institute*, Vol. 66, No. 2, Feb. 1969, pp. 119-128.
6. Nowlen, W. J., "Influence of Aggregate Properties on Effectiveness of Interlock Joints in Concrete Pavements," *Journal, Portland Cement Association Research and Development Laboratories*, Vol. 10, No. 2, May, 1968, pp. 2-8.
7. White, R. N., "Behavior of Pre-Cracked Concrete Subjected to Reversing Shearing Stresses," SWND-5, Stone & Webster Engineering Corp., Boston, Mass., Nov., 1969, also, *Department of Structural Engineering Report*, Cornell University, Ithaca, N.Y., Nov., 1969.

Journal of the
STRUCTURAL DIVISION
Proceedings of the American Society of Civil Engineers

STEEL COLUMN BUCKLING UNDER THERMAL GRADIENTS

By Charles G. Culver,¹ M. ASCE

INTRODUCTION

The influence of elevated temperature on the strength of structural members is an important design problem. Although considerable work has been done in this area for aircraft structures (2), similar information is not available for steel members used in buildings. The recent use of exposed steel members in buildings (11), for example, has pointed out the need for more information on the load carrying capacity of columns subjected for fires. In order to develop such information, an analytical research study was undertaken to determine the strength of steel members at elevated temperatures (5). A comprehensive review of previous work in this area is presented elsewhere (12).

The problem considered herein is the determination of the buckling loads for wide flange steel columns subjected to elevated temperatures.

PROBLEM STATEMENT

Elevated temperatures affect the behavior of steel columns in several ways. First, the material properties such as yield strength, modulus of elasticity and the coefficient of thermal expansion vary with temperature. The functional expressions relating these quantities to temperature which have been determined experimentally and used herein are presented elsewhere (3). Second, thermal stresses may be induced due to restraint of the expansion accompanying an increase in temperature. These stresses act in addition to those produced by the applied load and obviously affect the total load carrying capacity of the member. Thirdly, the thermal expansion produces deformations which may interact with the applied load to produce additional stresses. This occurs in columns subject to thermal gradients over the cross section which tend to

Note.—Discussion open until January 1, 1973. To extend the closing date one month, a written request must be filed with the Executive Director, ASCE. This paper is part of the copyrighted *Journal of the Structural Division, Proceedings of the American Society of Civil Engineers*, Vol. 98, No. ST8, August, 1972. Manuscript was submitted for review for possible publication on December 6, 1971.

¹Assoc. Prof., Dept. of Civ. Engrg., Carnegie-Mellon Univ., Pittsburgh, Pa.

sidered, corresponding to different factored load combinations, the bar quantities actually may be defined by stress states in which $S = 0$.

It can easily be shown that by providing a bar clamping capacity $1.5S$ on circumferential and meridional planes, the minimum clamping capacity on any other plane will be at least 1.0 times the shear to be transmitted along that plane. As the tests reported in Part I indicated that required clamping forces are much less than 1.0 times shear force, this recommendation will assure membrane shear equilibrium through mobilization of the surface roughness interlock mode.

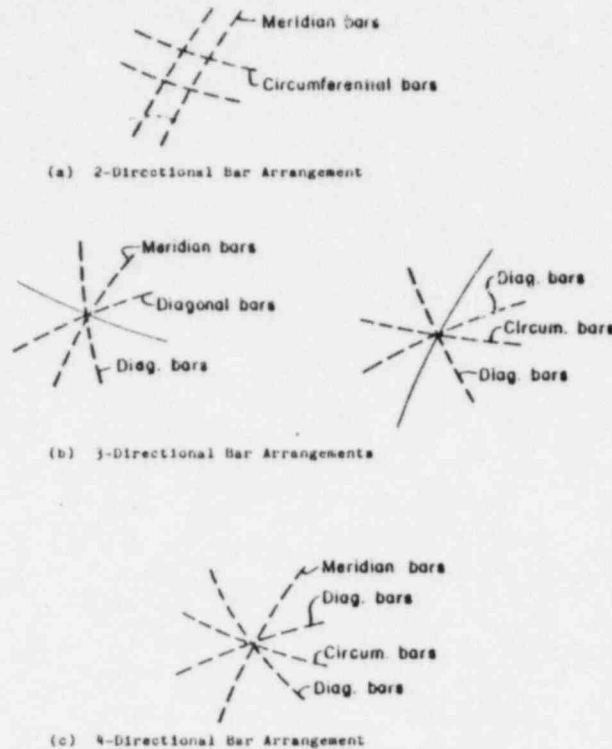


FIG. 12.—BAR ARRANGEMENTS FOR SHELL MEMBRANE STRESS STATES: (a) TWO-DIRECTIONAL BAR ARRANGEMENT; (b) THREE-DIRECTIONAL BAR ARRANGEMENTS; (c) FOUR-DIRECTIONAL BAR ARRANGEMENTS

It should be emphasized that the use of a two-directional bar arrangement, proportioned in accordance with the foregoing recommendations, is in no way analogous to the design of an R/C beam without shear reinforcement. It is, rather, analogous to the design of such a beam with transverse stirrups, and with such stirrups proportioned to resist 1.5 times the transverse shear force. Clearly, if the containment shell membrane shear problem is viewed from the viewpoint of diagonal tension cracking, the recommendation is extremely conservative.

Three-Bar and Four-Bar Arrangements.—Either by choice or because the unit shear stress corresponding to membrane shear, S , exceeds the limiting values presented on Fig. 11, one of the multidirectional bar arrangements shown in Fig. 12(b) and (c) may be used. It is, of course, possible to proportion the bars in any of these arrangements so that the membrane stress state, T_H , T_V , S , is held in equilibrium by bar axial forces alone. However, it is equally sound to take advantage of the capacity for shear transfer in the surface roughness interlock mode. Denoting this capacity by S_0 = shell thickness multiplied by limiting unit shear stress from Fig. 11 in those cases for which $S > S_0$, one may proportion the bars to provide equilibrium for a modified membrane stress state, $T_H + 1.5S_0$, $T_V + 1.5S_0$, and $S - S_0$. Because T_H , T_V , and S typically take their maximum values under different factored load combinations, it may be found that use of the modified membrane stress state leads to substantially reduced diagonal bar quantities without significantly increasing the required meridional or circumferential bar quantities. That is, the latter may be defined by factored load combinations for which $S = 0$ and the unmodified membrane stress state controls. Accordingly, it is strongly recommended that the modified membrane stress state be used for proportioning (or verifying) bars to resist membrane stress states in which $S \neq 0$. This recommendation is justified by: (1) The highly conservative limits of recommended unit shear stress presented on Fig. 11, and the fact that these stresses are developed at extremely small slip displacements; (2) by the test evidence that resistance in the surface roughness mode is ductile (see Fig. 5, 7, 8); and (3) by the fact that if the shear problem is viewed in the context of diagonal cracking it will be found that the resulting bar quantities are very conservative.

CONCLUSIONS

Transfer of cyclic shear stress on the order of 150 psi across cracks in reinforced concrete is possible, with only minor slippage, by the surface roughness interlock mode of shear transfer. The interlock mode is mobilized by restraint forces in the reinforcing located normal to the crack; the restraint forces range from 30% to 50% of the total applied shearing force.

ACKNOWLEDGMENTS

The test program reported in Part I was supported through the sponsorship of the Stone and Webster Engineering Corporation and three of its clients: the Virginia Electric and Power Co., the Duquesne Light Co., and the Long Island Lighting Company. The experimental program was conducted in the Structural Testing Laboratory of Cornell University.

The cooperation and ready assistance of William Klehn and Charles Miczek of Stone and Webster, acting for the group of sponsors, facilitated greatly the successful completion of the testing program. Peter Gergely and George Winter of Cornell University participated in an advisory capacity. Finally, three suppliers made important contributions: the Stressteel Corporation, Wilkes-Barre, Pa., and the Cayuga Cement Company and the University Sand and Gravel Co., both of Ithaca, N.Y.

(A) NOTED JUL 18 1984 J.A.L. WEN

Shear Transfer in Reinforced Concrete

By J. A. HOFBECK, I. O. IBRAHIM and

ALAN H. MATTOCK

Presents a study of shear transfer in reinforced concrete, that is, the transfer of shear across a plane, such as at the interface between a precast beam and a cast-in-place slab. Thirty-eight push-off specimens were tested, some with, some without a pre-existing crack along the shear plane. The shear-friction theory was found to give a conservative estimate of the shear transfer strength of initially cracked concrete. A method is presented for the calculation of shear transfer strength in initially uncracked concrete, based on the Zie envelope to Mohr circles representing failure conditions for concrete.

Keywords: composite construction (concrete to concrete); connections; precast concrete; reinforced concrete; research; shear strength; slippage.

■ SITUATIONS EXIST WHERE shear failure is constrained to occur along a plane, such as at the interface between a precast beam and a cast-in-place deck slab, or at certain locations in precast concrete connections. The transfer of shear across such a plane is called "shear transfer," to distinguish this type of shearing action from that which usually occurs in a reinforced concrete beam.

Instances where shear transfer across a definite plane must be considered in the design of precast concrete connections have been discussed by Birkeland and Birkeland¹ and by Mast.² Mast has further pointed out the need to consider the case where a crack may exist along the shear plane before shear is applied. Such cracks can occur for a variety of reasons unrelated to shear, such as tension forces caused by restrained shrinkage or temperature deformations, accidental dropping of a member, etc.

EXPERIMENTAL STUDY

This paper reports a study of the shear transfer strength of reinforced concrete, both with and without a crack existing along the shear plane

prior to the application of shear. The objectives of the study were as follows:

1. To determine the influence of a pre-existing crack in the shear plane on the shear transfer strength.
2. To determine the influence of strength, size and arrangement of reinforcement on the shear transfer strength.
3. To determine the influence of concrete strength on shear transfer strength.
4. To examine the possible contribution to shear transfer strength of "dowel action" of reinforcing bars crossing the shear plane.
5. To examine the applicability of the "shear friction" theory^{1,2} to the calculation of shear transfer strength when a crack pre-exists in the shear plane.

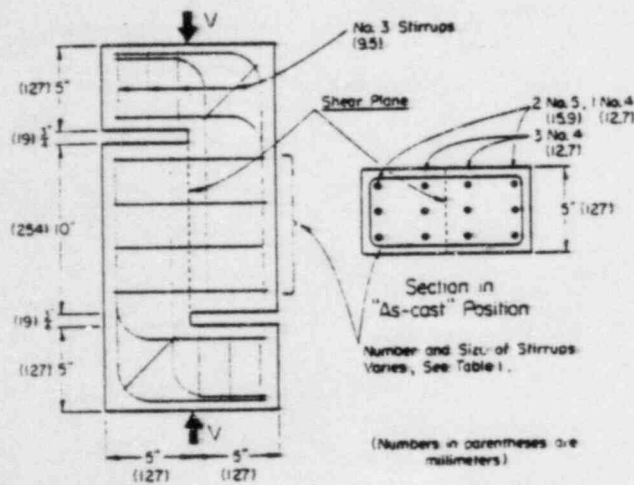


Fig. 1—Details of push-off specimen

6. To attempt to relate the shear transfer strength measured in push-off tests to the compressive and tensile strengths of concrete and steel.

The test specimens

A typical specimen is shown in Fig. 1. When loaded axially as indicated by the arrows V in Fig. 1, shear without moment is produced on the shear plane indicated. If adequate longitudinal and end reinforcement is provided, failure of this type of specimen occurs along the shear plane. Reinforcement across the shear plane is in the form of closed stirrups, anchored by wrapping round the longitudinal reinforcement. The actual shear reinforcement provided in each specimen is given in Table 1, together with the concrete strength.

Each specimen was cast horizontally in one piece, oriented as indicated by the section in Fig. 1. The concrete was made from Type III portland cement and 3/8 in. (22 mm) maximum size river gravel aggregate. The specimens and companion compression cylinders were cured in the forms under polyethylene sheet for 48 hr. At this time the specimens and cylinders were taken from the forms and were stored in air alongside one another until the time of test, usually at 6 days.

The specimens of Series 6 differed from the remainder of the specimens in that soft rubber sleeves 2 in. (50 mm) long and 1/8 in. (3.2 mm) thick were secured around the legs of the stirrups where they crossed the shear plane. The rubber sleeves were provided so as to eliminate as much as possible, any dowel action between the legs of the stirrups and the surrounding concrete in the shear plane.

TABLE 1—TEST SPECIMEN PROPERTIES

Specimen No.	Stirrups bar size \pm or in. (mm)	Number of stirrups	Stirrups yield point, ksi (kgf/mm ²)	Concrete strength f_c , psi (kgf/cm ²)	Specimen No.	Stirrups bar size \pm or in. (mm)	Number of stirrups	Stirrups yield point, ksi (kgf/mm ²)	Concrete strength f_c , psi (kgf/cm ²)
10*	—	0	—	4040 (284)	3.1	1/8 (3.2)	2	50.1 (35.2)	4040 (284)
11A	#2 (9.5)	1	50.7 (35.7)	3920 (276)	3.2	#2 (9.5)	2	56.8 (40.0)	4010 (282)
11B	#2 (9.5)	1	48.0 (33.8)	4340 (305)	3.3	#3 (9.5)	2	50.7 (35.7)	3100 (213)
12A	#2 (9.5)	2	50.7 (35.7)	3340 (270)	3.4	#4 (12.7)	2	47.2 (33.2)	4040 (284)
12B	#2 (9.5)	2	48.0 (33.8)	4180 (294)	3.5	#5 (15.9)	2	42.4 (29.9)	4040 (284)
13A	#2 (9.5)	3	50.7 (35.7)	3840 (270)	4.1	#3 (9.5)	1	66.1 (46.5)	4070 (286)
13B	#2 (9.5)	3	48.0 (33.8)	3920 (276)	4.2	#3 (9.5)	2	66.1 (46.5)	4070 (286)
14A	#1 (9.5)	4	50.7 (35.7)	4510 (317)	4.3	#3 (9.5)	3	66.1 (46.5)	4040 (284)
14B	#1 (9.5)	4	48.0 (33.8)	3655 (272)	4.4	#3 (9.5)	4	66.1 (46.5)	4040 (284)
15A	#2 (9.5)	5	50.7 (35.7)	4510 (317)	4.5	#3 (9.5)	5	66.1 (46.5)	3990 (272)
15B	#1 (9.5)	5	48.0 (33.8)	4065 (288)	5.1	#3 (9.5)	1	50.7 (35.7)	2450 (172)
16A	#1 (9.5)	6	50.7 (35.7)	4310 (303)	5.2	#3 (9.5)	2	50.7 (35.7)	2920 (207)
16B	#1 (9.5)	6	48.0 (33.8)	4050 (285)	5.3	#3 (9.5)	3	50.7 (35.7)	2330 (164)
17	#2 (9.5)	1	50.7 (35.7)	3100 (218)	5.4	#3 (9.5)	4	50.7 (35.7)	2500 (176)
18	#2 (9.5)	2	50.7 (35.7)	3190 (218)	5.5	#3 (9.5)	5	50.7 (35.7)	2420 (171)
19	#2 (9.5)	2	50.7 (35.7)	3990 (275)	6.1*	#3 (9.5)	1	44.0 (31.3)	3640 (256)
20	#2 (9.5)	2	50.7 (35.7)	3990 (275)	6.2*	#3 (9.5)	1	44.0 (31.3)	3640 (256)
21	#2 (9.5)	3	50.7 (35.7)	4420 (294)	6.3	#3 (9.5)	2	44.0 (31.3)	3640 (256)
22	#2 (9.5)	3	50.7 (35.7)	4420 (294)	6.4	#3 (9.5)	2	44.0 (31.3)	3640 (256)

* As a series 1 and 2 specimens, #1 and #2 were replaced in series 1 and 2. The specimens were tested in the same manner as the other specimens.
 * Reinforcement and concrete strength are given in parentheses in accordance with ASTM A 308 and A 318.

Test procedure

The specimens of Series I and II, Specimens 1.1 and 1.2 were tested in an initially uncracked condition. All other specimens were deliberately cracked along the shear plane before testing.

The crack along the shear plane was formed as follows. The specimen was placed horizontally in a hydraulic testing machine, oriented as indicated by the section in Fig. 1. Line loads were applied to opposite faces of the specimen at the location of the shear plane. The loads were increased until a crack formed in the shear plane.

The shear test was performed in the same testing machine. The specimen was placed in a vertical position and was loaded concentrically as indicated in Fig. 1. The load was increased by increments until failure occurred. After each increase in load, the slip along the shear plane was measured. For this purpose a 0.001 in. (0.0254 mm per division) dial gage was mounted on a bracket attached to the specimen on one side of the shear plane, with its tip resting on a horizontal steel plate secured to the specimen on the opposite side of the shear plane.

TEST RESULTS

Behavior under load

Typical load-slip curves for specimens with and without cracks before testing are shown in Fig. 2. There was measurable slip from the beginning of the shear test in the case of the initially cracked specimens. However, no movement could be detected in the initially uncracked specimens until diagonal tension cracks became visible at shear

J. A. Hobeck is a member of the American Concrete Institute and is currently an Assistant Professor of Civil Engineering at the University of Washington. He received his BS, MS, and PhD degrees in engineering from the University of Washington. He received his undergraduate education at the University of Washington.

I. O. Ibrahim is a bridge engineer, Road Section, Ministry of Works, Sudan. He was formerly a graduate student at the University of Washington where he obtained an MS degree in civil engineering in 1967. Mr. Ibrahim received his undergraduate education at the University of Khartoum.

ACI member Alan H. Mattock since 1964 has been professor of civil engineering, University of Washington, Seattle, Wash. Prior to 1964 he was principal engineer in the Structural Laboratory of the Portland Cement Association, Skokie, Ill. He received BS, MS, and PhD degrees in engineering from the University of London, England. Active in ACI technical committee work, Dr. Mattock is currently chairman of ACI-ASCE Committee 423, Prestressed Concrete, and ACI-ASCE Committee 428, Limit Design, and a member of ACI Committee 115, Current Research, ACI-ASCE Committee 426, Shear and Diagonal Tension, and ACI Committee 438, Torsion. He was awarded the ACI Wason Medal for most meritorious paper in 1967.

stresses of from about 500 to 700 psi (nom. 35 to 50 kgf/cm²). These diagonal tension cracks crossed the shear plane at an angle of from 40 to 50 deg. They were each about two inches (nom. 5 cm) in length, and were spaced one to two inches (nom. 2.5 to 5 cm) apart along the length of the shear plane. After formation of these cracks there was relative longitudinal movement of the two halves of the initially uncracked specimens, but this was not slip in the true sense of the word. The movement was rather due to rotation of the short concrete struts formed by the diagonal tension cracks, when the stirrup reinforcement stretched.

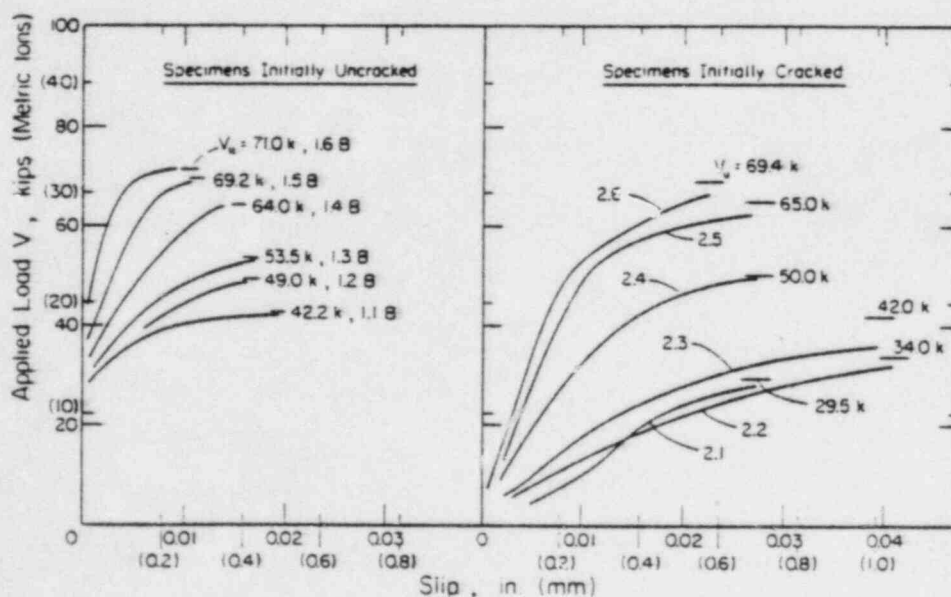


Fig. 2—Typical load-slip curves

Concrete strength f_c , psi	f_c , kgf/cm ²
4040 (284)	
4010 (282)	
3100 (218)	
4040 (284)	
4040 (284)	
4070 (286)	
4070 (286)	
4340 (305)	
4340 (305)	
3390 (239)	
2450 (172)	
2620 (184)	
2385 (168)	
2580 (182)	
2620 (184)	
2770 (197)	
2770 (197)	
2960 (212)	
2930 (210)	

Similar diagonal tension cracks occurred in initially cracked specimens that contained a high percentage of stirrup reinforcement. These diagonal tension cracks ran across the pre-existing crack in the shear plane.

Final failure was accompanied by compression spalling in the region of the diagonal tension cracks adjacent to the shear plane, and by the formation of additional cracks joining the diagonal tension cracks together.

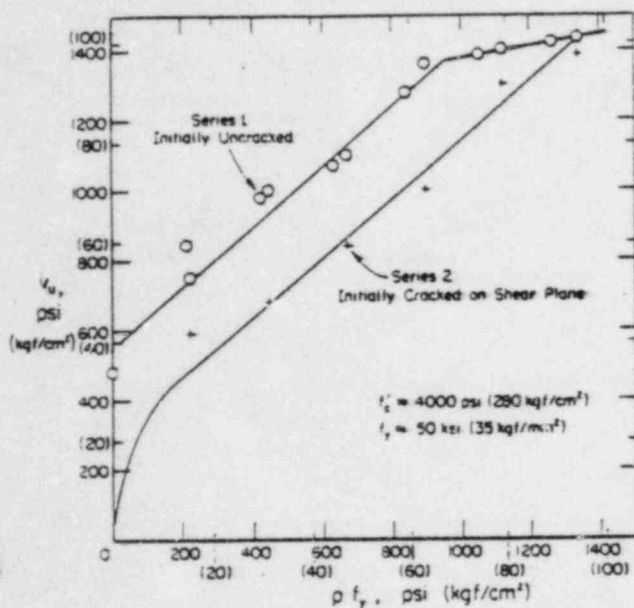


Fig. 3—Variation of shear strength with reinforcement parameter $p f_y$, with and without a crack along the shear plane

Ultimate strength

The ultimate shear strengths attained in all the tests are summarized in Table 2. For convenience they are expressed as average shear stresses v_u , obtained by dividing the ultimate shear force V_u by the area of the shear plane, bd (where d is the length of the shear plane and b its width).

DISCUSSION OF TEST RESULTS

Effect of cracking

The data indicate that if a crack exists in the shear plane before the application of shear, then the slip at all stages of loading will be greater than would have occurred if the crack had not been present. The existence of a crack in the shear plane also reduces the ultimate shear strength, as may be seen in Fig. 3. For values of the web reinforcement parameter $p f_y$, between about 200 (nom. 14 and 70 kgf/cm²) and 1000 psi, the difference between the ultimate shear stress in an initially cracked specimen and that achieved in a companion uncracked specimen is almost constant and equal to about 250 psi (nom. 17.5 kgf/cm²). For lower values of $p f_y$, the difference increases. For values of $p f_y$, above 1000 psi (70 kgf/cm²), the strength of the initially uncracked specimens increases at a very slow rate with increase in $p f_y$, while the strength of the initially cracked specimens continue to increase at the same rate as for lower values of $p f_y$. As a result of this, the strengths of the cracked and uncracked specimens are approximately equal for a $p f_y$ of 1340 psi (94 kgf/cm²).

TABLE 2—TEST RESULTS

Specimen No.	$p f_y$,* psi (kgf/cm ²)	v_u ,* psi (kgf/cm ²)	Specimen No.	$p f_y$,* psi (kgf/cm ²)	v_u ,* psi (kgf/cm ²)
1.0	0	150 (10.3)	3.1	49 (3.5)	210 (16.0)
1.1A	223 (15.7)	750 (52.8)	3.2	223 (15.7)	320 (26.6)
1.1B	211 (14.8)	314 (22.4)	3.3	446 (31.4)	680 (47.8)
1.2A	446 (31.4)	1000 (70.3)	3.4	740 (52.1)	1028 (72.3)
1.2B	422 (29.7)	980 (69.0)	3.5	1040 (73.2)	1152 (81.1)
1.2A	670 (47.2)	1100 (77.3)			
1.3B	622 (44.6)	1070 (75.3)	4.1	293 (20.6)	704 (49.5)
1.4A	313 (22.3)	1260 (89.7)	4.2	383 (27.0)	980 (68.0)
1.4B	314 (22.4)	1250 (89.0)	4.3	374 (26.5)	1180 (82.0)
1.5A	1120 (78.8)	1400 (98.5)	4.4	1165 (81.0)	1400 (98.5)
1.5B	1055 (74.2)	1331 (97.3)	4.5	1453 (102.3)	1320 (92.8)
1.6A	1340 (94.3)	1432 (100.8)			
1.6B	1296 (92.1)	1320 (93.9)	5.1	223 (15.7)	510 (35.2)
			5.2	446 (31.4)	700 (49.2)
			5.3	670 (47.2)	310 (21.0)
			5.4	893 (62.4)	795 (55.9)
			5.5	1120 (78.8)	1010 (71.0)
2.1	223 (15.7)	540 (38.5)	6.1	211 (14.8)	380 (26.3)
2.2	446 (31.4)	600 (42.4)	6.2	1055 (73.2)	1240 (87.2)
2.3	670 (47.2)	530 (37.3)	6.3	446 (31.4)	320 (22.3)
2.4	893 (62.4)	1080 (76.2)	6.4	670 (47.2)	920 (64.9)
2.5	1120 (78.8)	1000 (70.3)			
2.6	1340 (94.3)	1215 (87.5)			

It is of the proper values of the to she exister

Effect

If th reinfor ing the

v_u , psi (kgf/cm²)

Fig. 4 sh

the re to de reinfo the c and 2. p the h. In Se size (15.0 of 5 which betw

Effect

In

of r

It is interesting to note that the shear strength of the initially cracked specimens is not directly proportional to the amount of reinforcement. For values of pf_v above 200 psi (14 kgf/cm²) the trend of the data seems to indicate some contribution to shear strength by the concrete, despite the existence of a crack along the shear plane.

Effect of stirrup bar size and spacing

If the area of the shear plane is constant, the reinforcement ratio p can be changed by changing the bar size and/or the bar spacing. In Fig. 4,

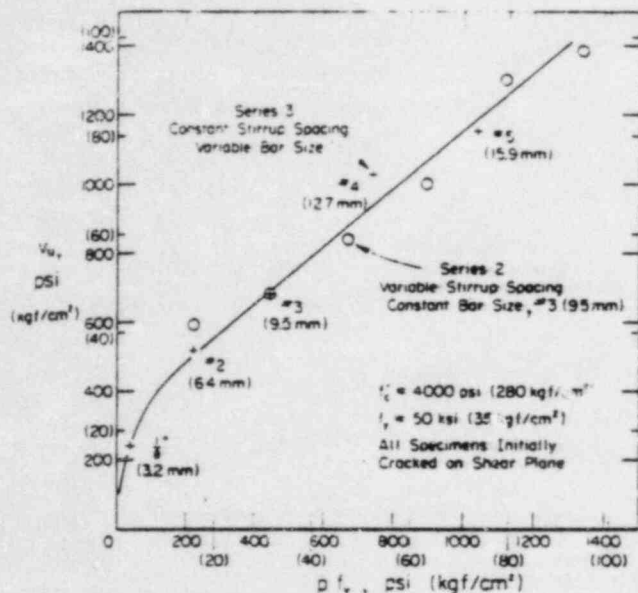


Fig. 4—Effect of stirrup bar size and spacing on the shear strength of initially cracked specimens

the results of Tests Series 2 and 3 are compared to determine whether the way in which the reinforcement ratio is changed has any effect on the relationship between ultimate shear strength and the reinforcement parameter pf_v . In Series 2, p was changed by varying the stirrup spacing, the bar size being constant. (#3) (9.5 mm dia.). In Series 3, p was changed by varying the bar size between $\frac{1}{8}$ in. (3.2 mm) diameter and #5 (15.9 mm), while maintaining a constant spacing of 5 in. (12.7 cm). It appears that the way in which p is changed does not affect the relationship between shear strength and the parameter pf_v .

Effect of stirrup reinforcement yield point

In the tests so far discussed, and in other available test data,^{3,4} the stirrup reinforcement was all of intermediate grade with a yield point of about 50 ksi (nom. 35 kgf/mm²). It was thought desirable to check whether the full yield strength of Type A432 reinforcing bars can be developed when they are used as shear transfer reinforcement.

In Fig. 5 the shear strength of specimens reinforced with A432 bar stirrups having a yield point of 96.1 ksi (68.5 kgf/mm²) and compared with the strength of specimens reinforced with stirrups having a yield point of 50.7 ksi (35.7 kgf/mm²). The concrete strength was 4000 psi (280 kgf/cm²) in both cases, and both series of specimens were deliberately cracked along the shear plane before test. With the exception of the most heavily reinforced specimen, the strength of the specimens reinforced with the A432 bar

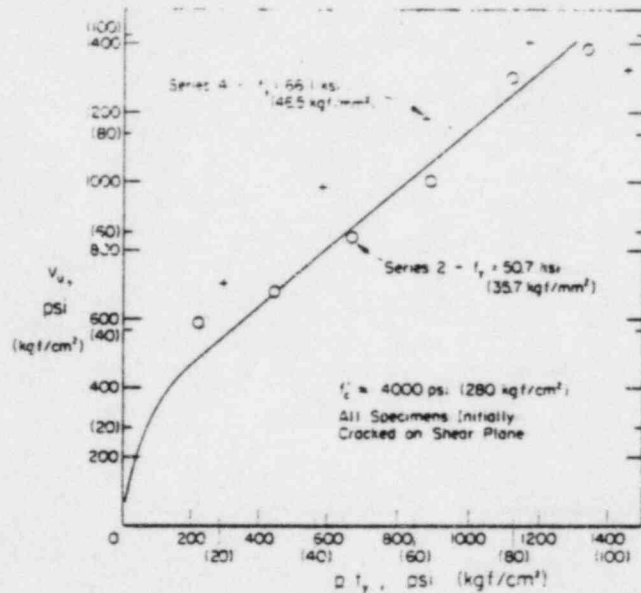


Fig. 5—Effect of stirrup reinforcement yield point on the shear strength of initially cracked specimens

stirrups was greater than that of the specimens reinforced with intermediate grade stirrups, for any particular value of reinforcement parameter pf_v . This appears to indicate that at ultimate strength the A432 stirrups developed a stress greater than their yield point, i.e., strain hardening occurred. This is quite possible, as the yield plateau of the A432 reinforcement is considerably shorter than that of the intermediate grade reinforcement. The test results indicate that it may safely be assumed in design that A432 reinforcing bars will develop their specified yield strength when used as shear transfer reinforcement.

Effect of concrete strength

The effect of variation in concrete strength on the shear strength of initially cracked specimens is illustrated in Fig. 6. The specimens of Series 2 and 5 were identical in all respects except concrete strength, Series 2 having 4000 psi (280 kgf/cm²) concrete and Series 5 having 2500 psi (175 kgf/cm²) concrete. For values of pf_v below about 600 psi (nom. 42 kgf/cm²) the concrete

strength does not appear to affect the shear transfer strength. For higher values of pf_v , the shear strength is lower for the lower strength concrete.

Referring to Fig. 3 it can be seen that there is a change in the behavior of the uncracked specimens of 4000 psi (280 kgf/cm²) concrete strength at about a pf_v of 950 psi (nom. 67 kgf/cm²). Thereafter the shear strength increases at a slower rate, and must also provide a ceiling to the strength of the cracked specimens. That is, if cracked and uncracked specimens had been tested with pf_v

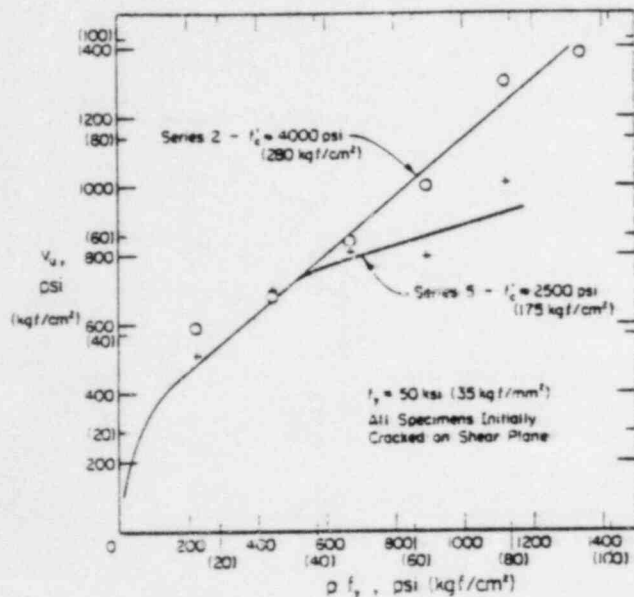


Fig. 6—Effect of concrete strength on the shear strength of initially cracked specimens.

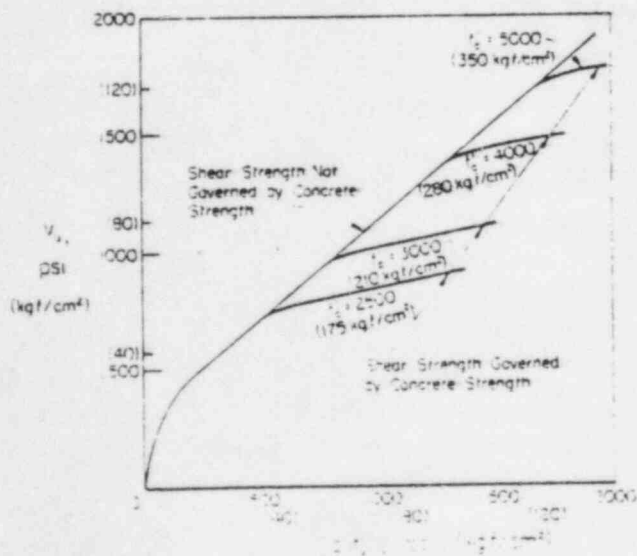


Fig. 7—Possible relationship between v_s and pf_v for initially cracked specimens of various concrete strengths (not to scale)

greater than 1400 psi (98 kgf/cm²) they would probably have had the same strength. No uncracked specimens were tested with 2500 psi (175 kgf/cm²) concrete strength, but it is possible to calculate the point of change in behavior of the uncracked specimens reasonably closely. (This is discussed later). For a 2500 psi (175 kgf/cm²) concrete, this point would be at a pf_v of about 400 psi (nom. 28 kgf/cm²) and v_s would be about 750 psi (nom. 53 kgf/cm²). A line through this point and approximately parallel to the line through the 4000 psi (280 kgf/cm²) data for uncracked specimens, for values of pf_v over 1000 psi (70 kgf/cm²), would pass through the experimental data for the 2500 psi (175 kgf/cm²) concrete when pf_v exceeds 600 psi (42 kgf/cm²).

The concrete strength therefore appears to set an upper limit value of pf_v , below which the relationship between v_s and pf_v established for 4000 psi (280 kgf/cm²) concrete would hold for any strength of concrete equal to or greater than that being considered, and above which the shear strength increases at a lesser rate. The shear strength versus pf_v relationships for cracked specimens of various concrete strengths might therefore be expected to be as sketched in Fig. 7.

Dowel action of stirrup reinforcement

(a) *Initially uncracked specimens*—The rubber sleeves provided in Specimens 6.1 and 6.2 eliminated any dowel action between the stirrup legs and the surrounding concrete for slips of less than about 1/8 in. (nom. 3 mm). The slips at any given load were no greater in the specimens with rubber sleeves than in companion specimens without. The strength of Specimen 6.1 is equal to the average strength of Specimens 1.1A and 1.1B. The strength of Specimen 6.2 is only 10 percent less than the strength of Companion Specimen 1.5B. These results indicate that dowel action does not contribute significantly to the shear transfer strength of initially uncracked specimens.

(b) *Initially cracked specimens*—The slip at ultimate strength in Specimens 6.3 and 6.4 with rubber sleeves reached 0.15 in. (3.8 mm), about six times the slip in the companion specimens without the rubber sleeves. The strengths of Specimens 6.3 and 6.4 were less by 34 and 23 percent, respectively than the strength of initially cracked specimens of the same pf_v value, without rubber sleeves (using the mean experimental line for Series 2). These results indicate that there is a considerable contribution to shear transfer strength by dowel action in initially cracked specimens.

(c) *General*—The different behavior of initially uncracked and initially cracked specimens at

parallel bond action probably stems from the different cracking pattern in the two types of specimens.

In initially uncracked specimens the cracking takes the form of a number of short diagonal cracks crossing the shear plane at close intervals. Movement of the two halves of the specimen relative to one another occurs by rotation of the concrete struts formed between the diagonal tension cracks. When this type of motion occurs, points on the opposite faces of the cracks move relative to one another in directions approximately parallel to the orientation of the stirrups. It would be difficult therefore for any appreciable dowel action to develop under these conditions. The reinforcement is put into tension as a truss-like action develops, rather than being subject to shearing action at the shear plane.

In the initially cracked specimens the stirrup legs cross the crack in the shear plane at right angles. They are therefore subject to a shearing action by the concrete on opposite sides of this crack. In this case therefore, dowel action can develop between the reinforcement and the concrete.

The shear-friction theory

The shear-friction theory has been discussed in detail by Birkeland and Birkeland,¹ and by Mast.² A crack is assumed to have occurred along the shear plane, and reinforcement having a total area A_s and a yield point f_y is assumed to cross the crack at right angles. The faces of the crack will be rough and irregular, so that when slip

occurs along the crack the pieces of concrete on either side of the crack will be made to separate slightly. This separation would create a tensile stress in tension, which would in turn create a compressive stress in the concrete across the crack. This compressive stress would provide resistance to slip along the crack by virtue of friction between the rough and irregular faces of the crack. It is assumed that the separation is sufficient to stress the reinforcement to its yield point, so that if $\tan\phi$ is the coefficient of friction between the faces of the crack, the shearing resistance along the crack will be given by:

$$V_u = A_s f_y \tan\phi \quad (1)$$

Alternatively, if we divide throughout by the area of the shear plane, the relationship can be expressed in terms of stress:

$$v_u = p f_y \tan\phi \quad (2)$$

Mast proposes that for a crack in monolithic concrete, or at a rough bonded interface between precast and cast-in-place concrete, $\tan\phi$ should be taken as 1.4, for values of $p f_y$ not greater than $0.15 f'_c$. He further limits the applicability of Eq.

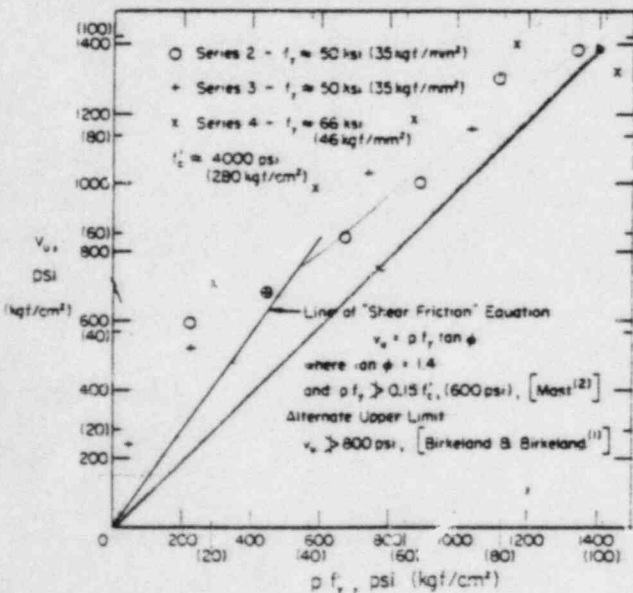


Fig. 8—Comparison of shear strength calculated using "shear friction" equation, with measured strength of initially cracked specimens having $f'_c \approx 4000$ psi

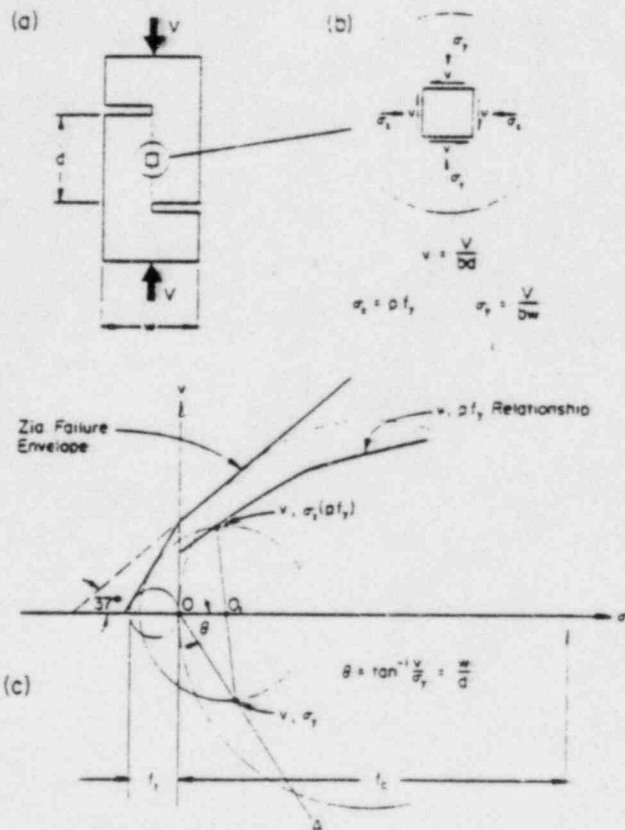


Fig. 9—Construction of relationship between shear strength v , and reinforcement parameter $p f_y$, in an initially uncracked push-off specimen

(2) to cases where intermediate grade reinforcement is used.

In Fig. 8, shear strength calculated using Eq. (2) is compared with the actual shear strength of all the initially cracked specimens with concrete strength of 4000 psi (280 kgf/cm²). Within the range of values of pf_v , set by Mast, the shear-friction equation yields a conservative estimate of the shear transfer strength of these initially cracked specimens. In view of the earlier discussion of the effect of concrete strength on shear transfer strength, it appears that Eq. (2) would start to become unconservative for concrete strengths of 4000 psi (280 kgf/cm²) or over when pf_v exceeds 600 psi (42 kgf/cm²). The upper limit to pf_v should therefore be $0.15f_c'$ but not more than 600 psi (42 kgf/cm²).

The distribution of the experimental results for the initially cracked specimens indicates that for values of pf_v in excess of about 200 psi (nom. 14 kgf/cm²) the shear strength is a combination of cohesion and friction effects, with an upper limit to shear strength of about $0.3f_c'$. The slope of the straight line through the data in this range is about 0.8. This is the same as the coefficient of friction between formed concrete surfaces measured by Gaston and Kriz.³ The shear-friction theory ignores the cohesion effect and compensates by using an apparent angle of internal friction which is much greater than the actual angle of internal friction. That the friction angle used is only "apparent," and is applicable only to low stress levels is noted by Mast.²

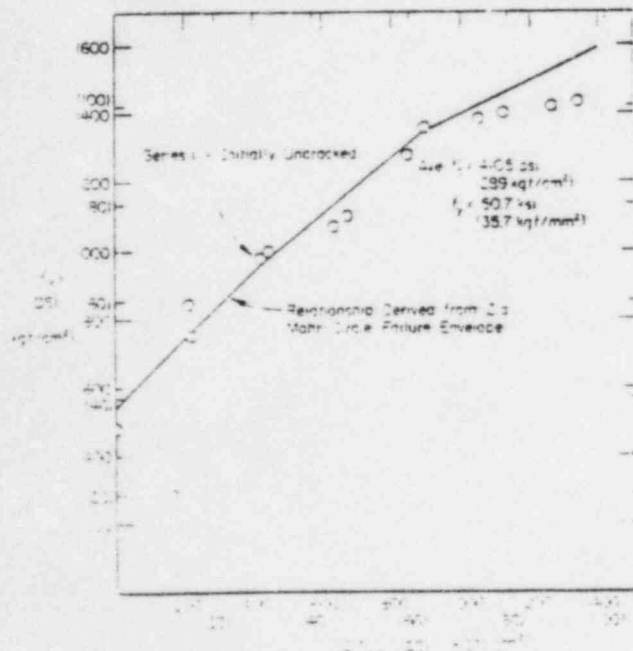


Fig. 8—Comparison of shear strength calculated using the ZIA failure envelope with measured strength of the initially uncracked specimens of Series I

The shear-friction theory is a simple and valuable tool in the design of connection details in precast and composite construction. The results of these tests indicate that, using $\tan\phi$ equal to 1.4, the shear-friction theory is reasonably conservative for values of pf_v , less than $0.15f_c'$ or 600 psi (42 kgf/cm²), (whichever is the less), using reinforcement with a specified yield point of 60 ksi (42 kgf/mm²) or less. This limits the ultimate shear stress to 840 psi (59 kgf/cm²). The test results show that with heavy reinforcement, shear stresses considerably in excess of this can be developed in cracked specimens. To take advantage of this in design, it would be necessary to use a lower value of $\tan\phi$ and a different upper limit to pf_v . Suitable values would be $\tan\phi$ equal to 1.0, and pf_v not greater than $0.3f_c'$ or 1500 psi (105 kgf/cm²), (whichever is the less).

Several examples of the use of the shear-friction theory in design are set out in References 1 and 2.

Shear strength of initially uncracked specimens

Consider a push-off specimen width w , thickness b , and with a shear plane of length d (Fig. 9). The stresses acting on a small element of concrete lying in the shear plane will be as shown at (b) in Fig. 9. Shear stresses v on all faces, normal stress σ_x due to the restraint provided by the stirrup reinforcement, and normal stresses σ_y due to

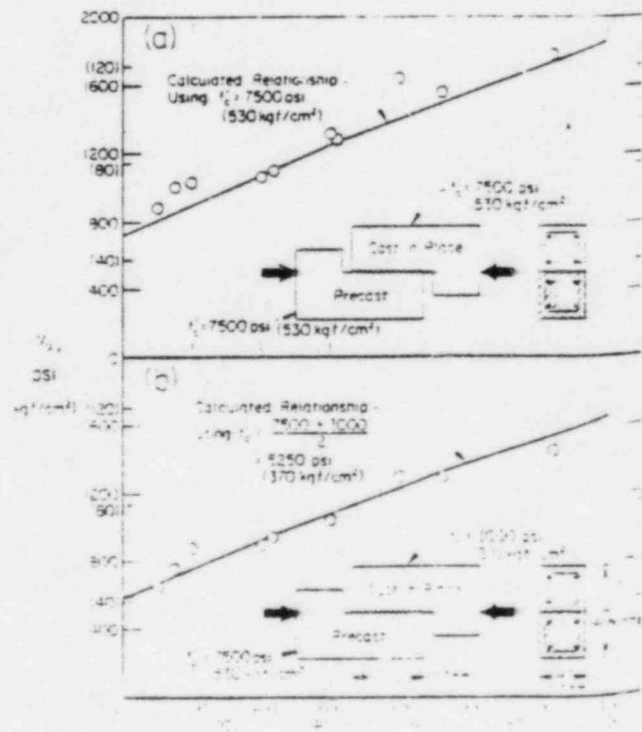


Fig. 11—Comparison of test results obtained by Anderson with relationships derived from ZIA failure envelope

... The exact distribution of the stresses is not known and so averaged stresses are used.

$$v = V/bd$$

$$\sigma_c = pf_v$$

$$\sigma_t = V/bw$$

The problem is to determine the combinations of these stresses which will result in failure of the concrete on the shear plane. To do this, use is made of a slightly modified version of the failure envelope proposed by Zia.⁶ This failure envelope is shown at (c) in Fig. 9 and consists of two parts: (1) a line inclined at 37 deg to the normal stress axis and tangent to the Mohr circle representing failure in uniaxial compression; (2) a line drawn from the point of intersection of the first line with the shear stress axis, and tangent to the Mohr circle representing failure in uniaxial tension. In constructing the failure envelope for a particular strength of concrete, the uniaxial compression strength f_c was taken as $0.85f'_c$ and the tensile strength was taken as $6\sqrt{f'_c}$ psi ($1.6\sqrt{f'_c}$ kgf/cm²).

Since for a particular pattern of push-off specimen v/σ_v is constant, points on the Mohr circles at failure corresponding to v and σ_v will all lie on the straight line OA inclined at angle θ to the normal stress axis, where θ is $\tan^{-1}(v/\sigma_v)$. The term (v/σ_v) is fixed by the proportions of the test specimen and is equal to w/d . A series of circles are drawn, each tangent to the failure envelope. Where Line OA cuts a circle establishes the point v, σ_v for the stress conditions at failure represented by that circle. A line is drawn through point v, σ_v and through the center of that circle. Where this line cuts the circle diametrically opposite from point v, σ_v fixes the point v, σ_t , that is, v, pf_v . By repeating this process for the several circles, a succession of points v, pf_v can be obtained. A line through these points is the v, pf_v relationship obtained in the push-off test.

The v, pf_v relationship was derived as described above for the Series 1 specimens of 4000 psi (280 kgf/cm²) concrete. This relationship is compared with the test data in Fig. 10 and is seen to be in good agreement for values of pf_v up to about 900 psi (nom. 63 kgf/cm²). The break in the relationship at about this point corresponds to the point at which the Mohr circles cease to be tangent to the more steeply sloping line, and become tangent to the line inclined at 37 deg. The implication of this is that the failure changes from a combination cleavage-sliding failure to a shear failure. Although the second part of the derived relation-

ship has not been tested, it is of interest to note that the break in the derived relationship corresponds closely to the break in the experimental relationship. Above this point the shear strength increases at a slower rate.

To check whether this method of deriving the v, pf_v relationship is applicable to composite push-off specimens, to concrete of other strengths, and to push-off specimens of different size and proportions, it was used to obtain the relationships for push-off specimens tested by Anderson.⁴ In Fig. 11(a) the derived relationship is compared with the experimental data for rough bonded composite push-off specimens in which both the precast and the cast-in-place concrete had a strength of 7500 psi (530 kgf/cm²). In Fig. 11(b) the derived relationship is compared with the experimental data for rough bonded composite push-off specimens in which the precast concrete had a strength of 7500 psi (530 kgf/cm²), and the cast-in-place concrete had a strength of 3000 psi (210 kgf/cm²). In this case the derived relationship was based on the average of the two concrete strengths. In both cases the agreement between the derived relationship and the experimental data is close.

It appears therefore that although this method of deriving the v, pf_v relationship is based on averaged stresses and a simplified failure envelope, it can be used with reasonable confidence for monolithic or rough bonded composite construction and for a wide range of concrete strengths and push-off specimen sizes.

CONCLUSIONS

1. A pre-existing crack along the shear plane will both reduce the ultimate shear transfer strength and increase the slip at all levels of load. For 4000 psi (280 kgf/cm²) normal weight concrete and values of pf_v between 200 and 1000 psi (14 and 70 kgf/cm²) the reduction in shear strength is a constant 250 psi (17.5 kgf/cm²).
2. The shear transfer strength is a function of the reinforcement parameter pf_v . When intermediate or A432 grade reinforcement is used, changes in strength, size and spacing of reinforcement affect the shear strength only insofar as they change the value of the reinforcement parameter pf_v .
3. In initially cracked concrete, the concrete strength sets an upper limit value for pf_v , below which the relationship between v and pf_v is the same for concretes of strength equal to or greater than that of the concrete being considered, and above which the shear transfer strength increases at a much reduced rate.

4. Dowel action of reinforcing bars crossing the shear plane is insignificant in initially uncracked concrete, but is substantial in concrete with a pre-existing crack along the shear plane.

5. The shear-friction theory gives a reasonably conservative estimate of shear transfer strength in normal weight concrete with a pre-existing crack along the shear plane and reinforced with intermediate or A432 grade reinforcement if μ is assumed equal to 1.40, providing p_f is less than $0.15f_c'$ or 600 psi (42 kgf/cm²) (whichever is the less).

6. The Zia failure envelope may be used to derive the relationship between shear transfer strength and reinforcement parameter p_f , for uncracked concrete, either monolithic, or at a rough bonded interface between precast and cast-in-place concrete.

ACKNOWLEDGMENTS

This study was carried out in the Structural Research Laboratory of the University of Washington. It was made possible by the support of donors to the Structural Concrete Research Fund at the University of Washington, and by the Bethlehem Steel Corporation who donated reinforcing bars.

REFERENCES

1. Birkeland, P. W., and Birkeland, H. W., "Connections in Precast Concrete Construction," *ACI JOURNAL, Proceedings* V. 63, No. 3, Mar. 1966, pp. 345-368.
2. Mast, R. F., "Auxiliary Reinforcement in Concrete Connections," *Proceedings, ASCE*, V. 94, ST6, June 1968, pp. 1425-1504.
3. Hanson, N. W., "Precast-Prestressed Concrete Bridges 2. Horizontal Shear Connections," *Journal, PCI Research and Development Laboratories*, V. 2, No. 2, May 1960, pp. 38-58. Also, *PCA Development Department Bulletin* D35.
4. Anderson, A. R., "Composite Designs in Precast and Cast-in-Place Concrete," *Progressive Architecture*, V. 41, No. 9, Sept. 1960, pp. 172-179.
5. Gaston, J. R., and Kriz, L. B., "Connections in Precast Concrete Structures -- Scarf Joints," *Journal, Prestressed Concrete Institute*, V. 9, No. 3, June 1964, pp. 37-59.
6. Zia, P., "Torsional Strength of Prestressed Concrete Members," *ACI JOURNAL, Proceedings* V. 37, No. 10, Apr. 1961, pp. 1337-1360.

Received by the Institute Apr. 13, 1968.

Sinopsis—Résumé—Zusammenfassung

Transmisión del Cortante en Concreto Reforzado

Se presenta un estudio de la transferencia del cortante en concreto reforzado, esto es, la transferencia del cortante a través de un plano tal como el de la superficie de contacto entre una viga precolada y una viga colada en el lugar. Se ensayaron 38 especímenes de extracción, algunos con, otros sin una grieta preexistente a lo largo del plano de cortante. Se encontró que la teoría cortante-fricción da una estimación conservadora de la resistencia transmitida por cortante en concreto con agrietamiento inicial. Se presenta un método para calcular la transferencia por cortante en concreto sin agrietamiento inicial, basado en la relación entre la envolvente de Zia y los círculos de Mohr representando condiciones de falla para el concreto.

Transfert de Cisaillement dans un Béton Armé

Cet article présente une étude de transfert de cisaillement dans un béton armé c'est à dire le transfert de cisaillement à travers un plan, telle que la face interne entre une poutre précoulée et une dalle coulée en place. Trente huit spécimen de poussée ont été essayés, quelques uns avec, d'autres sans craquelures pré-existante le long du plan de cisaillement. La théorie de cisaillement friction s'est montrée apportant une estimation conservatrice du transfert de résistance au cisaillement de béton initialement craquelé.

Une méthode est présentée pour le calcul de transfert de résistance au cisaillement dans des bétons non craquelés; elle est basée sur l'enveloppe Zia des cercles de Mohr représentant les conditions de rupture pour du béton.

Schubübertragung in Stahlbetonteilen

Eine Studie über die Schubübertragung in Stahlbetonteilen wird diskutiert. Darunter ist die Übertragung von Schubkräften über eine Fläche wie z.B. im Schnitt zwischen einem vorgefertigten Balken und einer nachträglich daraufbetonierten Platte verstanden. Achtunddreissig Wegdruckproben wurden untersucht, von denen einige bei Versuchsbeginn Risse in der Schubfläche enthielten. Es wurde festgestellt, dass die Schub-Reibungstheorie auf der sicheren Seite liegenden Werte für die Schubübertragungsfestigkeit von Proben ergab, welche bei Versuchsbeginn gerissen waren. Eine Methode für die Berechnung der Schubübertragungsfestigkeit von ursprünglich ungerissenen Proben wird gegeben, welche auf die Zia Einhüllende zu Mohrschen Kreisen als Bruchbedingung für Beton aufbaut.

ITEM III (from June 14 meeting with NRC)

Qualification of Leak Rate Test Channels in the Containment Liner for SAR Loadings

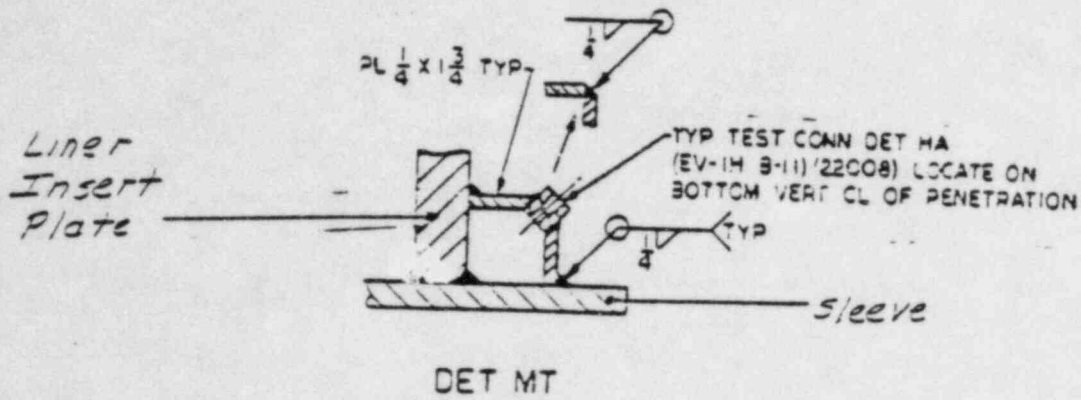
The applicant will determine the capability of the channels to withstand combined pressure and temperature loads.

RESPONSE:

- A. The accompanying sketches show the various leak chase members that were analyzed for the emergency, test, normal, and severe operational conditions listed in Table 3.8-1 of the FSAR.
- B. Analysis shows the stress levels for all load combination equations are within the acceptance criteria as defined in the FSAR Section 3.8, thereby maintaining the leak tight pressure boundary.

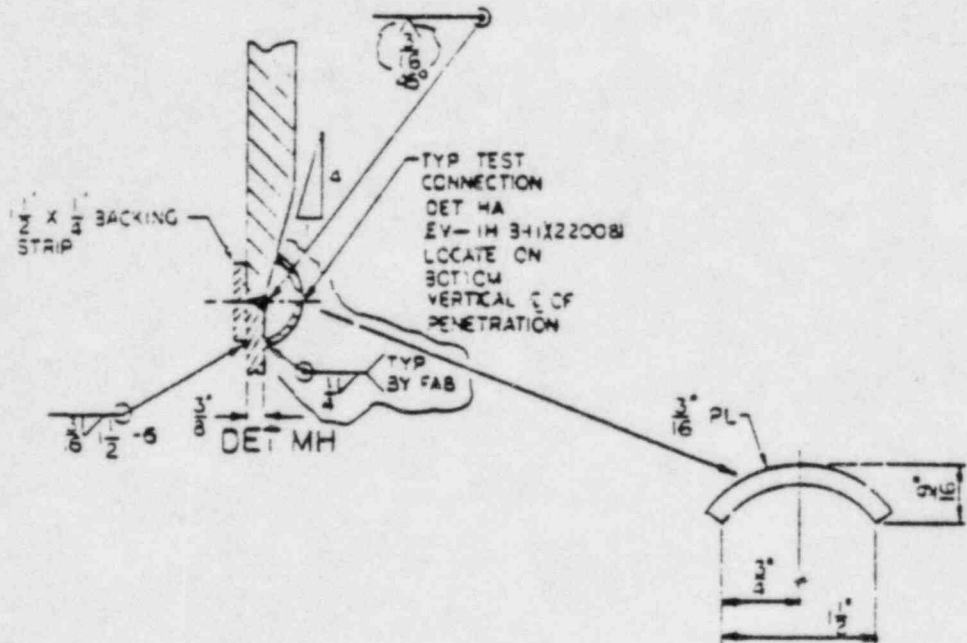
LEAK CHASE DETAILS

TYPE 1



Typical for Main Steam and Feedwater Penetrations

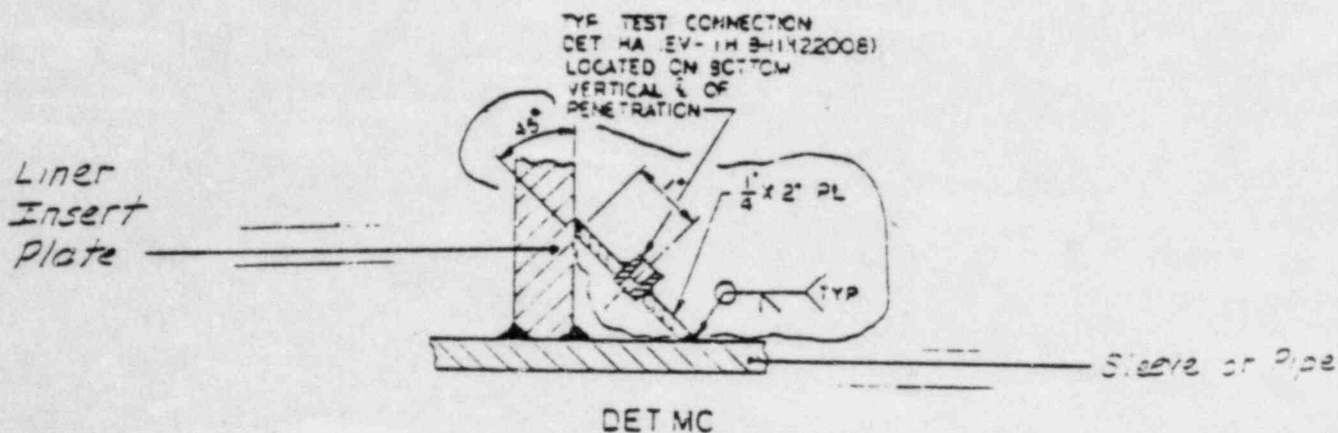
TYPE 2



Typical for all circular liner insert plates at penetrations

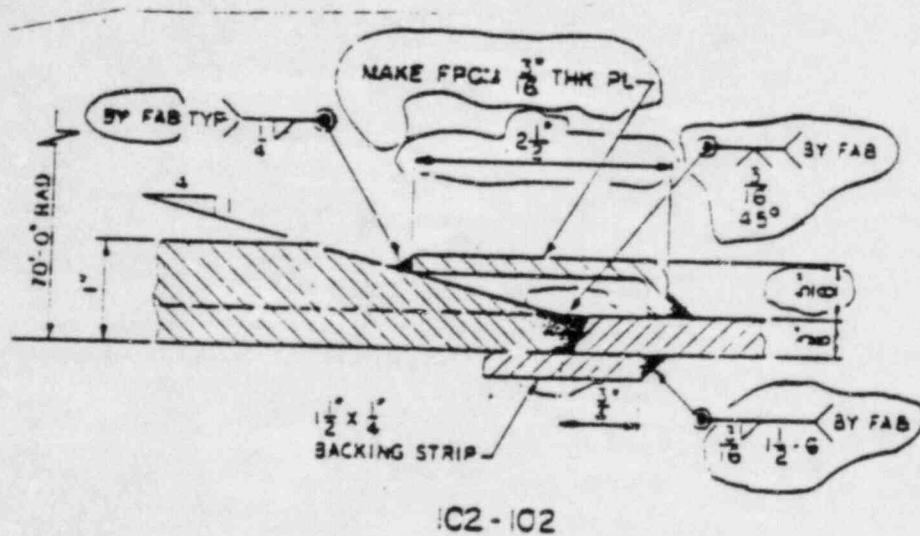
LEAK CHASE DETAILS

TYPE 3



Typical for all penetrations except the
Main Steam and Feedwater

TYPE 4



Typical for large rectangular insert plates